TALYS-1.0

A nuclear reaction program

A.J. Koning*, S. Hilaire† and M. Duijvestijn*

* NRG - Nuclear Research and Consultancy Group, 1755 ZG Petten, The Netherlands
† CEA, Service de Physique et Techniques Nucleaires, B.P. 12, F-91680 Bruyères-le-Châtel, France

USER MANUAL

December 21, 2007

Preface

TALYS is a nuclear reaction program created at NRG Petten, the Netherlands and CEA Bruyères-le-Châtel, France. The idea to make TALYS was born in 1998, when we decided to implement our combined knowledge of nuclear reactions into one single software package. Our objective is to provide a complete and accurate simulation of nuclear reactions in the 1 keV-200 MeV energy range, through an optimal combination of reliable nuclear models, flexibility and user-friendliness. TALYS can be used for the analysis of basic scientific experiments or to generate nuclear data for applications.

Like most scientific projects, TALYS is always under development. Nevertheless, at certain moments in time, we freeze a well-defined version of TALYS and subject it to extensive verification and validation procedures. You are now reading the manual of version 1.0.

Many people have contributed to the present state of TALYS: In no particular order, and realizing that we probably forget someone, we thank Jacques Raynal for extending the ECIS-code according to our special wishes and for refusing to retire, Jean-Paul Delaroche and Olivier Bersillon for theoretical support, Emil Betak, Vivian Demetriou and Connie Kalbach for input on the pre-equilibrium models, Stéphane Goriely for providing many nuclear structure tables and extending TALYS for astrophysical calculations, Eric Bauge for extending the optical model possibilities of TALYS, Pascal Romain, Emmeric Dupont and Michael Borchard for specific computational advice and code extensions, Steven van der Marck for careful reading of this manual, Roberto Capote and Mihaela Sin for input on fission models, Jura Kopecky and Robin Forrest for testing many of the results of TALYS, and Mark Chadwick, Phil Young and Mike Herman for helpful discussions and for providing us the motivation to compete with their software.

TALYS-1.0 falls in the category of GNU General Public License software. Please read the release conditions on the next page. Although we have invested a lot of effort in the validation of our code, we will not make the mistake to guarantee perfection. Therefore, in exchange for the free use of TALYS: If you find any errors, or in general have any comments, corrections, extensions, questions or advice, we would like to hear about it. You can reach us at **info@talys.eu**, if you need us personally, but information that is of possible interest to all TALYS users should be send to the mailing list **talys-l@nrg.eu**. The webpage for TALYS is **www.talys.eu**.

Arjan Koning
Stéphane Hilaire
Marieke Duijvestijn

TALYS release terms

TALYS-1.0 is copylefted free software: you can redistribute it and/or modify it under the terms of the GNU General Public License as published by the Free Software Foundation, see http://www.gnu.org.

This program is distributed in the hope that it will be useful, but WITHOUT ANY WARRANTY; without even the implied warranty of MERCHANTABILITY or FITNESS FOR A PARTICULAR PURPOSE. See the GNU General Public License in Appendix A for more details.

In addition to the GNU GPL *terms* we have a few *requests*:

- Please inform (one of) the authors when you distribute TALYS further. We like to keep track of the users.

- When TALYS is used for your reports, publications, etc., please make a proper reference to the code. For TALYS-1.0 this is:
  A.J. Koning, S. Hilaire and M.C. Duijvestijn, "TALYS: Comprehensive nuclear reaction modeling", *Proceedings of the International Conference on Nuclear Data for Science and Technology - ND2004*, AIP vol. 769, eds. R.C. Haight, M.B. Chadwick, T. Kawano, and P. Talou, Sep. 26 - Oct. 1, 2004, Santa Fe, USA, p. 1154 (2005).
  This should however be replaced in the near future by the more recent document
  A.J. Koning, S. Hilaire and M.C. Duijvestijn, "TALYS-1.0", *Proceedings of the International Conference on Nuclear Data for Science and Technology - ND2007*, April 22-27 2007 Nice France (2008).
  Please include the publisher, editors and page number in this reference once it becomes available.

- Inform us about, or send, extensions you have built into TALYS. Of course, proper credit will be given to the authors of such extensions in future versions of the code.

- Send us a copy/preprint of reports and publications in which TALYS is used.

Contents

Chapter 1

Introduction

TALYS is a computer code system for the analysis and prediction of nuclear reactions. The basic objective behind its construction is the simulation of nuclear reactions that involve neutrons, photons, protons, deuterons, tritons, ^{3}He- and alpha-particles, in the 1 keV - 200 MeV energy range and for target nuclides of mass 12 and heavier. To achieve this, we have implemented a suite of nuclear reaction models into a single code system. This enables us to evaluate nuclear reactions from the unresolved resonance range up to intermediate energies.

There are two main purposes of TALYS, which are strongly connected. First, it is a *nuclear physics* tool that can be used for the analysis of nuclear reaction experiments. The interplay between experiment and theory gives us insight in the fundamental interaction between particles and nuclei, and precise measurements enable us to constrain our models. In return, when the resulting nuclear models are believed to have sufficient predictive power, they can give an indication of the reliability of measurements. The many examples we present at the end of this manual confirm that this software project would be nowhere without the existing (and future) experimental database.

After the nuclear physics stage comes the second function of TALYS, namely as a *nuclear data* tool: Either in a default mode, when no measurements are available, or after fine-tuning the adjustable parameters of the various reaction models using available experimental data, TALYS can *generate* nuclear data for all open reaction channels, on a user-defined energy and angle grid, beyond the resonance region. The nuclear data libraries that are constructed with these calculated and experimental results provide essential information for existing and new nuclear technologies. Important applications that rely directly or indirectly on data generated by nuclear reaction simulation codes like TALYS are: conventional and innovative nuclear power reactors (GEN-IV), transmutation of radioactive waste, fusion reactors, accelerator applications, homeland security, medical isotope production, radiotherapy, single-event upsets in microprocessors, oil-well logging, geophysics and astrophysics. Before this release, TALYS has already been used for both basic and applied science. A non-exhaustive list of publications that contain an analysis with TALYS is given in Refs. [1]-[50].

The development of TALYS has always followed the "first completeness, then quality" principle. This should certainly not suggest that we use toy models to arrive at some quick and dirty results. Actually, we think that "completeness and quality" has been accomplished for several important parts of the program, since several reaction mechanisms coded in TALYS are based on theoretical models whose implementation is only possible with the current-day computer power. It rather means that, in our quest for completeness, we try to divide our effort equally among all nuclear reaction types. The precise description of *all* possible reaction channels in a single calculational scheme is such an enormous task that we have chosen, to put it bluntly, not to devote several years to the theoretical research and absolutely perfect implementation of one particular reaction channel which accounts for only a few millibarns of the total reaction cross section. Instead, we aim to enhance the quality of TALYS equally over the whole reaction range and always search for the largest shortcoming that remains after the last improvement. The reward of this approach is that with TALYS we can cover the whole path from fundamental nuclear reaction models to the creation of complete data libraries for nuclear applications, with the obvious side note that the implemented nuclear models will always need to be upgraded. An additional long-term aim is full transparency of the implemented nuclear models, in other words, an *understandable* source program, and a modular coding structure.

The idea to construct a computer program that gives a simultaneous prediction of many nuclear reaction channels, rather than a very detailed description of only one or a few reaction channels, is not new. Well-known examples of all-in-one codes from the past decades are GNASH [51], ALICE [52], STAPRE [53], and EMPIRE [54]. They have been, and are still, extensively used, not only for academical purposes but also for the creation of the nuclear data libraries that exist around the world. GNASH and EMPIRE are still being maintained and extended by the original authors, whereas various local versions of ALICE and STAPRE exist around the world, all with different extensions and improvements. TALYS is new in the sense that it has recently been written completely from scratch (with the exception of one very essential module, the coupled-channels code ECIS), using a consistent set of programming procedures.

As specific features of the TALYS package we mention

- In general, an exact implementation of many of the latest nuclear models for direct, compound, pre-equilibrium and fission reactions.
- A continuous, smooth description of reaction mechanisms over a wide energy range (0.001- 200 MeV) and mass number range ($12 < \mathrm{A} < 339$).
- Completely integrated optical model and coupled-channels calculations by the ECIS-06 code [55].
- Incorporation of recent optical model parameterisations for many nuclei, both phenomenological (optionally including dispersion relations) and microscopical.
- Total and partial cross sections, energy spectra, angular distributions, double-differential spectra and recoils.
- Discrete and continuum photon production cross sections.
- Excitation functions for residual nuclide production, including isomeric cross sections.
- An exact modeling of exclusive channel cross sections, e.g. $(n, 2np)$, spectra, and recoils.
- Automatic reference to nuclear structure parameters as masses, discrete levels, resonances, level density parameters, deformation parameters, fission barrier and gamma-ray parameters, generally from the IAEA Reference Input Parameter Library [56].
- Various width fluctuation models for binary compound reactions and, at higher energies, multiple Hauser-Feshbach emission until all reaction channels are closed.
- Various phenomenological and microscopic level density models.
- Various fission models to predict cross sections and fission fragment and product yields.

- Models for pre-equilibrium reactions, and multiple pre-equilibrium reactions up to any order.
- Astrophysical reaction rates using Maxwellian averaging.
- Option to start with an excitation energy distribution instead of a projectile-target combination.
- Use of systematics if an adequate theory for a particular reaction mechanism is not yet available or implemented, or simply as a predictive alternative for more physical nuclear models.
- Automatic generation of nuclear data in ENDF-6 format (not included in the free release).
- Automatic optimization to experimental data and generation of covariance data (not included in the free release).
- A transparent source program.
- Input/output communication that is easy to use and understand.
- An extensive user manual.
- A large collection of sample cases.

The central message is that we always provide a complete set of answers for a nuclear reaction, for all open channels and all associated cross sections, spectra and angular distributions. It depends on the current status of nuclear reaction theory, and our ability to model that theory, whether these answers are generated by sophisticated physical methods or by a simpler empirical approach. With TALYS, a complete set of cross sections can already be obtained with minimal effort, through a four-line input file of the type:

```
projectile n
element    Fe
mass       56
energy     14.
```

which, if you are only interested in reasonably good answers for the most important quantities, will give you all you need. If you want to be more specific on nuclear models, their parameters and the level of output, you simply add some of the more than 200 keywords that can be specified in TALYS. We thus do not ask you to understand the precise meaning of all these keywords: you can make your input file as simple or as complex as you want. Let us immediately stress that we realize the danger of this approach. This ease of use may give the obviously false impression that one gets a *good* description of *all* the reaction channels, with minimum reaction specification, as if we would have solved virtually all nuclear reaction problems (in which case we would have been famous). Unfortunately, nuclear physics is not that simple. Clearly, many types of nuclear reactions are very difficult to model properly and can not be expected to be covered by simple default values. Moreover, other nuclear reaction codes may outperform TALYS on particular tasks because they were specifically designed for one or a few reaction channels. In this light, Section 7.3 is very important, as it contains many sample cases which should give the user an idea of what TALYS can do. We wish to mention that the above sketched method for handling input files was born out of frustration: We have encountered too many computer codes containing an implementation of beautiful physics, but with an unnecessary high treshold to use the code, since its input files are supposed to consist of a large collection of mixed, and intercorrelated, integer and real values, for which values *must* be given, forcing the user to first read the entire manual, which often does not exist.

1.1 How to use this manual

Although we would be honored if you would read this manual from the beginning to the end, we can imagine that not all parts are necessary, relevant or suitable to you. For example if you are just an interested physicist who does not own a computer, you may skip

> Chapter 2: Installation guide.

while everybody else probably needs Chapter 2 to use TALYS. A complete description of all nuclear models and other basic information present in TALYS, as well as the description of the types of cross sections, spectra, angular distributions etc. that can be produced with the code can be found in the next three chapters:

> Chapter 3: A general discussion of nuclear reactions and the types of observables that can be obtained.

> Chapter 4: An outline of the theory behind the various nuclear models that are implemented in TALYS.

> Chapter 5: A description of the various nuclear structure parameters that are used.

If you are an experienced nuclear physicist and want to compute your own specific cases directly after a successful installation, then instead of reading Chapters 3-5 you may go directly to

> Chapter 6: Input description.

The next chapter we consider to be quite important, since it contains ready to use starting points (sample cases) for your own work. At the same time, it gives an impression of what TALYS can be used for. That and associated matters can be found in

> Chapter 7: Output description, sample cases and verification and validation.

People planning to enter the source code for extensions, changes or debugging, may be interested in

> Chapter 8: The detailed computational structure of TALYS.

Finally, this manual ends with

> Chapter 9: Conclusions and ideas for future work.

Chapter 2

Installation and getting started

2.1 The TALYS package

In what follows we assume TALYS will be installed on a Unix/Linux operating system. In total, you will need about 1.3 Gb of free disk space to install TALYS. (This rather large amount of memory is almost completely due to microscopic level density, radial density, gamma and fission tables in the nuclear structure database. Since these are, at the moment, not the default models for TALYS you could omit these if total memory storage poses a problem.) If you obtain the entire TALYS package from www.talys.eu, you should do

- **tar zxvf talys.tar**

and the total TALYS package will be automatically stored in the *talys/* directory. It contains the following directories and files:

- *README* outlines the contents of the package.

- *talys.setup* is a script that takes care of the installation.

- *source/* contains the source code of TALYS: 274 Fortran subroutines, and the file *talys.cmb*, which contains all variable declarations and common blocks. This includes the file *ecis06t.f*. This is basically Jacques Raynal's code ECIS-06, which we have transformed into a subroutine and slightly modified to enable communication with the rest of TALYS.

- *structure/* contains the nuclear structure database in various subdirectories. See Chapter 5 for more information.

- *doc/* contains the documentation: this manual in postscript and pdf format and the description of ECIS-06.

- *samples/* contains the input and output files of the sample cases.

The code has so far been tested by us on various Unix/Linux systems, so we can not guarantee that it works on all operating systems, although we know that some users have easily installed TALYS under Windows XP. The only machine dependences we can think of are the directory separators '/' we use in pathnames that are hardwired in the code. If there is any dependence on the operating system, the associated statements can be altered in the subroutine *machine.f*. Also, the output of the execution time in *timer.f* may be machine dependent. The rest of the code should work on any computer.

TALYS has been tested for the following compilers and operating systems:

- Fujitsu Fortran90/95 compiler v1.0 on Linux Red Hat 5
- Fujitsu/Lahey Fortran90/95 compiler v6.1/6.2 on Linux Red Hat 9
- gnu g77 Fortran77 compiler on all Linux systems
- g95 Fortran95 compiler on all Linux systems
- Workshop 6.2 Fortran77 compiler on the SUN workstation

ECIS-06 may contain one or a few peculiarities that generate warnings by some compilers, though the upgrade from ECIS-97 has remedied many problems.

2.2 Installation

The installation of TALYS is straightforward. For a Unix/Linux system, the installation is expected to be handled by the *talys.setup* script, as follows

- edit *talys.setup* and set the first two variables: the name of your compiler and the place where you want to store the TALYS executable.
- **talys.setup**

If this does not work for some reason, we here provide the necessary steps to do the installation manually. For a Unix/Linux system, the following steps should be taken:

- **chmod -R u+rwX talys** to ensure that all directories and files have read and write permission and the directories have execute permission. (These permissions are usually disabled when reading from a CD or DVD).
- **cd talys/source**
- Ensure that TALYS can read the nuclear structure database. This is done in subroutine *machine.f*. If *talys.setup* has not already replaced the path name in *machine.f*, do it yourself. We think this is the only Unix/Linux machine dependence of TALYS. Apart from a few trivial warning messages for *ecis06t.f*, we expect no complaints from the compiler.
- **f95 -c *.f**
- **f95 *.o -o talys**
- **mv talys ~/bin** (assuming you have a *~/bin* directory which contains all executables that can be called from any working directory)

After you or *talys.setup* has completed this, type

- **rehash**, to update your table with commands.

The above commands represent the standard compilation options. Consult the manual of your compiler to get an enhanced performance with optimization flags enabled. The only restriction for compilation is that *ecis06t.f* should *not* be compiled in double precision.

2.3 Verification

If TALYS is installed, testing the sample cases is the logical next step. The *samples/* directory contains the script *verify* that runs all the test cases. Each sample case has its own subdirectory, which contains a subdirectory *org/*, where we stored the input files and **our** calculated results, obtained with the Fujitsu/Lahey v6.2 compiler on Linux Red Hat 9. It also contains a subdirectory *new*, where we have stored the input files only and where the *verify* script will produce **your** output files. A full description of the keywords used in the input files is given in Chapter 6. Section 7.3 describes all sample cases in full detail. Note that under Linux/Unix, in each subdirectory a file with differences with our original output is created.

Should you encounter error messages upon running TALYS, like *'killed'* or *'segmentation fault'*, then probably the memory of your processor is not large enough (i.e. smaller than 256 Mb). Edit *talys.cmb* and reduce the value of **memorypar**.

2.4 Getting started

If you have created your own working directory with an input file named e.g. *input*, then a TALYS calculation can easily be started with:

talys $<$ **input** $>$ **output**

where the names *input* and *output* are not obligatory: you can use any name for these files.

Chapter 3

Nuclear reactions: General approach

An outline of the general theory and modeling of nuclear reactions can be given in many ways. A common classification is in terms of time scales: short reaction times are associated with direct reactions and long reaction times with compound nucleus processes. At intermediate time scales, pre-equilibrium processes occur. An alternative, more or less equivalent, classification can be given with the number of intranuclear collisions, which is one or two for direct reactions, a few for pre-equilibrium reactions and many for compound reactions, respectively. As a consequence, the coupling between the incident and outgoing channels decreases with the number of collisions and the statistical nature of the nuclear reaction theories increases with the number of collisions. Figs. 3.1 and 3.2 explain the role of the different reaction mechanisms during an arbitrary nucleon-induced reaction in a schematic manner. They will all be discussed in this manual.

This distinction between nuclear reaction mechanisms can be obtained in a more formal way by means of a proper division of the nuclear wave functions into open and closed configurations, as detailed for example by Feshbach's many contributions to the field. This is the subject of several textbooks and will not be repeated here. When appropriate, we will return to the most important theoretical aspects of the nuclear models in TALYS in Chapter 4.

When discussing nuclear reactions in the context of a computer code, as in this manual, a different starting point is more appropriate. We think it is best illustrated by Fig. 3.3. A particle incident on a target nucleus will induce several *binary* reactions which are described by the various competing reaction mechanisms that were mentioned above. The end products of the binary reaction are the emitted particle and the corresponding recoiling residual nucleus. In general this is, however, not the end of the process. A total nuclear reaction may involve a whole sequence of residual nuclei, especially at higher energies, resulting from multiple particle emission. All these residual nuclides have their own separation energies, optical model parameters, level densities, fission barriers, gamma strength functions, etc., that must properly be taken into account along the reaction chain. The implementation of this entire reaction chain forms the backbone of TALYS. The program has been written in a way that enables a clear and easy inclusion of all possible nuclear model ingredients for any number of nuclides in the reaction chain. Of course, in this whole chain the target and primary compound nucleus have a special status, since they are subject to *all* reaction mechanisms, i.e. direct, pre-equilibrium, compound and fission and, at low incident energies, width fluctuation corrections in compound nucleus decay. Also, at incident energies below a few MeV, only binary reactions take place and the target and compound nucleus are often the

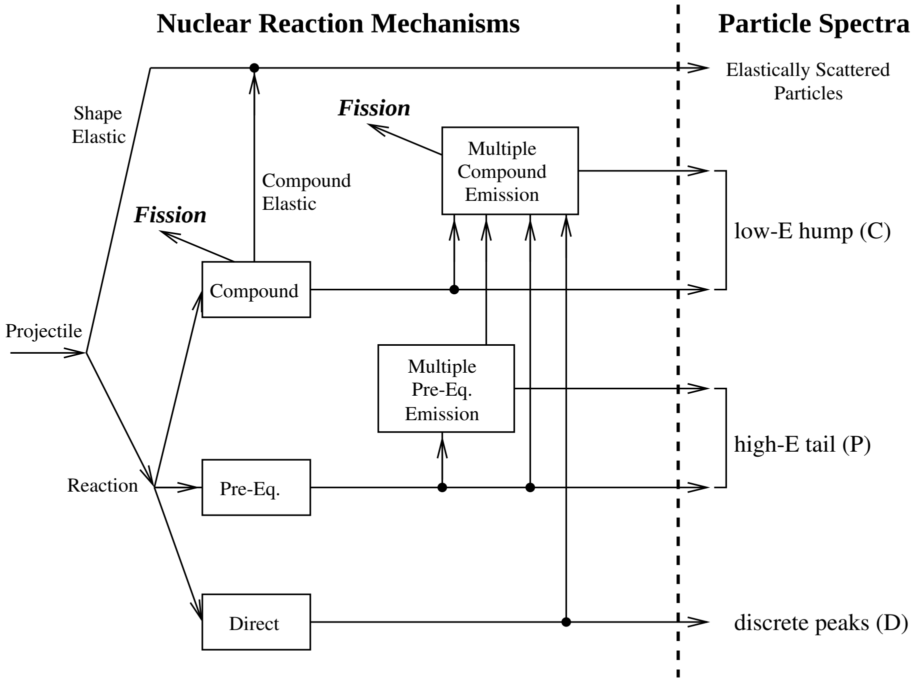

Figure 3.1: The role of direct, pre-equilibrium and compound processes in the description of a nuclear reaction and the outgoing particle spectra. The C, P and D labels correspond to those in Fig. 3.2

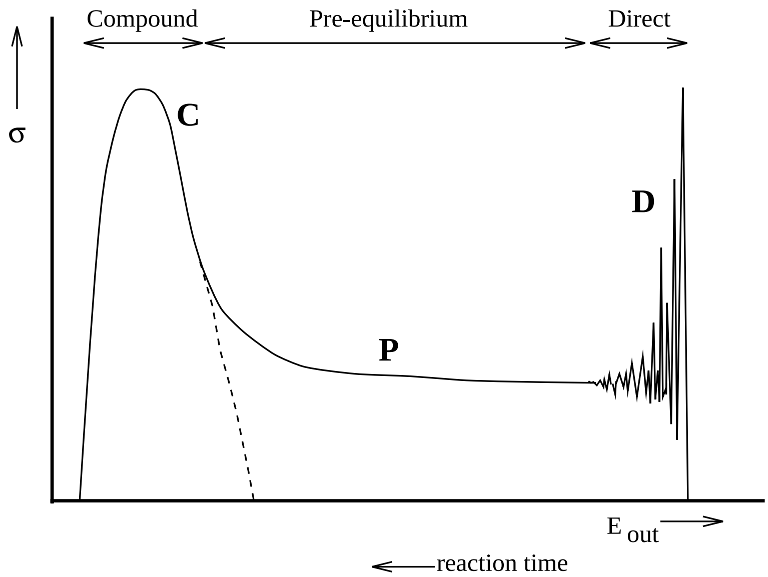

Figure 3.2: Schematical drawing of an outgoing particle spectrum. The energy regions to which direct (D), pre-equilibrium (P) and compound (C) mechanisms contribute are indicated. The dashed curve distinguishes the compound contribution from the rest in the transitional energy region.

only two nuclei involved in the whole reaction. Historically, it is for the binary reactions that most of the theoretical methods have been developed and refined, mainly because their validity, and their relation with nuclear structure, could best be tested with exclusive measurements. In general, however, Fig. 3.3 should serve as the illustration of a total nuclear reaction at any incident energy. The projectile, in this case a neutron, and the target $(Z_C, N_C - 1)$ form a compound nucleus (Z_C, N_C) with a total energy

$$E^{tot} = E_{CM} + S_n(Z_{CN}, N_{CN}) + E_x^0, \tag{3.1}$$

where E_{CM} is the incident energy in the CM frame, S_n is the neutron separation energy of the compound nucleus, and E_x^0 the excitation energy of the target (which is usually zero, i.e. representing the ground state). The compound nucleus is described by a range of possible spin (J) and parity (Π) combinations, which for simplicity are left out of Fig. 3.3. From this state, transitions to all open channels may occur by means of direct, pre-equilibrium and compound processes. The residual nuclei formed by these binary reactions may be populated in the discrete level part and in the continuum part of the available excitation energy range. In Fig. 3.3, we have only drawn three binary channels, namely the (Z_C, N_C-1), (Z_C-1, N_C) and (Z_C-1, N_C-1) nuclei that result from binary neutron, proton and deuteron emission, respectively. Each nucleus is characterized by a separation energy per possible ejectile. If the populated residual nucleus has a maximal excitation energy $E_x^{max}(Z, N)$ that is still above the separation energies for one or more different particles for that nucleus, further emission of these particles may occur and nuclei with lower Z and N will be populated. At the end of the nuclear reaction (left bottom part of Fig. 3.3), all the reaction population is below the lowest particle separation energy, and the residual nucleus $(Z_C - z, N_C - n)$ can only decay to its ground or isomeric states by means of gamma decay. In a computer program, the continuum must be discretized in excitation energy (E_x) bins. We have taken these bins equidistant, although we already want to stress the important fact here that the *emission* energy grid for the outgoing particles is non-equidistant in TALYS. After the aforementioned binary reaction, every continuum excitation energy bin will be further depleted by means of particle emission, gamma decay or fission. Computationally, this process starts at the initial compound nucleus and its highest energy bin, i.e. the bin just below $E_x^{max}(Z_C, N_C) = E^{tot}$, and subsequently in order of decreasing energy bin/level, decreasing N and decreasing Z. Inside each continuum bin, there is an additional loop over all possible J and Π, whereas for each discrete level, J and Π have unique values. Hence, a bin/level is characterized by the set $\{Z, N, E_x, J, \Pi\}$ and by means of gamma or particle emission, it can decay into all accessible $\{Z', N', E_{x'}, J', \Pi'\}$ bins/levels. In this way, the whole reaction chain is followed until all bins and levels are depleted and thus all channels are closed. In the process, all particle production cross sections and residual production cross sections are accumulated to their final values.

We will now zoom in on the various parts of Fig. 3.3 to describe the various stages of the reaction, depending on the incident energy, and we will mention the nuclear reaction mechanisms that apply.

3.1 Reaction mechanisms

In the projectile energy range between 1 keV and several hundreds of MeV, the importance of a particular nuclear reaction mechanism appears and disappears upon varying the incident energy. We will now describe the particle decay scheme that typically applies in the various energy regions. Because of the Coulomb barrier for charged particles, it will be clear that the discussion for low energy reactions usually

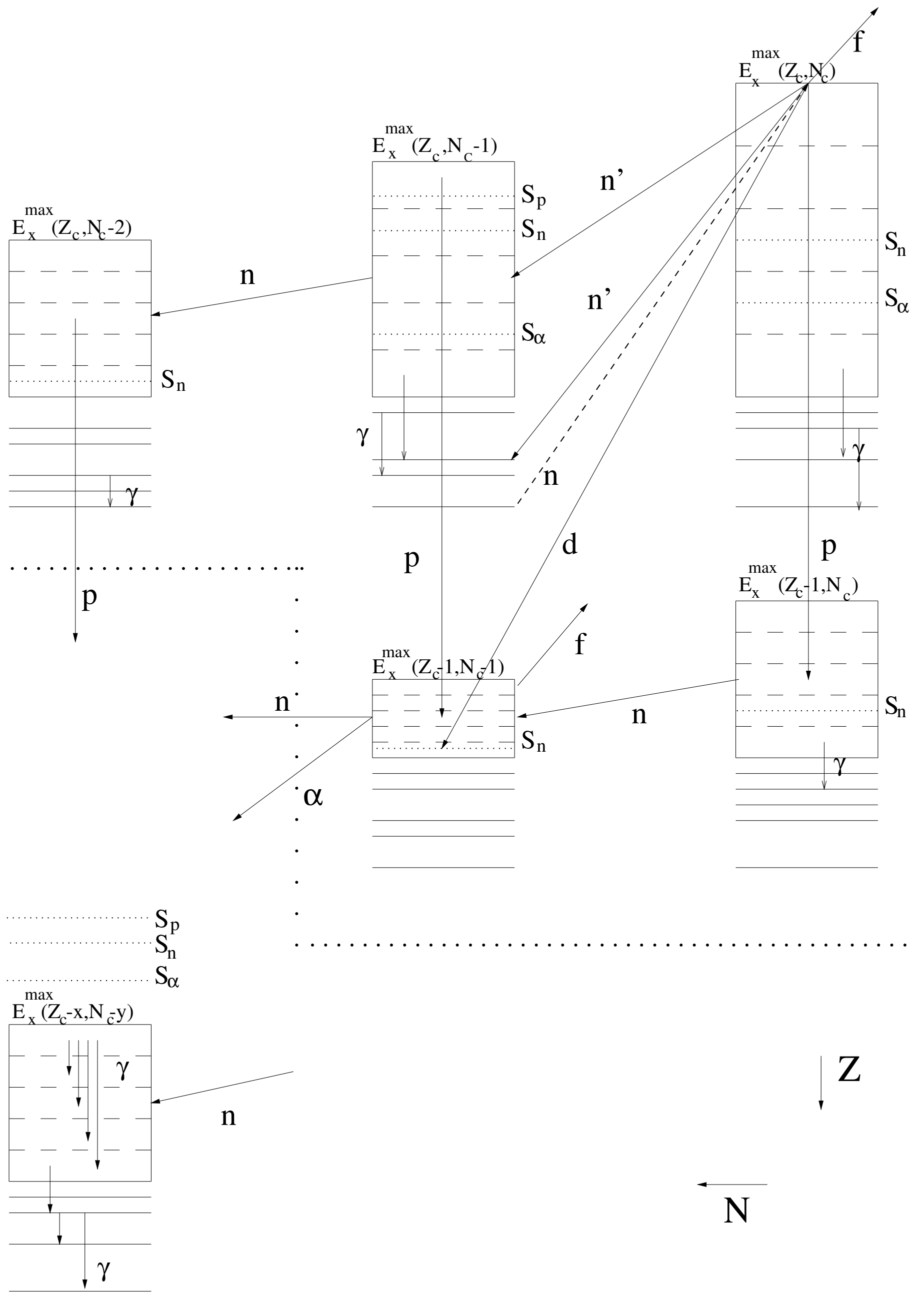

Figure 3.3: Neutron-induced reaction. The dashed arrow represents the incident channel, while the continuous arrows represent the decay possibilities. E_x^{max} denotes the maximal possible excitation energy of each nucleus and S_k is the particle separation energy for particle k. For each nucleus a few discrete levels are drawn, together with a few continuum energy bins. Spin and parity degrees of freedom are left out of this figure for simplicity. Fission is indicated by an f.

concerns incident neutrons. In general, however, what follows can be generalized to incident charged particles. The energy ranges mentioned in each paragraph heading are just meant as helpful indications, which apply for a typical medium mass nucleus.

3.1.1 Low energies

Elastic scattering and capture (E $<$ 0.2 MeV)

If the energy of an incident neutron is below the excitation energy of the first inelastic level, and if there are no (n, p), etc. reactions that are energetically possible, then the only reaction possibilities are elastic scattering, neutron capture and, for fissile nuclides, fission. At these low energies, only the $(Z_C, N_C - 1)$ and (Z_C, N_C) nuclides of Fig. 3.3 are involved, see Fig. 3.4. First, the shape (or direct) elastic scattering cross section can directly be determined from the optical model, which will be discussed in Section 4.1. The compound nucleus, which is populated by a reaction population equal to the reaction cross section, is formed at one single energy $E^{tot} = E_x^{max}(Z_C, N_C)$ and a range of J, Π-values. This compound nucleus either decays by means of compound elastic scattering back to the initial state of the target nucleus, or by means of neutron capture, after which gamma decay follows to the continuum and to discrete states of the compound nucleus. The competition between the compound elastic and capture channels is described by the compound nucleus theory, which we will discuss in Section 4.5. To be precise, the elastic and capture processes comprise the first *binary* reaction. To complete the description of the total reaction, the excited (Z_C, N_C) nucleus, which is populated over its whole excitation energy range by the primary gamma emission, must complete its decay. The highest continuum bin is depleted first, for all J and Π. The subsequent gamma decay increases the population of the lower bins, before the latter are depleted themselves. Also, continuum bins that are above the neutron separation energy S_n of the compound nucleus contribute to the feeding of the $(n, \gamma n)$ channel. This results in a weak continuous neutron spectrum, even though the elastic channel is the only true binary neutron channel that is open. The continuum bins and the discrete levels of the compound nucleus are depleted one by one, in decreasing order, until the ground or an isomeric state of the compound nucleus is reached by subsequent gamma decay. If a nuclide is fissile, fission may compete as well, both from the initial compound state $E_x^{max}(Z_C, N_C)$ and from the continuum bins of the compound nucleus, the latter resulting in a $(n, \gamma f)$ cross section. Both contributions add up to the so called first-chance fission cross section.

Inelastic scattering to discrete states (0.2 $<$ E $<$ 4 MeV)

At somewhat higher incident energies, the first inelastic channels open up, see Fig. 3.5. Reactions to these discrete levels have a compound and a direct component. The former is again described by the compound nucleus theory, while the latter is described by the Distorted Wave Born Approximation (DWBA) for spherical nuclei and by coupled-channels equations for deformed nuclei, see Section 4.2. When the incident energy crosses an inelastic threshold, the compound inelastic contribution rises rapidly and predominates, whereas the direct component increases more gradually. Obviously, the elastic scattering, capture and fission processes described in the previous subsection also apply here. In addition, there is now gamma decay to an isomeric state or the ground state in the target nucleus after inelastic scattering. When there are several, say 10, inelastic levels open to decay, the compound contribution to each individual level is still significant. However, the effect of the width fluctuation correction on the compound

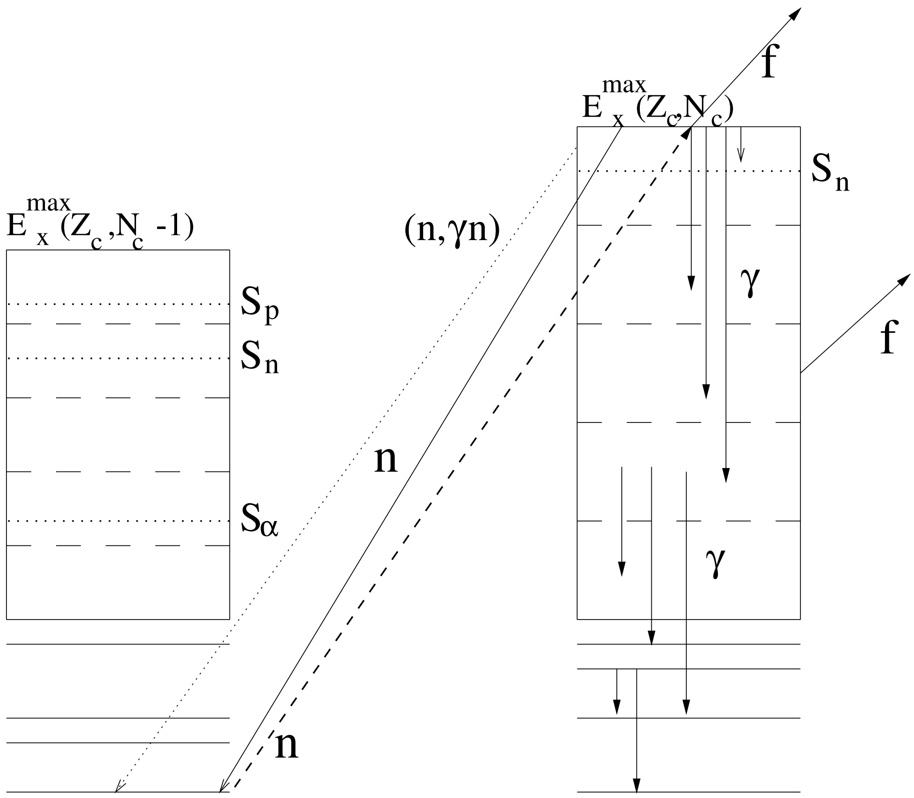

Figure 3.4: Neutron-induced reaction at low energy. The dashed arrow represents the incident channel, while the continuous arrows represents the elastic channel. The only possibilities are elastic scattering and capture of the neutron in the compound nucleus, with subsequent decay to the ground state or an isomeric state of the compound nucleus. A small part of the population may decay to the target nucleus by means of the $(n, \gamma n)$ channel (dotted arrow). For fissile nuclei, fission may be another open channel.

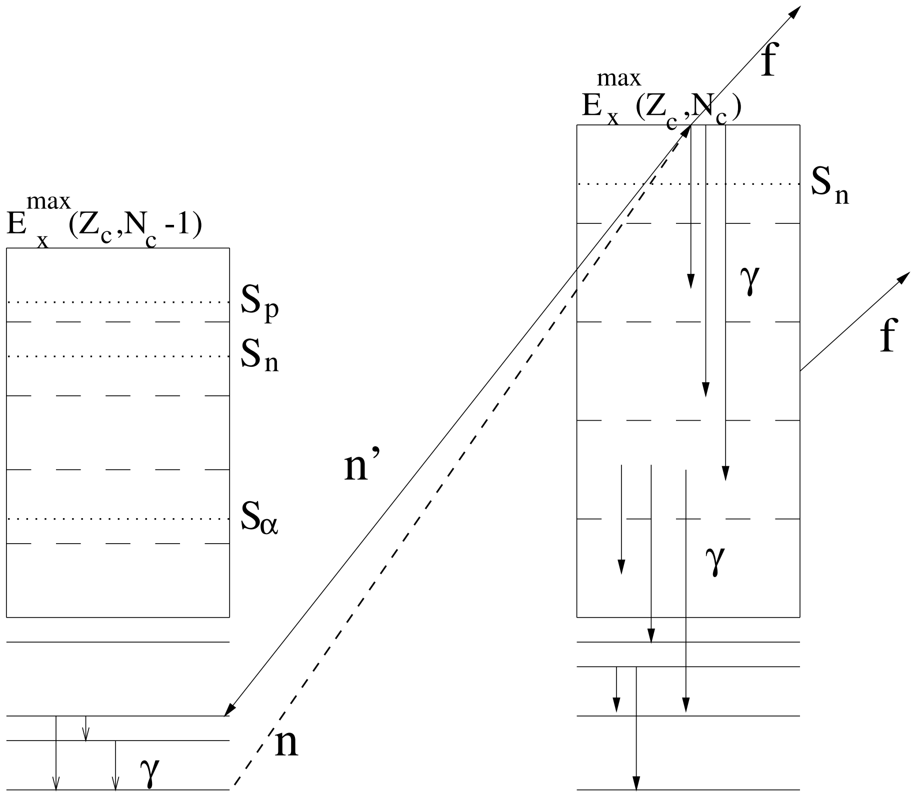

Figure 3.5: Neutron-induced reaction at somewhat higher energy. The dashed arrow represents the incident channel, while the continuous arrows represent the decay possibilities. In addition to the possibilities sketched in the previous figure, there is now inelastic scattering followed by gamma decay in the target nucleus.

cross section is already small in this case, as will be outlined in Section 4.5.

3.1.2 High energies

Pre-equilibrium reactions (E $>$ 4 MeV)

At higher incident energies, inelastic cross sections to both the discrete states and the continuum are possible, see Fig. 3.3. Like reactions to discrete states, reactions to the continuum also have a compound and a direct-like component. The latter are usually described by pre-equilibrium reactions which, by definition, include direct reactions to the continuum. They will be discussed in Section 4.4. Also non-elastic channels to other nuclides, through charge-exchange, e.g. (n,p), and transfer reactions, e.g. (n,α), generally open up at these energies, and decay to these nuclides can take place by the same direct, pre-equilibrium and compound mechanisms. Again, the channels described in the previous subsections also apply here. In addition, gamma decay to ground and isomeric states of all residual nuclides occurs. When many channels open up, particle decay to individual states (e.g. compound elastic scattering) rapidly becomes negligible. For the excitation of a discrete state, the direct component now becomes predominant, since that involves no statistical competition with the other channels. At about 15 MeV, the *total* compound cross section, i.e. summed over all final discrete states and the excited continuum, is however still larger than the summed direct and pre-equilibrium contributions.

Multiple compound emission (E $>$ 8 MeV)

At incident energies above about the neutron separation energy, the residual nuclides formed after the first binary reaction contain enough excitation energy to enable further decay by compound nucleus particle emission or fission. This gives rise to multiple reaction channels such as $(n, 2n)$, (n, np), etc. For higher energies, this picture can be generalized to many residual nuclei, and thus more complex reaction channels, as explained in the introduction of this Chapter, see also Fig. 3.3. If fission is possible, this may occur for all residual nuclides, which is known as multiple chance fission. All excited nuclides will eventually decay to their isomeric and ground states.

Multiple pre-equilibrium emission (E $>$ 40 MeV)

At still higher incident energies, above several tens of MeV, the residual nuclides formed after binary emission may contain so much excitation energy that the presence of further *fast* particles inside the nucleus becomes possible. These can be imagined as strongly excited particle-hole pairs resulting from the first binary interaction with the projectile. The residual system is then clearly non-equilibrated and the excited particle that is high in the continuum may, in addition to the first emitted particle, also be emitted on a short time scale. This so-called multiple pre-equilibrium emission forms an alternative theoretical picture of the intra-nuclear cascade process, whereby now not the exact location and momentum of the particles is followed, but instead the total energy of the system and the number of particle-hole excitations (exciton number). In TALYS, this process can be generalized to any number of multiple pre-equilibrium stages in the reaction by keeping track of all successive particle-hole excitations, see Section 4.6.2. For these incident energies, the binary compound cross section becomes small: the non-elastic cross section is almost completely exhausted by primary pre-equilibrium emission. Again, Fig. 3.3 applies.

3.2 Cross section definitions

In TALYS, cross sections for reactions to all open channels are calculated. Although the types of most of these partial cross sections are generally well known, it is appropriate to define them for completeness. This section concerns basically the book-keeping of the various cross sections, including all the sum rules they obey. The particular nuclear models that are needed to obtain them are described in Chapter 4. Thus, we do not yet give the definition of cross sections in terms of more fundamental quantities. Unless otherwise stated, we use incident neutrons as example in what follows and we consider only photons (γ), neutrons (n), protons (p), deuterons (d), tritons (t), helium-3 particles (h) and alpha particles (α) as competing particles. Also, to avoid an overburdening of the notation and the explanation, we will postpone the competition of fission to the last section of this Chapter.

3.2.1 Total cross sections

The most basic nuclear reaction calculation is that with the optical model, which will be explained in more detail in Section 4.1. Here, it is sufficient to summarize the relations that can be found in many nuclear reaction textbooks, namely that the optical model yields the *reaction cross section* σ_{reac} and, in the case of neutrons, the *total cross section* σ_{tot} and the *shape-elastic cross section* $\sigma_{shape-el}$. They are related by

$$\sigma_{tot} = \sigma_{shape-el} + \sigma_{reac}. \tag{3.2}$$

If the elastic channel is, besides shape elastic scattering, also fed by compound nucleus decay, the latter component is a part of the reaction cross section and is called the *compound elastic cross section* $\sigma_{comp-el}$. With this, we can define the *total elastic cross section* σ_{el},

$$\sigma_{el} = \sigma_{shape-el} + \sigma_{comp-el}, \tag{3.3}$$

and the *non-elastic cross section* σ_{non-el},

$$\sigma_{non-el} = \sigma_{reac} - \sigma_{comp-el}, \tag{3.4}$$

so that we can combine these equations to give

$$\sigma_{tot} = \sigma_{el} + \sigma_{non-el}. \tag{3.5}$$

The last equation contains the quantities that can actually be measured in an experiment. We also note that the competition between the many compound nucleus decay channels ensures that $\sigma_{comp-el}$ rapidly diminishes for incident neutron energies above a few MeV, in which case σ_{non-el} becomes practically equal to σ_{reac}.

A further subdivision of the outcome of a nuclear reaction concerns the breakdown of σ_{non-el}: this cross section contains all the partial cross sections. For this we introduce the exclusive cross sections, from which all other cross sections of interest can be derived.

3.2.2 Exclusive cross sections

In this manual, we call a cross section *exclusive* when the outgoing channel is precisely specified by the type and number of outgoing particles ($+$ any number of photons). Well-known examples are the inelastic or (n, n') cross section and the $(n, 2n)$ cross section, which corresponds with two, *and only* two, neutrons ($+$ accompanying photons) in the outgoing channel. We denote the *exclusive cross section* as $\sigma^{ex}(i_n, i_p, i_d, i_t, i_h, i_\alpha)$, where i_n stands for the number of outgoing neutrons, etc. In this notation, where the incident particle is assumed implicit, e.g. the $(n, 2np)$ cross section is given by $\sigma^{ex}(2, 1, 0, 0, 0, 0)$, for which we will also use the shorthand notation $\sigma_{n,2np}$. For a non-fissile nucleus, the sum over all exclusive cross sections is equal to the non-elastic cross section

$$\sigma_{non-el} = \sum_{i_n=0}^{\infty} \sum_{i_p=0}^{\infty} \sum_{i_d=0}^{\infty} \sum_{i_t=0}^{\infty} \sum_{i_h=0}^{\infty} \sum_{i_\alpha=0}^{\infty} \sigma^{ex}(i_n, i_p, i_d, i_t, i_h, i_\alpha), \tag{3.6}$$

provided we impose that $\sigma^{ex}(1, 0, 0, 0, 0, 0)$ is the exclusive *inelastic* cross section $\sigma_{n,n'}$, i.e. it does not include shape- or compound elastic scattering.

The precise calculation of exclusive cross sections and spectra is a complicated book-keeping problem which, to our knowledge, has not been properly documented. We will describe the exact formalism here. In what follows we use quantities with a prime for daughter nuclides and quantities without a prime for mother nuclides in a decay chain. Consider an excitation energy bin or discrete level E_x in a nucleus (Z,N). Let $P(Z,N,E_x)$ represent the population of this bin/level before it decays. Let $s_k(Z,N,E_x,E_{x'})$ be the part of the population that decays from the (Z,N,E_x) bin/level to the residual $(Z',N',E_{x'})$ bin/level, whereby (Z,N) and (Z',N') are connected through the particle type k, with the index k running from γ-rays up to α-particles. With these definitions, we can link the various residual nuclides while keeping track of all intermediate particle emissions. A special case for the population is the initial compound nucleus (Z_C,N_C), which contains all the initial reaction population at its total excitation energy E_x^{max} (projectile energy + binding energy), i.e.

$$P(Z_C,N_C,E_x^{max}) = \sigma_{non-el}, \tag{3.7}$$

while all other population bins/levels are zero. For the initial compound nucleus, $s_k(Z_C,N_C,E_x^{max},E_{x'})$ represents the binary feeding to the excitation energy bins of the first set of residual nuclides. This term generally consists of direct, pre-equilibrium and compound components.

The population of any bin in the decay chain is equal to the sum of the decay parts for all particles that can reach this bin from the associated mother bins, i.e.

$$P(Z',N',E_{x'}(i')) = \sum_{k=\gamma,n,p,d,t,h,\alpha} \sum_i s_k(Z,N,E_x(i),E_{x'}(i')), \tag{3.8}$$

where the sum over i runs over discrete level and continuum energy bins in the energy range from $E_{x'}(i')+S_k$ to $E_x^{max}(Z,N)$, where S_k is the separation energy of particle k so that the sum only includes decay that is energetically allowed, and $E_x^{max}(Z,N)$ is the maximum possible excitation energy of the (Z,N) nucleus. Note again that the particle type k determines (Z,N).

To obtain the exclusive cross sections, we need to start with the initial compound nucleus and work our way down to the last nucleus that can be reached. First, consider a daughter nucleus (Z',N') somewhere in the reaction chain. We identify all exclusive channels $(i_n,i_p,i_d,i_t,i_h,i_\alpha)$ that lead to this residual (Z',N') nucleus, i.e. all channels that satisfy

$$\begin{aligned} i_n + i_d + 2i_t + i_h + 2i_\alpha &= N_C - N' \\ i_p + i_d + i_t + 2i_h + 2i_\alpha &= Z_C - Z'. \end{aligned} \tag{3.9}$$

For each of these channels, the *inclusive* cross section per excitation energy bin S is equal to the sum of the feeding from all possible mother bins, i.e.

$$\begin{aligned} S(i_n,i_p,i_d,i_t,i_h,i_\alpha,E_{x'}(i')) &= \sum_{k=\gamma,n,p,d,t,h,\alpha} \sum_i \frac{s_k(Z,N,E_x(i),E_{x'}(i'))}{P(Z,N,E_x(i))} \\ \times \quad & S(i_n-\delta_{nk},i_p-\delta_{pk},i_d-\delta_{dk},i_t-\delta_{tk},i_h-\delta_{hk},i_\alpha-\delta_{\alpha k},E_x(i)), \end{aligned} \tag{3.10}$$

where we introduce Kronecker delta's, with characters as subscript, as

$$\begin{aligned} \delta_{nk} &= 1 \text{ if } k=n \text{ (neutron)} \\ &= 0, \text{ otherwise} \end{aligned} \tag{3.11}$$

and similarly for the other particles. Note that S is still inclusive in the sense that it is not yet depleted for further decay. The summation runs over the excitation energies of the mother bin from which decay into the $E_{x'}(i')$ bin of the residual nucleus is energetically allowed. Feeding by gamma decay from bins above the $(Z', N', E_{x'}(i'))$ bin is taken into account by the $k = \gamma$ term, in which case all of the Kronecker delta's are zero.

With Eq. (3.7) as initial condition, the recursive procedure is completely defined. For a fixed nucleus, Eq. (3.10) is calculated for all excitation energy bins, in decreasing order, until the remaining population is in an isomeric or the ground state of the nucleus. When there is no further decay possible, the exclusive cross section per ground state/isomer, numbered by i, can be identified,

$$\sigma_i^{ex}(i_n, i_p, i_d, i_t, i_h, i_\alpha) = S(i_n, i_p, i_d, i_t, i_h, i_\alpha, E_i). \tag{3.12}$$

The total exclusive cross section for a particular channel is then calculated as

$$\sigma^{ex}(i_n, i_p, i_d, i_t, i_h, i_\alpha) = \sum_{i=0,isomers} \sigma_i^{ex}(i_n, i_p, i_d, i_t, i_h, i_\alpha). \tag{3.13}$$

The procedure outlined above automatically sorts and stores all exclusive cross sections, irrespective of the order of particle emission within the reaction chain. For example, the (n, np) and (n, pn) channels are automatically added. The above formalism holds *exactly* for an arbitrary number of emitted particles.

We stress that keeping track of the excitation energy E_x throughout this formalism is essential to get the exact exclusive cross sections for two reasons:

(i) the exact determination of the branching ratios for exclusive isomeric ratios. The isomeric ratios for different exclusive reactions that lead to the same residual product, e.g. (n, np) and (n, d), both leading to $(Z_C - 1, N_C - 1)$, are generally different from each other and thus also from the isomeric ratios of the total residual product. Hence, it would be an approximation to apply isomeric branching ratios for residual products, obtained after the full reaction calculation, a posteriori on the exclusive channels. This is avoided with our method,

(ii) the exclusive spectra, which we will explain in Section 3.3.2.

Suppose one would only be interested in the total exclusive cross sections of Eq. (3.13), i.e. neither in the exclusive isomeric ratios, nor in the exclusive spectra. Only in that case, a simpler method would be sufficient. Since only the total reaction population that decays from nucleus to nucleus needs to be tracked, the total exclusive cross section for a certain channel is easily determined by subtracting the total ongoing flux from the total feeding flux to this channel. This is described in e.g. Section II.E.f of the GNASH manual[51]. We note that the exact treatment of TALYS does not require a large amount of computing time, certainly not when compared with more time-expensive parts of the full calculation.

When TALYS computes the binary reaction models and the multiple pre-equilibrium and Hauser-Feshbach models, it stores both $P(Z, N, E_x)$ (through the **popexcl** array) and $s_k(Z, N, E_x, E_{x'})$ (through the **feedexcl** array) for all residual nuclei and particles. This temporary storage enables us to first complete the full reaction calculation, including all its physical aspects, until all channels are closed. Then, we turn to the exclusive cross section and spectra problem afterwards in a separate subroutine: *channels.f*. It is thus considered as an isolated book-keeping problem.

The total number of different exclusive channels rapidly increases with the number of reaction stages. It can be shown that for m outgoing particles (i.e. reaction stages) which can be of k different types, the maximum number of exclusive cross sections is $\binom{m+k-1}{m}$. In general, we include neutrons up to alpha-particles as competing particles, i.e. $k = 6$, giving $\binom{m+5}{m}$ possible exclusive channels, or 6, 21, 56 and 126, respectively, for the first 4 stages. This clarifies why exclusive channels are usually only of interest for only a few outgoing particles (the ENDF format for evaluated data libraries includes reactions up to 4 particles). At higher energies, and thus more outgoing particles, exclusive cross sections loose their relevance and the cross sections per channel are usually accumulated in the total particle production cross sections and residual production cross sections. Certainly at higher energies, this apparent loss of information is no longer an issue, since the observable quantities to which nuclear models can be tested are of a cumulative nature anyway, when many particles are involved.

In TALYS, the cumulated particle production cross sections and residual production cross sections are always *completely* tracked down until all residual nuclides have decayed to an isomer or the ground state, regardless of the incident energy, whereas exclusive cross sections are only tracked up to a user-defined depth. To elucidate this important point we discuss the low and the high energy case. For low energies, say up to 20 MeV, keeping track of the exclusive cross section is important from both the fundamental and the applied point of view. It can be imagined that in a (n, np) measurement both the emitted neutron and proton have been measured in the detector. Hence the cross section is *not* the same as that of an activation measurement of the final residual nucleus, since the latter would also include a contribution from the (n, d) channel. Another example is the $(n, 2n)$ channel, distinguished from the (n, n') or the general (n, xn) cross section, which is of importance in some integral reactor benchmarks. If, on the other hand, we encounter in the literature a cross section of the type ^{120}Sn$(p, 7p18n)^{96}$Ru, we can be sure that the residual product ^{96}Ru was measured and not the indicated number of neutrons and protons in a detector. The $(p, 7p18n)$ symbol merely represents the number of neutron and proton units, while other light ions are generally included in the emission channel. Hence, for high energies the outcome of a nuclear reaction is usually tracked in parallel by two sets of quantities: the $(proj, xn), \ldots (proj, x\alpha)$ particle production cross sections and spectra, and the residual production cross sections. These will be exactly defined in the next sections.

3.2.3 Binary cross sections

Some of the exclusive channels need, and get, more attention than others. The exclusive binary cross sections, for reactions that are characterized by one, and only one, particle out, are special in the sense that they comprise both discrete and continuous energy transitions. Inelastic scattering can occur through both direct collective and compound transitions to the first few excited levels and through pre-equilibrium and compound reactions to the continuum. Let us assume that for a target nucleus the basic structure properties (spin, parity, deformation parameters) of the first N levels are known. Then, the *inelastic cross section*, $\sigma_{n,n'}$ is the sum of a *total discrete inelastic cross section* $\sigma^{disc}_{n,n'}$ and a *continuum inelastic cross section* $\sigma^{cont}_{n,n'}$

$$\sigma_{n,n'} = \sigma^{disc}_{n,n'} + \sigma^{cont}_{n,n'}, \tag{3.14}$$

where $\sigma^{disc}_{n,n'}$ is the sum over the inelastic cross sections for all the individual discrete states

$$\sigma^{disc}_{n,n'} = \sum_{i=1}^{N} \sigma^{i}_{n,n'}. \tag{3.15}$$

A further breakdown of each term is possible by means of reaction mechanisms. The inelastic cross section for each individual state i has a direct and a compound contribution:

$$\sigma^{i}_{n,n'} = \sigma^{i,direct}_{n,n'} + \sigma^{i,comp}_{n,n'}, \tag{3.16}$$

where the direct component comes from DWBA or coupled-channels calculations. Similarly, for the inelastic scattering to the continuum we can consider a pre-equilibrium and a compound contribution

$$\sigma^{cont}_{n,n'} = \sigma^{\mathrm{PE}}_{n,n'} + \sigma^{cont,comp}_{n,n'}. \tag{3.17}$$

The set of definitions (3.14-3.17) can be given in a completely analogous way for the other binary channels $\sigma_{n,p}$, i.e. $\sigma^{ex}(0,1,0,0,0,0)$, $\sigma_{n,d}$, $\sigma_{n,t}$, $\sigma_{n,h}$ and $\sigma_{n,\alpha}$. For the depletion of the reaction population that goes into the pre-equilibrium channels, which will be discussed in Section 4.4, it is helpful to define here the *total discrete direct cross section*,

$$\sigma^{disc,direct} = \sum_{i} \sum_{k=n',p,d,t,h,\alpha} \sigma^{i,direct}_{n,k}. \tag{3.18}$$

Finally, we also consider an alternative division for the non-elastic cross section. It is equal to the sum of the *inclusive* binary cross sections

$$\sigma_{non-el} = \sum_{k=\gamma,n',p,d,t,h,\alpha} \sigma^{inc,bin}_{n,k}, \tag{3.19}$$

where again at the present stage of the outline we do not consider fission and ejectiles heavier than α-particles. This is what we actually use in the inclusive nuclear reaction calculations. With the direct, pre-equilibrium and compound models, several residual nuclides can be formed after the binary reaction, with a total population per nucleus that is equal to the terms of Eq. (3.19). The residual nuclides then decay further until all channels are closed. Note that $\sigma^{inc,bin}$ is not a "true" cross section in the sense of a quantity for a final combination of a product and light particle(s).

3.2.4 Total particle production cross sections

Especially for incident energies higher than about 10 MeV, it is appropriate to define the composite or *total neutron production cross section*, $\sigma_{n,xn}$. It can be expressed in terms of the exclusive cross sections as follows

$$\sigma_{n,xn} = \sum_{i_n=0}^{\infty} \sum_{i_p=0}^{\infty} \sum_{i_d=0}^{\infty} \sum_{i_t=0}^{\infty} \sum_{i_h=0}^{\infty} \sum_{i_\alpha=0}^{\infty} i_n \sigma^{ex}(i_n, i_p, i_d, i_t, i_h, i_\alpha), \tag{3.20}$$

i.e. in the more common notation,

$$\sigma_{n,xn} = \sigma_{n,n'} + 2\sigma_{n,2n} + \sigma_{n,np} + 2\sigma_{n,2np} + ... \tag{3.21}$$

Again, $\sigma_{n,xn}$ is not a true cross section since the incident and outgoing channels are not exactly defined by its individual reaction components. (Contrary to our definition, in some publications $\sigma_{n,xn}$ is used to indicate activation measurements of a whole string of isotopes (e.g. $^{202-208}$Pb) in which case x is a number that varies case by case. In our work, this is called an exclusive cross section). The *neutron multiplicity*, or *yield*, Y_n is defined as

$$Y_n = \frac{\sigma_{n,xn}}{\sigma_{non-el}}. \tag{3.22}$$

Similarly, the *total proton production cross section*, $\sigma_{n,xp}$ is defined as

$$\sigma_{n,xp} = \sum_{i_n=0}^{\infty}\sum_{i_p=0}^{\infty}\sum_{i_d=0}^{\infty}\sum_{i_t=0}^{\infty}\sum_{i_h=0}^{\infty}\sum_{i_\alpha=0}^{\infty} i_p \sigma^{ex}(i_n, i_p, i_d, i_t, i_h, i_\alpha), \tag{3.23}$$

and the proton multiplicity, or yield, Y_p is defined as

$$Y_p = \frac{\sigma_{n,xp}}{\sigma_{non-el}}, \tag{3.24}$$

and similarly for the other particles. We note that we do not, in practice, use Eq. (3.20) to calculate the composite particle production cross section. Instead, we first calculate the inclusive binary cross section of Eq. (3.19) and then, during the depletion of each residual nucleus by further decay we directly add the reaction flux, equal to the $s_k(Z, N, E_x, E_{x'})$ term of Eq. (3.8), to $\sigma_{n,xn}$, $\sigma_{n,xp}$, etc. This procedure has already been sketched in the multiple decay scheme at the beginning of this Chapter. In the output of TALYS, we include Eq. (3.20) only as a numerical check. For a few outgoing particles Eq. (3.20) should exactly hold. For higher energies and thus more outgoing particles (typically more than 4, see the **maxchannel** keyword on page 140) the exclusive cross sections are no longer tracked by TALYS and Eq. (3.20) can no longer be expected to hold numerically. Remember, however, that we always calculate the total particle production cross sections, irrespective of the number of outgoing particles, since we continue the multiple emission calculation until all residual nuclides are in their isomeric or ground states.

3.2.5 Residual production cross sections

We can define another important type of derived cross section using the exclusive cross section, namely the residual production cross section σ_{prod}. All exclusive cross sections with the same number of neutron and proton units in the outgoing channel sum up to the same residual nucleus production cross section for the final nucleus (Z, N), i.e.

$$\sigma_{prod}(Z,N) = \sum_{i_n=0}^{\infty}\sum_{i_p=0}^{\infty}\sum_{i_d=0}^{\infty}\sum_{i_t=0}^{\infty}\sum_{i_h=0}^{\infty}\sum_{i_\alpha=0}^{\infty} \sigma^{ex}(i_n, i_p, i_d, i_t, i_h, i_\alpha)\delta_N\delta_Z, \tag{3.25}$$

where the Kronecker delta's are defined by

$$\begin{aligned} \delta_N &= 1 \text{ if } i_n + i_d + 2i_t + i_h + 2i_\alpha = N_C - N \\ &= 0 \text{ otherwise} \\ \delta_Z &= 1 \text{ if } i_p + i_d + i_t + 2i_h + 2i_\alpha = Z_C - Z \\ &= 0 \text{ otherwise,} \end{aligned} \tag{3.26}$$

where the first compound nucleus that is formed from the projectile and target nucleus is denoted by (Z_C, N_C). As an example, consider the $n+ {}^{56}\text{Fe} \rightarrow {}^{54}\text{Mn} + x$ reaction. The exclusive cross sections that add up to the ^{54}Mn production cross section are $\sigma_{n,2np}$, $\sigma_{n,nd}$, and $\sigma_{n,t}$, or $\sigma^{ex}(2,1,0,0,0,0)$, $\sigma^{ex}(1,0,1,0,0,0)$, and $\sigma^{ex}(0,0,0,1,0,0)$, respectively.

Since all exclusive cross sections contribute to the residual production cross section for one nuclide (Z, N) only, Eq. (3.6) automatically implies

$$\sigma_{non-el} = \sum_Z \sum_N \sigma_{prod}(Z, N). \tag{3.27}$$

Similar to Eq. (3.13), Eq. (3.25) is separated per isomer

$$\sigma_{prod,i}(Z, N) = \sum_{i_n=0}^{\infty} \sum_{i_p=0}^{\infty} \sum_{i_d=0}^{\infty} \sum_{i_t=0}^{\infty} \sum_{i_h=0}^{\infty} \sum_{i_\alpha=0}^{\infty} \sigma_i^{ex}(i_n, i_p, i_d, i_t, i_h, i_\alpha)\delta_N \delta_Z, \tag{3.28}$$

and the equivalent of Eq. (3.13) is

$$\sigma_{prod}(Z, N) = \sum_{i=0,isomers} \sigma_{prod,i}(Z, N). \tag{3.29}$$

Also here, we do not calculate σ_{prod} and $\sigma_{prod,i}$ using Eqs. (3.25) and (3.28), although optionally TALYS includes it as a numerical check in the output for residual nuclides close to the target. Analogous to the total particle production, we determine the residual production cross section, for both the isomers and the ground state, after the complete decay of each nucleus by means of an inclusive calculation.

3.3 Spectra and angular distributions

In addition to cross sections, TALYS also predicts energy spectra, angular distributions and energy-angle distributions.

3.3.1 Discrete angular distributions

The elastic angular distribution $\frac{d\sigma^{el}}{d\Omega}$ has a direct and a compound component:

$$\frac{d\sigma^{el}}{d\Omega} = \frac{d\sigma^{shape-el}}{d\Omega} + \frac{d\sigma^{comp-el}}{d\Omega}, \tag{3.30}$$

where the shape-elastic part comes directly from the optical model while the compound part comes from compound nucleus theory, namely Eq. (4.170). An analogous relation holds for inelastic scattering to a single discrete state i

$$\frac{d\sigma^i_{n,n'}}{d\Omega} = \frac{d\sigma^{i,direct}_{n,n'}}{d\Omega} + \frac{d\sigma^{i,compound}_{n,n'}}{d\Omega}, \tag{3.31}$$

where the direct component comes from DWBA or coupled-channels calculations. For charge exchange, we can write

$$\frac{d\sigma^i_{n,p}}{d\Omega} = \frac{d\sigma^{i,direct}_{n,p}}{d\Omega} + \frac{d\sigma^{i,compound}_{n,p}}{d\Omega} \tag{3.32}$$

and analogous expressions can be written for the other binary reactions (n, d), etc.

Of course, the integration over solid angle of every angular distribution defined here must be equal to the corresponding cross section, e.g.

$$\sigma^{i,direct}_{n,n'} = \int d\Omega \frac{d\sigma^{i,direct}_{n,n'}}{d\Omega}. \tag{3.33}$$

In the output of TALYS, we use a representation in terms of outgoing angle and one in terms of Legendre coefficients, i.e. Eq. (3.30) can also be written as

$$\frac{d\sigma^{el}}{d\Omega} = \sum_L (C_L^{shape-el} + C_L^{comp-el}) P_L(\cos\Theta), \tag{3.34}$$

where P_L are Legendre polynomials. For inelastic scattering we have

$$\frac{d\sigma^i_{n,n'}}{d\Omega} = \sum_L (C_L^{i,direct} + C_L^{i,comp}) P_L(\cos\Theta), \tag{3.35}$$

and similarly for the other binary channels. The Legendre expansion is required for the storage of the results in ENDF data libraries.

3.3.2 Exclusive spectra

An exclusive spectrum is not only specified by the exact number of emitted particles, but also by their outgoing energies.

In TALYS, exclusive spectra are calculated in the same loops that take care of the exclusive cross sections. The inclusive continuum spectra are obtained by taking the derivative of the inclusive cross sections per excitation energy of Eq. (3.10) with respect to the outgoing particle energy $E_{k'}$,

$$E_{k'} = E_x - E_{x'}(i') - S_{k'}, \tag{3.36}$$

where $S_{k'}$ is the separation energy for outgoing particle k'. Note that since the inclusive cross section per excitation energy S depends on $E_{k'}$ via s_k, the product rule of differentiation applies to Eq. (3.10). Therefore, the inclusive spectrum per excitation energy for an outgoing particle k' of a given $(i_n, i_p, i_d, i_t, i_h, i_\alpha)$ channel is

$$\begin{aligned}
&\frac{dS}{dE_{k'}}(i_n, i_p, i_d, i_t, i_h, i_\alpha, E_{x'}(i')) = \sum_{k=\gamma,n,p,d,t,h,\alpha} \sum_i \\
&[\frac{s_k(Z,N,E_x(i),E_{x'}(i'))}{P(Z,N,E_x(i))} \frac{dS}{dE_{k'}}(i_n-\delta_{nk}, i_p-\delta_{pk}, i_d-\delta_{dk}, i_t-\delta_{tk}, i_h-\delta_{hk}, i_\alpha-\delta_{\alpha k}, E_x(i)) \\
+ \quad &\delta_{kk'} \frac{ds_k(Z,N,E_x(i),E_{x'}(i'))}{dE_{k'}} \frac{S(i_n-\delta_{nk}, i_p-\delta_{pk}, i_d-\delta_{dk}, i_t-\delta_{tk}, i_h-\delta_{hk}, i_\alpha-\delta_{\alpha k}, E_x(i))}{P(Z,N,E_x(i))}],
\end{aligned} \tag{3.37}$$

where, as initial condition, the derivatives of $s_k(Z_C, N_C, E_x^{max}, E_{x'}(i'))$ are the binary emission spectra. The first term on the right-hand side corresponds to the spectrum of the feeding channel and the second term denotes the contribution of the last emitted particle. The calculation of Eq. (3.37) can be done simultaneously with the exclusive cross section calculation, i.e. we follow exactly the same recursive procedure. The final exclusive spectrum for outgoing particle k' is given by

$$\frac{d\sigma^{ex}}{dE_{k'}}(i_n, i_p, i_d, i_t, i_h, i_\alpha) = \sum_{i=0,isomers} \frac{dS}{dE_{k'}}(i_n, i_p, i_d, i_t, i_h, i_\alpha, E_i), \tag{3.38}$$

The terms on the right hand side are the exclusive spectra per ground state or isomer. The latter naturally result from our method, even though only the total exclusive spectra of the left hand side are of interest.

We stress that for a given $(i_n, i_p, i_d, i_t, i_h, i_\alpha)$ channel, Eq. (3.37) is calculated for *every* outgoing particle k' (i.e. n, p, d, t, h and α). Hence, e.g. the $(n, 2np\alpha)$ channel is characterized by only one exclusive cross section, $\sigma_{n,2np\alpha}$, but by three spectra, one for outgoing neutrons, protons and alpha's, respectively, whereby all three spectra are constructed from components from the first up to the fourth particle emission (i.e. the α can have been emitted in each of the four stages). In practice, this means that all spectra have a first order pre-equilibrium component (and for higher energies also higher order pre-equilibrium components), and a compound component from multiple emission. Upon integration over outgoing energy, the exclusive cross sections may be obtained,

$$\sigma^{ex}(i_n, i_p, i_d, i_t, i_h, i_\alpha) = \frac{1}{i_n + i_p + i_d + i_t + i_h + i_\alpha} \sum_{k'=n,p,d,t,h,\alpha} \int dE_{k'} \frac{d\sigma^{ex}}{dE_{k'}}(i_n, i_p, i_d, i_t, i_h, i_\alpha). \tag{3.39}$$

3.3.3 Binary spectra

Similar to the cross sections, the exclusive spectra determine various other specific spectra of interest. The exclusive *inelastic spectrum* is a special case of Eq. (3.38)

$$\frac{d\sigma_{n,n'}}{dE_{n'}} = \frac{d\sigma^{ex}}{dE_{n'}}(1, 0, 0, 0, 0, 0). \tag{3.40}$$

Since Eq. (3.37) represents an energy spectrum, it includes by definition only continuum transitions, i.e. it does not include the binary reactions to discrete states. Hence, upon integration, Eq. (3.40) only gives the continuum inelastic cross section of Eq. (3.14):

$$\sigma^{cont}_{n,n'} = \int dE_{n'} \frac{d\sigma_{n,n'}}{dE_{n'}}. \tag{3.41}$$

Similar relations hold for the binary (n,p), (n,d), (n,t), (n,h) and (n,α) spectra. The contributions to the binary spectra generally come from pre-equilibrium and continuum compound spectra.

3.3.4 Total particle production spectra

Similar to the total particle production cross sections, the *composite* or *total neutron spectrum* can be expressed in terms of exclusive spectra as follows

$$\frac{d\sigma_{n,xn}}{dE_{n'}} = \sum_{i_n=0}^{\infty} \sum_{i_p=0}^{\infty} \sum_{i_d=0}^{\infty} \sum_{i_t=0}^{\infty} \sum_{i_h=0}^{\infty} \sum_{i_\alpha=0}^{\infty} \frac{d\sigma^{ex}}{dE_{n'}}(i_n, i_p, i_d, i_t, i_h, i_\alpha), \tag{3.42}$$

i.e. in the other notation,

$$\frac{d\sigma_{n,xn}}{dE_{n'}} = \frac{d\sigma_{n,n'}}{dE_{n'}} + \frac{d\sigma_{n,2n}}{dE_{n'}} + \frac{d\sigma_{n,np}}{dE_{n'}} + \frac{d\sigma_{n,2np}}{dE_{n'}} + ... \tag{3.43}$$

Similar relations hold for the (n, xp), etc. spectra. Note that, in contrast with Eq. (3.20), the multiplicity is already implicit in the exclusive spectra.

Again, in practice we do not use Eq. (3.42) to calculate the composite spectra but instead add the $ds_k(Z, N, E_x, E_{x'})/dE_{k'}$ term that appears in Eq. (3.37) to the composite spectra while depleting all nuclides in an inclusive calculation. We do use Eq. (3.42) as a numerical check in the case of a few outgoing particles. Finally, integration of the total neutron spectrum and addition of the binary discrete cross section gives the total particle production cross section

$$\sigma_{n,xn} = \int dE_{n'} \frac{d\sigma_{n,xn}}{dE_{n'}} + \sigma^{disc}_{n,n'}, \tag{3.44}$$

and similarly for the other particles.

3.3.5 Double-differential cross sections

The generalization of the exclusive spectra to angular dependent cross sections is done by means of the exclusive double-differential cross sections

$$\frac{d^2\sigma^{ex}}{dE_{k'}d\Omega}(i_n, i_p, i_d, i_t, i_h, i_\alpha), \tag{3.45}$$

which are obtained by either physical models or systematics. Integration over angles yields the exclusive spectrum

$$\frac{d\sigma^{ex}}{dE_{k'}}(i_n, i_p, i_d, i_t, i_h, i_\alpha) = \int d\Omega \frac{d^2\sigma^{ex}}{dE_{k'}d\Omega}(i_n, i_p, i_d, i_t, i_h, i_\alpha). \tag{3.46}$$

The other relations are analogous to those of the spectra, e.g. the inelastic double-differential cross section for the continuum is

$$\frac{d^2\sigma_{n,n'}}{dE_{n'}d\Omega} = \frac{d^2\sigma^{ex}}{dE_{n'}d\Omega}(1, 0, 0, 0, 0, 0), \tag{3.47}$$

and the total neutron double-differential cross section can be expressed as

$$\frac{d^2\sigma_{n,xn}}{dE_{n'}d\Omega} = \sum_{i_n=0}^{\infty}\sum_{i_p=0}^{\infty}\sum_{i_d=0}^{\infty}\sum_{i_t=0}^{\infty}\sum_{i_h=0}^{\infty}\sum_{i_\alpha=0}^{\infty} \frac{d^2\sigma^{ex}}{dE_{n'}d\Omega}(i_n, i_p, i_d, i_t, i_h, i_\alpha). \tag{3.48}$$

For the *exclusive* calculation, the angular information is only tracked for the first particle emission. The reason is that for incident energies up to about 20 to 30 MeV, only the first emitted particle deviates from an isotropic angular distribution. Multiple compound emission to the continuum is essentially isotropic. The isotropic contribution to the exclusive double-differential spectrum is then simply determined by the part of the corresponding cross section that comes from Hauser-Feshbach decay. At higher incident energies, where the approximation of only one forward-peaked particle becomes incorrect, the interest in exclusive spectra, or for that matter, the computational check of Eq. (3.48), is no longer there. The presence of multiple pre-equilibrium emission at energies above several tens of MeV requires that we include angular information for every emitted particle in the *total* double-differential cross section, i.e. the left-hand side of Eq. (3.48). Again, this is all tracked correctly in the full inclusive calculation.

3.4 Fission cross sections

For clarity, we have kept the fission channel out of the discussion so far. The generalization to a picture in which fission is possible is however not too difficult. For fissile nuclides, the first expression that needs generalization is that of the non-elastic cross section expressed as a sum of exclusive cross sections, Eq. (3.6). It should read

$$\sigma_{non-el} = \sum_{i_n=0}^{\infty}\sum_{i_p=0}^{\infty}\sum_{i_d=0}^{\infty}\sum_{i_t=0}^{\infty}\sum_{i_h=0}^{\infty}\sum_{i_\alpha=0}^{\infty} \sigma^{ex}(i_n, i_p, i_d, i_t, i_h, i_\alpha) + \sigma_f, \tag{3.49}$$

where the *total fission* cross section σ_f is the sum over exclusive fission cross sections

$$\sigma_f = \sum_{i_n=0}^{\infty}\sum_{i_p=0}^{\infty}\sum_{i_d=0}^{\infty}\sum_{i_t=0}^{\infty}\sum_{i_h=0}^{\infty}\sum_{i_\alpha=0}^{\infty} \sigma_f^{ex}(i_n, i_p, i_d, i_t, i_h, i_\alpha), \tag{3.50}$$

where $\sigma_f^{ex}(i_n, i_p, i_d, i_t, i_h, i_\alpha)$ represents the cross section for fissioning *after* the emission of i_n neutrons, i_p protons, etc. Well-known special cases are $\sigma_{n,f} = \sigma_f^{ex}(0,0,0,0,0,0)$, $\sigma_{n,nf} = \sigma_f^{ex}(1,0,0,0,0,0)$ and $\sigma_{n,2nf} = \sigma_f^{ex}(2,0,0,0,0,0)$, which are also known as first-chance, second-chance and third-chance fission cross section, respectively. Eq. (3.50) is more general in the sense that it also includes cases where particles other than neutrons can be emitted before the residual nucleus fissions, e.g. (n, npf), which may occur at higher incident energies.

The generalization of the non-elastic cross section of Eq. (3.19) is

$$\sigma_{non-el} = \sum_{k=\gamma,n',p,d,t,h,\alpha} \sigma_{n,k}^{inc,bin} + \sigma_f^{bin}, \tag{3.51}$$

where σ_f^{bin} represents fission from the initial compound state (i.e. excluding $(n,\gamma f)$ processes).

Analogous to Eq. (3.25), we can define a cross section for each fissioning residual product

$$\sigma_{prod}^{fis}(Z,N) = \sum_{i_n=0}^{\infty}\sum_{i_p=0}^{\infty}\sum_{i_d=0}^{\infty}\sum_{i_t=0}^{\infty}\sum_{i_h=0}^{\infty}\sum_{i_\alpha=0}^{\infty} \sigma_f^{ex}(i_n, i_p, i_d, i_t, i_h, i_\alpha)\delta_N\delta_Z. \tag{3.52}$$

At higher energies, the meaning of $\sigma_{prod}^{fis}(Z,N)$ is more relevant than the exclusive fission cross sections. Consequently, for the total fission cross section we have

$$\sigma_f = \sum_Z\sum_N \sigma_{prod}^{fis}(Z,N). \tag{3.53}$$

What remains to be explained is how σ_f^{ex} is computed. First, we need to add to Eq. (3.8) a term we denote by $s_f(Z,N,E_x(i))$, which is the part of the population that fissions from the $(Z,N,E_x(i))$ bin. Hence, for fissile nuclides we have

$$P(Z,N,E_x(i)) = s_f(Z,N,E_x(i)) + \sum_{k=\gamma,n,p,d,t,h,\alpha}\sum_i s_k(Z,N,E_x(i),E_{x'}(i')). \tag{3.54}$$

where in this case the sum over i runs over discrete levels and continuum bins from 0 to $E_x(i) - S_k$. The exclusive fission cross section σ_f^{ex} is

$$\sigma_f^{ex}(i_n, i_p, i_d, i_t, i_h, i_\alpha) = \sum_i \frac{s_f(Z,N,E_x(i))}{P(Z,N,E_x(i))} S(i_n, i_p, i_d, i_t, i_h, i_\alpha, E_x(i)). \tag{3.55}$$

where i runs from 0 to $E_x^{max}(Z,N)$. The rest of the calculation of the exclusive particle cross section proceeds exactly as before. Eq. (3.10) is now automatically depleted from the fission cross section (3.55), in the sense that the s_k terms alone, summed over γ and particles only, no longer add up to the population P.

Finally, the exclusive fission cross sections are also accompanied by spectra. For example, the first two neutrons emitted in the $(n, 2nf)$ channel (third-chance fission) are described by an outgoing neutron spectrum. The exclusive spectrum of outgoing particle k' in a fission channel is

$$\frac{d\sigma_f^{ex}}{dE_{k'}}(i_n, i_p, i_d, i_t, i_h, i_\alpha) = \sum_i \frac{s_f(Z, N, E_x(i))}{P(Z, N, E_x(i))} \frac{dS}{dE_{k'}}(i_n, i_p, i_d, i_t, i_h, i_\alpha), \tag{3.56}$$

while the exclusive particle spectra are again described by Eq. (3.37). For double-differential spectra, the usual generalization holds. We also repeat here that the total (observable) fission cross section is always calculated by letting reaction population go into the fission channel from each (Z, N, E_x, J, Π) channel until all nuclides have ended up in their ground or isomeric state, irrespective of the user request for an exclusive channel calculation.

3.5 Recoils

3.5.1 Qualitative analysis

In a nuclear reaction code, the calculations are usually performed in the center of mass (CM) frame, while the experimental data are obtained in the Laboratory (LAB) frame. It is therefore necessary to perform a transformation either by (i) expressing the experimental data in the CM frame or by (ii) expressing the CM model results in the LAB frame. Of course, the cross sections are the same in both frames, but the spectra are certainly different. The best example is given by the elastic peak in an emission spectrum which is a Dirac delta peak in the CM frame and rather looks like a Gaussian when measured experimentally. The reason for this, apart from the fact that the projectile beam is not perfectly mono-energetic, is that the composite system has a velocity in the LAB frame before decay occurs. Consequently if one considers the emission of an ejectile with a well defined energy in the CM frame, the ejectile energy in the LAB frame will not be unique because of all the CM emission angles. More precisely, a maximum ejectile energy will be obtained when the emission occurs at 0°, and a minimum will be obtained at 180°, together with all the intermediate situations. Dealing with this situation is simple if only one nucleus decays, but if two particles are sequentially emitted, the first emission probabilities create a velocity distribution of the residual nuclei in the LAB frame. One must first loop over these velocities before one can compute the secondary emission.

3.5.2 General method

As mentioned in section 3.2.2, in TALYS each nucleus that can decay is described by an array $P(Z, N, E_x)$ which gives the population in a bin/level with excitation energy E_x of the nucleus (Z, N). A special case is the initial compound nucleus which contains all the initial reaction population at its total excitation energy E_x^{max}. For the kinematics of the binary reactions, it is necessary to keep track of the velocities and moving directions of these nuclei in the LAB frame, so that we can reconstruct the LAB spectra from the decays in the CM frame. We therefore have to add in principle three dimensions to the P array. The first one to keep track of the recoil energy, and the two other ones for the emission angles. However, such book-keeping would become very time consuming, especially for high energies.

Hence, we only take into account the recoil energies and the usual Θ angle and define another array $P_{rec}(Z, N, E_x, E_r, \Theta_r)$ which indicates the fraction of the total population $P(Z, N, E_x)$ moving with the kinetic energy E_r in the direction Θ_r with respect to the beam direction in the LAB frame. Obviously,

$$P(Z, N, E_x) = \sum_{E_r\ bins} \sum_{\Theta_r\ bins} P_{rec}(Z, N, E_x, E_r, \Theta_r). \tag{3.57}$$

Again, the initial compound nucleus (Z_C, N_C) is a special one. Its kinetic energy E_r^0 in the LAB frame is unique and is given by

$$E_r^0 = \sqrt{(E_p^2 + 2M_pE_p + M_C^2)} - M_C, \tag{3.58}$$

where E_p is the projectile kinetic energy in the LAB, M_p the projectile mass and M_C the compound nucleus mass, and it moves in the beam direction (i.e. $0°$). Before any emission is calculated, the initial reaction population is stored in the array element $P_{rec}(Z_c, N_c, E_x^{max}, E_r^0, 0)$. As explained before, the population of the residual nuclei bins are calculated by looping over all possible ejectiles, emission energies and angles in the CM frame. Therefore, each time we decay from a mother bin to a residual bin, we know exactly what fraction of the total bin population is emitted in a given CM (energy,angle) bin. We then simply couple the CM emission energies and angles with the CM kinetic energy and moving direction in the LAB frame to determine simultaneously the ejectile double-differential spectrum in the LAB and the residual nucleus population in the corresponding LAB (energy,angle) bin. This may seem simple from a qualitative point of view, it is however not trivial to implement numerically and can be time consuming.

3.5.3 Quantitative analysis

From now on, for simplicity, we assume that the kinematics of the binary reactions can be considered as a classical process, i.e. we exclude γ decay and relativistic kinematics in the recoil calculation. We here consider the emission of a given ejectile from a given energy bin i of the decaying nucleus (Z, N) which moves with a given velocity v_{cm} (or kinetic energy E_{cm}) in the direction Θ_{cm} with respect to the beam direction. The total population that is going to decay is $P(Z, N, E_i)$ and the fraction of this population moving with the velocity v_{cm} in the direction Θ_{cm} is given by $P_{rec}(Z, N, E_i, E_{cm}, \Theta_{cm})$. We can determine the total emitted flux for a given emission energy and a given emission angle in the CM frame. In practice, we rather decay from a initial bin to a residual bin in a given angular bin in the CM frame. If recoil effects are neglected we directly derive from such a decay an energy bin $[E_{low}^{CM}, E_{up}^{CM}]$ and an angular bin $[\Theta_{low}^{CM}, \Theta_{up}^{CM}]$ in which the total flux Φ_{ej}^{CM} is emitted. Accounting for recoil effects requires an intermediate step to share the available energy ΔE (difference between the energy bins of the initial nucleus and final nucleus) among the ejectile with mass m_{ej} and the residual nucleus with mass M_R.

To do this, we use the classical relation

$$\overrightarrow{v}_{ej}^{LAB} = \overrightarrow{v}_{cm} + \overrightarrow{v}_{ej}^{CM}, \tag{3.59}$$

which connects the LAB velocity $\overrightarrow{v}_{ej}^{LAB}$ of the ejectile with its velocity $\overrightarrow{v}_{ej}^{CM}$ in the CM frame and the CM frame velocity $\overrightarrow{v}_{cm}$. We need to connect $\overrightarrow{v}_{ej}^{CM}$ with ΔE.

This can be done upon writing

$$\Delta E = \frac{1}{2} m_{ej} (\overrightarrow{v}_{ej}^{CM})^2 + \frac{1}{2} M_R (\overrightarrow{v}_R^{CM})^2, \tag{3.60}$$

where $\overrightarrow{v}_R^{CM}$ is the residual nucleus velocity in the CM frame, and using the relation

$$m_{ej} \overrightarrow{v}_{ej}^{CM} + m_R \overrightarrow{v}_R^{CM} = \overrightarrow{0}. \tag{3.61}$$

Combining (3.60) and (3.61) yields

$$v_{ej}^{CM} = \sqrt{2 \frac{M_R}{m_{ej}(m_{ej} + M_R)} \Delta E}, \tag{3.62}$$

which reduces to the classical relation

$$v_{ej}^{CM} = \sqrt{\frac{2\Delta E}{m_{ej}}}, \tag{3.63}$$

if recoil effects are neglected (i.e. in the limit $M_R \to +\infty$).

Once this connection is established, Eq. (3.59) is used to determine the velocity and angle of both the emitted light particle and the residual nucleus by simple projections on the LAB axis.

Hence, given a decay situation in the CM frame, we can reconstruct both the energy and angle of emission in the LAB frame. We now have to determine the link between the double-differential decay characteristics in both frames. The solution is well known (see Ref. [57] for instance) and consists of using a Jacobian which accounts for the modification of an elementary solid angle $d\Omega$ in the CM frame when going into the LAB frame. However, in TALYS we have to employ another method because we do not generally calculate decays for well defined energies and angles but rather for a given energy bin and angular bin. Moreover, since we do not account for the azimuthal angle, we may also encounter some problems when calculating recoil for secondary emission. Indeed, only the first binary process has the azimuthal symmetry with respect to the beam direction.

3.5.4 The recoil treatment in TALYS

The way the double-differential spectra are calculated by TALYS in the LAB frame from those obtained in the CM frame is illustrated in Fig. 3.6. As stressed in Chapter 3, the emission energy grid for the outgoing particles is non-equidistant. Moreover, one has to keep in mind that the total flux $\Phi(i,j)$ in an energy-angular bin (i,j) is connected with the double differential cross section $xs(i,j)$ by

$$\Phi(i,j) = xs(i,j)\Delta E(i)\Delta cos\Theta(j). \tag{3.64}$$

Consequently, it is appropriate to locate the grid points using an energy-cosine grid. As an example, in Fig. 3.6, we consider the decay in the CM bin defined by the energy interval $[2,3]$ and the cosine interval $[0.25,0.5]$ (black region). We assume that the decay occurs from a composite system moving with a kinetic energy of 1 MeV in the direction 45° with respect to the initial beam direction. The mass of the ejectile is assumed to be $m_e = 1$ arb.unit, and that of the composite system 20 arb.unit. In that case, the region reached by the ejectile is a slightly deformed trapezoid (gray region) which covers several bins. Therefore, if the emitted flux is located in a single bin in the CM, it must be distributed over several bins

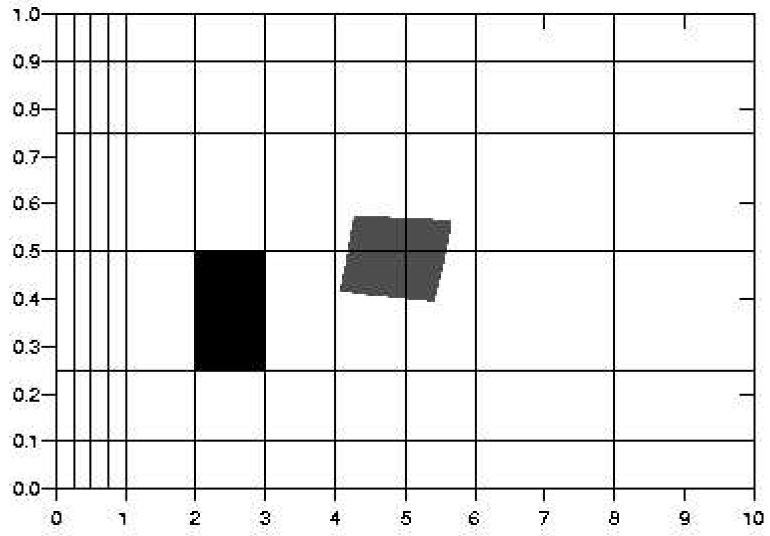

Figure 3.6: CM and LAB double-differential spectra in TALYS.

when going to the LAB frame. This is the key problem to be solved in TALYS. To solve this problem, we need to make assumptions to be able (i) to calculate the area covered in the LAB frame (gray region) and (ii) the way this global area is distributed over the bins it partially covers. The assumption made in TALYS consists of neglecting the deformation of the boundaries of the grey area and assuming this area to be a trapezoid. In other words, we make the assumption that a triangle in the CM frame is transformed into a triangle when going in the LAB. This is helpful since the area of a triangle is given by a simple analytic expression as function of the coordinates of the summits of the triangle. Therefore, we divide the starting CM bins into two triangles to determine the two triangles obtained in the LAB frame. With such a method, the whole problem can be solved and the decay calculated in the CM frame can be transformed to the LAB frame without any further approximations.

However, in practice, coupling the angular direction (in the LAB) of the nucleus that decays with the ejectile emission angle in the CM frame, while neglecting the azimuthal angle, gives double differential ejectile spectra in the LAB which are generally not correct. In fact, we believe that it is better not to account for the angular distribution of the decaying nucleus unless both Θ and ϕ are explicitly treated. Fortunately, the final angular distribution of the recoiling nucleus is seldom of interest.

3.5.5 Method of average velocity

As mentioned above, we do not loop over the angular distribution of the decaying nucleus. This is equivalent to replacing the array $P_{rec}(Z, N, E_i, E_r, \Theta_r)$ by $P_{rec}(Z, N, E_i, E_r)$. Then, we only have to keep track of the velocities of the nucleus that is going to decay, i.e. we have to loop over the E_r bins to reconstruct both the ejectile and residual nuclei spectra. Another approximation that we have implemented as an option (**recoilaverage y**) consists of using an average velocity before this reconstruction, a method first applied by Chadwick et al. [58, 59]. This approach avoids the loop over the E_r bins altogether and reduces the calculation time. However, for high energies, this might be too crude an approximation.

3.5.6 Approximative recoil correction for binary ejectile spectra

Maybe you are not interested in a full recoil calculation, but merely want to correct the outgoing particle spectra for the recoil of the nucleus. In that case you may use the following method which is implemented in TALYS for just that purpose and which is outlined below.

The assumptions are made that (*i*) only binary emission takes place, and that (*ii*) emission only occurs under 0^o. Hence, this approximation is basically expected to be valid for angle-integrated spectra only. The CM to LAB conversion of the ejectile spectra takes under these conditions the following simple form:

$$E_{ej}^{lab} = \frac{M_R}{M_C}\,\Delta E + \frac{m_{ej}M_p}{M_C^2}\,E_p + 2\sqrt{\frac{m_{ej}M_RM_p}{M_C^3}\,E_p\,\Delta E}, \tag{3.65}$$

in which E_{ej}^{lab} is the LAB ejectile energy. This correction is applied to the *full* ejectile spectrum including the multiple emission contributions. Hence, the approximation is rather crude. It saves, however, a lot of computer time. Since the high-energy tail originates completely from binary emission, this tail is correctly converted to the LAB system. Furthermore, the correction is small at low energies where the largest contributions from multiple emission reside.

Chapter 4

Nuclear models

Fig. 4.1 gives an overview of the nuclear models that are included in TALYS. They can generally be categorized into optical, direct, pre-equilibrium, compound and fission models, all driven by a comprehensive database of nuclear structure and model parameters. We will first describe the optical model and the various models for direct reactions that are used. Next, we give an outline of the various pre-equilibrium models that are included. Then, we describe compound nucleus models for both binary and multiple emission, and level densities, which are important ingredients of pre-equilibrium and compound models. Finally, we give an outline of the fission models.

4.1 Optical model

The central assumption underlying the optical model is that the complicated interaction between an incident particle and a nucleus can be represented by a complex mean-field potential, which divides the reaction flux into a part covering shape elastic scattering and a part describing all competing non-elastic channels. Solving the Schrödinger equation numerically with this complex potential yields a wealth of valuable information. First, it returns a prediction for the basic observables, namely the elastic angular distribution and polarisation, the reaction and total cross section and, for low energies, the s, p-wave strength functions and the potential scattering radius R'. The essential value of a good optical model is that it can reliably predict these quantities for energies and nuclides for which no measurements exist. Also, the quality of the not directly observable quantities that are provided by the optical model has an equally important impact on the evaluation of the various reaction channels. Well-known examples are transmission coefficients, for compound nucleus and multi-step compound decay, and the distorted wave functions that are used for direct inelastic reactions and for transitions to the continuum that describe statistical multi-step direct reactions. Also, the reaction cross sections that are calculated with the optical model are crucial for the semi-classical pre-equilibrium models.

All optical model calculations are performed by ECIS-06 [55], which is used as a subroutine in TALYS.

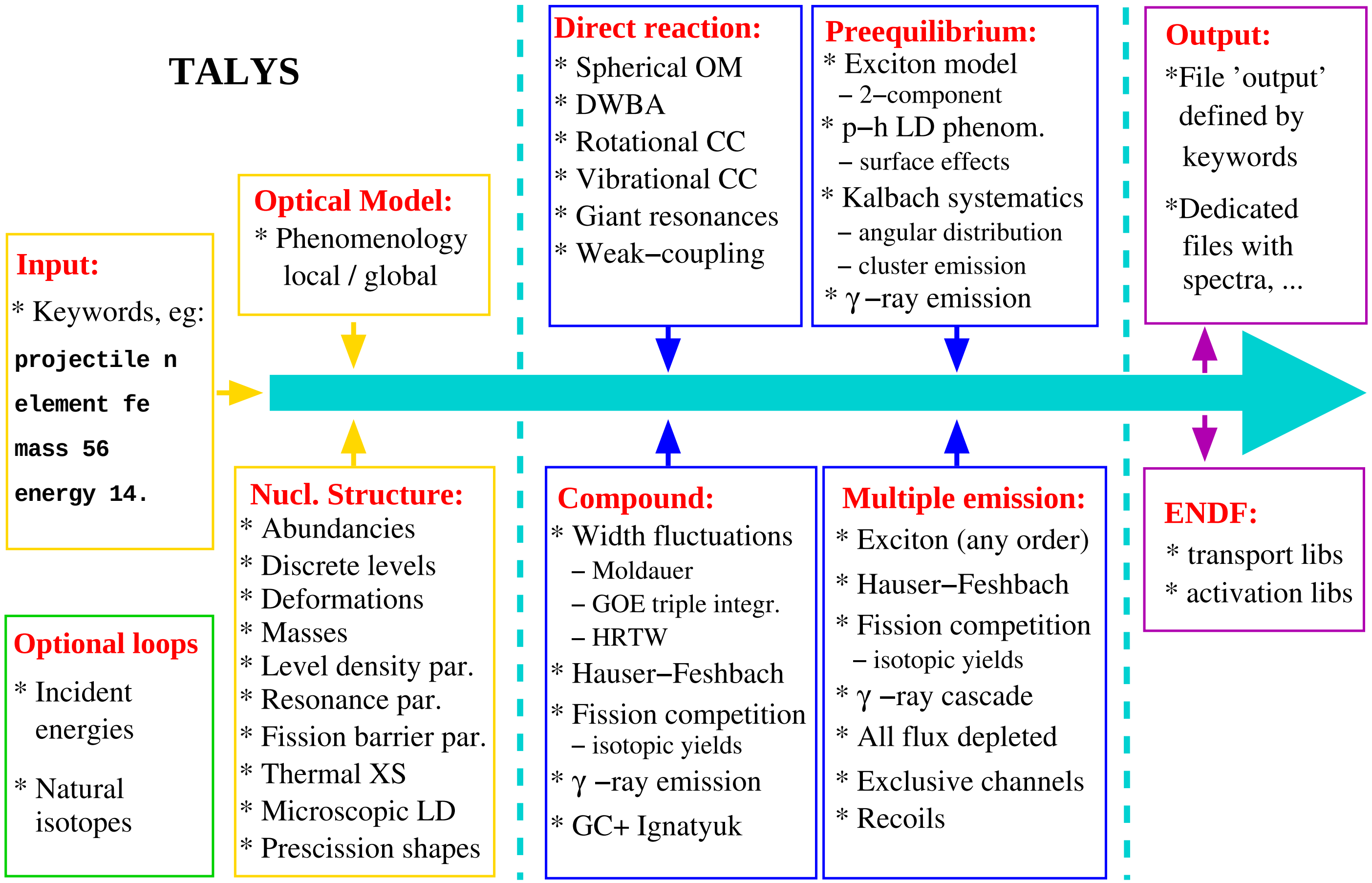

Figure 4.1: Nuclear models in TALYS

4.1.1 Spherical OMP: Neutrons and protons

The default optical model potentials (OMP) used in TALYS are the local and global parameterisations of Koning and Delaroche [60].

The phenomenological OMP for nucleon-nucleus scattering, $\mathcal{U}$, is defined as:

$$\begin{aligned}\mathcal{U}(r,E) &= -\mathcal{V}_V(r,E) - i\mathcal{W}_V(r,E) - i\mathcal{W}_D(r,E) \\ &\quad +\mathcal{V}_{SO}(r,E).\mathbf{l}.\sigma + i\mathcal{W}_{SO}(r,E).\mathbf{l}.\sigma + \mathcal{V}_C(r),\end{aligned} \tag{4.1}$$

where $\mathcal{V}_{V,SO}$ and $\mathcal{W}_{V,D,SO}$ are the real and imaginary components of the volume-central (V), surface-central (D) and spin-orbit (SO) potentials, respectively. E is the LAB energy of the incident particle in MeV. All components are separated in energy-dependent well depths, V_V, W_V, W_D, V_{SO}, and W_{SO}, and energy-independent radial parts f, namely

$$\begin{aligned}\mathcal{V}_V(r,E) &= V_V(E)f(r,R_V,a_V), \\ \mathcal{W}_V(r,E) &= W_V(E)f(r,R_V,a_V), \\ \mathcal{W}_D(r,E) &= -4a_DW_D(E)\frac{d}{dr}f(r,R_D,a_D), \\ \mathcal{V}_{SO}(r,E) &= V_{SO}(E)\left(\frac{\hbar}{m_\pi c}\right)^2\frac{1}{r}\frac{d}{dr}f(r,R_{SO},a_{SO}), \\ \mathcal{W}_{SO}(r,E) &= W_{SO}(E)\left(\frac{\hbar}{m_\pi c}\right)^2\frac{1}{r}\frac{d}{dr}f(r,R_{SO},a_{SO}).\end{aligned} \tag{4.2}$$

The form factor $f(r,R_i,a_i)$ is a Woods-Saxon shape

$$f(r,R_i,a_i) = (1+\exp[(r-R_i)/a_i])^{-1}, \tag{4.3}$$

where the geometry parameters are the radius $R_i = r_iA^{1/3}$, with A being the atomic mass number, and the diffuseness parameters a_i. For charged projectiles, the Coulomb term $\mathcal{V}_C$, as usual, is given by that of a uniformly charged sphere

$$\begin{aligned}\mathcal{V}_C(r) &= \frac{Zze^2}{2R_C}(3-\frac{r^2}{R_C^2}), \quad \text{for } r \le R_C \\ &= \frac{Zze^2}{r}, \quad \text{for } r \ge R_C,\end{aligned} \tag{4.4}$$

with $Z(z)$ the charge of the target (projectile), and $R_C = r_CA^{1/3}$ the Coulomb radius.

The functional forms for the potential depths depend on $(E-E_f)$, where E_f, the Fermi energy in MeV, is defined as the energy halfway between the last occupied and the first unoccupied shell of the nucleus. For incident neutrons,

$$E_f^n = -\frac{1}{2}[S_n(Z,N) + S_n(Z,N+1)], \tag{4.5}$$

with S_n the neutron separation energy for a nucleus with proton number Z and neutron number N, while for incident protons

$$E_f^p = -\frac{1}{2}[S_p(Z,N) + S_p(Z+1,N)], \tag{4.6}$$

with S_p the proton separation energy. We use the mass table of the nuclear structure database to obtain the values of the separation energies.

Our OMP parameterisation for either incident neutrons or protons is

$$\begin{aligned}
V_V(E) &= v_1[1 - v_2(E - E_f) + v_3(E - E_f)^2 - v_4(E - E_f)^3] \\
W_V(E) &= w_1 \frac{(E - E_f)^2}{(E - E_f)^2 + (w_2)^2} \\
r_V &= \text{constant} \\
a_V &= \text{constant} \\
W_D(E) &= d_1 \frac{(E - E_f)^2}{(E - E_f)^2 + (d_3)^2} \exp[-d_2(E - E_f)] \\
r_D &= \text{constant} \\
a_D &= \text{constant} \\
V_{SO}(E) &= v_{so1} \exp[-v_{so2}(E - E_f)] \\
W_{SO}(E) &= w_{so1} \frac{(E - E_f)^2}{(E - E_f)^2 + (w_{so2})^2} \\
r_{SO} &= \text{constant} \\
a_{SO} &= \text{constant} \\
r_C &= \text{constant},
\end{aligned} \tag{4.7}$$

where $E_f = E_f^n$ for incident neutrons and $E_f = E_f^p$ for incident protons. Here E is the incident energy in the LAB system. This representation is valid for incident energies from 1 keV up to 200 MeV. Note that V_V and W_V share the same geometry parameters r_V and a_V, and likewise for the spin-orbit terms.

In general, all parameters appearing in Eq. (4.7) differ from nucleus to nucleus. When enough experimental scattering data of a certain nucleus is available, a so called local OMP can be constructed. TALYS retrieves all the parameters v_1, v_2, etc. of these local OMPs automatically from the nuclear structure and model parameter database, see the next Chapter, which contains the same information as the various tables of Ref. [60]. If a local OMP parameterisation is not available in the database, the built-in global optical models are automatically used, which can be applied for any Z, A combination. A flag exists (the **localomp** keyword) to overrule the local OMP by the global OMP. The global neutron OMP, validated for $0.001 \leq E \leq 200$ MeV and $24 \leq A \leq 209$, is given by

$$\begin{aligned}
V_V(E) &= v_1^n[1 - v_2^n(E - E_f^n) + v_3^n(E - E_f^n)^2 - v_4^n(E - E_f^n)^3] \\
W_V(E) &= w_1^n \frac{(E - E_f^n)^2}{(E - E_f^n)^2 + (w_2^n)^2} \\
r_V &= 1.3039 - 0.4054A^{-1/3} \\
a_V &= 0.6778 - 1.487.10^{-4}A \\
W_D(E) &= d_1^n \frac{(E - E_f^n)^2}{(E - E_f^n)^2 + (d_3^n)^2} \exp[-d_2^n(E - E_f^n)] \\
r_D &= 1.3424 - 0.01585A^{1/3} \\
a_D &= 0.5446 - 1.656.10^{-4}A
\end{aligned}$$

$$\begin{aligned}
V_{SO}(E) &= v^n_{so1}\exp[-v^n_{so2}(E-E^n_f)] \\
W_{SO}(E) &= w^n_{so1}\frac{(E-E^n_f)^2}{(E-E^n_f)^2+(w^n_{so2})^2} \\
r_{SO} &= 1.1854-0.647A^{-1/3} \\
a_{SO} &= 0.59,
\end{aligned} \tag{4.8}$$

where the units are in fm and MeV and the parameters for the potential depths and E^n_f are given in Table 4.1.

The global proton OMP is given by

$$\begin{aligned}
V_V(E) &= v^p_1[1-v^p_2(E-E^p_f)+v^p_3(E-E^p_f)^2-v^p_4(E-E^p_f)^3] \\
&+ \bar{V}_C.v^p_1\left[v^p_2-2v^p_3(E-E^p_f)+3v^p_4(E-E^p_f)^2\right] \\
W_V(E) &= w^p_1\frac{(E-E^p_f)^2}{(E-E^p_f)^2+(w^p_2)^2} \\
r_V &= 1.3039-0.4054A^{-1/3} \\
a_V &= 0.6778-1.487.10^{-4}A \\
W_D(E) &= d^p_1\frac{(E-E^p_f)^2}{(E-E^p_f)^2+(d^p_3)^2}\exp[-d^p_2(E-E^p_f)] \\
r_D &= 1.3424-0.01585A^{1/3} \\
a_D &= 0.5187+5.205.10^{-4}A \\
V_{SO}(E) &= v^p_{so1}\exp[-v^p_{so2}(E-E^p_f)] \\
W_{SO}(E) &= w^p_{so1}\frac{(E-E^p_f)^2}{(E-E^p_f)^2+(w^p_{so2})^2} \\
r_{SO} &= 1.1854-0.647A^{-1/3} \\
a_{SO} &= 0.59 \\
r_C &= 1.198+0.697A^{-2/3}+12.994A^{-5/3},
\end{aligned} \tag{4.9}$$

where the parameters for the potential depths, $\bar{V}_C$ and E^p_f are given in Table 4.2. The functional form of the proton global OMP differs from the neutron global OMP only by the Coulomb correction term in $V_V(E)$.

The spherical optical model described above provides the transmission coefficients, DWBA cross sections, total and elastic cross sections, etc., mentioned in the beginning of this section. For deformed nuclides, strongly coupled collective levels need to be included. This will be explained in Section 4.2 on direct reactions.

All optical model parameters mentioned in this Section can be adjusted, not only by means of a local parameter file (see the **optmodfileN** keyword), but also via adjustable parameters through the **v1adjust**, **v2adjust** etc. keywords, with which the standard values can be multiplied.

v_1^n	$= 59.30 - 21.0(N-Z)/A - 0.024A$	MeV
v_2^n	$= 0.007228 - 1.48.10^{-6}A$	MeV^{-1}
v_3^n	$= 1.994.10^{-5} - 2.0.10^{-8}A$	MeV^{-2}
v_4^n	$= 7.10^{-9}$	MeV^{-3}
w_1^n	$= 12.195 + 0.0167A$	MeV
w_2^n	$= 73.55 + 0.0795A$	MeV
d_1^n	$= 16.0 - 16.0(N-Z)/A$	MeV
d_2^n	$= 0.0180 + 0.003802/(1+\exp[(A-156.)/8.)]$	MeV^{-1}
d_3^n	$= 11.5$	MeV
v_{so1}^n	$= 5.922 + 0.0030A$	MeV
v_{so2}^n	$= 0.0040$	MeV^{-1}
w_{so1}^n	$= -3.1$	MeV
w_{so2}^n	$= 160.$	MeV
E_f^n	$= -11.2814 + 0.02646A$	MeV

Table 4.1: Potential depth parameters and Fermi energy for the neutron global OMP of Eq. (4.8).

v_1^p	$= 59.30 + 21.0(N-Z)/A - 0.024A$	MeV
v_2^p	$= 0.007067 + 4.23.10^{-6}A$	MeV^{-1}
v_3^p	$= 1.729.10^{-5} + 1.136.10^{-8}A$	MeV^{-2}
v_4^p	$= v_4^n$	MeV^{-3}
w_1^p	$= 14.667 + 0.009629A$	MeV
w_2^p	$= w_2^n$	MeV
d_1^p	$= 16.0 + 16.0(N-Z)/A$	MeV
d_2^p	$= d_2^n$	MeV^{-1}
d_3^p	$= d_3^n$	MeV
v_{so1}^p	$= v_{so1}^n$	MeV
v_{so2}^p	$= v_{so2}^n$	MeV^{-1}
w_{so1}^p	$= w_{so1}^n$	MeV
w_{so2}^p	$= w_{so2}^n$	MeV
E_f^p	$= -8.4075 + 0.01378A$	MeV
$\bar{V}_C$	$= 1.73.Z.A^{-1/3}/r_C$	MeV

Table 4.2: Potential depth parameters and Fermi energy for the proton global OMP of Eq. (4.9). The parameter values for neutrons are given in Table 4.1. $\bar{V}_C$ appears in the Coulomb correction term $\Delta V_C(E)$, of the real central potential.

4.1.2 Spherical dispersive OMP: Neutrons

The theory of the nuclear optical model can be reformulated in terms of dispersion relations that connect the real and imaginary parts of the optical potential, and we have added an option in TALYS to take them into account. These dispersion relations are a natural result of the causality principle that a scattered wave cannot be emitted before the arrival of the incident wave. The dispersion component stems directly from the absorptive part of the potential,

$$\Delta\mathcal{V}(r,E) = \frac{\mathcal{P}}{\pi}\int_{-\infty}^{\infty}\frac{\mathcal{W}(r,E')}{E'-E}dE', \tag{4.10}$$

where $\mathcal{P}$ denotes the principal value. The total real central potential can be written as the sum of a Hartree-Fock term $\mathcal{V}_{HF}(r,E)$ and the the total dispersion potential $\Delta\mathcal{V}(r,E)$

$$\mathcal{V}(r,E) = \mathcal{V}_{HF}(r,E) + \Delta\mathcal{V}(r,E). \tag{4.11}$$

Since $\mathcal{W}(r,E)$ has a volume and a surface component, the dispersive addition is,

$$\begin{aligned}\Delta\mathcal{V}(r,E) &= \Delta\mathcal{V}_V(r,E) + \Delta\mathcal{V}_D(r,E)\\ &= \Delta V_V(E)f(r,R_V,a_V) - 4a_D\Delta V_D(E)\frac{d}{dr}f(r,R_D,a_D)\end{aligned} \tag{4.12}$$

where the volume dispersion term is given by

$$\Delta V_V(E) = \frac{\mathcal{P}}{\pi}\int_{-\infty}^{\infty}\frac{W_V(E')}{E'-E}dE', \tag{4.13}$$

and the surface dispersion term is given by

$$\Delta V_D(E) = \frac{\mathcal{P}}{\pi}\int_{-\infty}^{\infty}\frac{W_D(E')}{E'-E}dE'. \tag{4.14}$$

Hence, the real volume well depth of Eq. (4.2) becomes

$$V_V(E) = V_{HF}(E) + \Delta V_V(E), \tag{4.15}$$

and the real surface well depth is

$$V_D(E) = \Delta V_D(E). \tag{4.16}$$

In general, Eqs. (4.13)-(4.14) cannot be solved analytically. However, under certain plausible conditions, analytical solutions exist. Under the assumption that the imaginary potential is symmetric with respect to the Fermi energy E_F,

$$W(E_F - E) = W(E_F + E), \tag{4.17}$$

where W denotes either the volume or surface term, we can rewrite the dispersion relation as,

$$\Delta V(E) = \frac{2}{\pi}(E-E_F)\mathcal{P}\int_{E_F}^{\infty}\frac{W(E')}{(E'-E_F)^2-(E-E_F)^2}dE', \tag{4.18}$$

from which it easily follows that $\Delta V(E)$ is skew-symmetric around E_F,

$$\Delta V(E + E_F) = -\Delta V(E - E_F), \tag{4.19}$$

and hence $\Delta V(E_F) = 0$. This can then be used to rewrite Eq. (4.10) as

$$\begin{aligned}
\Delta V(E) &= \Delta V(E) - \Delta V(E_F) \\
&= \frac{\mathcal{P}}{\pi}\int_{-\infty}^{\infty} W(E')(\frac{1}{E'-E} - \frac{1}{E'-E_F})dE' \\
&= \frac{E-E_F}{\pi}\int_{-\infty}^{\infty} \frac{W(E')}{(E'-E)(E'-E_F)}dE'.
\end{aligned} \tag{4.20}$$

For the Hartree-Fock term we adopt the usual form for $V_V(E)$ given in Eq. (4.7). The dispersion integrals for the functions for absorption can be calculated analytically and are included as options in ECIS-06. This makes the use of a dispersive optical model parameterization completely equivalent to that of a non-dispersive OMP: the dispersive contributions are calculated automatically once the OMP parameters are given. Upon comparison with a nondispersive parameterization, we find that v_1 is rather different (as expected) and that r_V, a_V, v_2, v_3, w_1 and w_2 are slightly different. We have included dispersive spherical neutron OMP parameterization for about 70 nuclides (unpublished). They can be used with the keyword **dispersion y**.

4.1.3 Spherical OMP: Complex particles

For deuterons, tritons, Helium-3 and alpha particles, we use a simplification of the folding approach of Watanabe [61], see Ref. [62]. We take the nucleon OMPs described in the previous section, either local or global, as the basis for these complex particle potentials.

Deuterons

For deuterons, the real central potential depth at incident energy E is

$$V_V^{deuteron}(E) = V_V^{neutron}(E/2) + V_V^{proton}(E/2), \tag{4.21}$$

and similarly for W_V and W_D. For the spin-orbit potential depth we have

$$V_{SO}^{deuteron}(E) = (V_{SO}^{neutron}(E) + V_{SO}^{proton}(E))/2, \tag{4.22}$$

and similarly for W_{SO}. For the radius and diffuseness parameter of the real central potential we have

$$\begin{aligned}
r_V^{deuteron} &= (r_V^{neutron} + r_V^{proton})/2, \\
a_V^{deuteron} &= (a_V^{neutron} + a_V^{proton})/2,
\end{aligned} \tag{4.23}$$

and similarly for the geometry parameters of the other potentials.

Note that several of these formulae are somewhat more general than necessary, since the nucleon potentials mostly have geometry parameters, and also potential depths such as V_{SO}, which are equal for neutrons and protons (a_D is an exception). The general formulae above have been implemented to also account for other potentials, if necessary.

Tritons

For tritons, the real central potential depth at incident energy E is

$$V_V^{triton}(E) = 2V_V^{neutron}(E/3) + V_V^{proton}(E/3), \tag{4.24}$$

and similarly for W_V and W_D. For the spin-orbit potential depth we have

$$V_{SO}^{triton}(E) = (V_{SO}^{neutron}(E) + V_{SO}^{proton}(E))/6, \tag{4.25}$$

and similarly for W_{SO}. For the radius and diffuseness parameter of the real central potential we have

$$\begin{aligned} r_V^{triton} &= (2r_V^{neutron} + r_V^{proton})/3, \\ a_V^{triton} &= (2a_V^{neutron} + a_V^{proton})/3, \end{aligned} \tag{4.26}$$

and similarly for the geometry parameters of the other potentials.

Helium-3

For Helium-3, the real central potential depth at incident energy E is

$$V_V^{Helium-3}(E) = V_V^{neutron}(E/3) + 2V_V^{proton}(E/3), \tag{4.27}$$

and similarly for W_V and W_D. For the spin-orbit potential depth we have

$$V_{SO}^{Helium-3}(E) = (V_{SO}^{neutron}(E) + V_{SO}^{proton}(E))/6, \tag{4.28}$$

and similarly for W_{SO}. For the radius and diffuseness parameter of the real central potential we have

$$\begin{aligned} r_V^{Helium-3} &= (r_V^{neutron} + 2r_V^{proton})/3, \\ a_V^{Helium-3} &= (a_V^{neutron} + 2a_V^{proton})/3, \end{aligned} \tag{4.29}$$

and similarly for the geometry parameters of the other potentials.

Alpha particles

For alpha's, the real central potential depth at incident energy E is

$$V_V^{alphas}(E) = 2V_V^{neutron}(E/4) + 2V_V^{proton}(E/4), \tag{4.30}$$

and similarly for W_V and W_D. For the spin-orbit potential depth we have

$$V_{SO}^{alphas}(E) = W_{SO}^{alphas}(E) = 0. \tag{4.31}$$

For the radius and diffuseness parameter of the real central potential we have

$$\begin{aligned} r_V^{alphas} &= (r_V^{neutron} + r_V^{proton})/2, \\ a_V^{alphas} &= (a_V^{neutron} + a_V^{proton})/2, \end{aligned} \tag{4.32}$$

and similarly for the geometry parameters of the other potentials.

All optical model parameters for complex particles can be altered via adjustable parameters through the **v1adjust**, **rvadjust** etc. keywords, with which the standard values can be multiplied.

4.1.4 Semi-microscopic optical model (JLM)

Besides the phenomenological OMP, it is also possible to perform TALYS calculations with the semimicroscopic nucleon-nucleus spherical optical model potential as described in [63]. We have implemented Eric Bauge's MOM code [56] as a subroutine to perform so called Jeukenne-Lejeune-Mahaux (JLM) OMP calculations. The optical model potential of [63] and its extension to deformed and unstable nuclei has been widely tested [63, 64, 65, 66, 67] and produces predictions from A=30 to 240 and for energies ranging from 10 keV up to 200 MeV. MOM stands for "Modèle Optique Microscopique" in French, or "Microscopic Optical Model" in English. In this version of TALYS, only spherical JLM OMP's are included.

The MOM module reads the radial matter densities from the nuclear structure database and performs the folding of the Nuclear Matter (NM) optical model potential described in [63] with the densities to obtain a local OMP. This is then put in the ECIS-06 routine to compute observables by solving the Schrödinger equation for the interaction of the projectile with the aforementioned OMP. The OMP's are calculated by folding the target radial matter density with an OMP in nuclear matter based on the Brückner-Hartree-Fock work of Jeukenne, Lejeune and Mahaux [68, 69, 70, 71]. This NM OMP was then phenomenologically altered in [63, 72] in order to improve the agreement of predicted finite nuclei observables with a large set of experimental data. These improvements consist in unifying the low and high energy parameterizations of the NM interaction in [72], and in studying the energy variations of the potential depth normalization factors in [63]. These factors now include non-negligible normalizations of isovector components [63] that are needed in order to account simultaneously for (p,p) and (n,n) elastic scattering as well as (p,n)$_{IAS}$ quasi-elastic scattering. The final NM potential for a given nuclear matter density $\rho = \rho_n - \rho_p$ and asymmetry $\alpha = (\rho_n + \rho_p)/\rho$ reads

$$\begin{aligned} U_{NM}(E)_{\rho,\alpha} = & \quad \lambda_V(E)\left[V_0(\tilde{E}) \pm \lambda_{V1}(E)\alpha V_1(\tilde{E})\right] \\ + & \quad i\lambda_W(E)\left[W_0(\tilde{E}) \pm \lambda_{W1}(E)\alpha W_1(\tilde{E})\right], \end{aligned} \tag{4.33}$$

with E the incident nucleon energy, $\tilde{E} = E - V_c$ (where V_c is the Coulomb field), V_0, V_1, W_0, and W_1 the real isoscalar, real isovector, imaginary isoscalar, and imaginary isovector NM OMP components respectively, and λ_V, λ_{V1}, λ_W, and λ_{W1} the real (isoscalar+isovector), real isovector, imaginary, and imaginary isovector normalization factors respectively. The values of λ_V, λ_{V1}, λ_W, and λ_{W1} given in [63] read

$$\lambda_V(E) = 0.951 + 0.0008\ \ln(1000E) + 0.00018\ [\ln(1000E)]^2 \tag{4.34}$$

$$\begin{aligned} \lambda_W(E) = & \quad \left[1.24 - \left[1 + e^{\left(\frac{E-4.5}{2.9}\right)}\right]^{-1}\right]\left[1 + 0.06\, e^{-\left(\frac{E-14}{3.7}\right)^2}\right] \\ \times & \quad \left[1 - 0.09\, e^{-\left(\frac{E-80}{78}\right)^2}\right]\left[1 + \left(\frac{E-80}{400}\right)\Theta(E-80)\right] \end{aligned} \tag{4.35}$$

$$\lambda_{V1}(E) = 1.5 - 0.65\left[1 + e^{\frac{E-1.3}{3}}\right]^{-1} \tag{4.36}$$

$$\lambda_{W1}(E) = \left[1.1 + 0.44\left[1 + \left(e^{\frac{E-40}{50.9}}\right)^4\right]^{-1}\right] \times \left[1 - 0.065\, e^{-\left(\frac{E-40}{13}\right)^2}\right]\left[1 - 0.083\, e^{-\left(\frac{E-200}{80}\right)^2}\right]. \quad (4.37)$$

with the energy E expressed in MeV. As stated in [63], in the 20 to 50 MeV range, the uncertainties related to λ_V, λ_{V1}, λ_W, and λ_{W1} are estimated to be 1.5%, 10%, 10%, and 10%, respectively. Outside this energy range, uncertainties are estimated to be 1.5 times larger.

In order to apply the NM OMP to finite nuclei an approximation had to be performed. This is the Local Density Approximation (LDA) where the local value of the finite nucleus OMP is taken to be the NM OMP value for the local finite nucleus density: $U_{FN}(r) = U_{NM}(\rho(r))$. Since this LDA produces potentials with too small rms radii, the improved LDA, which broadens the OMP with a Gaussian form factor (4.38), is introduced. In [72, 63] different prescriptions for the improved Local Density approximation are compared and LDA range parameters are optimized.

$$U_{FN}(r,E) = (t\sqrt{\pi})^{-3}\int \frac{U_{NM}(\rho(r'),E)}{\rho(r')}\exp(-|\vec{r}-\vec{r'}|^2/t_r^2)\rho(r')d\vec{r'}, \quad (4.38)$$

with t the range of the Gaussian form factor. The $t_r = 1.25$ fm and $t_i = 1.35$ fm values were found [63] to be global optimal values for the real and imaginary ranges, respectively.

Finally, since no spin-orbit (SO) potential exists between a nucleon and NM, the Scheerbaum [73] prescription was selected in [72], coupled with the phenomenological complex potential depths $\lambda_{v_{so}}$, and $\lambda_{w_{so}}$. The SO potential reads

$$U^{so}_{n(p)}(r) = (\lambda_{v_{so}}(E) + i\lambda_{v_{so}}(E))\,\frac{1}{r}\frac{d}{dr}\left(\frac{2}{3}\rho_{p(n)} + \frac{1}{3}\rho_{n(p)}\right), \quad (4.39)$$

with

$$\lambda_{v_{so}} = 130\,\exp(-0.013\,E) + 40 \quad (4.40)$$

and

$$\lambda_{w_{so}} = -0.2\,(E-20). \quad (4.41)$$

All JLM OMP parameters can be altered via adjustable parameters through the **lvadjust**, **lwadjust** etc. keywords, with which the standard values can be multiplied.

4.1.5 Systematics for non-elastic cross sections

Since the reaction cross sections for complex particles as predicted by the OMP have not been tested and rely on a relatively simple folding model, we added a possibility to estimate the non-elastic cross sections from empirical expressions. The adopted *tripathi.f* subroutine that provides this does not coincide with the published expression as given by Tripathi et al. [74], but checking our results with the published figures of Ref. [74] made us decide to adopt this empirical model as an option. We sometimes use it for deuterons up to alpha-particles. A high-quality OMP for complex particles would make this option redundant.

4.2 Direct reactions

Various models for direct reactions are included in the program: DWBA for (near-)spherical nuclides, coupled-channels for deformed nuclides, the weak-coupling model for odd nuclei, and also a giant resonance contribution in the continuum. In all cases, TALYS drives the ECIS-06 code to perform the calculations. The results are presented as discrete state cross sections and angular distributions, or as contributions to the continuum.

4.2.1 Deformed nuclei: Coupled-channels

The formalism outlined in the previous section works, theoretically, for nuclides which are spherical and, in practice, for nuclides which are not too strongly deformed. In general, however, the more general coupled-channels method should be invoked to describe simultaneously the elastic scattering channel and the low-lying states which are, due to their collective nature, strongly excited in inelastic scattering. These collective excitations can be described as the result of static or dynamic deformations, which cause the homogeneous neutron-proton fluid to rotate or vibrate. The associated deformation parameters can be predicted from a (semi-)microscopic model or can be derived from an analysis of the experimental angular distributions.

The coupled-channels formalism for scattering and reaction studies is well known and will not be described in this manual. For a detailed presentation, we refer to Ref. [75]. We will only state the main aspects here to put the formalism into practice. Refs. [76] and [77] have been used as guidance. In general various different channels, usually the ground state and several inelastic states, are included in a coupling scheme while the associated coupled equations are solved. In ECIS-06, this is done in a so called sequential iterative approach [55]. Besides Ref. [55], Ref. [78] is also recommended for more insight in the use of the ECIS code.

Various collective models for deformed nuclei exist. Note that the spherical optical model of Eq. (4.2) is described in terms of the nuclear radius $R_i = r_i A^{1/3}$. For deformed nuclei, this expression is generalized to include collective motions. Various models have been implemented in ECIS-06, which enables us to cover many nuclides of interest. We will describe the ones that can be invoked by TALYS. The collective models are automatically applied upon reading the deformation parameter database, see Section 5.5.

Symmetric rotational model

In the symmetric rotational model, the radii of the different terms of the OMP are expressed as

$$R_i = r_i A^{1/3}\left[1 + \sum_{\lambda=2,4,....} \beta_\lambda Y_\lambda^0(\Omega)\right], \tag{4.42}$$

where the β_λ's are permanent, static deformation parameters, and the Y functions are spherical harmonics. The quadrupole deformation β_2 plays a leading role in the interaction process. Higher order deformations β_λ (with $\lambda = 4, 6, ...$) are systematically smaller in magnitude than β_2. The inclusion of β_4 and β_6 deformations in coupled-channels calculations produces changes in the predicted observables, but in general, only β_2 and β_4 are important in describing inelastic scattering to the first few levels in a rotational band. For even-even nuclides like ^{184}W and ^{232}Th, the symmetric rotational model provides a good description of the lowest $0^+, 2^+, 4^+$ (and often $6^+, 8+$, etc.) rotational band. The nuclear model and parameter database of TALYS specifies whether a rotational model can be used for a particular nucleus, together with the included levels and deformation parameters. Either a deformation parameter β_λ or a deformation length $\delta_\lambda = \beta_\lambda r_i A^{1/3}$ may be given. The latter one is generally recommended since it has more physical meaning than β_λ and should not depend on incident energy (while r_i may, in some optical models, depend on energy). We take δ_λ equal for the three OMP components V_V, W_V and W_D and take the spin-orbit potential undeformed. The same holds for the vibrational and other collective models.

By default, TALYS uses the global optical model by Soukhovitskii et al. [79] for actinides. For rotational non-fissile nuclides, if no specific potential is specified through one of the various input methods, we take our local or global spherical potential and subtract 15% from the imaginary surface potential parameter d_1, if rotational or vibrational levels are included in the coupling scheme.

Harmonic vibrational model

A vibrational nucleus possesses a spherically symmetric ground state. Its excited states undergo shape oscillations about the spherical equilibrium model. In the harmonic vibrational model, the radii of the different terms of the OMP are expressed as

$$R_i = r_i A^{1/3} \left[1 + \sum_{\lambda\mu} \alpha_{\lambda\mu} Y_\lambda^\mu(\Omega) \right], \tag{4.43}$$

where the $\alpha_{\lambda\mu}$ operators can be related to the coupling strengths β_λ, describing the vibration amplitude with multipolarity λ. Expanding the OMP to first or second order with this radius gives the OMP expressions for the excitation of one-phonon (first order vibrational model) and two-phonon (second order vibrational model) states [55]. For vibrational nuclei, the minimum number of states to couple is two. For even-even nuclei, we generally use the $(0^+, 2^+)$ coupling, where the 2^+ level is a one-quadrupole phonon excitation. The level scheme of a vibrational nucleus (e.g. ^{110}Pd) often consists of a one-phonon state (2^+) followed by a $(0^+, 2^+, 4^+)$ triplet of two-phonon states. When this occurs, all levels are included in the coupling scheme with the associated deformation length δ_2 (or deformation parameter β_2). If the 3^- and 5^- states are strongly collective excitations, that is when β_3 and β_5 are larger than 0.1, these levels may also be included in the coupling scheme. An example is ^{120}Sn [80], where the low lying $(0^+, 2^+, 3^-, 4^+, 5^-)$ states can all be included as one-phonon states in a single coupling scheme.

Again, if no specific potential is specified through one of the various input methods, we take our local or global spherical potential and subtract 15% from the imaginary surface potential parameter d_1.

Vibration-rotational model

For certain nuclides, the level scheme consists not only of one or more rotational bands, but also of one or more vibrational bands that can be included in the coupling scheme. An example is ^{238}U, where many vibrational bands can be coupled. In Chapter 5 on nuclear model parameters, it is explained how such calculations are automatically performed by TALYS. Depending on the number of levels included, the calculations can be time-consuming.

Asymmetric rotational model

In the asymmetric rotational model, in addition to the spheroidal equilibrium deformation, the nucleus can oscillate such that ellipsoidal shapes are produced. In this model the nucleus has rotational bands built on the statically deformed ground state and on the γ-vibrational state. The radius is now angular dependent,

$$R_i(\Theta) = r_i A^{1/3}\left[1 + \beta_2 \cos\gamma Y_2^0(\Omega) + \sqrt{\frac{1}{2}}\beta_2 \sin\gamma (Y_2^2(\Omega) + Y_2^{-2}(\Omega)) + \beta_4 Y_4^0(\Omega)\right], \tag{4.44}$$

where we restrict ourselves to a few terms. The deformation parameters β_2, β_4 and γ need to be specified. ^{24}Mg is an example of a nucleus that can be analyzed with the asymmetric rotational model. Mixing between bands is not yet automated as an option in TALYS.

4.2.2 Distorted Wave Born Approximation

The Distorted Wave Born Approximation (DWBA) is only valid for small deformations. Until the advent of the more general coupled-channels formalism, it was the commonly used method to describe inelastic scattering, for both weakly and strongly coupled levels. Nowadays, we see DWBA as a first order vibrational model for small deformation, with only a single iteration to be performed for the coupled-channels solution. (See, however Satchler [81] for the exact difference between this so called distorted wave method and DWBA). The interaction between the projectile and the target nucleus is modeled by the derivative of the OMP for elastic scattering times a strength parameter. The latter, the deformation parameter β_λ, is then often used to vary the overall magnitude of the cross section (which is proportional to β_λ^2).

In TALYS, we use DWBA

(a) if a deformed OMP is not available. This applies for the spherical OMPs mentioned in the previous Section, which are all based on elastic scattering observables only. Hence, if we have not constructed a coupled-channels potential, TALYS will automatically use (tabulated or systematical) deformation parameters for DWBA calculations.

(b) if a deformed OMP is used for the first excited states only. For the levels that do not belong to that basic coupling scheme, e.g. for the many states at somewhat higher excitation energy, we use DWBA with (very) small deformation parameters.

4.2.3 Odd nuclei: Weak coupling

Direct inelastic scattering off odd-A nuclei can be described by the weak-coupling model [82], which assumes that a valence particle or hole interacts only weakly with a collective core excitation. Hence the model implies that the nucleon inelastic scattering by the odd-A nucleus is very similar to that by the even core alone, i.e. the angular distributions have a similar shape. Let L be the spin of the even core state, and J_0 and J the spin of the ground and excited state, respectively, of the odd-A nucleus, resulting from the angular momentum coupling. Then, the spins J of the multiplet states in the odd-A nucleus range from $|L - J_0|$ to $(L + J_0)$. If the strength of the inelastic scattering is characterized by the square of the deformation parameters $\beta^2_{L,J}$, then the sum of all $\beta^2_{L,J}$ or $\sigma(E)$ for the transitions in the odd-A nucleus should be equal to the value β^2_L or $\sigma(E)$ for the single transition in the even core nucleus:

$$\sum_J \beta^2_{L,J} = \beta^2_L, \quad \sum_J \sigma_{J_0 \to J} = \sigma_{0 \to L}, \tag{4.45}$$

where the symbol $0 \to L$ indicates a transition between the ground state to the excited state with spin L in the even core nucleus. The deformation parameters $\beta^2_{L,J}$ are now given by

$$\beta^2_{L,J} = \frac{2J+1}{(2J_0+1)(2L+1)}\beta^2_L. \tag{4.46}$$

In practice, the DWBA cross sections are calculated for the real mass of the target nucleus and at the exact excitation energies of the odd-A states, but for the even-core spin L and with deformation parameters $\beta_{L,J}$.

We stress that our weak-coupling model is not full-proof. First of all, there are always two choices for the even-even core. The default used in TALYS (by means of the keyword **core -1**) is to use the even-even core obtained by subtracting a nucleon, but the other choice (**core 1**), to obtain the even-even core by adding a nucleon, may sometimes be more appropriate. The next uncertainty is the choice of levels in the odd-A core. We select the levels that are closest to the excitation energy of the even-spin state of the even-even core. Again, this may not always be the most appropriate choice. A future option is to designate these levels manually.

4.2.4 Giant resonances

The high-energy part of the continuum spectra are generally described by pre-equilibrium models. These models are essentially of a single-particle nature. Upon inspection of continuum spectra, some structure in the high-energy tail is observed that can not be accounted for by the smooth background of the single-particle pre-equilibrium model. For example, many 14 MeV inelastic neutron spectra show a little hump at excitation energies around 6-10 MeV. This structure is due to collective excitations of the nucleus that are known as giant resonances [83, 84]. We use a macroscopic, phenomenological model to describe giant resonances in the inelastic channel. For each multipolarity, an energy weighted sum rule (EWSR) S_ℓ applies,

$$S_\ell = \sum_i E_{\ell,i}\beta^2_{\ell,i} = 57.5A^{-5/3}l(2l+1) \quad \text{MeV}, \tag{4.47}$$

where $E_{\ell,i}$ is the excitation energy of the i-th state with multipolarity ℓ. The summation includes all the low-lying collective states, for each ℓ, that have already been included in the coupled-channels or DWBA formalism. The EWSR thus determines the remaining collective strength that is spread over the continuum. Our treatment is phenomenological in the sense that we perform a DWBA calculation with ECIS-06 for each giant resonance state and spread the cross section over the continuum with a Gaussian distribution. The central excitation energy for these states and the spreading width is different for each multipolarity and has been empirically determined. For the giant monopole resonance (GMR) EWSR we have

$$S_0 = 23A^{-5/3} \quad \text{MeV}, \tag{4.48}$$

with excitation energy and width

$$E_{0,GMR} = 18.7 - 0.025A \quad \text{MeV}, \quad \Gamma_{GMR} = 3 \quad \text{MeV}. \tag{4.49}$$

The EWSR for the giant quadrupole resonance (GQR) is

$$S_2 = 575A^{-5/3}\text{MeV}, \tag{4.50}$$

with

$$E_{0,GQR} = 65A^{-1/3}\text{MeV}, \quad \Gamma_{GQR} = 85A^{-2/3}\text{MeV}. \tag{4.51}$$

The EWSR for the giant octupole resonance is

$$S_3 = 1208A^{-5/3}\text{MeV}, \tag{4.52}$$

which has a low-energy (LEOR) and a high-energy (HEOR) component. Following Kalbach [84], we assume

$$S_{3,LEOR} = 0.3S_3, \quad S_{3,HEOR} = 0.7S_3, \tag{4.53}$$

with excitation energy and width

$$E_{0,LEOR} = 31A^{-1/3}\text{MeV}, \quad \Gamma_{LEOR} = 5\text{MeV}, \tag{4.54}$$

and

$$E_{0,HEOR} = 115A^{-1/3}\text{MeV}, \quad \Gamma_{HEOR} = 9.3 - A/48\text{MeV}, \tag{4.55}$$

respectively. We also take as width for the actual Gaussian distribution $\Gamma_{Gauss} = 0.42\Gamma_\ell$.

The contribution from giant resonances is automatically included in the total inelastic cross section. The effect is most noticeable in the single- and double-differential energy spectra.

4.3 Gamma-ray transmission coefficients

Gamma-ray transmission coefficients are important for the description of the gamma emission channel in nuclear reactions. This is an almost universal channel since gamma rays, in general, may accompany emission of any other emitted particle. Like the particle transmission coefficients that emerge from the optical model, gamma-ray transmission coefficients enter the Hauser-Feshbach model for the calculation of the competition of photons with other particles.

The gamma-ray transmission coefficient for multipolarity ℓ of type X (where $X = M$ or E) is given by

$$T_{X\ell}(E_\gamma) = 2\pi f_{X\ell}(E_\gamma)E_\gamma^{2\ell+1}, \tag{4.56}$$

where E_γ denotes the gamma energy and $f_{X\ell}(E_\gamma)$ is the energy-dependent gamma-ray strength function.

4.3.1 Gamma-ray strength functions

We have included 4 models for the gamma-ray strength function. The first is the so-called Brink-Axel option [85], in which a standard Lorentzian form describes the giant dipole resonance shape, i.e.

$$f_{X\ell}(E_\gamma) = K_{X\ell}\frac{\sigma_{X\ell}E_\gamma\Gamma_{X\ell}^2}{(E_\gamma^2 - E_{X\ell}^2)^2 + E_\gamma^2\Gamma_{X\ell}^2}, \tag{4.57}$$

where $\sigma_{X\ell}, E_{X\ell}$ and $\Gamma_{X\ell}$ are the strength, energy and width of the giant resonance, respectively, and

$$K_{X\ell} = \frac{1}{(2\ell+1)\pi^2\hbar^2c^2}. \tag{4.58}$$

At present, we use the Brink-Axel option for all transition types other than $E1$. For $E1$ radiation, the default option used in TALYS is the generalized Lorentzian form of Kopecky and Uhl [86],

$$f_{E1}(E_\gamma, T) = K_{E1}\left[\frac{E_\gamma\tilde{\Gamma}_{E1}(E_\gamma)}{(E_\gamma^2 - E_{E1}^2)^2 + E_\gamma^2\tilde{\Gamma}_{E1}(E_\gamma)^2} + \frac{0.7\Gamma_{E1}4\pi^2T^2}{E_{E1}^3}\right]\sigma_{E1}\Gamma_{E1}, \tag{4.59}$$

where the energy-dependent damping width $\tilde{\Gamma}(E_\gamma)$ is given by

$$\tilde{\Gamma}_{E1}(E_\gamma) = \Gamma_{E1}\frac{E_\gamma^2 + 4\pi^2T^2}{E_{E1}^2}, \tag{4.60}$$

and T is the nuclear temperature given by[87]

$$T = \sqrt{\frac{E_n + S_n - \Delta - E_\gamma}{a(S_n)}}, \tag{4.61}$$

where S_n is the neutron separation energy, E_n the incident neutron energy, Δ the pairing correction (see the Section on level densities) and a the level density parameter at S_n.

For $E1$-transitions, GDR parameters for various individual nuclides exist. These are stored in the nuclear structure database of TALYS, see Chapter 5. Certain nuclides have a split GDR, i.e. a second set of Lorentzian parameters. For these cases, the incoherent sum of two strength functions is taken. For all transitions other than $E1$, systematic formulae compiled by Kopecky [56], for the resonance parameters are used. For $E1$ transitions for which no tabulated data exist, we use

$$\sigma_{E1} = 1.2{\times}120NZ/(A\pi\Gamma_{E1}) \text{ mb}, \quad E_{E1} = 31.2A^{-1/3}{+}20.6A^{-1/6} \text{ MeV}, \quad \Gamma_{E1} = 0.026E_{E1}^{1.91} \text{ MeV}. \tag{4.62}$$

For $E2$ transitions we use

$$\sigma_{E2} = 0.00014Z^2E_{E2}/(A^{1/3}\Gamma_{E2}) \text{ mb}, \quad E_{E2} = 63.A^{-1/3} \text{ MeV}, \quad \Gamma_{E2} = 6.11 - 0.012A \text{ MeV}. \tag{4.63}$$

For multipole radiation higher than $E2$, we use

$$\sigma_{E\ell} = 8.10^{-4}\sigma_{E(\ell-1)}, \quad E_{E\ell} = E_{E(\ell-1)} \quad \Gamma_{E\ell} = \Gamma_{E(\ell-1)}, \tag{4.64}$$

For $M1$ transitions we use

$$f_{M1} = 1.58A^{0.47} \text{ at } 7 \text{ MeV}, \quad E_{M1} = 41.A^{-1/3} \text{ MeV}, \quad \Gamma_{M1} = 4 \text{ MeV}, \tag{4.65}$$

where Eq. (4.57) thus needs to be applied at 7 MeV to obtain the σ_{M1} value. For multipole radiation higher than $M1$, we use

$$\sigma_{M\ell} = 8.10^{-4}\sigma_{M(\ell-1)}, \quad E_{M\ell} = E_{M(\ell-1)} \quad \Gamma_{M\ell} = \Gamma_{M(\ell-1)}, \tag{4.66}$$

For all cases, the systematics can be overruled with user-defined input parameters.

Finally, there are also two microscopic options for $E1$ radiation. Stephane Goriely calculated gamma-ray strength functions according to the Hartree-Fock BCS model (**strength 3**) and the Hartree-Fock-Bogolyubov model (**strength 4**), see also Ref. [56]. Since these microscopical strenght functions, which we will call $f_{\rm HFM}$, have not been adjusted to experimental data, we add adjustment flexibility through a scaling function, i.e.

$$f_{E1}(E_\gamma) = f^{nor} f_{HFM}(E_\gamma + E_{\rm shift}) \tag{4.67}$$

where by default $f^{nor} = 1$ and $E_{\rm shift} = 0$ (i.e. unaltered values from the tables). The energy shift $E_{\rm shift}$ simply implies obtaining the level density from the table at a different energy. Adjusting f^{not} and $E_{\rm shift}$ together gives enough adjustment flexibility.

4.3.2 Renormalization of gamma-ray strength functions

At sufficiently low incident neutron energies, the average radiative capture width Γ_γ is due entirely to the s-wave interaction, and it is Γ_γ at the neutron separation energy S_n that is often used to normalize gamma-ray transmission coefficients [88]. The Γ_γ values are, when available, read from our nuclear structure database. For nuclides for which no experimental value is available, we use an interpolation table by Kopecky [89] for $40 < A < 250$, the simple form

$$\Gamma_\gamma = 1593/A^2 \ \ {\rm eV}, \tag{4.68}$$

for $A > 250$, while we apply no gamma normalization for $A < 40$.

The s-wave radiation width may be obtained by integrating the gamma-ray transmission coefficients over the density of final states that may be reached in the first step of the gamma-ray cascade. The normalization is then carried out as follows

$$\frac{2\pi\Gamma_\gamma}{D_0} = G_{norm} \sum_J \sum_\Pi \sum_{X\ell} \sum_{I'=|J-\ell|}^{J+\ell} \sum_{\Pi'} \int_0^{S_n} dE_\gamma T_{X\ell}(E_\gamma) \rho(S_n - E_\gamma, I', \Pi') f(X, \Pi', \ell), \tag{4.69}$$

where D_0 is the average resonance spacing and ρ is the level density. The J,Π sum is over the compound nucleus states with spin J and parity Π that can be formed with s-wave incident particles, and I',Π' denote the spin and parity of the final states. The multipole selection rules are $f(E,\Pi',\ell) = 1$ if $\Pi = \Pi'(-1)^\ell$, $f(M,\Pi',\ell) = 1$ if $\Pi = \Pi'(-1)^{\ell+1}$, and 0 otherwise. It is understood that the integral over dE_γ includes a summation over discrete states. G_{norm} is the normalization factor that ensures the equality (4.69). In practice, the transmission coefficients (4.56) are thus multiplied by G_{norm} before they enter the nuclear reaction calculation. G_{norm} can be specified by the user. The default is the value returned by Eq. (4.69). If $G_{norm} = 1$ is specified, no normalization is carried out and strength functions purely determined from giant resonance parameters are taken. Other values can be entered for G_{norm}, e.g. for fitting of the neutron capture cross section. Normalisation per multipolarity can be performed by adjusting the $\sigma_{X\ell}$ values in the input, see Chapter 6.

4.3.3 Photoabsorption cross section

TALYS requires photo-absorption cross sections for photo-nuclear reactions and for pre-equilibrium gamma-ray emission. Following Chadwick et al. [90], the photo-absorption cross section is given by

$$\sigma_{abs}(E_\gamma) = \sigma_{GDR}(E_\gamma) + \sigma_{QD}(E_\gamma). \tag{4.70}$$

The GDR component is related to the strength functions outlined above. It is given by

$$\sigma_{GDR}(E_\gamma) = \sum_i \sigma_{E1} \frac{(E_\gamma \Gamma_{E1,i})^2}{(E_\gamma^2 - E_{E1,i}^2)^2 + E_\gamma^2 \Gamma_{E1,i}^2}, \tag{4.71}$$

where the parameters where specified in the previous subsection. The sum over i is over the number of parts into which the GDR is split.

The quasi-deuteron component σ_{QD} is given by

$$\sigma_{QD}(E_\gamma) = L \frac{NZ}{A} \sigma_d(E_\gamma) f(E_\gamma). \tag{4.72}$$

Here, $\sigma_d(E_\gamma)$ is the experimental deuteron photo-disintegration cross section, parameterized as

$$\sigma_d(E_\gamma) = 61.2 \frac{(E_\gamma - 2.224)^{3/2}}{E_\gamma^3}, \tag{4.73}$$

for $E_\gamma > 2.224$ MeV and zero otherwise. The so-called Levinger parameter is $L = 6.5$ and the Pauli-blocking function is approximated by the polynomial expression

$$f(E_\gamma) = 8.3714.10^{-2} - 9.8343.10^{-3} E_\gamma + 4.1222.10^{-4} E_\gamma^2 - 3.4762.10^{-6} E_\gamma^3 + 9.3537.10^{-9} E_\gamma^4 \tag{4.74}$$

for $20 < E_\gamma < 140$ MeV,

$$f(E_\gamma) = \exp(-73.3/E_\gamma) \tag{4.75}$$

for $E_\gamma < 20$ MeV, and

$$f(E_\gamma) = \exp(-24.2348/E_\gamma) \tag{4.76}$$

for $E_\gamma > 140$ MeV.

4.4 Pre-equilibrium reactions

It is now well-known that the separation of nuclear reaction mechanisms into direct and compound is too simplistic. As Fig. 3.2 shows, the cross section as predicted by the pure compound process is too small with respect to measured continuum spectra, and the direct processes described in the previous section only excite the discrete levels at the highest outgoing energies. Furthermore, the measured angular distributions in the region between direct and compound are anisotropic, indicating the existence of a memory-preserving, direct-like reaction process. Apparently, as an intermediate between the two extremes, there exists a reaction type that embodies both direct- and compound-like features. These reactions are referred to as *pre-equilibrium, precompound* or, when discussed in a quantum-mechanical context, *multi-step processes*. Pre-equilibrium emission takes place after the first stage of the reaction but long before statistical equilibrium of the compound nucleus is attained. It is imagined that the incident particle step-by-step creates more complex states in the compound system and gradually loses its memory of the initial energy and direction. Pre-equilibrium processes cover a sizable part of the reaction cross section for incident energies between 10 and (at least) 200 MeV. Pre-equilibrium reactions have been modeled both classically and quantum-mechanically and both are included in TALYS.

4.4.1 Exciton model

In the exciton model (see Refs. [10, 91, 92] for extensive reviews), the nuclear state is characterized at any moment during the reaction by the total energy E^{tot} and the total number of particles above and holes below the Fermi surface. Particles (p) and holes (h) are indiscriminately referred to as excitons. Furthermore, it is assumed that all possible ways of sharing the excitation energy between different particle-hole configurations with the same exciton number $n = p + h$ have equal a-priori probability. To keep track of the evolution of the scattering process, one merely traces the temporal development of the exciton number, which changes in time as a result of intranuclear two-body collisions. The basic starting point of the exciton model is a time-dependent master equation, which describes the probability of transitions to more and less complex particle-hole states as well as transitions to the continuum (emission). Upon integration over time, the energy-averaged emission spectrum is obtained. These assumptions makes the exciton model amenable for practical calculations. The price to be paid, however, is the introduction of a free parameter, namely the average matrix element of the residual two-body interaction, occurring in the transition rates between two exciton states. When this matrix element is properly parameterized, a very powerful model is obtained.

Qualitatively, the equilibration process of the excited nucleus is imagined to proceed as follows, see Fig. 4.2. After entering the target nucleus, the incident particle collides with one of the nucleons of the Fermi sea, with depth E_F. The formed state with $n = 3$ (2p1h), in the case of a nucleon-induced reaction, is the first that is subject to particle emission, confirming the picture of the exciton model as a compound-like model rather than a direct-like model. Subsequent interactions result in changes in the number of excitons, characterized by $\Delta n = +2$ (a new particle-hole pair) or $\Delta n = -2$ (annihilation of a particle-hole pair) or $\Delta n = 0$ (creation of a different configuration with the same exciton number). In the first stage of the process, corresponding to low exciton numbers, the $\Delta n = +2$ transitions are predominant. Apart from transitions to more complex or less complex exciton states, at any stage there is a non-zero probability that a particle is emitted. Should this happen at an early stage, it is intuitively clear that the emitted particle retains some "memory" of the incident energy and direction: the hypothesis of a fully equilibrated compound nucleus is not valid. This phase is called the pre-equilibrium phase, and it is responsible for the experimentally observed high-energy tails and forward-peaked angular distributions. If emission does not occur at an early stage, the system eventually reaches a (quasi-) equilibrium. The equilibrium situation, corresponding to high exciton numbers, is established after a large number of interactions, i.e. after a long lapse of time, and the system has "forgotten" about the initial state. Accordingly, this stage may be called the compound or evaporation stage. Hence, in principle the exciton model enables to compute the emission cross sections in a unified way, without introducing adjustments between equilibrium and pre-equilibrium contributions. However, in practical cases it turns out that it is simpler and even more accurate to distinguish between a pre-equilibrium and an equilibrium phase and to perform the latter with the usual Hauser-Feshbach formalism. This is the approach followed in TALYS.

Two versions of the exciton model are implemented in TALYS: The default is the two-component model in which the neutron or proton types of particles and holes are followed throughout the reaction. We describe this model first, and then discuss the simpler, and more generally known, one-component model which is also implemented as an option. The following Section contains basically the most important equations of the recent exciton model study of [10].

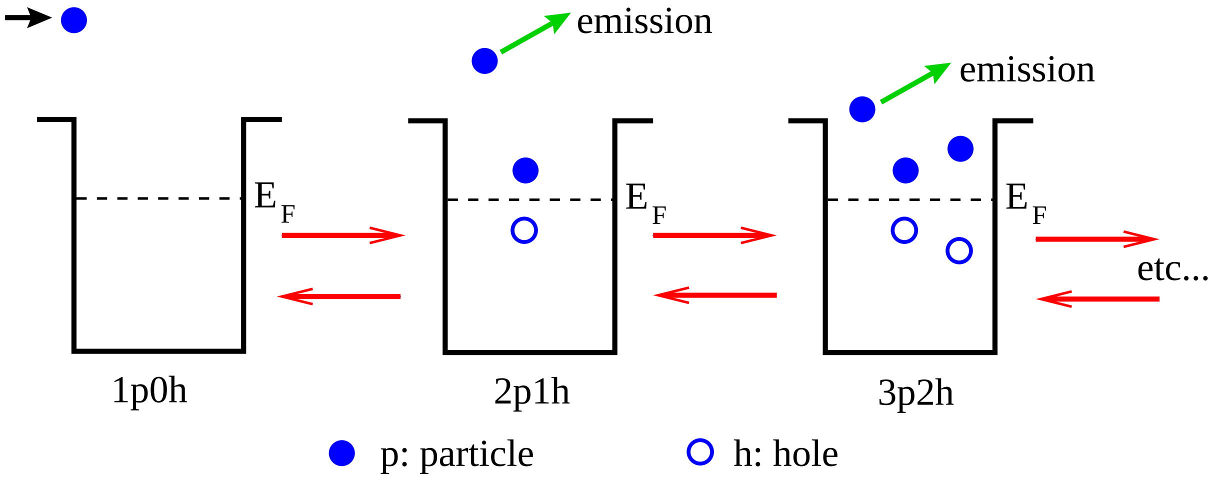

Figure 4.2: Reaction flow in exciton model

Two-component exciton model

In the following reaction equations, we use a notation in which p_π (p_ν) is the proton (neutron) particle number and h_π (h_ν) the proton (neutron) hole number. From this, we define the proton exciton number $n_\pi = p_\pi + h_\pi$ and the neutron exciton number $n_\nu = p_\nu + h_\nu$. From this, we can construct the charge-independent particle number $p = p_\pi + p_\nu$, the hole number $h = h_\pi + h_\nu$ and the exciton number $n = n_\pi + n_\nu$.

The temporal development of the system can be described by a master equation, describing the gain and loss terms for a particular class of exciton states, see [10]. Integrating the master equation over time up to the equilibration time τ_{eq} yields the mean lifetime of the exciton state τ that can be used to calculate the differential cross section [93]. The primary pre-equilibrium differential cross section for the emission of a particle k with emission energy E_k can then be expressed in terms of τ, the composite-nucleus formation cross section $\sigma^{\rm CF}$, and an emission rate W_k,

$$\begin{aligned} \frac{d\sigma_k^{\rm PE}}{dE_k} &= \sigma^{\rm CF} \sum_{p_\pi = p_\pi^0}^{p_\pi^{\max}} \sum_{p_\nu = p_\nu^0}^{p_\nu^{\max}} W_k(p_\pi, h_\pi, p_\nu, h_\nu, E_k)\tau(p_\pi, h_\pi, p_\nu, h_\nu) \\ &\times P(p_\pi, h_\pi, p_\nu, h_\nu), \end{aligned} \tag{4.77}$$

where the factor P represents the part of the pre-equilibrium population that has survived emission from the previous states and now passes through the $(p_\pi, h_\pi, p_\nu, h_\nu)$ configurations, averaged over time. Expressions for all quantities appearing in this expression will be detailed in the rest of this Section. The initial proton and neutron particle numbers are $p_\pi^0 = Z_p$, and $p_\nu^0 = N_p$, respectively with Z_p (N_p) the proton (neutron) number of the projectile. For any exciton state in the reaction process, $h_\pi = p_\pi - p_\pi^0$ and $h_\nu = p_\nu - p_\nu^0$, so that for primary pre-equilibrium emission the initial hole numbers are $h_\pi^0 = h_\nu^0 = 0$. For e.g. a neutron-induced reaction, the initial exciton number is given by $n^0 = n_\nu^0 = 1$ ($0p_\pi 0h_\pi 1p_\nu 0h_\nu$), but only pre-equilibrium gamma emission can occur from this state (nucleon emission from this state is essentially elastic scattering and this is already covered by the optical model). Particle emission only occurs from $n = 3$ ($2p1h$) and higher exciton states. We use a hardwired value of $p_\pi^{\max} = p_\nu^{\max} = 6$ as the upper limit of the summation, see [10]. We use the never-come-back approximation, i.e. throughout the cascade one neglects the interactions that decrease the exciton number, although the adopted solution of Eq. (4.77) does include transitions that convert a proton particle-hole pair into a neutron pair and vice versa. The maximum values $p_\pi^{\max}$ and $p_\nu^{\max}$ thus entail an automatic separation of the pre-equilibrium population and the compound nucleus population. The latter is then handled by the more adequate Hauser-Feshbach mechanism. We now discuss the various ingredients of Eq. (4.77).

A. Reaction cross sections The basic feeding term for pre-equilibrium emission is the compound formation cross section σ^{CF}, which is given by

$$\sigma^{\mathrm{CF}} = \sigma_{\mathrm{reac}} - \sigma_{\mathrm{direct}}, \tag{4.78}$$

where the reaction cross section σ_{reac} is directly obtained from the optical model and σ_{direct} is the sum of the cross sections for direct reactions to discrete states $\sigma^{disc,direct}$ as defined in Eq. (3.18), and for giant resonances, see Section 4.2.4.

B. Emission rates and particle-hole state densities The emission rate W_k has been derived by Cline and Blann [94] from the principle of microreversibility, and can easily be generalized to a two-component version [95]. The emission rate for an ejectile k with relative mass μ_k and spin s_k is

$$\begin{aligned} W_k(p_\pi, h_\pi, p_\nu, h_\nu, E_k) &= \frac{2s_k+1}{\pi^2\hbar^3}\mu_k E_k \sigma_{k,\mathrm{inv}}(E_k) \\ &\times \frac{\omega(p_\pi - Z_k, h_\pi, p_\nu - N_k, h_\nu, E^{\mathrm{tot}} - E_k)}{\omega(p_\pi, h_\pi, p_\nu, h_\nu, E^{\mathrm{tot}})}, \end{aligned} \tag{4.79}$$

where $\sigma_{k,\mathrm{inv}}(E_k)$ is the inverse reaction cross section, again calculated with the optical model, Z_k (N_k) is the charge (neutron) number of the ejectile and E^{tot} is the total energy of the composite system.

For the particle-hole state density $\omega(p_\pi, h_\pi, p_\nu, h_\nu, E_x)$ we use the expression of Běták and Dobeš [95, 96]. Their formula is based on the assumption of equidistant level spacing and is corrected for the effect of the Pauli exclusion principle and for the finite depth of the potential well. The two-component particle-hole state density is

$$\begin{aligned} \omega(p_\pi, h_\pi, p_\nu, h_\nu, E_x) &= \frac{g_\pi^{n_\pi} g_\nu^{n_\nu}}{p_\pi! h_\pi! p_\nu! h_\nu! (n-1)!}(U - A(p_\pi, h_\pi, p_\nu, h_\nu))^{n-1} \\ &\times f(p, h, U, V), \end{aligned} \tag{4.80}$$

where g_π and g_ν are the single-particle state densities, A the Pauli correction, f the finite well function, and $U = E_x - P_{p,h}$ with $P_{p,h}$ Fu's pairing correction [97],

$$\begin{aligned} P_{p,h} &= \Delta - \Delta \left[0.996 - 1.76\left(\frac{n}{n_{\mathrm{crit}}}\right)^{1.6}\left(\frac{E_x}{\Delta}\right)^{0.68}\right]^2 \\ & \quad \text{if} \quad E_x/\Delta \geq 0.716 + 2.44\left(\frac{n}{n_{\mathrm{crit}}}\right)^{2.17}, \\ &= \Delta \quad \text{otherwise}, \end{aligned} \tag{4.81}$$

with

$$n_{\rm crit} = 2gT_{\rm crit}\ln 2, \tag{4.82}$$

where $T_{\rm crit} = 2\sqrt{\Delta/\frac{1}{4}g}/3.5$ and $g = g_\pi + g_\nu$. The pairing energy Δ for total level densities is given by

$$\Delta = \chi\frac{12}{\sqrt{A}}, \tag{4.83}$$

where here A is the mass number and $\chi = 0, 1$ or 2 for odd-odd, odd or even-even nuclei. The Pauli correction term is given by

$$\begin{aligned} A(p_\pi, h_\pi, p_\nu, h_\nu) &= \frac{[\max(p_\pi, h_\pi)]^2}{g_\pi} + \frac{[\max(p_\nu, h_\nu)]^2}{g_\nu} \\ &- \frac{p_\pi^2 + h_\pi^2 + p_\pi + h_\pi}{4g_\pi} - \frac{p_\nu^2 + h_\nu^2 + p_\nu + h_\nu}{4g_\nu}. \end{aligned} \tag{4.84}$$

For the single-particle state densities we take

$$g_\pi = Z/15, \qquad g_\nu = N/15, \tag{4.85}$$

which is, through the relationship $g = a\pi^2/6$, in line with the values for our total level density parameter a, see Eq. (4.232), and also provides a globally better description of spectra than the generally adopted $g = A/13$.

The finite well function $f(p, h, E_x, V)$ accounts for the fact that a hole cannot have an energy below that of the bottom of the potential well depth V. It is given by

$$f(p, h, E_x, V) = 1 + \sum_{i=1}^{h}(-1)^i \begin{pmatrix} h \\ i \end{pmatrix} \left[\frac{E_x - iV}{E_x}\right]^{n-1} \Theta(E_x - iV), \tag{4.86}$$

where Θ is the unit step function. Note that f is different from 1 only for excitation energies greater than V. In the original version of Běták and Dobeš, V is given by the depth E_f of the Fermi well. This was generalized by Kalbach [98, 84] to obtain an effective method to include surface effects in the first stage of the interaction, leading to a harder pre-equilibrium spectrum. For the first stage the maximum depth of the hole should be significantly reduced, since in the surface region the potential is shallower than in the interior. This automatically leaves more energy to be adopted by the excited particle, yielding more emission at the highest outgoing energies. We use the following functional form for V in terms of the projectile energy E_p and the mass A,

$$\begin{aligned} V &= 22 + 16\frac{E_p^4}{E_p^4 + (450/A^{1/3})^4}\ \text{MeV for } h = 1 \text{ and incident protons,} \\ V &= 12 + 26\frac{E_p^4}{E_p^4 + (245/A^{1/3})^4}\ \text{MeV for } h = 1 \text{ and incident neutrons,} \\ V &= E_f = 38\ \text{MeV for } h > 1. \end{aligned} \tag{4.87}$$

See Ref. [10] for a further justification of this parameterisation.

C. Lifetimes The lifetime τ of exciton state $(p_\pi, h_\pi, p_\nu, h_\nu)$ in Eq. (4.77) is defined as the inverse sum of the total emission rate and the various internal transition rates,

$$\tau(p_\pi, h_\pi, p_\nu, h_\nu) = [\lambda_\pi^+(p_\pi, h_\pi, p_\nu, h_\nu) + \lambda_\nu^+(p_\pi, h_\pi, p_\nu, h_\nu) + \lambda_{\pi\nu}^0(p_\pi, h_\pi, p_\nu, h_\nu) + \lambda_{\nu\pi}^0(p_\pi, h_\pi, p_\nu, h_\nu) + W(p_\pi, h_\pi, p_\nu, h_\nu)]^{-1}, \tag{4.88}$$

where λ_π^+ (λ_ν^+) is the internal transition rate for proton (neutron) particle-hole pair creation, $\lambda_{\pi\nu}^0$ $(\lambda_{\nu\pi}^0)$ is the rate for the conversion of a proton (neutron) particle-hole pair into a neutron (proton) particle-hole pair, and λ_π^- (λ_ν^-) is the rate for particle-hole annihilation. These transition rates will be discussed in Sec. 4.4.1. The total emission rate W is the integral of Eq. (4.79) over all outgoing energies, summed over all outgoing particles,

$$W(p_\pi, h_\pi, p_\nu, h_\nu) = \sum_{k=\gamma,n,p,d,t,h,\alpha} \int dE_k W_k(p_\pi, h_\pi, p_\nu, h_\nu, E_k). \tag{4.89}$$

The final ingredient of the exciton model equation, Eq. (4.77), is the part of the pre-equilibrium population P that has survived emission from all previous steps and has arrived at the exciton state $(p_\pi, h_\pi, p_\nu, h_\nu)$. The expression for P is somewhat more complicated than that of the depletion factor that appears in the one-component exciton model [92]. For two components, contributions from both particle creation *and* charge exchange reactions need to be taken into account, whereas transitions that do not change the exciton number cancel out in the one-component model.

For the $(p_\pi, h_\pi, p_\nu, h_\nu)$ state, P is given by a recursive relation:

$$\begin{aligned} P(p_\pi, h_\pi, p_\nu, h_\nu) &= P(p_\pi-1, h_\pi-1, p_\nu, h_\nu)\Gamma_\pi^+(p_\pi-1, h_\pi-1, p_\nu, h_\nu) && (A) \\ &+ P(p_\pi, h_\pi, p_\nu-1, h_\nu-1)\Gamma_\nu^+(p_\pi, h_\pi, p_\nu-1, h_\nu-1) && (B) \\ &+ [P(p_\pi-2, h_\pi-2, p_\nu+1, h_\nu+1)\Gamma_\pi'^+(p_\pi-2, h_\pi-2, p_\nu+1, h_\nu+1) \\ &+ P(p_\pi-1, h_\pi-1, p_\nu, h_\nu)\Gamma_\nu'^+(p_\pi-1, h_\pi-1, p_\nu, h_\nu)] \\ &\times \Gamma_{\nu\pi}^0(p_\pi-1, h_\pi-1, p_\nu+1, h_\nu+1) && (C+D) \\ &+ [P(p_\pi, h_\pi, p_\nu-1, h_\nu-1)\Gamma_\pi'^+(p_\pi, h_\pi, p_\nu-1, h_\nu-1) \\ &+ P(p_\pi+1, h_\pi+1, p_\nu-2, h_\nu-2)\Gamma_\nu'^+(p_\pi+1, h_\pi+1, p_\nu-2, h_\nu-2)] \\ &\times \Gamma_{\pi\nu}^0(p_\pi+1, h_\pi+1, p_\nu-1, h_\nu-1) && (E+F). \end{aligned} \tag{4.90}$$

This relation contains 6 distinct feeding terms: (A) creation of a proton particle-hole pair from the $(p_\pi-1, h_\pi-1, p_\nu, h_\nu)$ state, (C) creation of a proton particle-hole pair from the $(p_\pi-2, h_\pi-2, p_\nu+1, h_\nu+1)$ state followed by the conversion of a neutron particle-hole pair into a proton particle-hole pair, and (D) creation of a neutron particle-hole pair from the $(p_\pi-1, h_\pi-1, p_\nu, h_\nu)$ state followed by its conversion into a proton particle-hole pair. The three remaining terms (B), (E), and (F) are obtained by changing protons into neutrons and vice versa. The probabilities of creating new proton or neutron particle-hole pairs and for converting a proton (neutron) pair into a neutron (proton) pair are calculated as follows:

$$\begin{aligned} \Gamma_\pi^+(p_\pi, h_\pi, p_\nu, h_\nu) &= \lambda_\pi^+(p_\pi, h_\pi, p_\nu, h_\nu)\tau(p_\pi, h_\pi, p_\nu, h_\nu), \\ \Gamma_\nu^+(p_\pi, h_\pi, p_\nu, h_\nu) &= \lambda_\nu^+(p_\pi, h_\pi, p_\nu, h_\nu)\tau(p_\pi, h_\pi, p_\nu, h_\nu), \end{aligned}$$

$$\begin{aligned}
\Gamma'^{+}_{\pi}(p_\pi,h_\pi,p_\nu,h_\nu) &= \lambda^{+}_{\pi}(p_\pi,h_\pi,p_\nu,h_\nu)\tau'(p_\pi,h_\pi,p_\nu,h_\nu),\\
\Gamma'^{+}_{\nu}(p_\pi,h_\pi,p_\nu,h_\nu) &= \lambda^{+}_{\nu}(p_\pi,h_\pi,p_\nu,h_\nu)\tau'(p_\pi,h_\pi,p_\nu,h_\nu),\\
\Gamma^{0}_{\pi\nu}(p_\pi,h_\pi,p_\nu,h_\nu) &= \lambda^{0}_{\pi\nu}(p_\pi,h_\pi,p_\nu,h_\nu)\tau(p_\pi,h_\pi,p_\nu,h_\nu),\\
\Gamma^{0}_{\nu\pi}(p_\pi,h_\pi,p_\nu,h_\nu) &= \lambda^{0}_{\nu\pi}(p_\pi,h_\pi,p_\nu,h_\nu)\tau(p_\pi,h_\pi,p_\nu,h_\nu),\\
\tau'(p_\pi,h_\pi,p_\nu,h_\nu) &= [\lambda^{+}_{\pi}(p_\pi,h_\pi,p_\nu,h_\nu)+\lambda^{+}_{\nu}(p_\pi,h_\pi,p_\nu,h_\nu)\\
&+ W(p_\pi,h_\pi,p_\nu,h_\nu)]^{-1}.
\end{aligned} \tag{4.91}$$

The use of τ' in the probability Γ'^{+}_{π} (Γ'^{+}_{ν}), to create a new proton (neutron) particle-hole pair preceding an exchange interaction, originates from the approximation that only one exchange interaction is allowed in each pair-creation step. The appropriate lifetime in this case consists merely of pair creation and emission rates [93].

The initial condition for the recursive equations is

$$P(p^0_\pi,h^0_\pi,p^0_\nu,h^0_\nu)=1, \tag{4.92}$$

after which P can be solved for any configuration.

To calculate the pre-equilibrium spectrum, the only quantities left to determine are the internal transition rates λ^{+}_{π}, λ^{+}_{ν}, $\lambda^{0}_{\pi\nu}$ and $\lambda^{0}_{\nu\pi}$.

D. Internal transition rates The transition rate λ^{+}_{π} for the creation of a proton particle-hole pair is given by four terms, accounting for p_π, h_π, p_ν and h_ν scattering that leads to a new (p_π,h_π) pair,

$$\begin{aligned}
\lambda^{+}_{\pi}(p_\pi,h_\pi,p_\nu,h_\nu) &= \frac{1}{\omega(p_\pi,h_\pi,p_\nu,h_\nu,E^{\rm tot})}\\
[& \int_{L_1^{p\pi}}^{L_2^{p\pi}} \lambda^{1p}_{\pi\pi}(u)\omega(p_\pi-1,h_\pi,p_\nu,h_\nu,E^{\rm tot}-u)\omega(1,0,0,0,u)du\\
+ & \int_{L_1^{h\pi}}^{L_2^{h\pi}} \lambda^{1h}_{\pi\pi}(u)\omega(p_\pi,h_\pi-1,p_\nu,h_\nu,E^{\rm tot}-u)\omega(0,1,0,0,u)du\\
+ & \int_{L_1^{p\nu}}^{L_2^{p\nu}} \lambda^{1p}_{\nu\pi}(u)\omega(p_\pi,h_\pi,p_\nu-1,h_\nu,E^{\rm tot}-u)\omega(0,0,1,0,u)du\\
+ & \int_{L_1^{h\nu}}^{L_2^{h\nu}} \lambda^{1h}_{\nu\pi}(u)\omega(p_\pi,h_\pi,p_\nu,h_\nu-1,E^{\rm tot}-u)\omega(0,0,0,1,u)du],
\end{aligned} \tag{4.93}$$

where the first and third term represent particle scattering and the second and fourth term hole scattering. The integration limits correct for the Pauli exclusion principle,

$$\begin{aligned}
L_1^{p\pi} &= A(p_\pi+1,h_\pi+1,p_\nu,h_\nu)-A(p_\pi-1,h_\pi,p_\nu,h_\nu),\\
L_2^{p\pi} &= E^{\rm tot}-A(p_\pi-1,h_\pi,p_\nu,h_\nu),\\
L_1^{h\pi} &= A(p_\pi+1,h_\pi+1,p_\nu,h_\nu)-A(p_\pi,h_\pi-1,p_\nu,h_\nu),\\
L_2^{h\pi} &= E^{\rm tot}-A(p_\pi,h_\pi-1,p_\nu,h_\nu),\\
L_1^{p\nu} &= A(p_\pi,h_\pi,p_\nu+1,h_\nu+1)-A(p_\pi,h_\pi,p_\nu-1,h_\nu),
\end{aligned}$$

$$\begin{aligned}
L_2^{p\nu} &= E^{\rm tot} - A(p_\pi, h_\pi, p_\nu - 1, h_\nu), \\
L_1^{h\nu} &= A(p_\pi + 1, h_\pi + 1, p_\nu, h_\nu) - A(p_\pi, h_\pi, p_\nu, h_\nu - 1), \\
L_2^{h\nu} &= E^{\rm tot} - A(p_\pi, h_\pi, p_\nu, h_\nu - 1),
\end{aligned} \tag{4.94}$$

which demands that (a) the minimal energy available to the scattering particle or hole creating a new particle-hole pair equals the Pauli energy of the final state minus the Pauli energy of the inactive particles and holes not involved in the scattering process, and (b) the maximal energy available equals the total excitation energy minus the latter Pauli energy.

The term $\lambda^{1p}_{\pi\pi}(u)$ is the collision probability per unit time for a proton-proton interaction leading to an additional proton particle-hole pair. In general, the corresponding term for a hole is obtained by relating it to the particle collision probability through the accessible state density of the interacting particles and holes,

$$\lambda^{1h}_{\pi\pi}(u) = \lambda^{1p}_{\pi\pi}(u)\frac{\omega(1,2,0,0,u)}{\omega(2,1,0,0,u)}. \tag{4.95}$$

Similarly, $\lambda^{1p}_{\nu\pi}(u)$ is the collision probability per unit time for a neutron-proton interaction leading to an additional proton particle-hole pair, and for the corresponding hole term we have

$$\lambda^{1h}_{\nu\pi}(u) = \lambda^{1p}_{\nu\pi}(u)\frac{\omega(1,1,0,1,u)}{\omega(1,1,1,0,u)}. \tag{4.96}$$

The transition rate for conversion of a proton particle-hole pair into a neutron pair is

$$\begin{aligned}
\lambda^0_{\pi\nu}(p_\pi, h_\pi, p_\nu, h_\nu) &= \frac{1}{\omega(p_\pi, h_\pi, p_\nu, h_\nu, E^{\rm tot})}\int_{L_1^{p\pi}}^{L_2^{p\pi}} \lambda^{1p1h}_{\pi\nu}(u) \\
&\quad \omega(p_\pi - 1, h_\pi - 1, p_\nu, h_\nu, E^{\rm tot} - u)\omega(1,1,0,0,u)du,
\end{aligned} \tag{4.97}$$

with integration limits

$$\begin{aligned}
L_1^{p\pi} &= A(p_\pi, h_\pi, p_\nu, h_\nu) - A(p_\pi - 1, h_\pi - 1, p_\nu, h_\nu) \\
L_2^{p\pi} &= E^{\rm tot} - A(p_\pi - 1, h_\pi - 1, p_\nu, h_\nu).
\end{aligned} \tag{4.98}$$

The term $\lambda^{1p1h}_{\pi\nu}$ is the associated collision probability. Interchanging π and ν in Eqs. (4.93-4.98) gives the expressions for λ^+_ν, $\lambda^{1h}_{\nu\nu}$, $\lambda^{1h}_{\pi\nu}$ and $\lambda^0_{\nu\pi}$.

We distinguish between two options for the collision probabilities:

D1. Effective squared matrix element

Expressing the transition rate in terms of an effective squared matrix element has been used in many exciton model analyses. Also in TALYS, it is one of the options for our calculations and comparisons with data. The collision probabilities of Eqs. (4.93) and (4.97) are determined with the aid of Fermi's golden rule of time-dependent perturbation theory, which for a two-component model gives

$$\begin{aligned}
\lambda^{1p}_{\pi\pi}(u) &= \frac{2\pi}{\hbar}M^2_{\pi\pi}\omega(2,1,0,0,u), \\
\lambda^{1h}_{\pi\pi}(u) &= \frac{2\pi}{\hbar}M^2_{\pi\pi}\omega(1,2,0,0,u),
\end{aligned}$$

$$\begin{aligned}
\lambda^{1p}_{\nu\pi}(u) &= \frac{2\pi}{\hbar}M^2_{\nu\pi}\omega(1,1,1,0,u),\\
\lambda^{1h}_{\nu\pi}(u) &= \frac{2\pi}{\hbar}M^2_{\nu\pi}\omega(1,1,0,1,u),\\
\lambda^{1p1h}_{\pi\nu}(u) &= \frac{2\pi}{\hbar}M^2_{\pi\nu}\omega(0,0,1,1,u), \qquad (4.99)
\end{aligned}$$

where the relations (4.95)-(4.96) have been applied. Interchanging π and ν gives the expressions for $\lambda^{1p}_{\nu\nu}$, $\lambda^{1h}_{\nu\nu}$, $\lambda^{1p}_{\pi\nu}$, $\lambda^{1h}_{\pi\nu}$, and $\lambda^{1p1h}_{\nu\pi}$. Here, the $M^2_{\pi\pi}$, etc. are average squared matrix elements of the residual interaction, which are assumed to depend on the total energy $E^{\rm tot}$ of the whole composite nucleus only. Such a matrix element thus represents a truly *effective* residual interaction, whereby all individual residual interactions taking place inside the nucleus can be cast into an average form for the squared matrix element to which one assigns a global $E^{\rm tot}$-dependence a posteriori.

The average residual interaction inside the nucleus is not necessarily the same for like and unlike nucleons. The two-component matrix elements are given, in terms of an average M^2, by

$$\begin{aligned}
M^2_{\pi\pi} &= R_{\pi\pi}M^2,\\
M^2_{\nu\nu} &= R_{\nu\nu}M^2,\\
M^2_{\pi\nu} &= R_{\pi\nu}M^2,\\
M^2_{\nu\pi} &= R_{\nu\pi}M^2. \qquad (4.100)
\end{aligned}$$

In TALYS, we take

$$R_{\nu\nu} = 1.5, R_{\nu\pi} = R_{\pi\pi} = R_{\pi\nu} = 1., \qquad (4.101)$$

which is in line with the, more parameter-free, optical model based exciton model that we describe later. Note that this deviates somewhat from the parameters adopted in Ref. [10]. The current parameterization gives slightly better performance for cross section excitation functions. In TALYS, the above parameters are adjustable (**Rpinu**, etc. keywords) with Eq. (4.101) as default. The following semi-empirical expression for the squared matrix element has been shown to work for incident energies between 7 and 200 MeV [10]:

$$M^2 = \frac{C_1A_p}{A^3}\left[7.48C_2 + \frac{4.62\times10^5}{(\frac{E^{\rm tot}}{n.A_p}+10.7C_3)^3}\right]. \qquad (4.102)$$

Eq. (4.102) is a generalization of older parameterisations such as given in Refs. [93, 84], which apply in smaller (lower) energy ranges. Here C_1, C_2 and C_3 are adjustable constants (see the **M2constant**, **M2limit** and **M2shift** keywords) that are all equal to 1 by default, and A_p is the mass number of the projectile, which allows generalization for complex-particle reactions. Again, Eq. (4.102) is slightly different (10%) from the expression given in Ref. [10] to allow for better fits of excitation functions.

Finally, for matrix element based transition rates and equidistant particle-hole level densities, the integrals in the transition rates can be approximated analytically [93], giving

$$\begin{aligned}
\lambda_{\pi+}(p_\pi,h_\pi,p_\nu,h_\nu) &= \frac{2\pi}{\hbar}\frac{g^2_\pi}{2n(n+1)}\frac{\left[E^{tot}-A(p_\pi+1,h_\pi+1,p_\nu,h_\nu)\right]^{n+1}}{\left[E^{tot}-A(p_\pi,h_\pi,p_\nu,h_\nu)\right]^{n-1}}\\
&\times\ (n_\pi g_\pi M^2_{\pi\pi}+2n_\nu g_\nu M^2_{\pi\nu})f(p+1,h+1,E^{tot},V)\\
\lambda_{\nu+}(p_\pi,h_\pi,p_\nu,h_\nu) &= \frac{2\pi}{\hbar}\frac{g^2_\nu}{2n(n+1)}\frac{\left[E^{tot}-A(p_\pi,h_\pi,p_\nu+1,h_\nu+1)\right]^{n+1}}{\left[E^{tot}-A(p_\pi,h_\pi,p_\nu,h_\nu)\right]^{n-1}}
\end{aligned}$$

$$
\begin{aligned}
& \times \quad (n_\nu g_\nu M^2_{\nu\nu} + 2n_\pi g_\pi M^2_{\nu\pi}) f(p+1, h+1, E^{tot}, V) \\
\lambda_{\pi\nu}(p_\pi, h_\pi, p_\nu, h_\nu) \quad &= \quad \frac{2\pi}{\hbar} M^2_{\pi\nu} \frac{p_\pi h_\pi}{n} g_\nu^2 f(p, h, E^{tot}, V) \left[\frac{E^{tot} - B_{\pi\nu}(p_\pi, h_\pi, p_\nu, h_\nu)}{E^{tot} - A(p_\pi, h_\pi, p_\nu, h_\nu)} \right]^{n-1} \\
& \times \quad (2[E^{tot} - B_{\pi\nu}(p_\pi, h_\pi, p_\nu, h_\nu)] \\
& + \quad n|A(p_\pi, h_\pi, p_\nu, h_\nu) - A(p_\pi - 1, h_\pi - 1, p_\nu + 1, h_\nu + 1)|) \\
\lambda_{\nu\pi}(p_\pi, h_\pi, p_\nu, h_\nu) \quad &= \quad \frac{2\pi}{\hbar} M^2_{\nu\pi} \frac{p_\nu h_\nu}{n} g_\pi^2 f(p, h, E^{tot}, V) \left[\frac{E^{tot} - B_{\nu\pi}(p_\pi, h_\pi, p_\nu, h_\nu)}{E^{tot} - A(p_\pi, h_\pi, p_\nu, h_\nu)} \right]^{n-1} \\
& \times \quad (2[E^{tot} - B_{\nu\pi}(p_\pi, h_\pi, p_\nu, h_\nu)] \\
& + \quad n|A(p_\pi, h_\pi, p_\nu, h_\nu) - A(p_\pi + 1, h_\pi + 1, p_\nu - 1, h_\nu - 1)|), \qquad (4.103)
\end{aligned}
$$

with

$$
\begin{aligned}
B_{\pi\nu}(p_\pi, h_\pi, p_\nu, h_\nu) &= max[A(p_\pi, h_\pi, p_\nu, h_\nu), A(p_\pi - 1, h_\pi - 1, p_\nu + 1, h_\nu + 1)] \\
B_{\nu\pi}(p_\pi, h_\pi, p_\nu, h_\nu) &= max[A(p_\pi, h_\pi, p_\nu, h_\nu), A(p_\pi + 1, h_\pi + 1, p_\nu - 1, h_\nu - 1)]. \qquad (4.104)
\end{aligned}
$$

which is also included as an option. The default is however to use the numerical solutions for the internal transition rates. This analytical solution requires a value for M^2 that is 20% larger than that of Eq. (4.102), which apparently is the energy-averaged effect of introducing such approximations.

D2. Collision rates based on the optical model

Instead of modeling the intranuclear transition rate by an average squared matrix element, one may also relate the transition rate to the average imaginary optical model potential depth [10]. The collision probabilities, when properly averaged over all particle-hole configurations as in Eq. (4.93), in principle would yield a parameter free expression for the transition rate.

The average well depth W_i can be obtained by averaging the total imaginary part of the potential $\mathcal{W}$ over the whole volume of the nucleus

$$
W_i(E) = \frac{\int \mathcal{W}_i(r, E)\rho(r)dr}{\int \rho(r)dr}, \qquad (4.105)
$$

where ρ represents the density of nuclear matter for which we take the form factor $f(r, R, a)$ of the volume part of the optical model potential, given by the usual Woods-Saxon shape of Eq. (4.3). The total imaginary potential is given by

$$
\mathcal{W}_i(r, E) = \mathcal{W}_{V,i}(E) f(r, R_{V,i}, a_{V,i}) - 4a_{D,i}\mathcal{W}_{D,i}(E)\frac{d}{dr} f(r, R_{D,i}, a_{D,i}). \qquad (4.106)
$$

Next, we define an *effective* imaginary optical potential [10] related to nucleon-nucleon collisions in nuclear matter:

$$
W_i^{\text{eff}}(E) = C^{\text{comp}}\, W_i(E). \qquad (4.107)
$$

We use as best overall parameter

$$
C^{\text{comp}} = 0.55. \qquad (4.108)
$$

This parameter can be adjusted with the **M2constant** keyword, which serves as a multiplier for the value given in Eq. (4.108). The collision probabilities are now related as follows to the *effective* imaginary optical potential:

$$\begin{aligned}
\lambda_{\pi\pi}^{1p}(u) &= \frac{1}{4} \quad \frac{2W_p^{\rm eff}(u-S(p))}{\hbar} \\
\lambda_{\pi\pi}^{1h}(u) &= \frac{1}{4} \quad \frac{2W_p^{\rm eff}(u-S(p))}{\hbar}\frac{\omega(1,2,0,0,u)}{\omega(2,1,0,0,u)} \\
\lambda_{\nu\pi}^{1p}(u) &= \frac{3}{4} \quad \frac{2W_n^{\rm eff}(u-S(n))}{\hbar} \\
\lambda_{\nu\pi}^{1h}(u) &= \frac{3}{4} \quad \frac{2W_n^{\rm eff}(u-S(n))}{\hbar}\frac{\omega(1,1,0,1,u)}{\omega(1,1,1,0,u)} \\
\lambda_{\nu\pi}^{1p1h}(u) &= \frac{1}{2} \quad \frac{2W_n^{\rm eff}(u-S(n))}{\hbar},
\end{aligned} \tag{4.109}$$

and similarly for the components of λ_ν^+ and $\lambda_{\nu\pi}^0$. The transition rates for the exciton model are then obtained by inserting these terms in Eqs. (4.93) and (4.97). Apart from Eq. (4.108), a parameter-free model is obtained.

One-component exciton model

The one-component exciton model has been made redundant by the more flexible and physically more justified two-component model. Nevertheless, it is included as an option since it connects to many older pre-equilibrium studies and thus may be helpful as comparison. In the one-component exciton model, the pre-equilibrium spectrum for the emission of a particle k at an energy E_k is given by

$$\frac{d\sigma_k^{\rm PE}}{dE_k} = \sigma^{\rm CF}\sum_{p=p_0}^{p_{\rm max}} W_k(p,h,E_k)\tau(p,h), \tag{4.110}$$

where $p_{\rm max} = 6$ and $\sigma^{\rm CF}$ are defined as below Eq. (4.77). For the initial particle number p_0 we have $p_0 = A_p$ with A_p the mass number of the projectile. In general, the hole number $h = p - p_0$ in Eq. (4.110), so that the initial hole number is always zero, i.e. $h_0 = 0$ for primary pre-equilibrium emission.

The emission rate W_k is

$$W_k(p,h,E_k) = \frac{2s_k+1}{\pi^2\hbar^3}\mu_k E_k \sigma_{k,\rm inv}(E_k)\frac{\omega(p-A_k,h,E_{\rm tot}-E_k)}{\omega(p,h,E^{\rm tot})}Q_k(p), \tag{4.111}$$

with all quantities explained below Eq. (4.79), and A_k is the mass number of the ejectile and $Q_k(p)$ is a factor accounting for the distinguishability of neutrons and protons [99]

$$\begin{aligned}
Q_k(p) &= \frac{(p-A_k)!}{p!}\left[\sum_{p_\pi=Z_k}^{p-N_k}(\frac{Z}{A})^{n_\pi-Z_k}(\frac{A}{N})^{n_\nu-N_k}\frac{1}{h_\pi!h_\nu!}\frac{1}{(p_\pi-Z_k)!(p_\nu-N_k)!}\right] \\
&/ \quad \left[\sum_{p_\pi=Z_k}^{p-N_k}(\frac{Z}{A})^{n_\pi}(\frac{N}{A})^{n_\nu}\frac{1}{p_\pi!p_\nu!h_\pi!h_\nu!}\right].
\end{aligned} \tag{4.112}$$

For gamma's we set $Q_\gamma(p) = 1$.

Finally, $\omega(p, h, E_x)$ is the particle-hole state density for which we use the one-component expression by Běták and Dobeš [96], again corrected for the effect of the Pauli exclusion principle and for the finite depth of the potential well. The one-component particle-hole state density has a simpler form than that of Eq. (4.80),

$$\omega(p, h, E_x) = \frac{g^n}{p!h!(n-1)!}[E_x - A(p, h)]^{n-1} f(p, h, E_x, V), \tag{4.113}$$

where $g = A/15$ is the single-particle state density and

$$A(p, h) = \frac{[max(p, h)]^2}{g} - \frac{p^2 + h^2 + p + h}{4g}, \tag{4.114}$$

is the Pauli correction factor. The finite well function f is given by Eq. (4.86).

To obtain the lifetimes $\tau(p, h)$ that appear in Eq. (4.110), we first define the total emission rate $W(p, h)$ as the integral of Eq. (4.111) over all outgoing energies, summed over all outgoing particles:

$$W(p, h) = \sum_{k=\gamma,n,p,d,t,h,\alpha} \int dE_k W_k(p, h, E_k). \tag{4.115}$$

As mentioned already, we have implemented the never-come-back solution of the master equation. This is based on the assumption that at the beginning of the cascade one neglects the interactions that decrease the exciton number. Then, for the one-component model the expression for the lifetime is (see e.g. Ref. [92])

$$\tau(p, h) = \frac{1}{\lambda^+(p, h) + W(p, h)} D_{p,h}, \tag{4.116}$$

where $D_{p,h}$ is a depletion factor that accounts for the removal of reaction flux, through emission, by the previous stages

$$D_{p,h} = \prod_{p'=p_0}^{p-1} \frac{\lambda^+(p', h')}{\lambda^+(p', h') + W(p', h')}, \tag{4.117}$$

with again $h' = p' - p_0$. The initial case of Eq. (4.116) is

$$\tau(p_0, h_0) = \frac{1}{\lambda^+(p_0, h_0) + W(p_0, h_0)}. \tag{4.118}$$

To calculate the pre-equilibrium spectrum, the only quantity left to determine is the internal transition rate $\lambda^+(p, h)$ from state (p, h) to state $(p + 1, h + 1)$. The general definition of $\lambda^+(p, h)$ is

$$\begin{aligned} \lambda^+(p, h) &= \frac{1}{\omega(p, h, E^{\text{tot}})}[\int_{L_1^p}^{L_2^p} du \lambda^{1p}(u)\omega(p-1, h, E^{\text{tot}} - u)\omega(1, 0, u) \\ &+ \int_{L_1^h}^{L_2^h} du \lambda^{1h}(u)\omega(p, h-1, E^{\text{tot}} - u)\omega(0, 1, u)]. \end{aligned} \tag{4.119}$$

where the two terms account for particle and hole scattering, respectively, and the integration limits

$$\begin{aligned} L_1^p &= A(p+1, h+1) - A(p-1, h) \\ L_2^p &= E^{\text{tot}} - A(p-1, h) \\ L_1^h &= A(p+1, h+1) - A(p, h-1) \\ L_2^h &= E^{\text{tot}} - A(p, h-1), \end{aligned} \tag{4.120}$$

correct for the Pauli exclusion principle.

We again distinguish between two options:

1. Effective squared matrix element

The collision probabilities are determined with the aid of Fermi's golden rule of time-dependent perturbation theory, which for the one-component model are

$$\begin{aligned}\lambda^{1p}(u) &= \frac{2\pi}{\hbar}M^2\omega(2,1,u)\\ \lambda^{1h}(u) &= \frac{2\pi}{\hbar}M^2\omega(1,2,u),\end{aligned} \tag{4.121}$$

with M^2 the average squared matrix element of the residual interaction. In the one-component model, "forbidden" transitions are taken into account, so that a squared matrix element smaller than that of Eq. (4.102) of the two-component model is needed to compensate for these transitions. We find that for the one-component model we need to multiply M^2 of Eq. (4.102) by 0.5 to obtain a global comparison with data that is closest to our two-component result, i.e.

$$M^2 = \frac{0.5C_1A_p}{A^3}\left[7.48C_2 + \frac{4.62\times 10^5}{(\frac{E^{\rm tot}}{n.A_p}+10.7C_3)^3}\right]. \tag{4.122}$$

For completeness, we note that the transition rate can be well approximated by an analytical form as discussed in Refs. [100, 96, 98]. The result is

$$\lambda^+(p,h) = \frac{2\pi}{\hbar}M^2\frac{g^3}{2(n+1)}\frac{\left[E^{\rm tot}-A(p+1,h+1)\right]^{n+1}}{\left[E^{\rm tot}-A(p,h)\right]^{n-1}}f(p+1,h+1,E^{\rm tot},V). \tag{4.123}$$

However, the overall description of experimental data obtained with the one-component model is however worse that that of the two-component model, so we rarely use it.

2. Collision rates based on the optical model

Also in the one-component model the transition rates can be related to the effective nucleon-nucleon interaction $\bar{\sigma}$ and thereby to the imaginary optical potential,

$$\begin{aligned}\lambda^{1p}(u) &= \frac{1}{2}\frac{2W^{\rm eff}(u-S)}{\hbar}\\ \lambda^{1h}(u) &= \frac{1}{2}\frac{2W^{\rm eff}(u-S)}{\hbar}\frac{\omega(1,2,u)}{\omega(2,1,u)},\end{aligned} \tag{4.124}$$

with S the separation energy of the particle. Since the one-component model makes no distinction between neutron and proton particle-hole pairs, W_V^{eff} is evaluated as follows,

$$W_i^{\rm eff}(E) = 0.5C^{\rm omp}\,W_i(E), \tag{4.125}$$

analogous to the multiplication with a factor 0.5 for M^2.

Energy width representation The formalism given above, i.e. Eqs. (4.110), (4.111) and (4.116), forms a representation in which the time appears, i.e. the dimensions of $W(p,h)$ and $\tau(p,h)$ are $[s]^{-1}$ and $[s]$ respectively. An alternative expression for the exciton model that is often used is in terms of energy widths. Since this may be more recognisable to some users we also give it here. The partial escape width $\Gamma_k^{\uparrow}(p,h,E_k)$ is related to the emission rate by

$$\Gamma_k^{\uparrow}(p,h,E_k) = \hbar W_k(p,h,E_k). \tag{4.126}$$

Integrated over energy we have

$$\Gamma_k^{\uparrow}(p,h) = \hbar W_k(p,h), \tag{4.127}$$

and the total escape width is

$$\Gamma^{\uparrow}(p,h) = \sum_{k=\gamma,n,p,d,t,h,\alpha} \Gamma_k^{\uparrow}(p,h) = \hbar W(p,h). \tag{4.128}$$

The damping width $\Gamma^{\downarrow}$ is related to the internal transition rate by

$$\Gamma^{\downarrow}(p,h) = \hbar\lambda^{+}(p,h). \tag{4.129}$$

Defining the total width by

$$\Gamma^{\mathrm{tot}}(p,h) = \Gamma^{\downarrow}(p,h) + \Gamma^{\uparrow}(p,h), \tag{4.130}$$

we can rewrite the exciton model cross section (4.110) as

$$\frac{d\sigma_k^{\mathrm{PE}}}{dE_k} = \sigma^{\mathrm{CF}} \sum_{p=p_0}^{p_{\max}} \frac{\Gamma_k^{\uparrow}(p,h,E_k)}{\Gamma^{\mathrm{tot}}(p,h)} \left(\prod_{p'=p_0}^{p-1} \frac{\Gamma^{\downarrow}(p',h')}{\Gamma^{\mathrm{tot}}(p',h')} \right). \tag{4.131}$$

In the output file of TALYS, the results for the various quantities in both the time and the energy width representation are given.

In sum, the default model used by TALYS is the two-component exciton model with collision probabilities based on the effective squared matrix element of Eq. (4.102).

4.4.2 Photon exciton model

For pre-equilibrium photon emission, we have implemented the model of Akkermans and Gruppelaar [101]. This model gives a simple but powerful simulation of the direct-semidirect capture process within the framework of the exciton model. Analogous to the particle emission rates, the continuum γ-ray emission rates may be derived from the principle of detailed balance or microscopic reversibility, assuming that only $E1$-transitions contribute. This yields

$$W_{\gamma}(p,h,E_{\gamma}) = \frac{E_{\gamma}^2}{\pi^2\hbar^3c^2} \frac{\sigma_{\gamma,abs}(E_{\gamma})}{\omega(p,h,E^{tot})} \left(\frac{g^2E_{\gamma}\omega(p-1,h-1,E_x-E_{\gamma})}{g(n-2)+g^2E_{\gamma}} + \frac{gn\omega(p,h,E_x-E_{\gamma})}{gn+g^2E_{\gamma}} \right) \tag{4.132}$$

where $\sigma_{\gamma,abs}(E_{\gamma})$ is the photon absorption cross section of Eq. (4.70). The initial particle-hole configuration in Eq. (4.110) is $n_0 = 1$ ($1p0h$) for photon emission. For "direct" γ-ray emission in nucleon-induced reactions only the second term between brackets ($n = 1$) contributes. The "semi-direct" γ-ray emission ($n = 3$) consists of both terms.

The emission rate (4.132) is included in Eqs. (4.110) and (4.115) so that the pre-equilibrium photon cross section automatically emerges.

For the two-component model, we use

$$\begin{aligned} W_\gamma(p_\pi, h_\pi, p_\nu, h_\nu, E_\gamma) &= \frac{E_\gamma^2}{\pi^2\hbar^3c^2}\frac{\sigma_{\gamma,abs}(E_\gamma)}{\omega(p_\pi, h_\pi, p_\nu, h_\nu, E^{tot})} \\ \times & \Big(\frac{g^2 E_\gamma \frac{1}{2}\left[\omega(p_\pi-1, h_\pi-1, p_\nu, h_\nu, E_x-E_\gamma)+\omega(p_\pi, h_\pi, p_\nu-1, h_\nu-1, E_x-E_\gamma)\right]}{g(n-2)+g^2E_\gamma} \\ + & \frac{gn\omega(p_\pi, h_\pi, p_\nu, h_\nu, E_x-E_\gamma)}{gn+g^2E_\gamma}\Big). \end{aligned} \quad (4.133)$$

4.4.3 Pre-equilibrium spin distribution

Since the exciton model described above does not provide a spin distribution for the residual states after pre-equilibrium emission, a model needs to be adopted that provides the spin population in the continuum in binary reactions. TALYS provides two options for this. The default is to adopt the compound nucleus spin distribution (described in Section 4.5) also for the excited states resulting from pre-equilibrium emission. Another option that has been quite often used in the past is to assign a spin distribution to the particle-hole state density. For that, we adopt the usual decomposition of the state density into a J-dependent part and an energy-dependent part,

$$\rho(p,h,J,E_x) = (2J+1)R_n(J)\omega(p,h,E_x). \quad (4.134)$$

The function $R_n(J)$ represents the spin distribution of the states in the continuum. It is given by

$$R_n(J) = \frac{2J+1}{\pi^{1/2}n^{3/2}\sigma^3}\exp\left[-\frac{(J+\frac{1}{2})^2}{n\sigma^2}\right], \quad (4.135)$$

and satisfies, for any exciton number n,

$$\sum_J (2J+1)R_n(J) = 1. \quad (4.136)$$

The used expression for the spin cut-off parameter σ is [102],

$$\sigma^2 = 0.24nA^{\frac{2}{3}}, \quad (4.137)$$

where A is the mass number of the nucleus. Similarly, for the two-component particle-hole level density we have

$$\rho(p_\pi, h_\pi, p_\nu, h_\nu, J, E_x) = (2J+1)R_n(J)\omega(p_\pi, h_\pi, p_\nu, h_\nu, E_x). \quad (4.138)$$

In practice, with this option (**preeqspin y**) the residual states formed by pre-equilibrium reactions would be multiplied by R_n a posteriori. There are various arguments to prefer the compound nucleus spin distribution, so we use that default.

4.4.4 Continuum stripping, pick-up, break-up and knock-out reactions

For pre-equilibrium reactions involving deuterons, tritons, Helium-3 and alpha particles, a contribution from the exciton model is automatically calculated with the formalism of the previous subsections. It is however well-known that for nuclear reactions involving projectiles and ejectiles with different particle numbers, mechanisms like stripping, pick-up, break-up and knock-out play an important role and these direct-like reactions are not covered by the exciton model. Therefore, Kalbach [103] developed a phenomenological contribution for these mechanisms, which we have included in TALYS. In total, the pre-equilibrium cross section for these reactions is given by the sum of an exciton model (EM), nucleon transfer (NT), and knock-out (KO) contribution:

$$\frac{d\sigma_k^{\mathrm{PE}}}{dE_k} = \frac{d\sigma_k^{EM}}{dE_k} + \frac{d\sigma_k^{NT}}{dE_k} + \frac{d\sigma_k^{KO}}{dE_k} \tag{4.139}$$

where the contribution from the exciton model was outlined in the previous subsection.

Transfer reactions

The general differential cross section formula for a nucleon transfer reaction of the type $A(a,b)B$ is

$$\begin{aligned} \frac{d\sigma_{a,b}^{NT}}{dE_b} &= \frac{2s_b+1}{2s_a+1}\frac{A_b}{A_a}\frac{E_b\sigma_{b,inv}(E_b)}{A_a}K\left(\frac{A_a}{E_a+V_a}\right)^{2n}\left(\frac{C}{A_B}\right)^{n} \\ &\times\ N_a\left(\frac{2Z_A}{A_A}\right)^{2(Z_a+2)h_\pi+2p_\nu} \qquad \omega_{NT}(p_\pi,h_\pi,p_\nu,h_\nu,U) \end{aligned} \tag{4.140}$$

where

$$\begin{aligned} C_a &= 5500 \ \text{for incident neutrons,} \\ &= 3800 \ \text{for incident charged particles,} \end{aligned} \tag{4.141}$$

$$\begin{aligned} N_a &= \frac{1}{80E_a} \ \text{for pickup,} \\ &= \frac{1}{580\sqrt{E_a}} \ \text{for stripping,} \\ &= \frac{1}{1160\sqrt{E_a}} \ \text{for exchange.} \end{aligned} \tag{4.142}$$

K is an enhancement factor taking into account the fact that d, t and 3-He are loosely bound:

$$\begin{aligned} K &= 12 \ \text{for} \ (N,\alpha), \\ &= 12 - 11\frac{E_a-20}{E_a} \ \text{for} \ (\alpha,N) \ \text{and} \ E_a > 20, \\ &= 1 \ \text{otherwise,} \end{aligned} \tag{4.143}$$

where N stands for either neutron or proton. The well depth V_a is set at

$$V_a = 12.5A_a \ \text{MeV}, \tag{4.144}$$

and represents the average potential drop seen by the projectile between infinity and the Fermi level. The possible degrees of freedom for the reaction are all included in the residual state density $\omega_{NT}(p_\pi, h_\pi, p_\nu, h_\nu, U)$. Since we do not use this model to describe exchange reactions in inelastic scattering, there is no need to sum the various terms of Eq. (4.140) over p_π, as in Ref. [103]. The exciton numbers are automatically determined by the transfer reaction, i.e. $n = |A_a - A_b|$, $n_\pi = h_\pi = |Z_a - Z_b|$, $n_\nu = h_\nu = |N_a - N_b|$, $p_\pi = p_\nu = 0$. The accessible state density that is directly determined by the reaction is $\omega(p_\pi, h_\pi, p_\nu, h_\nu, U)$, given by Eq. (4.80). The total residual state density however also takes into account more complex configurations that can be excited by the transfer reaction. It is given by

$$\begin{aligned}\omega_{NT}(p_\pi, h_\pi, p_\nu, h_\nu, U) &= \sum_{i=0}^{3}\sum_{j=0}^{3-i}(X_{NT})^{i+j}\omega(p_\pi + i, h_\pi + i, p_\nu + j, h_\nu + j, U) \\ + &\sum_{i=0}^{p_\pi}\sum_{j=0}^{h_\pi}\sum_{k=0}^{p_\nu}\sum_{l=0}^{h_\nu}\omega(p_\pi - i, h_\pi - j, p_\nu - k, h_\nu - l, U)\Theta(i + j + k + l - \frac{1}{2}) \qquad (4.145)\end{aligned}$$

The first term allows that up to three particle-hole pairs can be excited in a transfer reaction. The factor X_{NT} represents the probability for exciting such a pair and is given by

$$X_{NT} = \frac{7\sqrt{E_a/A_a}}{V_1 A_A^2}(p_\nu^2 + p_\pi^2 + h_\nu^2 + 1.5h_\pi^2) \qquad (4.146)$$

For neutrons and protons we adopt for V_1 the value given by Eq.(4.87), for deuterons and tritons we take V_1=17 MeV, and for Helium-3 and alpha particles we take V_1=25 MeV. The finite well depth correction for Eq. (4.145) are made using a well depth of

$$\begin{aligned} V &= V_1\left(\frac{2Z}{A}\right) \text{ if } n_\pi = 0 \\ &= V_1 \text{ otherwise.} \qquad (4.147)\end{aligned}$$

The second term of Eq. (4.145) allows for transfer of nucleons at the Fermi level. Here, the Heaviside function is merely used to avoid double counting of $\omega(p_\pi, h_\pi, p_\nu, h_\nu, U)$.

Knockout reactions

For $(nucleon, \alpha)$ reactions a knockout contribution is added. The general differential cross section formula for a knockout reaction of the type $A(a, b)B$ is

$$\begin{aligned}\frac{d\sigma_{a,b}^{KO}}{dE_b} &= \frac{\sigma_{a,inv}(E_a)}{14}(2s_b + 1)A_b E_b \sigma_{b,inv}(E_b) \\ &\times \frac{P_b g_a g_b \left[U - A_{KO}(p_a, h_b)\right]}{\sum_{c=a,b}(2s_c + 1)A_c \langle\sigma_c\rangle (E_{max} + 2B_{coul,c})(E_{max} - B_{coul,c})^2 g_a g_b^2/6g_c} \qquad (4.148)\end{aligned}$$

where P_b is the probability of exciting a b-type particle-hole pair, E_{max} is the maximum emission energy, and $B_{coul,c}$ is the Coulomb barrier for a particle c. The average inverse cross section $\langle\sigma_c\rangle$ is given by

$$\langle\sigma_c\rangle = \int_{B_{coul,c}}^{E_{max}} dE\sigma_c(E) \qquad (4.149)$$

For the knockout model, the single-particle state density parameters for the cluster degrees of freedom g represent the number of cluster states per unit energy. The relevant values are given by

$$g_n = N/13, \quad g_p = Z/13, \quad g_\alpha = A/208 \ \text{MeV}. \tag{4.150}$$

The Pauli correction factor A_{KO} is given by

$$A_{KO}(p_a, h_b) = \frac{1}{2g_a^2} - \frac{1}{2g_b^2} \tag{4.151}$$

The probabilities for exciting the various particle-hole pairs are

$$\begin{aligned} P_n &= \frac{N_A - \phi Z_A}{A_A - 2\phi Z_A + \phi Z_A/2} \\ P_p &= \frac{Z_A - \phi Z_A}{A_A - 2\phi Z_A + \phi Z_A/2} \\ P_\alpha &= \frac{\phi Z_A/2}{A_A - 2\phi Z_A + \phi Z_A/2} \end{aligned} \tag{4.152}$$

The factors ϕ are a kind of pre-formation parameters [103]. The following values are adopted

$$\begin{aligned} N_A \leq 116 &\ : \ \phi = 0.08 \\ 116 \leq N_A < 126 &\ : \ \phi = 0.02 + 0.06(126 - N_A)/10 \\ 126 \leq N_A < 129 &\ : \ \phi = 0.02 + 0.06(N_A - 126)/3 \\ 129 \leq N_A &\ : \ \phi = 0.08 \end{aligned} \tag{4.153}$$

Break-up reactions

For reactions induced by complex particles, break-up may play an important role. This holds especially for weakly bound projectiles like deuterons. Break-up is here defined as having a projectile fragment emerge from the reaction in a relatively narrow peak centered close to the beam velocity and strongly directed toward forward angles. For deuterons only, a simple model by Kalbach has been included [104]. This leads to an extra contribution in the (d,n) and (d,p) channels.

The centroid energy of the breakup peak, in MeV, is given by

$$\epsilon_0 = \frac{A_b}{A_a}\left(\epsilon_a - B_{a,b} - \frac{Z_a Z_A}{9.5}\right) + \frac{Z_b Z_B}{9.5}, \tag{4.154}$$

where ϵ_a represents the channel energy (the energy of both the emitted particle and the recoiling nucleus in the center of mass), and $B_{a,b}$ is the binding energy in the projectile for the indicated breakup channel (2.224 MeV for deuterons). The peak is assumed to be described by a Gaussian line shape with a width parameter of

$$\Gamma = 1.15 + 0.12E_a - \frac{A_A}{140}, \tag{4.155}$$

where E_a is the laboratory energy of the incident deuteron, and the width parameter is given in MeV. The break-up cross section is assumed to be

$$\sigma_{BU} = K_{d,b}\frac{(A_A^{1/3} + 0.8)^2}{1 + \exp(\frac{13 - E_a}{6})}, \tag{4.156}$$

where the normalization factors are

$$\begin{aligned} K_{d,n} &= 18, \\ K_{d,p} &= 21. \end{aligned} \quad (4.157)$$

Finally, the differential break-up cross section is given by

$$\frac{d\sigma_{a,b}^{BU}}{dE_b} = \sigma_{BU} \frac{1}{\Gamma\sqrt{2\pi}} \exp\left(-\frac{(\epsilon_0 - E_b)^2}{\Gamma^2}\right). \quad (4.158)$$

In the output, we have stored the break-up contribution in the column "knockout" (which is normally only used for nucleon-induced reactions with alpha particles as ejectiles).

The stripping, pick-up, break-up and knock-out contributions can be adjusted with the **Cstrip** and **Cknock** keywords.

4.4.5 Angular distribution systematics

A sound pre-equilibrium theory should, besides the angle-integrated spectra, also describe the smooth forward peaked angular distributions in the continuum. A physics method to do so will be included in a future version of TALYS (multi-step direct reactions). Semi-classical models, such as the exciton model, have always had some problems to describe angular distributions (essentially because it is based on a compound-like concept instead of a direct one [105]). A powerful phenomenological method is given by Kalbach [106]. It is based on experimental information only and the insight that in general, a pre-equilibrium process consists of a forward peaked part (multi-step direct) and an isotropic part (multi-step compound), and that the angular distributions are fairly structureless and all look alike. The Kalbach formula for the double-differential cross section for a projectile a and an ejectile b is

$$\frac{d^2\sigma_{a,xb}}{dE_b d\Omega} = \frac{1}{4\pi}\left[\frac{d\sigma^{\rm PE}}{dE_b} + \frac{d\sigma^{comp}}{dE_b}\right] \frac{a}{\sinh(a)}[\cosh(a\cos\Theta) + f_{MSD}(E_b)\sinh(a\cos\Theta)] \quad (4.159)$$

where $\frac{d\sigma^{\rm PE}}{dE_b}$ and $\frac{d\sigma^{comp}}{dE_b}$ are the angle-integrated pre-equilibrium and compound spectra, respectively, and f_{MSD} is the so-called multi-step direct or pre-equilibrium ratio:

$$f_{MSD}(E_b) = \frac{d\sigma^{\rm PE}}{dE_b} / \left[\frac{d\sigma^{\rm PE}}{dE_b} + \frac{d\sigma^{comp}}{dE_b}\right] \quad (4.160)$$

which thus increases from practically 0 at very low emission energy to 1 at the highest emission energies. Hence, once the angle-integrated spectra are known, the parameter a determines the angular distribution. Kalbach parameterized it as

$$\begin{aligned} a(e'_a, e'_b) &= 0.04\frac{E_1 e'_b}{e'_a} + 1.8\times 10^{-6}(\frac{E_1 e'_b}{e'_a})^3 + 6.7\times 10^{-7} M_a m_b (\frac{E_3 e'_b}{e'_a})^4, \\ E_1 &= \min(e'_a, 130\mathrm{MeV}) \\ E_3 &= \min(e'_a, 41\mathrm{MeV}) \\ e'_b &= E_b + S_b \end{aligned}$$

$$
\begin{aligned}
e'_a &= E_a + S_a. \\
M_a &= 1 \text{ for neutrons, protons, deuterons, tritons and Helium} - 3 \\
&= 0 \text{ for alpha's} \\
m_b &= 1 \text{ for protons, deuterons, tritons and Helium} - 3 \\
&= \frac{1}{2} \text{ for neutrons} \\
&= 2 \text{ for alpha's} \\
S_b &= 15.68(A_C - A_B) - 28.07\left[\frac{(N_C - Z_C)^2}{A_C} - \frac{(N_B - Z_B)^2}{A_B}\right] \\
&- 18.56(A_C^{2/3} - A_B^{2/3}) + 33.22\left[\frac{(N_C - Z_C)^2}{A_C^{4/3}} - \frac{(N_B - Z_B)^2}{A_B^{4/3}}\right] \\
&- 0.717\left[\frac{Z_C^2}{A_C^{1/3}} - \frac{Z_B^2}{A_B^{1/3}}\right] + 1.211\left[\frac{Z_C^2}{A_C} - \frac{Z_B^2}{A_B}\right] - I_b \\
I_d &= 2.225 \\
I_t &= 8.482 \\
I_h &= 7.718 \\
I_\alpha &= 28.296,
\end{aligned}
\tag{4.161}
$$

Here, E_a and E_b are the incident and the outgoing energy, respectively. The number M_a represents the incident particle, while m_b represents the outgoing particle, C is a label for the compound nucleus, B for the final nucleus and the Myers and Swiatecki mass formula [107] for spherical nuclides should be used here to determine the separation energy S. Finally I_b is the energy required to break the emitted particle up into its constituents.

Since we calculate the pre-equilibrium and compound cross sections explicitly (and actually only use f_{MSD} for ENDF-6 data libraries), Eq. (4.159) can be reduced to a formula for the double-differential pre-equilibrium cross section

$$
\frac{d^2\sigma^{\rm PE}_{a,xb}}{dE_b d\Omega} = \frac{1}{4\pi}\frac{d\sigma^{\rm PE}}{dE_b}\frac{a}{\sinh(a)}\exp(a\cos\Theta), \tag{4.162}
$$

to which the isotropic compound angular distribution can be added. In sum, given the angle-integrated spectrum $\frac{d\sigma^{\rm PE}}{dE_b}$ by some physics model, the double-differential cross section is returned quite simply and reasonably accurate by Eq. (4.162).

4.5 Compound reactions

The term compound nucleus reaction is commonly used for two different mechanisms: (i) the process of the capture of the projectile in the target nucleus to form a compound nucleus, which subsequently emits a particle or gamma, (ii) the multiple emission process of highly excited residual nuclei formed after the binary reaction. The latter, which is known as multiple compound emission, will be explained in Section 4.6. We first treat the binary compound nucleus reaction that plays a role at low incident energy. It differs from the multiple compound emission at two important points: (a) the presence of width fluctuation corrections and (b) non-isotropic, though still symmetric, angular distributions.

4.5.1 Binary compound cross section and angular distribution

In the compound nucleus picture, the projectile and the target nucleus form a compound nucleus with a total energy E^{tot} and a range of values for the total spin J and parity Π. The following energy, angular momentum and parity conservation laws need to be obeyed,

$$\begin{aligned} E_a + S_a &= E_{a'} + E_x + S_{a'} = E^{tot} \\ s + I + l &= s' + I' + l' = J \\ \pi_0 \Pi_0 (-1)^l &= \pi_f \Pi_f (-1)^{l'} = \Pi. \end{aligned} \tag{4.163}$$

The compound nucleus formula for the binary cross section is given by

$$\begin{aligned} \sigma_{\alpha\alpha'}^{comp} &= D^{comp} \frac{\pi}{k^2} \sum_{J=mod(I+s,1)}^{l_{max}+I+s} \sum_{\Pi=-1}^{1} \frac{2J+1}{(2I+1)(2s+1)} \sum_{j=|J-I|}^{J+I} \sum_{l=|j-s|}^{j+s} \sum_{j'=|J-I'|}^{J+I'} \sum_{l'=|j'-s'|}^{j'+s'} \\ &\times \quad \delta_\pi(\alpha)\delta_\pi(\alpha') \frac{T_{\alpha l j}^J(E_a) \left\langle T_{\alpha' l' j'}^J(E_{a'}) \right\rangle}{\sum_{\alpha'',l'',j''} \delta_\pi(\alpha'') \left\langle T_{\alpha'' l'' j''}^J(E_{a''}) \right\rangle} W_{\alpha l j \alpha' l' j'}^J, \end{aligned} \tag{4.164}$$

In the above equations, the symbols have the following meaning:

$E_a =$ projectile energy

$s =$ spin of the projectile

$\pi_0 =$ parity of the projectile

$l =$ orbital angular momentum of the projectile

$j =$ total angular momentum of the projectile

$\delta_\pi(\alpha) =$ 1, if $(-1)^l \pi_0 \Pi_0 = \Pi$ and 0 otherwise

$\alpha =$ channel designation of the initial system of projectile and target nucleus: $\alpha = \{a, s, E_a, E_x^0, I, \Pi_0\}$, where a is the projectile type and E_x^0 the excitation energy of the target nucleus (usually zero)

$l_{max} =$ maximum l-value for projectile

$S_a =$ separation energy

$E_{a'} =$ ejectile energy

$s' =$ spin of the ejectile

$\pi_f =$ parity of the ejectile

$l' =$ orbital angular momentum of the ejectile

$j' =$ total angular momentum of the ejectile

$\delta_\pi(\alpha') =$ 1, if $(-1)^{l'}\pi_f\Pi_f = \Pi$ and 0 otherwise

$\alpha' =$ channel designation of the final system of ejectile and residual nucleus: $\alpha' = \{a', s', E_{a'}, E_x, I', \Pi_f\}$, where a' is the ejectile type, E_x the excitation energy of the residual nucleus

$I =$ spin of the target nucleus

$\Pi_0 =$ parity of the target

$I' =$ spin of the residual nucleus

$\Pi_f =$ parity of the residual nucleus

$\Pi =$ parity of the compound system

$J =$ total angular momentum of the compound system

$D^{comp} =$ depletion factor to account for direct and pre-equilibrium effects

$k =$ wave number of relative motion

$T =$ transmission coefficient

$W =$ width fluctuation correction (WFC) factor, see the next Section.

In order to let Eq. (4.164) represent the general case, we have denoted the outgoing transmission coefficient by $\left\langle T^J_{\alpha' l' j'}\right\rangle$. For this, two cases can be distinguished. If the excitation energy E_x, that is implicit in the definition of channel α', corresponds to a discrete state of the final nucleus, then we simply have

$$\left\langle T^J_{\alpha' l' j'}(E_{a'})\right\rangle = T^J_{\alpha' l' j'}(E_{a'}) \tag{4.165}$$

and $E'_{a'}$ is exactly determined by Eq. (4.163). For α' channels in which E_x is in the continuum, we have an effective transmission coefficient for an excitation energy bin with width ΔE_x,

$$\left\langle T^J_{\alpha' l' j'}(E_{a'})\right\rangle = \int_{E_x-\frac{1}{2}\Delta E_x}^{E_x+\frac{1}{2}\Delta E_x} dE_{x'}\rho(E_{x'}, J, \Pi) T^J_{\alpha' l' j'}(E_{a'}) \tag{4.166}$$

where ρ is the level density, which will be discussed in Section 4.7, and T is evaluated at an emission energy $E_{a'}$ that corresponds to the middle of the excitation energy bin, i.e. $E_{a'} = E^{tot} - E_x - S_{a'}$. Hence, both transitions to discrete states and transitions to the whole accessible continuum are covered by the sum over α' in Eq. (4.164). The normalization factor D^{comp} is

$$D^{comp} = [\sigma_{reac} - \sigma^{disc,direct} - \sigma^{\rm PE}]/\sigma_{reac} \tag{4.167}$$

This indicates that in TALYS we assume that direct and compound contributions can be added incoherently. This formula for D^{comp} is only applied for weakly coupled channels that deplete the flux, such as contributions from DWBA or pre-equilibrium. In the case of coupled-channels calculations for the discrete collective states, the transmission coefficients of Eq. (4.164) are automatically reduced by ECIS-06 to account for direct effects and TALYS only subtracts the direct cross section for the weakly coupled levels (DWBA), i.e. if

$$\sigma^{disc,direct} = \sigma^{disc,cc} + \sigma^{disc,DWBA} \tag{4.168}$$

then

$$D^{comp} = [\sigma_{reac} - \sigma^{disc,DWBA} - \sigma^{\mathrm{PE}}]/\sigma_{reac} \tag{4.169}$$

TALYS also computes the compound nucleus formula for the angular distribution. It is given by

$$\frac{d\sigma^{comp}_{\alpha\alpha'}(\theta)}{d\Omega} = \sum_L C^{comp}_L P_L(\cos\Theta), \tag{4.170}$$

where P_L are Legendre polynomials. The Legendre coefficients C^{comp}_L are given by

$$\begin{aligned} C^{comp}_L &= D^{comp}\frac{\pi}{k^2}\sum_{J,\Pi}\frac{2J+1}{(2I+1)(2s+1)}\sum_{j=|J-I|}^{J+I}\sum_{l=|j-s|}^{j+s}\sum_{j'=|J-I'|}^{J+I'}\sum_{l'=|j'-s'|}^{j'+s'} \\ &\times\ \delta_\pi(\alpha)\delta_\pi(\alpha')\frac{T^J_{\alpha lj}(E_a)\left\langle T^J_{\alpha' l' j'}(E_{a'})\right\rangle}{\sum_{\alpha'',l'',j''}\delta_\pi(\alpha'')\left\langle T^J_{\alpha'' l'' j''}(E_{a''})\right\rangle}W^J_{\alpha lj\alpha' l' j'}A^J_{IljI'l'j';L}, \end{aligned} \tag{4.171}$$

where the Blatt-Biedenharn factor A is given by

$$\begin{aligned} A^J_{IljI'l'j';L} &= \frac{(-1)^{I'-s'-I+s}}{4\pi}(2J+1)(2j+1)(2l+1)(2j'+1)(2l'+1) \\ (ll00|L0)\,&\mathcal{W}(JjJj;IL)\mathcal{W}(jjll;Ls)\,(l'l'00|L0)\,\mathcal{W}(Jj'Jj';I'L)\mathcal{W}(j'j'l'l';Ls'), \end{aligned} \tag{4.172}$$

where (|) are Clebsch-Gordan coefficients and $\mathcal{W}$ are Racah coefficients.

Formulae (4.164) and (4.170-4.172) show that the width fluctuation correction factors and the angular distribution factors depend on all the angular momentum quantum numbers involved, and thus have to be re-evaluated each time inside all the summations. We generally need these formulae for relatively low incident energy, where the WFC has a significant impact and where the compound nucleus cross section to each individual discrete state is large enough to make its angular distribution of interest. For projectile energies above several MeV (we generally take the neutron separation energy for safety), the width fluctuations have disappeared, meaning that $W^J_{\alpha lj\alpha' l' j'} = 1$ for all channels. Then for the angle-integrated compound cross section, instead of performing the full calculation, Eq. (4.164) can be decoupled into two parts that represent the incoming and outgoing reaction flux, respectively. It simplifies to

$$\sigma^{comp}_{\alpha\alpha'} = \sum_{J=mod(I+s,1)}^{l_{max}+I+s}\sum_{\Pi=-1}^{1}\sigma^{CF}_{J\Pi}(E^{tot})\frac{\Gamma_{\alpha'}(E^{tot},J,\Pi\longrightarrow E_x,I',\Pi_f)}{\Gamma^{tot}(E^{tot},J,\Pi)} \tag{4.173}$$

where $\sigma^{CF}_{J\Pi}$ is the compound formation cross section per spin and parity:

$$\sigma^{CF}_{J\Pi}(E^{tot}) = D^{comp}\frac{\pi}{k^2}\frac{2J+1}{(2I+1)(2s+1)}\sum_{j=|J-I|}^{J+I}\sum_{l=|j-s|}^{j+s}T^J_{\alpha lj}(E_a)\delta_\pi(\alpha) \tag{4.174}$$

which itself obeys

$$\sum_{J=mod(I+s,1)}^{l_{max}+I+s}\sum_{\Pi=-1}^{1}\sigma^{CF}_{J\Pi}(E^{tot}) = D^{comp}\sigma_{reac} \tag{4.175}$$

The partial decay widths are

$$\Gamma_{\alpha'}(E^{tot}, J, \Pi \longrightarrow E_x, I', \Pi_f) = \frac{1}{2\pi\rho(E^{tot}, J, \Pi)} \sum_{j'=|J-I'|}^{J+I'} \sum_{l'=|j'-s'|}^{j'+s'} \delta_\pi(\alpha') \left\langle T^J_{\alpha' l' j'}(E'_{a'}) \right\rangle \quad (4.176)$$

and the total decay width is

$$\Gamma^{tot}(E^{tot}, J, \Pi) = \sum_{\alpha''} \Gamma_{\alpha''}(E^{tot}, J, \Pi \longrightarrow E_x, I'', \Pi_f) \quad (4.177)$$

where we sum over all possible states in the residual nuclides through the sum over α''. Note that the term with the compound nucleus level density, $2\pi\rho$, is present in both Eq. (4.176) and Eq. (4.177) and therefore does not need to be calculated in practice for Eq. (4.173). A formula similar to Eq. (4.173) is used for multiple emission, see Section 4.6.

In sum, we use Eqs. (4.164) and (4.171) if either width fluctuations (**widthfluc y**, p. 158) or compound angular distributions (**outangle y**, p. 190) are to be calculated and Eq. (4.173) if they are both not of interest.

A final note to make here is that the formulae of this whole Section can also be applied for excited (isomeric) target states.

4.5.2 Width fluctuation correction factor

The WFC factor W accounts for the correlations that exist between the incident and outgoing waves. From a qualitative point of view, these correlations enhance the elastic channel and accordingly decrease the other open channels. Above a few MeV of projectile energy, when many competing channels are open, the WFC factor can be neglected and the simple Hauser-Feshbach model is adequate to describe the compound nucleus decay. To explain the WFC factors, we now switch to a more compact notation in which we leave out J and define $a = \{\alpha, l, j\}$ and $b = \{\alpha', l', j'\}$. With such a notation the compound nucleus cross section can be written in the compact form

$$\sigma_{ab} = \frac{\pi}{k_a^2} \frac{T_a T_b}{\sum_c T_c} W_{ab} \quad (4.178)$$

for each combination of a and b. In general, the WFC factor may be calculated using three different expressions, which have all been implemented in TALYS: The Hofmann-Richert-Tepel-Weidenmüller (HRTW) model [108, 109, 110], the Moldauer model [111, 112], and the model using the Gaussian Orthogonal Ensemble (GOE) of Hamiltonian matrices [113]. A comparison between the three models is given in Ref. [25].

For each expression, flux conservation implies that

$$T_a = \sum_b \frac{T_a T_b}{\sum_c T_c} W_{ab} \quad (4.179)$$

This equation can be used to check the numerical accuracy of the WFC calculation (see the **flagcheck** keyword in Chapter 6).

The HRTW method

The simplest approach is the HRTW method. It is based on the assumption that the main effect of the correlation between incident and outgoing waves is in the elastic channel. In that case, it is convenient to express the compound nucleus cross section (4.178) as

$$\sigma_{ab} = \frac{\pi}{k^2} \frac{V_a V_b}{\sum_c V_c} \left[1 + \delta_{ab}(W_a - 1)\right], \tag{4.180}$$

where the V_i's are effective transmission coefficients that take into account the correlations.

This expression means that only the elastic channel enhancement is described since for $a = b$, Eq. (4.180) becomes

$$\sigma_{aa} = \frac{\pi}{k_a^2} \frac{V_a^2}{\sum_c V_c} W_a \tag{4.181}$$

while for $a \neq b$,

$$\sigma_{ab} = \frac{\pi}{k_a^2} \frac{V_a V_b}{\sum_c V_c} \tag{4.182}$$

An expression for the V_i values can be determined from the flux conservation condition

$$\sum_b \sigma_{ab} = \frac{\pi}{k_a^2} T_a, \tag{4.183}$$

which yields using Eq. (4.180)

$$T_a = V_a + (W_a - 1)\frac{V_a^2}{\sum_c V_c}, \tag{4.184}$$

or

$$V_a = \frac{T_a}{1 + \frac{(W_a - 1)V_a}{\sum_c V_c}}. \tag{4.185}$$

The only required information is thus the expression for W_a, which can be derived from an analysis using random matrix calculations. In TALYS, the expression of Ref. [110] is used. It reads

$$W_a = 1 + \frac{2}{1 + T_a^F} + 87 \left(\frac{T_a - \overline{T}}{\sum\limits_c T_c} \right)^2 \left(\frac{T_a}{\sum\limits_c T_c} \right)^5, \tag{4.186}$$

with $\overline{T} = \dfrac{\sum\limits_c T_c^2}{\sum\limits_c T_c}$ and the exponent $F = \dfrac{4\dfrac{\overline{T}}{\sum\limits_c T_c}\left(1 + \dfrac{T_a}{\sum\limits_c T_c}\right)}{1 + \dfrac{3\overline{T}}{\sum\limits_c T_c}}$.

The result for V_a is obtained after iterating Eq. (4.185) several times, starting from the initial value

$$V_a(i = 0) = \frac{T_a}{1 + (W_a - 1)\dfrac{T_a}{\sum\limits_c T_c}} \tag{4.187}$$

and calculating $V_a(i+1)$ using

$$V_a(i+1) = \frac{T_a}{1 + (W_a - 1)\dfrac{V_a(i)}{\sum\limits_c V_c(i)}} \tag{4.188}$$

until $V_a(i+1) \approx V_a(i)$. In a calculation, a few tens of iterations are generally required to reach a stable result.

For each J and Π, expressions (4.185)-(4.188) only need to be evaluated once. This is done in *hrtwprepare.f*, before all the loops over l, j, l' and j', etc. quantum numbers are performed. For the calculation of $W^J_{\alpha lj\alpha' l' j'}$ in Eq. (4.164), which takes place inside all loops, the correct V_a and V_b are then addressed. The WFC factor can then be derived from Eqs. (4.178) and (4.180),

$$W_{ab} = \frac{V_a V_b}{\sum_c V_c}\left[1 + \delta_{ab}(W_a - 1)\right]\frac{\sum_c T_c}{T_a T_b} \tag{4.189}$$

which is calculated in *hrtw.f*.

Moldauer expression

This is the default option for the WFC in TALYS. Moldauer's expression for W_{ab} is based on the assumption that a χ^2 law with ν degrees of freedom applies for the partial widths Γ, which can be calculated from a Porter-Thomas distribution. These are associated with transmission coefficients as

$$T = \frac{2\pi\left\langle\Gamma\right\rangle}{D} \tag{4.190}$$

provided $\langle\Gamma\rangle << D$, where D is the mean level spacing. The WFC factor W_{ab} reads

$$W_{ab} = \left(1 + \frac{2\delta_{ab}}{\nu_a}\right)\int_0^{+\infty}\prod_c\left(1 + \frac{2T_c\,x}{\nu_c\sum_i T_i}\right)^{-(\delta_{ac}+\delta_{bc}+\nu_c/2)} dx \tag{4.191}$$

Moldauer has parameterised ν using Monte Carlo calculations, giving

$$\nu_a = 1.78 + \left(T_a^{1.212} - 0.78\right)\exp\left(-0.228\sum_c T_c\right) \tag{4.192}$$

In TALYS, the integral in Eq. (4.191) is evaluated numerically. For this, the Gauss-Laguerre method has been chosen and we find that 40 integration points are enough to reach convergence, the criterion being the flux conservation of Eq. (4.179). As for the HRTW model, the calculation can be split into parts dependent and independent of the channel quantum numbers. First, in *molprepare.f*, for each J and Π, we calculate Eq. (4.192) for all channels and the product $\prod\limits_c\left(1 + \dfrac{2T_c\,x}{\nu_c\sum_i T_i}\right)^{-\nu_c/2}$ that appears in Eq. (4.191). Inside all the loops, we single out the correct a and b channel and calculate Eq. (4.191) in *moldauer.f*.

Eq. (4.191) involves a product over all possible open channels. When the number of channels is large, the product calculation drastically increases the time of computation, forcing us to consider another method. Many open channels are considered for capture reactions and reactions to the continuum.

A. Capture reactions If the projectile is captured by the target nucleus, the compound nucleus is formed with an excitation energy at least equal to the projectile separation energy in the compound system. Since the γ transmission coefficient calculation involves all the possible states to which a photon can be emitted from the initial compound nucleus state, the number of radiative open channels is almost infinite, but each has a very small transmission coefficient. Following Ref. [114], the product over the radiative channels in Eq. (4.191) can be transformed as

$$\prod_{c\in\gamma}\left(1+\frac{2T_c\,x}{\nu_c\sum_i T_i}\right)^{-\nu_c/2} \approx \lim_{\nu_\gamma\to+\infty}\left(1+\frac{2T_\gamma\,x}{\bar{\nu}_\gamma\sum_i T_i}\right)^{-\bar{\nu}_\gamma/2} = \exp\left(-\frac{T_\gamma^{eff}\,x}{\sum_i T_i}\right) \tag{4.193}$$

where T_γ^{eff} is given by the procedure sketched in Section 4.3. The derivation is based on the hypothesis that all the individual T_γ are almost identical to 0. Therefore, to calculate W_{ab} when b denotes the gamma channel, we set $T_b = 0$ in Eqs. (4.191) and use Eqs. (4.193) to calculate the product for γ channels.

B. Continuum reactions For high excitation energies, it is impossible to describe all the open channels individually. It is then necessary to introduce energy bins to discretize the continuum of levels and define continuum (or effective) transmission coefficients as

$$T_{eff}(U) = \int_{E_{min}}^{E_{max}} \rho(\varepsilon)T(\varepsilon)d\varepsilon, \tag{4.194}$$

where U is generally taken as the middle of the interval $[E_{min}, E_{max}]$ and ρ is the density of levels under consideration. This effective transmission coefficient corresponds to an effective number of channels $N_{eff}(U)$, given by

$$N_{eff}(U) = \int_{E_{min}}^{E_{max}} \rho(\varepsilon)d\varepsilon. \tag{4.195}$$

Calculating the product term in Eq. (4.191) is tedious, unless one assumes that the energy variation of $T(\varepsilon)$ is smooth enough to warrant that each of the $N_{eff}(U)$ channels has the same average transmission coefficient

$$T_{mean}(U) = \frac{T_{eff}(U)}{N_{eff}(U)}. \tag{4.196}$$

Then, the product over the channels c belonging to such a continuum bin in the Moldauer integral Eq. (4.191) can be replaced by a single term, i.e.

$$\prod_c\left(1+\frac{2T_c}{\nu_c\sum\limits_i T_i}x\right)^{-\nu_c/2} \approx \left(1+\frac{2T_{mean}(U)}{\nu_{mean}\sum\limits_i T_i}x\right)^{-N_{eff}(U)\nu_{mean}/2}, \tag{4.197}$$

where

$$\nu_{mean} = 1.78 + \left(T_{mean}^{1.212} - 0.78\right)\exp\left(-0.228\sum_c T_c\right) \tag{4.198}$$

C. Fission reactions The fission reaction is treated as one global channel, regardless of the nature of the fission fragments that result from fission. We will see later on in Section 4.8, how the global fission transmission coefficient is calculated. It is however important to state here that the fission transmission coefficient is generally greater than 1 since it results from a summation over several fission paths and can therefore be defined as

$$T_{fis}(U) = \int_{E_{min}}^{E_{max}} \rho_{fis}(\varepsilon) T_f(\varepsilon) d\varepsilon. \tag{4.199}$$

Of course, one has $0 \le T_f(\varepsilon) \le 1$, but one can not assume that T_f is constant over the whole integration energy range as in the case of continuum reactions. To bypass this problem, instead of using a global fission transmission coefficient, we have grouped the various components of Eq. (4.199) according to their values. Instead of dealing with a global fission transmission coefficient, we use N different global transmission coefficients (where N is an adjustable parameter) such that

$$T_{fis}(U) = \sum_{i=0}^{N} T_{fis}(i, U) \tag{4.200}$$

where

$$T_{fis}(i, U) = \int_{E_{min}}^{E_{max}} \rho_{fis}(\varepsilon) T_f(\varepsilon) \delta_{i,N} d\varepsilon \tag{4.201}$$

and $\delta_{i,N} = 1$ is $i/N \le T_f(\varepsilon) \le (i+1)/N$ and 0 otherwise.

In this case one can define, as for continuum reactions, an effective number of channels $N_{fis}(i, U)$, and use N average fission transmission coefficients defined by

$$T_{fismean}(i) = \frac{T_{fis}(i, U)}{N_{fis}(i, U)}. \tag{4.202}$$

If N is large enough, these N average coefficients can be used for the width fluctuation calculation without making a too crude approximation.

The GOE triple integral

The two previously described methods to obtain W_{ab} are readily obtained since both are relatively simple to implement. However, in each case, a semi-empirical parameterisation is used. The GOE formulation avoids such a parameterisation, in which sense it is the more general expression. In the GOE approach, W_{ab} reads

$$W_{ab} = \frac{\sum_c T_c}{8} \int_0^{+\infty} d\lambda_1 \int_0^{+\infty} d\lambda_2 \int_0^1 d\lambda\ f(\lambda_1, \lambda_2, \lambda) \prod_c (\lambda_1, \lambda_2, \lambda)\ g_{ab}(\lambda_1, \lambda_2, \lambda) \tag{4.203}$$

with

$$f(\lambda_1, \lambda_2, \lambda) = \frac{\lambda(1-\lambda)|\lambda_1 - \lambda_2|}{\sqrt{\lambda_1 \lambda_2 (1+\lambda_1)(1+\lambda_2)}(\lambda+\lambda_1)^2(\lambda+\lambda_2)^2}, \tag{4.204}$$

$$\prod_c (\lambda_1, \lambda_2, \lambda) = \prod_c \frac{1 - \lambda T_c}{\sqrt{(1+\lambda_1 T_c)(1+\lambda_2 T_c)}}, \tag{4.205}$$

and

$$g_{ab}\left(\lambda_1,\lambda_2,\lambda\right)=\delta_{ab}(1-T_a)\left(\frac{\lambda_1}{1+\lambda_1 T_a}+\frac{\lambda_2}{1+\lambda_2 T_a}+\frac{2\lambda}{1-\lambda T_a}\right)^2+(1+\delta_{ab})$$
$$\times\left[\frac{\lambda_1(1+\lambda_1)}{(1+\lambda_1 T_a)(1+\lambda_1 T_b)}+\frac{\lambda_2(1+\lambda_2)}{(1+\lambda_2 T_a)(1+\lambda_2 T_b)}+\frac{2\lambda(1-\lambda)}{(1-\lambda T_a)(1-\lambda T_b)}\right] \quad (4.206)$$

The numerical method employed to compute this complicated triple integral is explained in Ref. [25].

Also here, a particular situation exists for the capture channel, where we set

$$\prod_{c\in\gamma}\frac{1-\lambda T_c}{\sqrt{(1+\lambda_1 T_c)(1+\lambda_2 T_c)}}\approx\exp\left[-\left(2\lambda+\lambda_1+\lambda_2\right)T_\gamma^{eff}/2\right] \quad (4.207)$$

and for the continuum, for which we set

$$\prod_c(\lambda_1,\lambda_2,\lambda)=\prod_{c\in continuum}\frac{(1-\lambda\,\bar{T}_c)^{N_c}}{\sqrt{(1+\lambda_1\bar{T}_c)^{N_c}(1+\lambda_2 T_c)^{N_c}}}. \quad (4.208)$$

Again, for each J and Π, the multiplications that do not depend on a or b are first prepared in *goeprepare.f*, while the actual WFC calculation takes place in *goe.f*.

4.6 Multiple emission

At incident energies above approximately the neutron separation energy, the residual nuclides formed after the first binary reaction are populated with enough excitation energy to enable further decay by particle emission or fission. This is called multiple emission. We distinguish between two mechanisms: multiple compound (Hauser-Feshbach) decay and multiple pre-equilibrium decay.

4.6.1 Multiple Hauser-Feshbach decay

This is the conventional way, and for incident energies up to several tens of MeV a sufficient way, to treat multiple emission. It is assumed that pre-equilibrium processes can only take place in the binary reaction and that secondary and further particles are emitted by compound emission.

After the binary reaction, the residual nucleus may be left in an excited discrete state i' or an excited state within a bin i' which is characterized by excitation energy $E_x'(i')$, spin I' and parity Π'. The population of this state or set of states is given by a probability distribution for Hauser-Feshbach decay P^{HF} that is completely determined by the binary reaction mechanism. For a binary neutron-induced reaction to a discrete state i', i.e. when $E_{x'}(i'), I'$ and Π' have unique values, the residual population is given by

$$P^{\mathrm{HF}}(Z',N',E_{x'}(i'),I',\Pi')=\sigma^{i'}_{n,k'}(E^{tot},I,\Pi\rightarrow E_{x'}(i'),I',\Pi'), \quad (4.209)$$

where the non-elastic reaction cross section for a discrete state $\sigma^{i'}_{n,k'}$ was defined in Section 3.2.3 and where the ejectile k' connects the initial compound nucleus (Z_C,N_C) and the residual nucleus (Z',N'). For binary reactions to the continuum, the residual population of states characterised by (I',Π') per $E_{x'}(i')$ bin is given by the sum of a pre-equilibrium and a compound contribution

$$P^{\mathrm{HF}}(Z',N',E_{x'}(i'),I',\Pi')=\int dE_{k'}\frac{d\sigma^{comp,cont}}{dE_{k'}}(E^{tot},I,\Pi\rightarrow E_{x'}(i'),I',\Pi')$$
$$+\quad\mathcal{P}^{\mathrm{pre}}(Z',N',p_\pi^{max}+1,h_\pi^{max}+1,p_\nu^{max}+1,h_\nu^{max}+1,E_{x'}(i')), \quad (4.210)$$

where the integration range over $dE_{k'}$ corresponds exactly with the bin width of $E_x'(i')$ and $\mathcal{P}^{\rm pre}$ denotes the population entering the compound stage after primary preequilibrium emission. The expression for $\mathcal{P}^{\rm pre}$ will be given in Eq. (4.214) of the next section. Once the first generation of residual nuclides/states has been filled, the picture can be generalized to tertiary and higher order multiple emission.

In general, the population $P^{\rm HF}$ before decay of a level i' or a set of states $(I', \Pi', E_{x'}(i'))$ in bin i' of a nucleus (Z', N') in the reaction chain is proportional to the feeding, through the ejectiles k', from all possible mother bins i with an energy $E_x(i)$ in the (Z, N) nuclides, i.e.

$$\begin{aligned} P^{\rm HF}(Z', N', E_{x'}(i'), I', \Pi') &= \sum_{I,\Pi}\sum_{k'}\sum_{i}[P^{\rm HF}(Z, N, E_x(i), I, \Pi) \\ &+ \mathcal{P}^{\rm pre}(Z, N, p_\pi^{max}+1, h_\pi^{max}+1, p_\nu^{max}+1, h_\nu^{max}+1, E_x(i))] \\ &\times \frac{\Gamma_{k'}(E_x(i), I, \Pi \rightarrow E_{x'}(i'), I', \Pi')}{\Gamma^{tot}(E_x(i), I, \Pi)}. \end{aligned} \tag{4.211}$$

The appearance of the indices p_π^{max} indicates that only the reaction population that has not been emitted via the (multiple) pre-equilibrium mechanism propagates to the multiple compound stage. Similar to Eq. (4.176) the decay widths are given by

$$\Gamma_{k'}(E_x(i), I, \Pi \longrightarrow E_{x'}(i'), I', \Pi') = \frac{1}{2\pi\rho(E_x(i), I, \Pi)} \sum_{j'=|J-I'|}^{J+I'} \sum_{l'=|j'-s'|}^{j'+s'} \delta_\pi(\alpha') \left\langle T^J_{\alpha' l' j'}(E'_{\alpha'}) \right\rangle . \tag{4.212}$$

Again, the term $2\pi\rho$ (compound nucleus level density) of the decay width (4.212) falls out of the multiple emission equation (4.211) and therefore does not need to be calculated in practice. The total decay width is

$$\Gamma^{tot}(E_x(i), I, \Pi) = \sum_{k''} \sum_{I''=mod(J+s,1)}^{J+l_{max}} \sum_{\Pi''=-1}^{1} \sum_{i''} \Gamma_{k''}(E_x(i), I, \Pi \longrightarrow E_{x''}(i''), I'', \Pi''). \tag{4.213}$$

In sum, the only differences between binary and multiple compound emission are that width fluctuations and angular distributions do not enter the model and that the initial compound nucleus energy E^{tot} is replaced by an excitation energy bin E_x of the mother nucleus. The calculational procedure, in terms of sequences of decaying bins, was already explained in Chapter 3.

4.6.2 Multiple pre-equilibrium emission

At high excitation energies, resulting from high incident energies, the composite nucleus is far from equilibrated and it is obvious that the excited nucleus should be described by more degrees of freedom than just E_x, J and Π. In general, we need to keep track of the particle-hole configurations that are excited throughout the reaction chain and thereby calculate multiple pre-equilibrium emission up to any order. This is accomplished by treating multiple pre-equilibrium emission within the exciton model. This is the default option for multiple pre-equilibrium calculations in TALYS (selected with the keyword **mpreeqmode 1**). TALYS contains, furthermore, an alternative more approximative model for multiple pre-equilibrium emission (**mpreeqmode 2**), called the *s-wave transmission coefficient method*. Both approaches are discussed below.

Multiple emission within the exciton model

We introduce the pre-equilibrium population $\mathcal{P}^{\rm pre}(Z,N,p_\pi,h_\pi,p_\nu,h_\nu,E_x(i))$ which holds the amount of the reaction population present in a unique (Z,N) nucleus, $(p_\pi,h_\pi,p_\nu,h_\nu)$ exciton state and excitation energy bin $E_x(i)$. A special case is the pre-equilibrium population for a particular exciton state after binary emission, which can be written as

$$\begin{aligned} & \mathcal{P}^{\rm pre}(Z',N',p_\pi-Z_{k'},h_\pi,p_\nu-N_{k'},h_\nu,E_{x'}(i')) = \\ = \; & \sigma^{\rm CF}(Z_C,N_C,E^{\rm tot})W_{k'}(Z_C,N_C,E^{\rm tot},p_\pi,h_\pi,p_\nu,h_\nu,E_{k'}) \\ \times \; & \tau(Z_C,N_C,E^{\rm tot},p_\pi,h_\pi,p_\nu,h_\nu)P(Z_C,N_C,E^{\rm tot},p_\pi,h_\pi,p_\nu,h_\nu), \end{aligned} \tag{4.214}$$

where Z_C (N_C) again is the compound nucleus charge (neutron) number and $Z_{k'}$ ($N_{k'}$) corresponds to the ejectile charge (neutron) number. The residual excitation energy $E_x(i')$ is linked to the total energy $E^{\rm tot}$, the ejectile energy $E_{k'}$, and its separation energy $S(k')$ by $E_x(i')=E^{\rm tot}-E_{k'}-S(k')$. This $\mathcal{P}^{\rm pre}$ represents the feeding term for secondary pre-equilibrium emission. Note that for several particle-hole configurations this population is equal to zero.

In general, the pre-equilibrium population can be expressed in terms of the mother nucleus, excitation energy bins, and particle-hole configurations from which it is fed. The residual population is given by a generalization of Eq. (4.77), in which $\sigma^{\rm CF}(Z_C,N_C,E^{\rm tot})$ is replaced by the population of the particle-hole states left after the previous emission stage $\mathcal{P}^{\rm pre}(Z,N,p^0_\pi,h^0_\pi,p^0_\nu,h^0_\nu,E_x(i))$. Since several combinations of emission and internal transitions may lead to the same configuration, a summation is applied over the ejectiles treated in multiple pre-equilibrium (neutrons and protons), over the $(p^0_\pi,h^0_\pi,p^0_\nu,h^0_\nu)$ configurations with which the next step is started and over the mother excitation energy bins:

$$\begin{aligned} \mathcal{P}^{\rm pre}(Z',N',p'_\pi,h'_\pi,p'_\nu,h'_\nu,E_{x'}(i')) \;=\; & \sum_{k'=n,p}\sum_{p^0_\pi=1}^{p^{\max}_\pi}\sum_{h^0_\pi=1}^{h^{\max}_\pi}\sum_{p^0_\nu=1}^{p^{\max}_\nu}\sum_{h^0_\nu=1}^{h^{\max}_\nu} \\ & \sum_i \mathcal{P}^{\rm pre}(Z,N,p^0_\pi,h^0_\pi,p^0_\nu,h^0_\nu,E_x(i)) \\ & W_k(Z,N,p_\pi,h_\pi,p_\nu,h_\nu,E_x(i),E_{k'})\tau(Z,N,p_\pi,h_\pi,p_\nu,h_\nu,E_x(i)) \\ \times \; & P(Z,N,p_\pi,h_\pi,p_\nu,h_\nu,E_x(i)), \end{aligned} \tag{4.215}$$

where the mother and daughter quantities are related by

$$\begin{aligned} Z &= Z'+Z_{k'}, \\ N &= N'+N_{k'}, \\ p_\pi &= p'_\pi+Z_{k'}, \\ h_\pi &= h'_\pi, \\ p_\nu &= p'_\nu+N_{k'}, \\ h_\nu &= h'_\nu, \\ E_x &= E_{x'}(i')+E_{k'}+S_{k'}. \end{aligned} \tag{4.216}$$

In the computation, we thus need to keep track of every possible $(Z',N',p'_\pi,h'_\pi,p'_\nu,h'_\nu,E_{x'}(i'))$ configuration, which is uniquely linked to a mother exciton state $(Z,N,p_\pi,h_\pi,p_\nu,h_\nu,E_x(i))$ through the ejectile characterized by $(Z_{k'}, N_{k'}, E_{k'})$. The term $P(Z, N, p_\pi, h_\pi, p_\nu, h_\nu, E_x(i))$ represents the part of the pre-equilibrium cross section that starts in $(Z, N, p^0_\pi, h^0_\pi, p^0_\nu, h^0_\nu, E_x(i))$ and survives emission up to a new particle-hole state $(Z, N, p_\pi, h_\pi, p_\nu, h_\nu, E_x(i))$. Again (see Eq. (4.92)),

$$P(Z, N, p^0_\pi, h^0_\pi, p^0_\nu, h^0_\nu, E_x(i)) = 1, \tag{4.217}$$

and the calculation for each newly encountered $(Z, N, p_\pi, h_\pi, p_\nu, h_\nu, E_x(i))$ configuration proceeds according to Eq. (4.90).

The part of $\mathcal{P}^{\rm pre}$ that does not feed a new multiple pre-equilibrium population automatically goes to the multiple Hauser-Feshbach chain of Eq. (4.211).

The final expression for the multiple pre-equilibrium spectrum is very similar to Eq.(4.77)

$$\begin{aligned}
\frac{d\sigma_k^{\rm MPE}}{dE_{k'}} &= \sum_{p^0_\pi=1}^{p^{\max}_\pi} \sum_{h^0_\pi=1}^{h^{\max}_\pi} \sum_{p^0_\nu=1}^{p^{\max}_\nu} \sum_{h^0_\nu=1}^{h^{\max}_\nu} \\
& \sum_i \mathcal{P}^{\rm pre}(Z, N, p^0_\pi, h^0_\pi, p^0_\nu, h^0_\nu, E_x(i)) \\
& \sum_{p_\pi=p^0_\pi}^{p^{\max}_\pi} \sum_{h_\pi=h^0_\pi}^{h^{\max}_\pi} \sum_{p_\nu=p^0_\nu}^{p^{\max}_\nu} \sum_{h_\nu=h^0_\nu}^{h^{\max}_\nu} W_k(Z, N, p_\pi, h_\pi, p_\nu, h_\nu, E_x(i), E_{k'}) \\
\times \quad & \tau(Z, N, p_\pi, h_\pi, p_\nu, h_\nu, E_x(i))\ P(Z, N, p_\pi, h_\pi, p_\nu, h_\nu, E_x(i))
\end{aligned} \tag{4.218}$$

Multiple emission with the s-wave transmission coefficient method

Apart from the exciton model, TALYS offers another, slightly faster, method to determine multiple pre-equilibrium emission [115, 116]. Within this approach the multiple pre-equilibrium spectrum is given by the following expression:

$$\begin{aligned}
\frac{d\sigma_k^{\rm MPE}}{dE_{k'}} &= \sum_{p^0_\pi=1}^{p^{\max}_\pi} \sum_{h^0_\pi=1}^{h^{\max}_\pi} \sum_{p^0_\nu=1}^{p^{\max}_\nu} \sum_{h^0_\nu=1}^{h^{\max}_\nu} \\
& \sum_i \mathcal{P}^{\rm pre}(Z, N, p^0_\pi, h^0_\pi, p^0_\nu, h^0_\nu, E_x(i)) \\
& \frac{1}{p^0_\pi + p^0_\nu} \frac{\omega(Z_{k'}, h^0_\pi, N_{k'}, h^0_\nu, E_{k'} + S_{k'})\omega(p^0_\pi - Z_{k'}, h^0_\pi, p^0_\nu - N_{k'}, h^0_\nu, E_x(i) - E_{k'} - S_{k'})}{\omega(p^0_\pi, h^0_\pi, p^0_\nu, h^0_\nu, E_x(i))} \\
\times \quad & T_s(E_{k'})
\end{aligned} \tag{4.219}$$

In this approach each residual particle-hole configuration created in the primary pre-equilibrium decay may have one or more excited particles in the continuum. Each of these excited particles can either be emitted or captured. The emission probability is assumed to be well represented by the s-wave transmission coefficient $T_s(E_{k'})$.

4.7 Level densities

In statistical models for predicting cross sections, nuclear level densities are used at excitation energies where discrete level information is not available or incomplete. We use several models for the level density in TALYS, which range from phenomenological analytical expressions to tabulated level densities derived from microscopic models. The complete details can be found in Ref. [117].

To set the notation, we first give some general definitions. The *level density* $\rho(E_x, J, \Pi)$ corresponds to the number of nuclear levels per MeV around an excitation energy E_x, for a certain spin J and parity Π. The *total level density* $\rho^{\rm tot}(E_x)$ corresponds to the total number of levels per MeV around E_x, and is obtained by summing the level density over spin and parity:

$$\rho^{\rm tot}(E_x) = \sum_J \sum_\Pi \rho(E_x, J, \Pi). \tag{4.220}$$

The nuclear levels are degenerate in M, the magnetic quantum number, which gives rise to the *total state density* $\omega^{\rm tot}(E_x)$ which includes the $2J+1$ states for each level, i.e.

$$\omega^{\rm tot}(E_x) = \sum_J \sum_\Pi (2J+1)\rho(E_x, J, \Pi). \tag{4.221}$$

When level densities are given by analytical expressions they are usually factorized as follows

$$\rho(E_x, J, \Pi) = P(E_x, J, \Pi)R(E_x, J)\rho^{\rm tot}(E_x), \tag{4.222}$$

where $P(E_x, J, \Pi)$ is the parity distribution and $R(E_x, J)$ the spin distribution. In all but one level density model in TALYS (**ldmodel 5**), the parity equipartition is assumed, i.e.

$$P(E_x, J, \Pi) = \frac{1}{2}, \tag{4.223}$$

However, in our programming, we have accounted for the possibility to adopt non-equidistant parities, such as e.g. in the case of microscopic level density tables.

4.7.1 Effective level density

We first describe the simplest expressions that are included in TALYS for level densities. We here use the term ”effective” to denote that the nuclear collective effects are not explicitly considered, but instead are effectively included in the level density expression.

The Fermi Gas Model

Arguably the best known analytical level density expression is that of the Fermi Gas model (FGM). It is based on the assumption that the single particle states which construct the excited levels of the nucleus are equally spaced, and that collective levels are absent. For a two-fermion system, i.e. distinguishing between excited neutrons and protons, the total Fermi gas state density reads

$$\omega_F^{\rm tot}(E_x) = \frac{\sqrt{\pi}}{12} \frac{\exp\left[2\sqrt{aU}\right]}{a^{1/4}U^{5/4}}, \tag{4.224}$$

with U defined by

$$U = E_x - \Delta, \tag{4.225}$$

where the energy shift Δ is an empirical parameter which is equal to, or for some models closely related to, the pairing energy which is included to simulate the known odd-even effects in nuclei. The underlying idea is that Δ accounts for the fact that pairs of nucleons must be separated before each component can be excited individually. In practice, Δ plays an important role as adjustable parameter to reproduce observables, and its definition can be different for the various models we discuss here. Eq. (4.224) indicates that throughout this manual we will use both the *true* excitation energy E_x, as basic running variable and for expressions related to discrete levels, and the *effective* excitation energy U, mostly for expressions related to the continuum.

Eq. (4.224) also contains the level density parameter a, which theoretically is given by $a = \frac{\pi^2}{6}(g_\pi + g_\nu)$, with g_π (g_ν) denoting the spacing of the proton (neutron) single particle states near the Fermi energy. In practice a is determined, through Eq. (4.224), from experimental information of the specific nucleus under consideration or from global systematics. In contemporary analytical models, it is energy-dependent. This will be discussed in more detail below.

Under the assumption that the projections of the total angular momentum are randomly coupled, it can be derived [118] that the Fermi gas level density is

$$\rho_F(E_x, J, \Pi) = \frac{1}{2}\frac{2J+1}{2\sqrt{2\pi}\sigma^3}\exp\left[-\frac{(J+\frac{1}{2})^2}{2\sigma^2}\right]\frac{\sqrt{\pi}}{12}\frac{\exp\left[2\sqrt{aU}\right]}{a^{1/4}U^{5/4}}, \tag{4.226}$$

where the first factor $\frac{1}{2}$ represents the aforementioned equiparity distribution and σ^2 is the spin cut-off parameter, which represents the width of the angular momentum distribution. It depends on excitation energy and will also be discussed in more detail below. Eq. (4.226) is a special case of the factorization of Eq. (4.222), with the Fermi gas spin distribution given by,

$$R_F(E_x, J) = \frac{2J+1}{2\sigma^2}\exp\left[-\frac{(J+\frac{1}{2})^2}{2\sigma^2}\right]. \tag{4.227}$$

Summing $\rho_F(E_x, J, \Pi)$ over all spins and parities yields for the total Fermi gas level density

$$\rho_F^{\rm tot}(E_x) = \frac{1}{\sqrt{2\pi}\sigma}\frac{\sqrt{\pi}}{12}\frac{\exp\left[2\sqrt{aU}\right]}{a^{1/4}U^{5/4}}, \tag{4.228}$$

which is, through Eq. (4.224), related to the total Fermi gas state density as

$$\rho_F^{\rm tot}(E_x) = \frac{\omega_F^{\rm tot}(E_x)}{\sqrt{2\pi}\sigma}. \tag{4.229}$$

These equations show that $\rho_F^{\rm tot}$ and ρ_F are determined by three parameters, a, σ and Δ. The first two of these have specific energy dependencies that will now be discussed separately, while we postpone the discussion of Δ to the Section on the various specific level density models.

In the Fermi gas model, the level density parameter a can be derived from D_0, the average s-wave level spacing at the neutron separation energy S_n, which is usually obtained from the available experimental set of s-wave resonances. The following equation can be used:

$$\frac{1}{D_0} = \sum_{J=|I-\frac{1}{2}|}^{J=I+\frac{1}{2}} \rho_F(S_n, J, \Pi) \tag{4.230}$$

where I is the spin of the target nucleus. From this equation, the level density parameter a can be extracted by an iterative search procedure.

In the TALYS-output, all quantities of interest are printed, if requested.

Model	α	β	γ_1	δ_{global}
BFM effective	0.0722396	0.195267	0.410289	0.173015
BFM collective	0.0381563	0.105378	0.546474	0.743229
CTM effective	0.0692559	0.282769	0.433090	0.
CTM collective	0.0207305	0.229537	0.473625	0.
GSM effective	0.110575	0.0313662	0.648723	1.13208
GSM collective	0.0357750	0.135307	0.699663	-0.149106

Table 4.3: Global level density parameters for the phenomenological models

The level density parameter a

The formulae described above may suggest a nuclide-specific constant value for the level density parameter a, and the first level density analyses spanning an entire range of nuclides [119, 120, 121] indeed treated a as a parameter independent of energy. Later, Ignatyuk et al. [122] recognized the correlation between the parameter a and the shell correction term of the liquid-drop component of the mass formula. They argued that a more realistic level density is obtained by assuming that the Fermi gas formulae outlined above are still valid, but that energy-dependent shell effects should be effectively included through an energy dependent expression for a. This expression takes into account the presence of shell effects at low energy and their disappearance at high energy in a phenomenological manner. It reads,

$$a = a(E_x) = \tilde{a}\left(1 + \delta W \frac{1 - \exp[-\gamma U]}{U}\right). \tag{4.231}$$

Here, $\tilde{a}$ is the asymptotic level density value one would obtain in the absence of any shell effects, i.e. $\tilde{a} = a(E_x \longrightarrow \infty)$ in general, but also $\tilde{a} = a(E_x)$ for all E_x if $\delta W = 0$. The damping parameter γ determines how rapidly $a(E_x)$ approaches $\tilde{a}$. Finally, δW is the shell correction energy. The absolute magnitude of δW determines how different $a(E_x)$ is from $\tilde{a}$ at low energies, while the sign of δW determines whether $a(E_x)$ decreases or increases as a function of E_x.

The asymptotic value $\tilde{a}$ is given by the smooth form

$$\tilde{a} = \alpha A + \beta A^{2/3}, \tag{4.232}$$

where A is the mass number, while the following systematical formula for the damping parameter is used,

$$\gamma = \frac{\gamma_1}{A^{\frac{1}{3}}} + \gamma_2. \tag{4.233}$$

In Eqs. (4.232)-(4.233), α, β and $\gamma_{1,2}$ are global parameters that have been determined to give the best average level density description over a whole range of nuclides. They are given in Table 4.3, where also the average pairing correction δ_{global} is given. Also, $\gamma_2 = 0$ by default. The α and β parameters can be changed with the **alphald** and **betald** keywords, see page 171. The parameters γ_1 and γ_2 can be adjusted with the **gammashell1** and **gammashell2** keywords, see page 172, and δ_{global} with the **Pshiftconstant** keyword, see page 175.

We define δW, expressed in MeV, as the difference between the experimental mass of the nucleus M_{exp} and its mass according to the spherical liquid-drop model mass M_{LDM} (both expressed in MeV),

$$\delta W = M_{\text{exp}} - M_{\text{LDM}}. \tag{4.234}$$

For the real mass we take the value from the experimental mass compilation [123]. Following Mengoni and Nakajima [124], for $M_{\rm LDM}$ we take the formula by Myers and Swiatecki [107]:

$$\begin{aligned}
M_{\rm LDM} &= M_n N + M_H Z + E_{\rm vol} + E_{\rm sur} + E_{\rm coul} + \delta \\
M_n &= 8.07144 \ \text{MeV} \\
M_H &= 7.28899 \ \text{MeV} \\
E_{\rm vol} &= -c_1 A \\
E_{\rm sur} &= c_2 A^{2/3} \\
E_{\rm coul} &= c_3 \frac{Z^2}{A^{1/3}} - c_4 \frac{Z^2}{A} \\
c_i &= a_i \left[1 - \kappa \left(\frac{N-Z}{A} \right)^2 \right], \ \ i = 1, 2 \\
a_1 &= 15.677 \ \text{MeV} \\
a_2 &= 18.56 \ \text{MeV} \\
\kappa &= 1.79 \\
c_3 &= 0.717 \ \text{MeV} \\
c_4 &= 1.21129 \ \text{MeV} \\
\delta &= -\frac{11}{\sqrt{A}} \ \text{even} - \text{even} \\
&= 0 \quad \text{odd} \\
&= \frac{11}{\sqrt{A}} \ \text{odd} - \text{odd}.
\end{aligned} \tag{4.235}$$

Eq. (4.231) should in principle be applied at all excitation energies, unless a different level density prescription is used at low energies, as e.g. for the CTM. Therefore, a helpful extra note for practical calculations is that for small excitation energies, i.e. $E_x \leq \Delta$, the limiting value of Eq. (4.231) is given by its first order Taylor expansion

$$\lim_{E_x - \Delta \to 0} a(E_x) = \tilde{a} \left[1 + \gamma \delta W \right]. \tag{4.236}$$

From now on, wherever the level density parameter a appears in the formalism, we implicitly assume the form (4.231) for $a(E_x)$.

It is important to define the order in which the various parameters of Eq. (4.231) are calculated in TALYS, because they can be given as an adjustable parameter in the input file, they can be known from experiment or they can be determined from systematics.

If the level density parameter at the neutron separation energy $a(S_n)$ is *not* known from an experimental D_0 value, we use the above systematical formulae for the global level density parameters. In this case, all parameters in Eq. (4.231) are defined and $a(E_x)$ can be completely computed at any excitation energy. However, for several nuclei $a(S_n)$ can be derived from an experimental D_0 value through Eq. (4.230), and one may want to use this information. In TALYS, this occurs when an input value for $a(S_n)$ is given and when **asys n** is set, meaning that instead of using the systematical formulae (4.232)-(4.234) the resonance parameter database is used to determine level density parameters. If we want to use this "experimental" $a(S_n)$ we are immediately facing a constraint: Eq. (4.231) gives the following condition that must be obeyed

$$a(S_n) = \tilde{a}\left[1 + \delta W \frac{1 - \exp(-\gamma(S_n - \Delta))}{S_n - \Delta}\right] \tag{4.237}$$

This means also that $a(S_n), \tilde{a}, \delta W$ and γ cannot *all* be given simultaneously in the input, since it would lead to inconsistency. In the case of an experimental $a(S_n)$, at least another parameter must be re-adjusted. The asymptotic level density parameter $\tilde{a}$ is the first choice. This is not as strange as it seems at first sight. Even though the values for δW depend strongly on the particular theoretical mass model and are merely adopted to reproduce the global trend of shell effects for various regions of the nuclide chart, we do not alter them when going from a global to a local model. Likewise, we feel that it is dangerous to adjust γ_1 merely on the basis of discrete level information and the mean resonance spacing at the neutron separation energy, since its presence in the exponent of Eq. (4.231) may lead to level density values that deviate strongly from the global average at high energy.

Hence, if $a(S_n)$ is given, and also γ and δW are given in the input or from tables then the asymptotic level density parameter $\tilde{a}$ is automatically obtained from

$$\tilde{a} = a(S_n) / \left[1 + \delta W \frac{1 - \exp(-\gamma(S_n - \Delta))}{S_n - \Delta}\right] \tag{4.238}$$

Other choices can however be forced with the input file. If $a(S_n)$, $\tilde{a}$ and δW are given while γ is not given in the input, γ is eliminated as a free parameter and is obtained by inverting Eq. (4.237),

$$\gamma = -\frac{1}{S_n - \Delta} \ln\left[1 - \frac{S_n - \Delta}{\delta W}\left(\frac{\tilde{a}}{a(S_n)} - 1\right)\right] \tag{4.239}$$

If δW is the only parameter not given in the input, it is automatically determined by inverting Eq. (4.237),

$$\delta W = \frac{(S_n - \Delta)(\frac{a(S_n)}{\tilde{a}} - 1)}{1 - \exp(-\gamma(S_n - \Delta))} \tag{4.240}$$

All this flexibility is not completely without danger. Since both δW and $a(S_n)$ are independently derived from experimental values, it may occur that Eq. (4.239) poses problems. In particular, δW may have a sign opposite to $[a(S_n) - \tilde{a}]$. In other words, if the argument of the natural logarithm is not between 0 and 1, our escape route is to return to Eq. (4.233) for γ and to readjust δW through Eq. (4.240.

The recipe outlined above represents a full-proof method to deal with all the parameters of Eq. (4.231), i.e. it always gives a reasonable answer since we are able to invert the Ignatyuk formula in all possible ways. We emphasize that in general, consistent calculations are obtained with Eqs. (4.234), (4.232), (4.233), and when available, a specific $a(S_n)$ value from the tables. The full range of possibilities of parameter specification for the Ignatyuk formula is summarized in Table 4.4. The reason to include all these parameter possibilities is simple: fitting experiments. Moreover, these variations are not as unphysical as they may seem: Regardless of whether they are derived from experimental data or from microscopic nuclear structure models, the parameters $a(S_n), \tilde{a}, \delta W$ and γ always have an uncertainty. Hence, as long as the deviation from their default values is kept within bounds, they can be helpful fitting parameters.

Table 4.4: Specification of parameter handling for Ignatyuk formula

Input	Calculation
- (Default)	γ: Eq. (4.233), $\tilde{a}$: Eq. (4.232) or Eq. (4.238), δW: Eq. (4.234), $a(S_n)$: Eq. (4.237)
$a(S_n), \gamma, \tilde{a}, \delta W$	TALYS-Error: Conflict
$a(S_n)(\text{table}), \gamma, \tilde{a}, \delta W$	$a(S_n)$: Eq. (4.237) (Input overruled)
$\gamma, \tilde{a}, \delta W$	$a(S_n)$: Eq. (4.237)
$\gamma, \tilde{a}$	δW: Eq. (4.234), $a(S_n)$: Eq. (4.237)
$\gamma, \delta W$	$\tilde{a}$: Eq. (4.232), $a(S_n)$: Eq. (4.237)
$\tilde{a}, \delta W$	γ: Eq. (4.233), $a(S_n)$: Eq. (4.237)
γ	$\tilde{a}$: Eq. (4.232), δW: Eq. (4.234), $a(S_n)$: Eq. (4.237)
$\tilde{a}$	γ: Eq. (4.233), δW: Eq. (4.234), $a(S_n)$: Eq. (4.237)
δW	γ: Eq. (4.233), $\tilde{a}$: Eq. (4.232), $a(S_n)$: Eq. (4.237)
$a(S_n)$	γ: Eq. (4.239) or (4.233), $\tilde{a}$: Eq. (4.238), δW: Eq. (4.234) or (4.240)
$a(S_n), \tilde{a}, \delta W$	γ: Eq. (4.239)
$a(S_n), \delta W$	$\tilde{a}$: Eq. (4.238) γ: Eq. (4.239)
$a(S_n), \tilde{a}$	δW: Eq. (4.234), γ: Eq. (4.239) or γ: Eq. (4.233), δW: Eq. (4.240)
$a(S_n), \gamma$	δW: Eq. (4.234), $\tilde{a}$: Eq. (4.238)
$a(S_n), \gamma, \delta W$	$\tilde{a}$: Eq. (4.238)
$a(S_n), \gamma, \tilde{a}$	δW: Eq. (4.240)

The spin cut-off parameter

The spin cut-off parameter σ^2 represents the width of the angular momentum distribution of the level density. The general expression for the continuum is based on the observation that a nucleus possesses collective rotational energy that can not be used to excite the individual nucleons. In this picture, one can relate σ^2 to the (undeformed) moment of inertia of the nucleus I_0 and the thermodynamic temperature t,

$$t = \sqrt{\frac{U}{a}}. \tag{4.241}$$

Indeed, an often used expression is $\sigma^2 = \sigma_{\|}^2 = I_0 t$, where the symbol $\sigma_{\|}^2$ designates the parallel spin cut-off parameter, obtained from the projection of the angular momentum of the single-particle states on the symmetry axis. However, it has has been observed from microscopic level density studies that the quantity σ^2/t is not constant [125, 126], but instead shows marked shell effects, similar to the level density parameter a. To take that effect into account we follow Refs. [125, 127] and adopt the following expression,

$$\sigma^2 = \sigma_{\|}^2 = \sigma_F^2(E_x) = I_0 \frac{a}{\tilde{a}} t, \tag{4.242}$$

with $\tilde{a}$ from Eq. (4.232) and

$$I_0 = \frac{\frac{2}{5} m_0 R^2 A}{(\hbar c)^2}, \tag{4.243}$$

where $R = 1.2A^{1/3}$ is the radius, and m_0 the neutron mass in amu. This gives

$$\sigma_F^2(E_x) = 0.01389\frac{A^{5/3}}{\tilde{a}}\sqrt{aU}. \tag{4.244}$$

On average, the $\sqrt{aU}/\tilde{a}$ has the same energy- and mass-dependent behaviour as the temperature $\sqrt{U/a}$. The differences occur in the regions with large shell effects. Eq. (4.244) can be altered by means of the **spincut** keyword, see page 176.

Analogous to the level density parameter, we have to account for low excitation energies for which Eq. (4.244) is not defined ($E_x \leq \Delta$) or less appropriate. This leads us to an alternative method to determine the spin cut-off parameter, namely from the spins of the low-lying discrete levels. Suppose we want to determine this discrete spin cut-off parameter σ_d^2 in the energy range where the total level density agrees well with the discrete level sequence, i.e. from a lower discrete level N_L with energy E_L to an upper level N_U with energy E_U. It can be derived that

$$\sigma_d^2 = \frac{1}{3\sum_{i=N_L}^{N_U}(2J_i+1)}\sum_{i=N_L}^{N_U} J_i(J_i+1)(2J_i+1). \tag{4.245}$$

where J_i is the spin of discrete level i. Reading these spins from the discrete level file readily gives the value for σ_d^2. In TALYS, σ_d^2 can be used on a nucleus-by-nucleus basis, when discrete levels are known. For cases where either Eqs. (4.244) or (4.245) are not applicable, e.g. because there are no discrete levels and $U = E_x - P$ is negative, we take the systematical formula

$$\sigma^2 = \left(0.83A^{0.26}\right)^2 \tag{4.246}$$

which gives a reasonable estimate for energies in the order of 1-2 MeV.

The final functional form for $\sigma^2(E_x)$ is a combination of Eqs. (4.244) and (4.245). Defining $E_d = \frac{1}{2}(E_L + E_U)$ as the energy in the middle of the $N_L - N_U$ region, we assume σ_d^2 is constant up to this energy and can then be linearly interpolated to the expression given by Eq. (4.244). We choose the matching point to be the neutron separation energy S_n of the nucleus under consideration, i.e.

$$\begin{aligned}\sigma^2(E_x) &= \sigma_d^2 && \text{for } 0 \leq E_x \leq E_d \\ &= \sigma_d^2 + \frac{E_x - E_d}{S_n - E_d}(\sigma_F^2(E_x) - \sigma_d^2) && \text{for } E_d \leq E_x \leq S_n \\ &= \sigma_F^2(E_x) && \text{for } E_x \geq S_n.\end{aligned} \tag{4.247}$$

Analogous to the level density parameter a, from now on we implicitly assume the energy dependence for $\sigma^2(E_x)$ whenever σ^2 appears in the formalism.

Constant Temperature Model

In the Constant Temperature Model (CTM), as introduced by Gilbert and Cameron [119], the excitation energy range is divided into a low energy part from 0 MeV up to a matching energy E_M, where the so-called constant temperature law applies and a high energy part above E_M, where the Fermi gas model applies. Hence, for the total level density we have

$$\begin{aligned}\rho^{\text{tot}}(E_x) &= \rho_T^{\text{tot}}(E_x), \quad \text{if } E_x \leq E_M, \\ &= \rho_F^{\text{tot}}(E_x), \quad \text{if } E_x \geq E_M,\end{aligned} \tag{4.248}$$

and similarly for the level density

$$\begin{aligned}\rho(E_x,J,\Pi) &= \frac{1}{2}R_F(E_x,J)\rho_T^{\rm tot}(E_x), \quad \text{if } E_x \leq E_M, \\ &= \rho_F(E_x,J,\Pi), \qquad\qquad \text{if } E_x \geq E_M. \end{aligned} \tag{4.249}$$

Note that the spin distribution of Eq. (4.227) is also used in the constant temperature region, including the low-energy behaviour for the spin cut-off parameter as expressed by Eq. (4.247).

For the Fermi gas expression, we use the effective excitation energy $U = E_x - \Delta^{\rm CTM}$, where the energy shift is given by

$$\Delta^{CTM} = \chi\frac{12}{\sqrt{A}}, \tag{4.250}$$

with

$$\begin{aligned}\chi &= 0, \;\; \text{for odd} - \text{odd}, \\ &= 1, \;\; \text{for odd} - \text{even}, \\ &= 2, \;\; \text{for even} - \text{even}. \end{aligned} \tag{4.251}$$

Note that by default no adjustable pairing shift parameter is used in the CTM. In TALYS, the number 12 in the enumerator of Eq. (4.250) can be altered using the **pairconstant** keyword, see page 173. This also applies to the other level density models.

For low excitation energy, the CTM is based on the experimental evidence that the cumulated histogram $N(E_x)$ of the first discrete levels can be well reproduced by an exponential law of the type

$$N(E_x) = \exp(\frac{E_x - E_0}{T}), \tag{4.252}$$

which is called the constant temperature law. The nuclear temperature T and E_0 are parameters that serve to adjust the formula to the experimental discrete levels. Accordingly, the constant temperature part of the total level density reads

$$\rho_T^{\rm tot}(E_x) = \frac{dN(E_x)}{dE_x} = \frac{1}{T}\exp(\frac{E_x - E_0}{T}). \tag{4.253}$$

For higher energies, the Fermi gas model is more suitable and the total level density is given by Eq. (4.228). The expressions for $\rho_T^{\rm tot}$ and $\rho_F^{\rm tot}$ have to be matched at a matching energy E_M where they, and their derivatives, are identical. First, continuity requires that

$$\rho_T^{\rm tot}(E_M) = \rho_F^{\rm tot}(E_M). \tag{4.254}$$

Inserting Eq. (4.253) in this equation directly leads to the condition

$$E_0 = E_M - T\ln\left[T\rho_F^{\rm tot}(E_M)\right]. \tag{4.255}$$

Second, continuity of the derivatives requires that

$$\frac{d\rho_T^{\rm tot}}{dE_x}(E_M) = \frac{d\rho_F^{\rm tot}}{dE_x}(E_M). \tag{4.256}$$

Inserting Eq. (4.253) in this equation directly leads to the condition

$$\frac{\rho_T^{\rm tot}(E_M)}{T} = \frac{d\rho_F^{\rm tot}}{dE_x}(E_M), \tag{4.257}$$

or

$$\frac{1}{T} = \frac{d\ln\rho_F^{\rm tot}}{dE_x}(E_M). \tag{4.258}$$

In principle, for all Fermi gas type expressions, including the energy dependent expressions for a, σ^2, $K_{\rm rot}$ etc., Eq. (4.258) could be elaborated analytically, but in practice we use a numerical approach to allow any level density model to be used in the matching problem. For this, we determine the inverse temperature of Eq. (4.258) numerically by calculating $\rho_F^{\rm tot}$ on a sufficiently dense energy grid.

The matching problem gives us two conditions, given by Eqs. (4.255) and (4.258), with three unknowns: T, E_0 and E_M. Hence, we need another constraint. This is obtained by demanding that in the discrete level region the constant temperature law reproduces the experimental discrete levels, i.e. $\rho_T^{\rm tot}$ needs to obey

$$N_U = N_L + \int_{E_L}^{E_U} dE_x \rho^{\rm tot}(E_x), \tag{4.259}$$

or, after inserting Eq. (4.253),

$$N_U = N_L + \left(\exp[\frac{E_U}{T}] - \exp[\frac{E_L}{T}]\right)\exp[\frac{-E_0}{T}]. \tag{4.260}$$

The combination of Eqs. (4.255), (4.258) and (4.260) determines T, E_0 and E_M. Inserting Eq. (4.255) in Eq. (4.260) yields:

$$T\rho_F^{\rm tot}(E_M)\exp[\frac{-E_M}{T}]\left(\exp[\frac{E_U}{T}] - \exp[\frac{E_L}{T}]\right) + N_L - N_U = 0, \tag{4.261}$$

from which E_M can be solved by an iterative procedure with the simultaneous use of the tabulated values given by Eq. (4.258). The levels N_L and N_U are chosen such that $\rho_T(E_x)$ gives the best description of the observed discrete states and are stored in the nuclear structure database. For nuclides for which no, or not enough, discrete levels are given we rely on empirical formula for the temperature. For the effective model,

$$T = -0.22 + \frac{9.4}{\sqrt{A(1+\gamma\delta W)}} \tag{4.262}$$

and for the collective model

$$T = -0.25 + \frac{10.2}{\sqrt{A(1+\gamma\delta W)}} \tag{4.263}$$

where γ is taken from Eq. (4.233) and Table 4.3. Next, we directly obtain E_M from Eq. (4.258) and E_0 from Eq. (4.255). Again, Eqs. (4.262) and (4.263) were obtained by fitting all individual values of the nuclides for which sufficient discrete level information exists. In a few cases, the global expression for T leads to a value for E_M which is clearly off scale. In that case, we resort to empirical expressions for the matching energy. For the effective model

$$E_M = 2.33 + 253/A + \Delta^{CTM}, \tag{4.264}$$

and for the collective model

$$E_M = 2.67 + 253/A + \Delta^{CTM}, \tag{4.265}$$

after which we obtain T from Eq. (4.258).

The Back-shifted Fermi gas Model

In the Back-shifted Fermi gas Model (BFM) [120], the pairing energy is treated as an adjustable parameter and the Fermi gas expression is used all the way down to 0 MeV. Hence for the total level density we have

$$\rho_F^{\rm tot}(E_x) = \frac{1}{\sqrt{2\pi}\sigma}\frac{\sqrt{\pi}}{12}\frac{\exp\left[2\sqrt{aU}\right]}{a^{1/4}U^{5/4}}, \tag{4.266}$$

and for the level density,

$$\rho_F(E_x,J,\Pi) = \frac{1}{2}\frac{2J+1}{2\sqrt{2\pi}\sigma^3}\exp\left[-\frac{(J+\frac{1}{2})^2}{2\sigma^2}\right]\frac{\sqrt{\pi}}{12}\frac{\exp\left[2\sqrt{aU}\right]}{a^{1/4}U^{5/4}}, \tag{4.267}$$

respectively. These expressions, as well as the energy-dependent expressions for a and σ^2, contain the effective excitation energy $U = E_x - \Delta^{\rm BFM}$, where the energy shift is given by

$$\Delta^{BFM} = \chi\frac{12}{\sqrt{A}} + \delta, \tag{4.268}$$

with

$$\begin{aligned} \chi &= -1, \text{for odd} - \text{odd}, \\ &= 0, \text{ for odd} - \text{even}, \\ &= 1, \text{ for even} - \text{even}, \end{aligned} \tag{4.269}$$

and δ an adjustable parameter to fit experimental data per nucleus.

A problem of the original BFM, which may have hampered its use as the default level density option in nuclear model analyses, is the divergence of Eqs. (4.266)-(4.267) when U goes to zero. A solution to this problem has been provided by Grossjean and Feldmeier [129], has been put into a practical form by Demetriou and Goriely [133], and is adopted in TALYS. The expression for the total BFM level density is

$$\rho_{\rm BFM}^{\rm tot}(E_x) = \left[\frac{1}{\rho_F^{\rm tot}(E_x)} + \frac{1}{\rho_0(t)}\right]^{-1}, \tag{4.270}$$

where ρ_0 is given by

$$\rho_0(t) = \frac{\exp(1)}{24\sigma}\frac{(a_n+a_p)^2}{\sqrt{a_n a_p}}\exp(4a_n a_p t^2), \tag{4.271}$$

where $a_n = a_p = a/2$ and t is given by Eq. (4.241).

With the usual spin distribution, the level density reads

$$\rho_{\rm BFM}(E_x,J,\Pi) = \frac{1}{2}\frac{2J+1}{2\sigma^2}\exp\left[-\frac{(J+\frac{1}{2})^2}{2\sigma^2}\right]\rho_{\rm BFM}^{\rm tot}(E_x). \tag{4.272}$$

In sum, there are two adjustable parameters for the BFM, a and δ.

The Generalized Superfluid Model

The Generalized Superfluid Model (GSM) takes superconductive pairing correlations into account according to the Bardeen-Cooper-Schrieffer theory. The phenomenological version of the model [137, 138] is characterized by a phase transition from a superfluid behaviour at low energy, where pairing correlations strongly influence the level density, to a high energy region which is described by the FGM. The GSM thus resembles the CTM to the extent that it distinguishes between a low energy and a high energy region, although for the GSM this distinction follows naturally from the theory and does not depend on specific discrete levels that determine a matching energy. Instead, the model automatically provides a constant temperature-like behaviour at low energies. For the level density expressions, it is useful to recall the general formula for the total level density,

$$\rho^{\rm tot}(E_x) = \frac{1}{\sqrt{2\pi}\sigma}\frac{e^S}{\sqrt{D}}, \tag{4.273}$$

where S is the entropy and D is the determinant related to the saddle-point approximation. For the GSM this expression has two forms: one below and one above the so called critical energy U_c.

For energies below U_c, the level density is described in terms of thermodynamical functions defined *at* U_c, which is given by

$$U_c = a_c T_c^2 + E_{\rm cond}. \tag{4.274}$$

Here, the critical temperature T_c is

$$T_c = 0.567\Delta_0, \tag{4.275}$$

where the pairing correlation function is given by

$$\Delta_0 = \frac{12}{\sqrt{A}}. \tag{4.276}$$

This correlation function also determines the condensation energy $E_{\rm cond}$, which characterizes the decrease of the superfluid phase relative to the Fermi gas phase. It is given by the expression

$$E_{\rm cond} = \frac{3}{2\pi^2}a_c\Delta_0^2, \tag{4.277}$$

where the critical level density parameter a_c is given by the iterative equation

$$a_c = \tilde{a}\left[1 + \delta W\frac{1-\exp(-\gamma a_c T_c^2)}{a_c T_c^2}\right], \tag{4.278}$$

which is easily obtained once $\tilde{a}$, δW and γ are known. Eq. (4.278) indicates that shell effects are again appropriately taken into account. For the determination of the level density we also invoke the expression for the critical entropy S_c,

$$S_c = 2\,a_c\,T_c, \tag{4.279}$$

the critical determinant D_c,

$$D_c = \frac{144}{\pi}\,a_c^3\,T_c^5, \tag{4.280}$$

and the critical spin cut-off parameter σ_c^2,

$$\sigma_c^2 = 0.01389A^{5/3}\frac{a_c}{\tilde{a}}T_c. \tag{4.281}$$

Now that everything is specified at U_c, we can use the superfluid Equation Of State (EOS) to define the level density below U_c. For this, we define an effective excitation energy

$$U' = E_x + \chi\Delta_0 + \delta, \tag{4.282}$$

where

$$\begin{aligned} \chi &= 2, \text{ for odd} - \text{odd}, \\ &= 1, \text{ for odd} - \text{even}, \\ &= 0, \text{ for even} - \text{even}, \end{aligned} \tag{4.283}$$

and δ is an adjustable shift parameter to obtain the best description of experimental data per nucleus. Note that the convention for χ is again different from that of the BFM or CTM. Defining

$$\varphi^2 = 1 - \frac{U'}{U_c}, \tag{4.284}$$

then for $U' \leq U_c$ the quantities φ and T obey the superfluid EOS [137],

$$\varphi = \tanh\left(\frac{T_c}{T}\varphi\right), \tag{4.285}$$

which is equivalent to

$$T = 2T_c\ \varphi\left[\ln\frac{1+\varphi}{1-\varphi}\right]^{-1}. \tag{4.286}$$

The other required functions for $U' \leq U_c$ are the entropy S,

$$S = S_c\frac{T_c}{T}\left(1-\varphi^2\right) = S_c\frac{T_c}{T}\frac{U'}{U_c}, \tag{4.287}$$

the determinant D,

$$D = D_c\left(1-\varphi^2\right)\left(1+\varphi^2\right)^2 = D_c\frac{U'}{U_c}\left(2-\frac{U'}{U_c}\right)^2, \tag{4.288}$$

and the spin cut-off parameter

$$\sigma^2 = \sigma_c^2\left(1-\varphi^2\right) = \sigma_c^2\frac{U'}{U_c}. \tag{4.289}$$

In sum, the level density can now be specified for the entire energy range. For $U' \leq U_c$, the total level density is given by

$$\rho^{\rm tot}_{\rm GSM}(E_x) = \frac{1}{\sqrt{2\pi}\sigma}\frac{e^S}{\sqrt{D}}, \tag{4.290}$$

using Eqs. (4.287)-(4.289). Similarly, the level density is

$$\rho_{\rm GSM}(E_x, J, \Pi) = \frac{1}{2}R_F(E_x, J)\rho^{\rm tot}_{\rm GSM}(E_x). \tag{4.291}$$

For $U' \geq U_c$ the FGM applies, though with an energy shift that is different from the pairing correction of the CTM and BFM. The total level density is

$$\rho^{\rm tot}_{\rm GSM}(E_x) = \frac{1}{\sqrt{2\pi}\sigma}\frac{\sqrt{\pi}}{12}\frac{\exp\left[2\sqrt{aU}\right]}{a^{1/4}U^{5/4}}, \tag{4.292}$$

where the effective excitation energy is defined by $U = E_x - \Delta^{GSM}$, with

$$\Delta^{GSM} = E_{\text{cond}} - \chi\Delta_0 - \delta. \tag{4.293}$$

The spin cut-off parameter in the high-energy region reads

$$\sigma^2 = I_0 \frac{a}{\tilde{a}}\sqrt{\frac{U}{a}}, \tag{4.294}$$

and I_0 is given by Eq. (4.243). The level density is given by

$$\rho_{\text{GSM}}(E_x, J, \Pi) = \frac{1}{2} R_F(E_x, J)\rho^{\text{tot}}_{\text{GSM}}(E_x). \tag{4.295}$$

At the matching energy, i.e., for $E'_x = U_c - \chi\Delta_0 - \delta$, it is easy to verify that Eqs. (4.290) and (4.292) match so that the total level density is perfectly continuous. In sum, there are two adjustable parameters for the GSM, a and δ.

4.7.2 Collective effects in the level density

All the previously described models do not explicitly account for collective effects. However, it is well known that generally the first excited levels of nuclei result from coherent excitations of the fermions it contains. The Fermi gas model is not appropriate to describe such levels. Nevertheless, the models presented so far can still be applied successfully in most cases since they incorporate collectivity in the level density in an effective way through a proper choice of the energy-dependent level density parameter values.

In some calculations, especially if the disappearance of collective effects with excitation energy plays a role (e.g. in the case of fission), one would like to model the collective effects in more detail. It can be shown that the collective effects may be accounted for explicitly by introducing collective enhancement factors on top of an intrinsic level density $\rho_{F,\text{int}}(E_x, J, \Pi)$. Then the deformed Fermi gas level density $\rho_{F,\text{def}}(E_x, J, \Pi)$ reads

$$\rho_{F,\text{def}}(E_x, J, \Pi) = K_{\text{rot}}(E_x)K_{\text{vib}}(E_x)\rho_{F,\text{int}}(E_x, J, \Pi), \tag{4.296}$$

while the total level densities $\rho^{\text{tot}}_{F,\text{def}}$ and $\rho^{\text{tot}}_{F,\text{int}}$ are related in the same way. K_{rot} and K_{vib} are called the rotational and vibrational enhancement factors, respectively. If K_{rot} and K_{vib} are explicitly accounted for, $\rho_{F,\text{int}}(E_x, J, \Pi)$ should now describe purely single-particle excitations, and can be determined again by using the Fermi gas formula. Obviously, the level density parameter a of $\rho_{F,\text{int}}$ will be different from that of the effective level density described before.

The vibrational enhancement of the level density is approximated [56] by

$$K_{\text{vib}} = \exp[\delta S - (\delta U/t)], \tag{4.297}$$

where δS and δU are changes in the entropy and excitation energy, respectively, resulting from the vibrational modes and T is the nuclear temperature given by Eq. (4.241). These changes are described by the Bose gas relationships, i.e

$$\begin{aligned} \delta S &= \sum_i (2\lambda_i + 1)\Big[(1 + n_i)\ln(1 + n_i) - n_i \ln n_i\Big], \\ \delta U &= \sum_i (2\lambda_i + 1)\omega_i n_i, \end{aligned} \tag{4.298}$$

where ω_i are the energies, λ_i the multipolarities, and n_i the occupation numbers for vibrational excitations at a given temperature. The disappearance of collective enhancement of the level density at high temperatures can be taken into account by defining the occupation numbers in terms of the equation

$$n_i = \frac{\exp(-\gamma_i/2\omega_i)}{\exp(\omega_i/T) - 1}, \tag{4.299}$$

where γ_i are the spreading widths of the vibrational excitations. This spreading of collective excitations in nuclei should be similar to the zero-sound damping in a Fermi liquid, and the corresponding width can be written as

$$\gamma_i = C(\omega_i^2 + 4\pi^2 T^2). \tag{4.300}$$

The value of $C = 0.0075\ A^{1/3}$ was obtained from the systematics of the neutron resonance densities of medium-weight nuclei [130]. We use a modified systematics [56] which includes shell effects to estimate the phonon energies (in MeV), namely

$$\omega_2 = 65A^{-5/6}/(1 + 0.05\delta W), \tag{4.301}$$

for the quadrupole vibrations and

$$\omega_3 = 100A^{-5/6}/(1 + 0.05\delta W), \tag{4.302}$$

for the octupole excitations.

An alternative, liquid drop model, estimation of the vibrational collective enhancement factor is given by [128]

$$K_{\rm vib}(E_x) = \exp\left(0.0555A^{\frac{2}{3}}t^{\frac{4}{3}}\right). \tag{4.303}$$

The **kvibmodel** keyword can be used to choose between these models.

A more important contribution to the collective enhancement of the level density originates from rotational excitations. Its effect is not only much stronger ($K_{\rm rot} \sim 10 - 100$ whereas $K_{\rm vib} \sim 3$), but the form for the rotational enhancement depends on the nuclear shape as well. This makes it crucial, among others, for the description of fission cross sections.

The expression for the rotational enhancement factor depends on the deformation [56, 131]. Basically, $K_{\rm rot}$ is equal to the perpendicular spin cut-off parameter $\sigma_\perp^2$,

$$\sigma_\perp^2 = I_\perp t, \tag{4.304}$$

with the rigid-body moment of inertia perpendicular to the symmetry axis given by

$$I_\perp = I_0\left(1 + \frac{\beta_2}{3}\right) = 0.01389A^{5/3}\left(1 + \frac{\beta_2}{3}\right), \tag{4.305}$$

where β_2 is the ground-state quadrupole deformation, which we take from the nuclear structure database. Hence,

$$\sigma_\perp^2 = 0.01389A^{5/3}\left(1 + \frac{\beta_2}{3}\right)\sqrt{\frac{U}{a}}. \tag{4.306}$$

For high excitation energies, it is known that the rotational behavior vanishes. To take this into account, it is customary to introduce a phenomenological damping function $f(E_x)$ which is equal to 1 in the purely deformed case and 0 in the spherical case. The expression for the level density is then

$$\begin{aligned}\rho(E_x, J, \Pi) &= [1 - f(E_x)]K_{\rm vib}(E_x)\rho_{F,{\rm int}}(E_x, J, \Pi) + f(E_x)\rho_{F,{\rm def}}(E_x, J, \Pi) \\ &= K_{\rm rot}(E_x)K_{\rm vib}(E_x)\rho_{F,{\rm int}}(E_x, J, \Pi) \end{aligned} \tag{4.307}$$

where

$$K_{\rm rot}(E_x) = \max([\sigma_\perp^2 - 1]f(E_x) + 1, 1). \tag{4.308}$$

The function $f(E_x)$ is taken as a combination of Fermi functions,

$$f(E_x) = \frac{1}{1 + \exp(\frac{E_x - E_{col}^{g.s.}}{d_{col}^{g.s.}})}, \tag{4.309}$$

which yields the desired property of $K_{\rm rot}$ going to 1 for high excitation energy. Little is known about the parameters that govern this damping, although attempts have been made (see e.g. [132]). We arbitrarily take $E_{col}^{g.s.} = 30$ MeV, $d_{col}^{g.s.} = 5$ MeV.

The formulae given above hold for the ground state, and for inner barriers with neutron number $N \leq 144$, which are all assumed to be axially symmetric (specified by the keyword **axtype 1**). Inner barriers with $N > 144$, e.g. the Am-isotopes, are taken to be axially asymmetric (**axtype 3**), and the rotational enhancement is

$$K_{rot}(E_x) = K_{rot}^{asym}(E_x, \beta_2) = \max([\sqrt{\frac{\pi}{2}}\sigma_\perp^2(1 - \frac{2\beta_2}{3})\sigma_\parallel - 1]f(E_x) + 1, 1). \tag{4.310}$$

For outer barriers, we apply an extra factor of 2 to $K_{\rm rot}$, due to the mass asymmetry. For fission barriers, the default parameters for the damping function Eq. (4.309) are $U_f^{bar} = 45$ MeV, $C_f^{bar} = 5$ MeV.

Finally, these collective enhancement expressions can be applied to the various phenomenological level density models. The CTM formalism can be extended with explicit collective enhancement, i.e. the total level density reads

$$\begin{aligned}\rho^{\rm tot}(E_x) &= \rho_T^{\rm tot}(E_x), \quad \text{if } E_x \leq E_M, \\ &= K_{\rm rot}(E_x)K_{\rm vib}(E_x)\rho_{F,{\rm int}}^{\rm tot}(E_x), \quad \text{if } E_x \geq E_M, \end{aligned} \tag{4.311}$$

and similarly for the level density $\rho(E_x, J, \Pi)$. Note that the collective enhancement is not applied to the constant temperature region, since collectivity is assumed to be already implicitly included in the discrete levels. The matching problem is completely analogous to that described before, although the resulting parameters E_M, E_0 and T will of course be different.

The BFM can also be extended with explicit collective enhancement, i.e.

$$\rho_{\rm BFM}^{\rm tot}(E_x) = K_{\rm rot}(E_x)K_{\rm vib}(E_x)\left[\frac{1}{\rho_{F,{\rm int}}^{\rm tot}(E_x)} + \frac{1}{\rho_0(t)}\right]^{-1}, \tag{4.312}$$

and similarly for the level density $\rho(E_x, J, \Pi)$. Finally, the GSM can be extended as follows

$$\rho_{\rm GSM}^{\rm tot}(E_x) = K_{\rm rot}(E_x)K_{\rm vib}(E_x)\rho_{GSM,{\rm int}}^{\rm tot}(E_x). \tag{4.313}$$

(In fact, the term “general” in the GSM was originally meant for the collective enhancement).

4.7.3 Microscopic level densities

Besides the phenomenological models that are used in TALYS, there is also an option to employ more microscopic approaches. For the RIPL database, S. Goriely has calculated level densities from drip line to drip line on the basis of Hartree-Fock calculations [134] for excitation energies up to 150 MeV and for spin values up to $I = 30$. If **ldmodel 4**, see page 169, these tables with microscopic level densities can be read. Moreover, new energy-, spin- and parity-dependent nuclear level densities based on the microscopic combinatorial model have been proposed by Hilaire and Goriely [135]. The combinatorial model includes a detailed microscopic calculation of the intrinsic state density and collective enhancement. The only phenomenological aspect of the model is a simple damping function for the rotational effects, see also Eq. (4.307). The calculations make coherent use of nuclear structure properties determined within the deformed Skyrme-Hartree-Fock-Bogolyubov framework. Level densities for more than 8500 nuclei are made available in tabular format, for excitation energies up to 200 MeV and for spin values up to $J = 49$. These level densities are used with **ldmodel 5**.

Since these microscopical level densities, which we will call $\rho_{\rm HFM}$, have not been adjusted to experimental data, we add adjustment flexibility through a scaling function, i.e.

$$\rho(E_x, J, \pi) = \exp(c\sqrt{E_x - \delta})\rho_{HFM}(E_x - \delta, J, \pi) \qquad (4.314)$$

where by default $c = 0$ and $\delta = 0$ (i.e. unaltered values from the tables). The "pairing shift" δ simply implies obtaining the level density from the table at a different energy. The constant c plays a role similar to that of the level density parameter a of phenomenological models. Adjusting c and δ together gives adjustment flexibility at both low and higher energies.

For both microscopic level density models, tables for level densities on top of the fission barriers are automatically invoked for **ldmodel 4** or **5**, when available in the structure database. For nuclides outside the tabulated microscopic database, the default Fermi gas model is used.

4.8 Fission

4.8.1 Fission transmission coefficients

For fission, the default model implemented in TALYS is based on the transition state hypothesis of Bohr and the Hill-Wheeler expression. This yields transmission coefficients that enter the Hauser-Feshbach model to compete with the particle and photon transmission coefficients.

Transmission coefficient for one fission barrier

The Hill-Wheeler expression gives the probability of tunneling through a barrier with height B_f and width $\hbar\omega_f$ for a compound nucleus with excitation energy E_x. It reads

$$T_f(E_x) = \frac{1}{1 + \exp\left[-2\pi\frac{(E_x - B_f)}{\hbar\omega_f}\right]} \qquad (4.315)$$

For a transition state with excitation energy ε_i above the top of the same barrier, one has

$$T_f(E_x, \varepsilon_i) = \frac{1}{1 + \exp\left[-2\pi\frac{(E_x - B_f - \varepsilon_i)}{\hbar\omega_f}\right]} \qquad (4.316)$$

which means that the barrier is simply shifted up by ε_i.

For a compound nucleus with excitation energy E_x, spin J, and parity Π, the total fission transmission coefficient is the sum of the individual transmissions coefficients for each barrier through which the nucleus may tunnel, and thus reads in terms of the previously introduced $T_f(E_x, \varepsilon_i)$

$$T_f^{J,\Pi}(E_x) = \sum_i T_f(E_x, \varepsilon_i) f(i, J, \Pi) + \int_{E_{th}}^{E_x} \rho(\varepsilon, J, \Pi) T_f(E_x, \varepsilon) d\varepsilon \tag{4.317}$$

The summation runs over all discrete transition states on top of the barrier and E_{th} marks the beginning of the continuum. In this equation, $f(i, J, \Pi) = 1$ if the spin and parity of the transition state equal that of the compound nucleus and 0 otherwise. Moreover, $\rho(\varepsilon, J, \Pi)$ is the level density of fission channels with spin J and parity Π for an excitation energy ε. The main difference with the usually employed expressions is that the upper limit in the integration is finite. This expression also enables to define the number of fission channels by replacing $T_f(E_x, \varepsilon_i)$ by 1 in Eq. (4.317). This is needed for width fluctuation calculations where the fission transmission coefficient is treated as a continuum transmission coefficient.

4.8.2 Transmission coeffi cient for multi-humped barriers

For double humped barriers, the generally employed expression is based on an effective transmission coefficient T_{eff} defined by

$$T_{eff} = \frac{T_A T_B}{T_A + T_B} \tag{4.318}$$

where T_A and T_B are the transmission coefficients for barrier A and B respectively, calculated with Eq. (4.317).

If a triple humped barrier needs to be considered, the expression for T_{eff} reads

$$T_{eff} = \frac{T_{AB} T_C}{T_{AB} + T_C} \tag{4.319}$$

where T_{AB} is given by Eq. (4.318). Consequently, the expression used in TALYS reads

$$T_{eff} = \frac{T_A T_B T_C}{T_A T_B + T_A T_C + T_B T_C} \tag{4.320}$$

For any number of barrier, the effective number of fission channels is calculated as in the case for one barrier [25].

4.8.3 Class II/III states

Class II (resp. III) states may be introduced when double (resp. triple) humped barriers are considered. In the particular situation where the excitation energy E_{CN} of the compound nucleus is lower than the barrier heights, fission transmission coefficients display resonant structures which are due to the presence of nuclear excited levels (Class II) in the second, or in the third (Class III) well of the potential energy surface. When such resonant structures occur, the expression for the effective fission transmission coefficient has to be modified (generally enhanced).

The way this resonant effect is determined depends on the number of barriers that are considered.

Double humped fission barrier

In the case where two barriers occur, the effective fission transmission coefficient T_{eff} can be written as

$$T_{eff} = \frac{T_A T_B}{T_A + T_B} \times F_{AB}(E_{CN}) \tag{4.321}$$

where $F_{AB}(E_{CN})$ is a factor whose value depends on the energy difference between the excitation energy of the nucleus and that of the a class II state located in the well between barrier A and B. It has been shown [136] that the maximum value of $F_{AB}(E)$ reaches $\frac{4}{T_A+T_B}$ and gradually decreases over an energy interval defined as the width Γ_{II} of the class II state with excitation energy E_{II}. This is accounted for using the empirical quadratic expression

$$F_{AB}(E) = \frac{4}{T_A + T_B} + \left(\frac{E - E_{II}}{0.5\Gamma_{II}}\right)^2 \times \left(1 - \frac{4}{T_A + T_B}\right) \tag{4.322}$$

if $E_{II} - 0.5\Gamma_{II} \leq E \leq E_{II} + 0.5\Gamma_{II}$ and $F_{AB} = 1$ otherwise.

Theoretically, this expression is valid for the tunneling through a single double humped barrier whereas in realistic situations, both T_A and T_B are obtained from a summation over several transition states. One may thus have large T_A and T_B values so that Eq. 4.322 may give $F_{AB}(E) \leq 1$. Such a situation can only occur for high enough excitation energies for which the individual Hill-Wheeler contributions in Eq. (4.317) are large enough. However, in TALYS, we only consider class II states with excitation energies lower than the height of the first barrier. Consequently, the resonant effect can only occur if the compound nucleus energy E_{CN} is (i) lower than the top of the first barrier and (ii) close to a resonant class II state ($E_{II} - 0.5\Gamma_{II} \leq E_{CN} \leq E_{II} + 0.5\Gamma_{II}$). With such requirements, the individual Hill-Wheeler terms are clearly small, and $T_A + T_B \ll 1$.

Triple humped fission barrier

If three barriers A, B and C are considered, the situation is more complicated. In this case, three situations can occur depending on the positions of the class II and class III states. Indeed the enhancement can be due either to a class II state or to a class III state, but on top of that, a double resonant effect can also occur if both a class II and a class III state have an excitation energy close to the compound nucleus energy. For any situation, the enhancement is first calculated for the first and the second barrier giving the transmission coefficient

$$T_{eff}^{AB} = T_{AB} \times F_{AB} \tag{4.323}$$

with F_{AB} given by Eq. (4.322) as in the previous case.

Next, the eventual coupling with a class III state with energy E_{III} of width Γ_{III} is accounted for by generalizing Eq. (4.321) writing

$$T_{eff}^{ABC} = \frac{T_{eff}^{AB} T_C}{T_{eff}^{AB} + T_C} \times F_{ABC}(E_{CN}) \tag{4.324}$$

where $F_{ABC}(E_{CN})$ is given by generalizing Eq. (4.322) writing

$$F_{ABC}(E) = \frac{4}{T_{eff}^{AB} + T_C} + \left(\frac{E - E_{III}}{0.5\Gamma_{III}}\right)^2 \times \left(1 - \frac{4}{T_{eff}^{AB} + T_C}\right) \tag{4.325}$$

if $E_{III} - 0.5\Gamma_{III} \leq E \leq E_{III} + 0.5\Gamma_{III}$ and $F_{ABC} = 1$ otherwise.

4.8.4 Fission barrier parameters

In TALYS several options are included for the choice of the fission barrier parameters:

1. Experimental parameters [56]: collection of a large set of actinide fission barrier heights and curvatures for both the inner and outer barrier based on a fit to experimental data, compiled by V. Maslov. Moreover, this compilation contains head band transition states.

2. Mamdouh parameters [142]: set of double-humped fission barrier heights for numerous isotopes derived from Extended Thomas-Fermi plus Strutinsky Integral calculations.

3. Rotating-Finite-Range Model (RFRM) by Sierk [139]: single-humped fission barrier heights are determined within a rotating liquid drop model, extended with finite-range effects in the nuclear surface energy and finite surface-diffuseness effects in the Coulomb energy.

4. Rotating-Liquid-Drop Model (RLDM) by Cohen *et al* [140].

In the current version of TALYS, the dependence on angular momentum of the fission barriers is discarded. If LDM barriers are employed in the calculation, they are corrected for the difference between the ground-state and fission barrier shell correction energy:

$$B_f^{LDM}(T) = B_f^{LDM}(0) - (\delta W_{groundstate} - \delta W_{barrier}) * g(T) \tag{4.326}$$

This correction gradually disappears with temperature due to the washing out of the shell effects [143]:

$$g(T) = \begin{cases} 1 & for \quad T < 1.65\text{MeV}, \\ g(T) = 5.809 \exp(-1.066\ T) & for \quad T \geq 1.65\text{MeV}. \end{cases} \tag{4.327}$$

Shell corrections on top of the fission barrier are generally unknown. They obviously play an important role for the level density as well. Default values are adopted: for subactinides $\delta W_{barrier} = 0$ MeV, for actinides $\delta W_{barrier,inner} = 2.5$ MeV and $\delta W_{barrier,outer} = 0.6$ MeV [56].

4.8.5 WKB approximation

As an alternative to the Hill-Wheeler approach, it is also possible to use the WKB approximation to calculate fission transmission coefficients We use an implementation by Mihaela Sin and Roberto Capote and refer to Ref. [141] for the full details of this method. It can be invoked with the keyword **fismodel 5**.

4.8.6 Fission fragment properties

The description of fission fragment and product yields follows the procedure outlined in Ref. [145]. The Hauser-Feshbach formalism gives a fission cross section per excitation energy bin for each fissioning system. The fission fragment masses and charges are, subsequently, determined per given excitation energy bin E_x, in a fissioning system FS, characterised by (Z_{FS}, A_{FS}, E_x), for which the fission cross section exceeds some minimum value. The total fragment mass distribution is given by a sum over all contributing bins weighted with the corresponding fission cross sections:

$$\sigma(A_{FF}) = \sum_{Z_{FS},A_{FS},E_x} \sigma_f(Z_{FS}, A_{FS}, E_x) Y(A_{FF}; Z_{FS}, A_{FS}, E_x), \tag{4.328}$$

where $Y(A_{FF}; Z_{FS}, A_{FS}, E_x)$ is the relative yield of a fission fragment with mass A_{FF} originating from a fissioning system. Combining this expression with the result of a fission fragment charge distribution calculation yields the final production cross section of a fission fragment with mass A_{FF} and charge Z_{FF}:

$$\begin{aligned} \sigma_{prod}(Z_{FF}, A_{FF}) &= \sum_{Z_{FS},A_{FS},E_x} \sigma_f(Z_{FS}, A_{FS}, E_x) Y(A_{FF}; Z_{FS}, A_{FS}, E_x) \\ &\quad \times Y(Z_{FF}; A_{FF}, Z_{FS}, A_{FS}, E_x) \end{aligned} \tag{4.329}$$

$Y(Z_{FF}; A_{FF}, Z_{FS}, A_{FS}, E_x)$ is the relative yield of a fission fragment with charge Z_{FF} given its mass A_{FF} and the fissioning system characterised by (Z_{FS}, A_{FS}, E_x).

In general, an excitation energy distribution is connected to these fission *fragment* production cross sections. In theory, this could be used to deduce the fission *product* yields through a full evaporation calculation of the fission fragments. This is not yet possible in TALYS. Instead a rather crude approximation, outlined later in this section, is adopted to estimate the number of post-scission neutrons emitted from each fragment. This procedure leads to relative yields for the fission product masses $Y(A_{FP}; Z_{FS}, A_{FS}, E_x)$ and charges $Y(Z_{FP}; A_{FP}, Z_{FS}, A_{FS}, E_x)$ and, hence, to expressions similar to Eq. (4.328) and Eq. (4.329) for the final fission products.

Fission fragment mass distribution

The fission fragment mass distribution is determined with a revised version of the multi-modal random neck-rupture model (MM-RNRM). The original model has been developed by Brosa to calculate properties of fission fragments at zero temperature [144]. However, fission calculations within TALYS require fragment mass distributions up to higher temperatures.

In the recent version of the model [145] the temperature is added to the calculation of the potential energy landscape of the nucleus. A search for the fission channels in deformation space yields the superlong (SL), standard I (ST I), and standard II (ST II) fission barriers and prescission shapes as a function of temperature. In this manner, the incorporated melting of shell effects naturally gives rise to the vanishing of the asymmetric fission modes ST I and ST II with increasing excitation energies. The obtained temperature-dependent fission barrier and prescission shape parameters serve as input for the fragment mass distribution computations in TALYS.

Each mass distribution is a sum over contributions of the three dominant fission modes FM:

$$Y(A_{FF}; Z_{FS}, A_{FS}, E_x) = \sum_{FM=SL,STI,STII} W_{FM}(Z_{FS}, A_{FS}, E_x) Y_{FM}(A_{FF}; Z_{FS}, A_{FS}, E_x), \tag{4.330}$$

where $W_{FM}(Z_{FS}, A_{FS}, E_x)$ denotes the weight of a fission mode, and $Y_{FM}(A_{FF}; Z_{FS}, A_{FS}, E_x)$ is the corresponding mass distribution. $Y(A_{FF}; Z_{FS}, A_{FS}, E_x)$ can then be substituted in Eq. (4.328) to determine the full fission fragment mass distribution for the reaction under consideration. An analogous expression can be written down for $Y(A_{FP}; Z_{FS}, A_{FS}, E_x)$.

Each mass distribution calculation is started by determining the relative contributions of the different fission modes. These are evaluated with the Hill-Wheeler penetrability through inverted parabolic barriers using temperature-dependent barrier parameters and, consequently (the reader is referred to [145] for a detailed explanation), ground-state level densities:

$$T_{f,FM}(Z_{FS}, A_{FS}, E_x) = \int_0^\infty d\epsilon\, \rho_{gs}(Z_{FS}, A_{FS}, \epsilon) \frac{1}{1 + \exp\left[\frac{2\pi(B_{f,FM}(Z_{FS}, A_{FS}, T(\epsilon)) + \epsilon - E_x)}{\hbar\omega_{f,FM}(Z_{FS}, A_{FS}, T(\epsilon))}\right]}. \tag{4.331}$$

All actinides encounter a double-humped barrier on their way to fission. The effective transmission coefficient can be expressed in terms of the transmission coefficient through the first and second barrier denoted by T_f^A and T_f^B respectively by Eq. (4.318). Since, however, the theoretical inner barrier is much lower than the outer barrier, the relative contribution $W_{FM}(Z_{FS}, A_{FS}, E_x)$ of the three fission modes may simply be determined by an equation of the following form:

$$W_{SL}(Z_{FS}, A_{FS}, E_x) = \frac{T^B_{f,SL}}{T^B_{f,SL} + T^B_{f,STI} + T^B_{f,STII}}. \tag{4.332}$$

Equivalent formulas hold for $W_{STI}(Z_{FS}, A_{FS}, E_x)$ and $W_{STII}(Z_{FS}, A_{FS}, E_x)$.

For subactinides it is not possible to calculate the competition between symmetric and asymmetric fission modes, since the computed fission channels exhibit rather broad and strangely shaped outer barriers, which makes a parabola fit to these barriers impossible. Hence, the Hill-Wheeler approach cannot be applied. Fortunately, the SL barriers are much lower than the ST barriers. Therefore, in all these calculations the asymmetric fission modes are simply discarded and the dominant symmetric SL mode is solely taken into account for subactinides.

The RNRM is employed to calculate the mass distribution per fission mode. An extensive description of the RNRM may be found in [144]. Here it is merely attempted to communicate its main ideas. In this model, the fission process is regarded as a series of instabilities. After the passage over the barriers, a neck starts to form. If this neck becomes flat its rupture may happen anywhere, which means that the point of future constriction can shift over the neck. This motion of the dent is called the shift instability. In the instant that the Rayleigh instability starts to deepen the dent, the position of the asymmetry is frozen and rupture is taking place. The RNRM translates the effect of both mechanisms into measurable quantities.

In order for the shift instability to do its work, a perfectly flat neck is required. Hence, the so-called

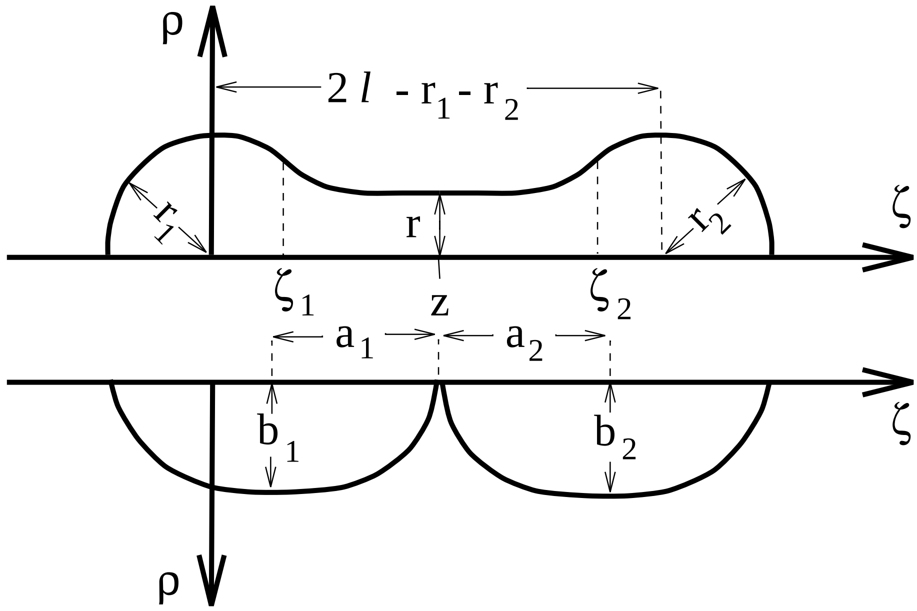

Figure 4.3: The upper part illustrates the flat-neck representation. The lower part contains the embedded spheroids parameterisation.

flat-neck parameterisation is introduced: (see Fig. 4.3):

$$\rho(\zeta) = \begin{cases} (r_1^2 - \zeta^2)^{1/2} & -r_1 \leq \zeta \leq \zeta_1 \\ r + a^2 c \left(\cosh\left(\frac{\zeta - z + l - r_1}{a}\right) - 1\right) & \zeta_1 \leq \zeta \leq \zeta_2 \\ \left(r_2^2 - (2l - r_1 - r_2 - \zeta)^2\right)^{1/2} & \zeta_2 \leq \zeta \leq 2l - r_1. \end{cases} \tag{4.333}$$

The radius of the nucleus is given by ρ as a function of a parameter ζ in terms of several parameters: the semilength *l*, the neck radius *r*, the position *z* of the dent, the curvature *c*, the extension of the neck *a*, the radii of the spherical heads r_1 and r_2, and the transitional points ζ_1 and ζ_2. By requiring continuity and differentiability of the shape, volume conservation and a minimal value of c for a really flat neck, only (*l*, *r*, *z*) remain as independent parameters. Subsequently, the neck radius is eliminated by the Rayleigh criterion, which relates the total length $2l$ of the prescission shape to the neck radius r by $2l = 11r$. The value of *z* can be transformed into the heavy fragment mass A_h by:

$$A_h = \frac{3A}{4r_{cn}^3} \int_{-l}^{z} \rho^2(\zeta) d\zeta, \tag{4.334}$$

where r_{cn} is the compound nucleus radius. The actual values of A_h and l originate from the channel searches and are called the prescission shape parameters. They have been stored in the structure database and are input to the RNRM calculations.

One last ingredient is missing for the computation of the mass distribution, namely the surface tension:

$$\gamma_0 = 0.9517 \left(1 - 1.7828 \left(\frac{N - Z}{A}\right)^2\right) MeV fm^{-2}. \tag{4.335}$$

This is taken from the LDM by Myers and Swiatecki [107].

Fluctuations amplified by the shift instability alter the shape slightly and enable the rupture of the nucleus to take place at another point than the most probable point z. In order to determine the fission-fragment mass distribution, the probability of cutting the neck at an arbitrary position z_r has to be calculated. This probability is given by the change in potential energy from z_r to z: $E(z_r) - E(z)$. This is replaced by the energy to cut the nucleus at the two positions: $E_{cut}(z_r) - E_{cut}(z)$, with $E_{cut}(z_r) = 2\pi\gamma_0\rho^2(z_r)$. The rupture probability is now proportional to the Boltzmann factor:

$$y(A_{FF}) \propto \exp\left(\frac{-2\pi\gamma_0\left(\rho^2(z_r) - \rho^2(z)\right)}{T}\right). \tag{4.336}$$

The fragment mass number A_{FF} can be computed according to the analogue of Eq. (4.334):

$$A_{FF}(z_r) = \frac{3A}{4r_{cn}^3}\int_{-l}^{z_r} \rho^2(\zeta)\, d\zeta. \tag{4.337}$$

The theoretical yield is finally determined with the following relation in which $Y(A_{FF})$ stands for the normalized fission fragment mass yield:

$$Y_{FM}(A_{FF}; Z_{FS}, A_{FS}, E_x) = y(A_{FF}) + y(A - A_{FF}). \tag{4.338}$$

In Eq. (4.336) the temperature of the scissioning nucleus must be provided. All calculations of the PES and the crossing of the fission barriers have been isothermal. However, for the RNRM the loss and gain of excitation energy in crossing the barrier is taken into account into a new excitation energy and temperature at scission:

$$E_x^{scission} = E_x^{groundstate} + F_{def,scission}. \tag{4.339}$$

The new excitation energy has two components: the original excitation energy in the ground state $E_x^{groundstate}$ and the deformation energy at scission $F_{def,scission}$. $F_{def,scission}$ is positive for actinides and becomes negative in the subactinide region. The new excitation energy is related to a new temperature $T_{scission}$. However, a new prescission temperature corresponds to a different prescission shape with a somewhat different value for $F_{def,scission}$. Therefore, the temperature $T_{scission}$ has to be determined in a self-consistent manner together with the final prescission shape. If a prescission shape has a high temperature or a very long neck, the mass distribution will be broad. Low temperatures and short necks result in a narrow mass distribution.

Post-scission neutron multiplicities

The mass distribution calculated above belongs to the primary fission fragments. Most fragments, however, are highly excited directly after their creation. They take their share of total excitation energy available at scission (4.339). Moreover, they are strongly deformed, which manifests itself in an extra amount of excitation energy set free when this deformation relaxes towards the ground-state deformation of the fragments by the strong surface tension. The superfluous excitation energy is released during the process of post-scission neutron and gamma emission. The neutron emission is responsible for a shift of the pre-neutron emission mass distribution to somewhat smaller masses.

The total excitation energy in a newly created fragment with mass A_{FF} results from:

$$E_x^{fragment}(A_{FF}) = E_{def,fragment}(A_{FF}) + \frac{A_{FF}}{A}\,E_x^{scission}. \tag{4.340}$$

$E_{def,fragment}(A_{FF})$ denotes the deformation energy of the fragment, and the second term contains the portion of the thermal energy at scission of the whole fissioning system picked up by the fragment. The assumption is that the fragment receives a share proportional to its mass.

For the calculation of $E_{def,fragment}(A_{FF})$ another shape parameterisation is employed: the embedded spheroids (see Fig. 4.3). The newborn fragments are modeled as two contacting spheroids with major axes a_1 and a_2, which are linked to *2l* and z_r by:

$$a_1 = \frac{1}{2}(r_1 + z_r), \qquad a_2 = l - \frac{1}{2}(r_1 + z_r). \tag{4.341}$$

The minor axes b_1 and b_2 follow from volume conservation:

$$b_1^2 = \frac{3}{4a_1}\int_{-r_1}^{z_r} \rho^2 d\zeta, \qquad b_2^2 = \frac{3}{4a_2}\int_{z_r}^{2l-r_1} \rho^2 d\zeta. \tag{4.342}$$

The energy difference of the spheroidally deformed and the spherical fragment $E_{def,fragment}(A_{FF})$ is given by:

$$\begin{aligned} E_{def,fragment}(A_{FF},\epsilon) \;=\;& E_{surf}^{sph}(A_{FF})\left(\frac{\arcsin(\epsilon) + \epsilon\,(1-\epsilon^2)^{1/2}}{2\epsilon\,(1-\epsilon^2)^{1/6}} - 1\right) + \\ & E_{Coul}^{sph}(A_{FF})\left(\frac{(1-\epsilon^2)^{1/3}}{2\epsilon} ln\left(\frac{1+\epsilon}{1-\epsilon}\right) - 1\right). \end{aligned} \tag{4.343}$$

The eccentricity is defined as:

$$\epsilon_i = \left(1 - \left(\frac{b_i}{a_i}\right)^2\right)^{1/2}, \tag{4.344}$$

and $E_{surf}^{sph}(A_{FF})$ and $E_{Coul}^{sph}(A_{FF})$ represent the LDM surface and the Coulomb energy of a spherical nucleus obtained from Ref. [146].

The neutron multiplicity $\nu_{FM}(A_{FF})$ for a fragment with mass A_{FF} is now derived by finding the root of the following relation:

$$E_x^{fragment}(A_{FF}) = \sum_{n=1}^{\nu_{FM}(A_{FF})} (S_n + \eta_n) + E_\gamma. \tag{4.345}$$

The separation energy S_n is calculated from the mass formula [146]. The average kinetic energy of the neutrons is taken to be $\frac{3}{2}$ times the fragment temperature, and the energy carried off by γ-rays E_γ is approximately half the separation energy of the first non-evaporated neutron.

The final fission product mass yield per fission mode is given by:

$$Y_{FM}(A_{FP}; Z_{FS}, A_{FS}, E_x) = Y_{FM}(A_{FF} - \nu_{FM}(A_{FF})) + Y_{FM}(A - A_{FF} - \nu_{FM}(A - A_{FF})). \tag{4.346}$$

Fission fragment charge distribution

Unfortunately, the MM-RNRM only yields information on the mass yields of the fission fragments. Predictions of charge distributions are performed in TALYS within a scission-point-model-like approach (Wilkins *et al.* [147]). Corresponding to each fission fragment mass A_{FF} a charge distribution is computed using the fact that the probability of producing a fragment with a charge Z_{FF} is given by the total potential energy of the two fragment system inside a Boltzmann factor:

$$Y_{FM}(Z_{FF};A_{FF},Z_{FS},A_{FS},E_x)=\frac{\exp\left(\frac{-E(Z_{FF},A_{FF},Z,A)}{T}\right)}{\sum_{Z_{FF_i}}\exp\left(\frac{-E(Z_{FF_i},A_{FF},Z,A)}{T}\right)} \tag{4.347}$$

In the original scission-point model this potential energy is integrated over all deformation space. Within the MM-RNRM, however, fission channel calculations already define the deformation at the scission point. Furthermore, a strong coupling between the collective and single particle degrees of freedom is assumed near the scission point. This means that the nucleus is characterised by a single temperature T.

The potential energy for the creation of one fragment with (Z_{FF},A_{FF}) and a second fragment with $(Z-Z_{FF},A-A_{FF})$ consists of a sum over the binding energy of the deformed fragments by the droplet model without shell corrections and their mutual Coulomb repulsion energy as well as the nuclear proximity repulsion energy:

$$E(Z_{FF},A_{FF},Z,A)=B(Z_{FF},A_{FF})+B(Z-Z_{FF},A-A_{FF})+E_{Coul}+V_{prox}. \tag{4.348}$$

The single constituents of this formula are defined by the following relations:

$$\begin{aligned}
B(Z_{FF},A_{FF}) &= -a_1\left[1-\kappa\left(\frac{A_{FF}-2Z_{FF}}{A_{FF}}\right)^2\right]A_{FF} && (4.349)\\
&\quad +a_2\left[1-\kappa\left(\frac{A_{FF}-2Z_{FF}}{A_{FF}}\right)^2\right]A_{FF}^{\frac{2}{3}}f(shape)\\
&\quad +\frac{3}{5}\frac{e^2}{r_0}\frac{Z_{FF}^2}{A_{FF}^{\frac{1}{3}}}\,g(shape)-\frac{\pi^2}{2}\frac{e^2}{r_0}\left(\frac{d}{r_0}\right)^2\frac{Z_{FF}^2}{A_{FF}} && (4.350)\\
E_{Coul} &= e^2Z_{FF}(Z-Z_{FF})S_{form}/(a_1+a_2) && (4.351)\\
V_{prox} &= -1.7817\frac{4\pi\gamma_0 b_1^2b_2^2}{a_1b_2^2+a_2b_1^2} && (4.352)
\end{aligned}$$

The parameters in the binding energy formula are taken from Ref. [146]. The function $f(shape)$ is the form factor for the Coulomb term whereas $g(shape)$ denotes the form factor for the surface energy. S_{form} is the form factor for the Coulomb interaction energy between two spheroids.

The fission product charge distribution is obtained from the calculated fission fragment charge distribution by shifting the corresponding fragment masses A_{FF} to the fission product masses A_{FP} with the aid of the post-scission neutron multiplicity $\nu_{FM}(A_{FF})$:

$$Y_{FM}(Z_{FP};A_{FP},Z_{FS},A_{FS},E_x)=Y_{FM}(Z_{FF};A_{FF}-\nu_{FM}(A_{FF}),Z_{FS},A_{FS},E_x). \tag{4.353}$$

Since proton evaporation of the fission fragments is neglected, the charge distribution connected with A_{FF} becomes simply linked to the fission product mass A_{FP}.

4.9 Thermal reactions

The Introduction states that TALYS is meant for the analysis of data in the 1 keV - 200 MeV energy region. The lower energy of 1 keV should not be taken too literally. More accurate is: above the resolved resonance range. The start of the unresolved resonance range differs from nucleus to nucleus and is related to the average resonance spacing D_0 or, equivalently, the level density at the binding energy. Generally, the starting energy region is higher for light nuclides than for heavy nuclides. Only beyond this energy, the optical and statistical models are expected to yield reasonable results, at least for the non-fluctuating cross sections. The lower energies are the domain of R-matrix theory, which describes the resonances. Nevertheless, it would be useful to have a first-order estimate of the non-threshold reactions, not only for the obvious neutron capture channel, but also for the exothermal (n,p), (n,α) and fission channels. The fact that a nuclear model calculation in TALYS is only performed down to about 1 keV should not prevent us to give at least an estimate of the $1/v$-like behaviour of the excitation function down to 10^{-5} eV (the lower energy limit in ENDF-6 files). In collaboration with J. Kopecky, we constructed a method that provides this.

4.9.1 Capture channel

First, we decide on the lower energy of validity of a TALYS nuclear model calculation E_L. Somewhat arbitrarily, we set as default $E_L = D_0$ when we wish to construct evaluated data libraries, where D_0 is taken from the nuclear model database or, if not present, derived from the level density. E_L can also be entered as an input keyword (**Elow**). Next, we determine the neutron capture cross section at the thermal energy $E_{th} = 2.53.10^{-8}$ MeV, either from the experimental database, see Chapter 5, or, if not present, from the systematical relation [148]

$$\sigma_{n,\gamma}(E_{th}) = 1.5 \times 10^{-3} a(S_n - \Delta)^{3.5} \quad \text{mb} \tag{4.354}$$

with a the level density parameter at the separation energy S_n and Δ the pairing energy. We assign a $1/v$, i.e. $1/\sqrt{E}$, dependence to the cross section from 10^{-5} eV to an upper limit $E_{1/v}$ which we set, again arbitrarily, at $E_{1/v} = 0.2E_L$. The $1/v$ line obviously crosses $\sigma_{n,\gamma}(E_{th})$ at E_{th}. The points at $E_{1/v}$ and E_L are connected by a straight line. The resulting capture cross section then looks like Fig. 4.4. In reality, the region between $E_{1/v}$ and E_L is filled with resolved resonances, the only feature we did not try to simulate.

4.9.2 Other non-threshold reactions

For other reactions with positive Q-values, such as (n,p) and (n,α), only a few experimental values at thermal energy are available and a systematical formula as for (n,γ) is hard to construct. If we do have a value for these reactions at thermal energy, the same method as for capture is followed. If not, we assume that the ratio between the gamma decay width and e.g. the proton decay width is constant for incident energies up to E_L. Hence, we determine $R_p = \sigma_{n,p}/\sigma_{n,\gamma}$ at E_L, and since we know the thermal (n,γ) value we can produce the (n,p) excitation function down to 10^{-5} eV by multiplying the capture cross section by R_p. A similar procedure is applied to all other non-threshold reactions.

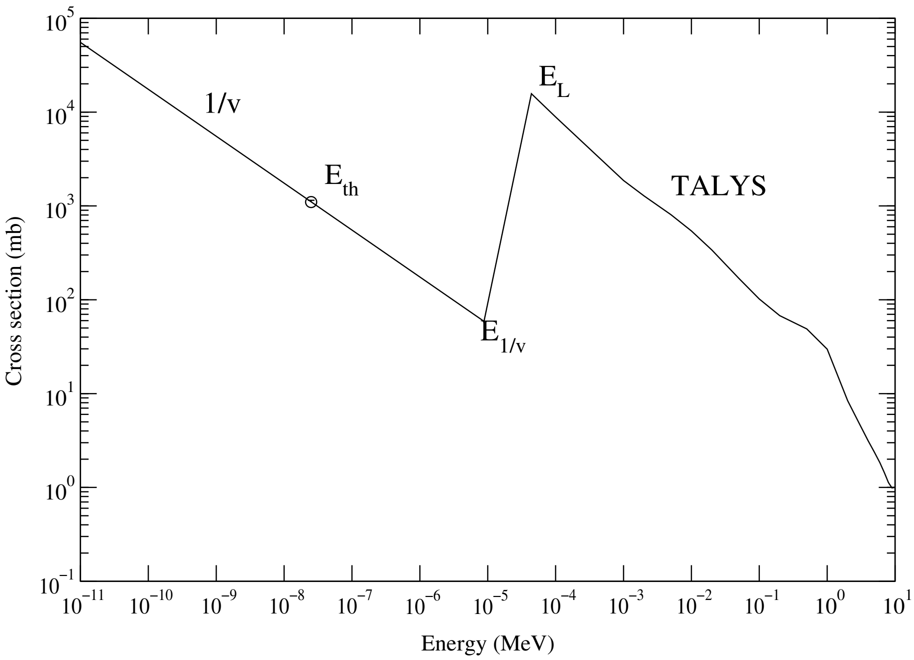

Figure 4.4: Capture cross section at low energies. The origin of the various energy regions are indicated.

4.10 Populated initial nucleus

Usually, a TALYS calculation will concern a projectile with a certain incident energy and a target, either in its ground or an excited state. However, it is also possible to start the decay from an initial population, i.e. an excited nucleus with a population distributed over excitation energy. An example of an interesting application is the neutron spectrum from fission fragments. One could calculate the fragment distribution from fission, e.g. as described in Section 4.8.6 or from empirical methods, and assume a population per excitation energy and spin, of the excited light and heavy fission fragment (models for such distributions exist, see e.g. Ref. [149]). This distribution can then be the starting point for a TALYS calculation. The initial population enters the Hauser-Feshbach scheme and the compound nucleus calculation proceeds as usual. The emitted neutrons can be recorded as well as the path from fission fragment to fission product. All relevant nuclear structure quantities are available since we simulate the process by a photon-induced reaction, the only difference being that we do not excite a single compound nucleus energy but directly fill the continuum bins and discrete levels according to our specified starting population. TALYS can be used in this mode by simply specifying **projectile 0**, see page 130, and providing an energy file as input, see page 131. The initial population can be provided at two levels of detail. A full excitation energy-spin population can be given, which is then interpolated on the internal excitation energy scheme of TALYS. Alternatively, only the total population per excitation energy can be given, after which the spin-dependent population is determined by multiplying it with the spin distribution of Eq. (4.227). For the fission neutron spectrum example mentioned above, one could loop over all fission fragments (by writing a clever script), sum the results, and obtain the fission neutron spectrum. There are more applications for this feature, such as TALYS taking care of the low energy evaporation part of a calculation that is started by a high-energy intranuclear cascade code.

4.11 Astrophysical reaction rates

In stellar interiors, nuclides not only exist in their ground states but also in different thermally excited states and a thermodynamic equilibrium holds locally to a very good approximation. Therefore, most of nuclear astrophysics calculations have made use of nuclear reaction rates evaluated within the statistical model [150]. The assumption of a thermodynamic equilibrium combined with the compound nucleus cross sections for the various excited states then allows to produce Maxwellian-averaged reaction rates, which is important input for stellar evolution models. Calculation of stellar reaction rates is obviously not new, but TALYS provides some features which automatically makes the extension to reaction rate calculations very worthwhile. In contrast with existing dedicated astrophysical reaction rate codes, the present Chapter shows that we provide the inclusion of pre-equilibrium reaction mechanism, the detailed competition between all open channels, the inclusion of multi-particle emission (neglected in most astrophysics codes), the inclusion of detailed width fluctuation corrections, the inclusion of parity-dependent level densities, the inclusion of coupled channel description for deformed nuclei, and the coherent inclusion of fission channel. Different prescriptions are also used when normalizing nuclear models on available experimental data, such nuclear level densities on s-wave spacings or E1 resonance strength on photoabsorption data.

The energies of both the targets and projectiles, as well as their relative energies E, obey Maxwell-Boltzmann distributions corresponding to the temperature T at that location (or a black-body Planck spectrum for photons). The astrophysical rate is obtained by integrating the cross section given by Eq. (4.164) over a Maxwell-Boltzmann distribution of energies E at the given temperature T. In addition, in hot astrophysical plasmas, a target nucleus exists in its ground as well as excited states. In a thermodynamic equilibrium situation, the relative populations of the various levels of nucleus with spins I^μ and excitation energies E_x^μ obey a Maxwell-Boltzmann distribution. Hence, in the formulae to follow, it is understood that the definition of the incident α channel, see below Eq. (4.164), now includes an explicit superscript μ to distinguish between the excited states The effective stellar rate of $\alpha \to \alpha'$ in the entrance channel at temperature T taking due account of the contributions of the various target excited states is finally expressed as

$$N_A\langle\sigma v\rangle^*_{\alpha\alpha'}(T) = \Big(\frac{8}{\pi m}\Big)^{1/2}\frac{N_A}{(kT)^{3/2}\,G(T)}\int_0^\infty\sum_\mu\frac{(2I^\mu+1)}{(2I^0+1)}\times \sigma^\mu_{\alpha\alpha'}(E)E\exp\Big(-\frac{E+E^\mu_x}{kT}\Big)dE, \tag{4.355}$$

where k is the Boltzmann constant, m the reduced mass of the α channel, N_A the Avogadro number, and

$$G(T)=\sum_\mu(2I^\mu+1)/(2I^0+1)\exp(-E^\mu_x/kT) \tag{4.356}$$

the T-dependent normalized partition function. Reverse reactions can also be estimated making use of the reciprocity theorem [150]. In particular, the stellar photodissociation rates are classically derived from the radiative capture rates by

$$\lambda^*_{(\gamma,\alpha)}(T) = \frac{(2I+1)(2j+1)}{(2I'+1)}\,\frac{G_I(T)}{G_{I'}(T)}\Big(\frac{AA_a}{A'}\Big)^{3/2}\Big(\frac{kT}{2\pi\hbar^2N_A}\Big)^{3/2}\times$$

$$N_A \langle \sigma v \rangle^*_{(\alpha,\gamma)} \, \mathrm{e}^{-Q_{\alpha\gamma}/kT}, \tag{4.357}$$

where $Q_{\alpha\gamma}$ is the Q-value of the $I^0(\alpha,\gamma)I'^0$ capture channel. Note that, in stellar conditions, the reaction rates for targets in thermal equilibrium are usually believed to obey reciprocity since the forward and reverse channels are symmetrical, in contrast to the situation which would be encountered for targets in their ground states only [150]. In TALYS, the total stellar photodissociation rate is determined from

$$\lambda^*_{(\gamma,j)}(T) = \frac{\sum_\mu (2J^\mu + 1) \; \lambda^\mu_{(\gamma,\alpha)}(T) \; \exp(-E^\mu_x/kT)}{\sum_\mu (2J^\mu + 1) \; \exp(-E^\mu_x/kT)}, \tag{4.358}$$

where the photodissociation rate $\lambda^\mu_{(\gamma,\alpha)}$ of state μ with excitation energy E^μ_x is given by

$$\lambda^\mu_{(\gamma,\alpha)}(T) = \int_0^\infty c \, n_\gamma(E,T) \; \sigma^\mu_{(\gamma,\alpha)}(E) \, dE \,, \tag{4.359}$$

where c is the speed of light, $\sigma^\mu_{(\gamma,j)}(E)$ the photodisintegration cross section at energy E, and n_γ the stellar γ-ray distribution well described by the back-body Planck spectrum at the given temperature T.

In TALYS, an appropriate incident energy grid for astrophysical calculations is made which overrules any incident energy given by the user.

Chapter 5

Nuclear structure and model parameters

5.1 General setup of the database

We have aimed to unify the nuclear structure and model parameter database of TALYS as much as possible. In the *talys/structure/* directory you can find the *masses/, abundance/, levels/, fission/, resonances/, deformation/, optical/, thermal/, gamma/* and *density/* subdirectories. Most subdirectories contain about 100 files, where each individual file points to a nuclear element and has the name *zZZZ* where ZZZ is the charge number of the element. One file contains the info for all the isotopes of one element. For example, the file *talys/structure/masses/z026* contains the theoretical and experimental masses of all Fe (Z=26) isotopes. As you will see below, the chemical symbol is always present in the file itself, allowing an easy search. Every directory has this same substructure and also the formats in which the data are stored have been kept uniform as much as possible.

The nuclear structure database has been created from a collection of "raw" data files, which for a large part come from the Reference Input Parameter Library RIPL [56], that we used as a basis for TALYS.

5.2 Nuclear masses

The nuclear masses are stored in the *talys/structure/masses/* directory. In TALYS, we use three different sources. In order of priority:

1. Experimental masses: The Audi Wapstra table (2003) [123]

2. Theoretical masses: The Möller mass table [151] or Goriely's mass table [152].

3. The Duflo-Zuker mass formula [153], included as a subroutine in TALYS.

The Audi-Wapstra and theoretical mass tables have been processed into our database. There, we have stored both the real mass M in atomic mass units ($amu = 931.49386$ MeV) and the mass excess $\Delta M = (M - A) * amu$ in MeV for both the experimental mass (if available) and the theoretical mass. The mass excesses are stored for a more precise calculation of separation energies.

For reaction Q-values one needs the masses of two nuclides. If for only one of them the experimental mass is known, we take the two *theoretical* mass excesses to calculate the Q-value, for consistency. This only occurs for nuclides far from the line of stability. If a nuclide is even outside the tables given in the database, we use the formula of Duflo-Zuker, which is included as a subroutine in TALYS.

As an example, below are the masses of some of the Fe-isotopes as given in file *masses/z026*. We have stored Z, A, experimental mass (amu), Möller theoretical mass (amu), experimental mass excess (MeV), Möller theoretical mass excess (MeV), Goriely theoretical mass excess (MeV), nuclear symbol with the format (2i4,5f12.6,6x,i4,a2).

26	42		42.053033		49.40	44.21	42Fe
26	43		43.040784		37.99	31.91	43Fe
26	44		44.025357		23.62	19.42	44Fe
26	45	45.014578	45.013859	13.579000	12.91	8.31	45Fe
26	46	46.000810	45.999979	0.755000	-0.02	-3.58	46Fe
26	47	46.992890	46.991283	-6.623000	-8.12	-11.09	47Fe
26	48	47.980504	47.979678	-18.160000	-18.93	-19.91	48Fe
26	49	48.973610	48.973076	-24.582000	-25.08	-26.91	49Fe
26	50	49.962988	49.962855	-34.475541	-34.60	-35.35	50Fe
26	51	50.956819	50.956178	-40.222341	-40.82	-42.41	51Fe
26	52	51.948113	51.948094	-48.331615	-48.35	-47.87	52Fe
26	53	52.945307	52.944251	-50.945323	-51.93	-50.68	53Fe
26	54	53.939610	53.938722	-56.252456	-57.08	-54.77	54Fe
26	55	54.938293	54.937606	-57.479368	-58.12	-56.24	55Fe
26	56	55.934937	55.934814	-60.605352	-60.72	-58.87	56Fe
26	57	56.935393	56.935577	-60.180130	-60.01	-59.19	57Fe
26	58	57.933275	57.933462	-62.153418	-61.98	-60.73	58Fe
26	59	58.934875	58.935383	-60.663114	-60.19	-59.34	59Fe
26	60	59.934071	59.933988	-61.411832	-61.49	-60.32	60Fe

5.3 Isotopic abundances

We have included the possibility to evaluate nuclear reactions for natural elements. If **mass 0**, see page 130, a calculation is performed for each isotope, after which the results are averaged with the isotopic abundance as weight. The isotopic abundances are stored in the *talys/structure/abundance/* directory and they are taken from RIPL (which are equal to those of the Nuclear Wallet Cards from Brookhaven National Laboratory). As an example, below are the isotopic abundances for Fe from the file *abundance/z026*. For each isotope, we have stored Z, A, its abundance, its uncertainty (not used in TALYS), nuclear symbol with the format (2i4,f11.6,f10.6,45x,i4,a2).

26	54	5.845000	0.035000	54Fe
26	56	91.754000	0.036000	56Fe
26	57	2.119000	0.010000	57Fe
26	58	0.282000	0.004000	58Fe

5.4 Discrete level file

The discrete level schemes are in the *talys/structure/levels/* directory. It is based on the discrete level file of Belgya, as stored in the RIPL-3 database. We have transformed it to a format that corresponds with that of the other parameter files in our database. Also, we filled in some omissions, repaired several errors and added some information necessary for Hauser-Feshbach calculations. As an example, below are the first discrete levels of ^{93}Nb as given in file *z041*. We have stored Z, A, total number of lines for this isotope, number of levels for this isotope, nuclear symbol with the format (2i4,2i5,56x,i4,a2). There is a loop over the levels in which we first read the level number, level energy in MeV, spin, parity, number of gamma-ray branchings, lifetime, spin assignment character, parity assignment character, original ENSDF string with the format (i4,f11.6,f6.1,3x,i2,i3,19x,e9.3,1x,2a1,a18). If the spin of a level does not come from the original file but instead is assigned in RIPL or by us, we place a 'J' in column 59. Analogously, an assigned parity is denoted by a 'P' in column 60. Note also that we have retained the original ENSDF string in columns 61-78. This string indicates the possible choices for spins and parities. If TALYS produces odd results for a nuclear reaction, a possible cause could be the wrong assignment of spin or parity. Columns 59 and 60 and the ENSDF string will reveal whether there are other possibilities that can be (and maybe should have been) adopted. For each level, there may be an inner loop over the number of gamma-ray branchings, and for each branching we read the number of the level to which the gamma-ray decay takes place and the corresponding branching ratio and electron-conversion factor. If a branching ratio has been assigned by us, a 'B' is placed in column 58. The format for this line is (29x,i3,f10.6,e10.3,5x,a1).

```
  41  93  285  100                                                        93Nb
   0    0.000000   4.5    1  0                                          9/2+
   1    0.030820   0.5   -1  1                  5.090E+08               1/2-
                              0  1.000000 1.750E+05
   2    0.687000   1.5   -1  1                  2.800E-13               3/2-
                              1  1.000000 1.833E-03
   3    0.743910   3.5    1  1                  5.700E-13               7/2+
                              0  1.000000 1.381E-03
   4    0.808580   2.5    1  2                  6.160E-12               5/2+
                              3  0.038049 7.810E-01
                              0  0.961951 1.170E-03
   5    0.810410   2.5   -1  1                  1.000E-12               5/2-
                              1  1.000000 1.282E-03
   6    0.949830   6.5    1  1                  4.360E-12              13/2+
                              0  1.000000 7.931E-04
   7    0.970000   1.5   -1  2                            J        1/2-,3/2-
                              2  0.500000 0.000E+00     B
                              4  0.500000 0.000E+00     B
   8    0.978940   5.5    1  1                  2.510E-13              11/2+
                              0  1.000000 7.564E-04
   9    1.082670   4.5    1  2                  2.900E-12               9/2+
                              3  0.712735 9.051E-03
                              0  0.287265 5.500E-04
  10    1.126850   2.5   -1  1                                         (5/2)
                              4  1.000000 4.407E-03
  11    1.284400   0.5    1  1                                        (1/2+)
                              1  1.000000 1.791E-04
  12    1.290000   0.5   -1  2                            J        1/2-,3/2-
                              1  0.500000 0.000E+00     B
```

```
                                 5  0.500000 0.000E+00     B
  13   1.297240   4.5    1  3                    2.100E-13                 9/2+
                                 8  0.232989 1.070E-02
                                 3  0.259831 2.721E-03
                                 0  0.507181 3.770E-04
  14   1.315140   2.5   -1  2                                              5/2(-)
                                 4  0.190340 1.311E-03
                                 3  0.809660 1.053E-03
  15   1.330000   1.5    1  2                              J        (3/2+,5/2+)
                                 1  0.500000 0.000E+00     B
                                 3  0.500000 0.000E+00     B
```

5.5 Deformation parameters

Deformation parameters and lengths are put in directory *talys/structure/deformation/*. They are strongly linked to the discrete level file when deformation parameters per level are given. The first subdirectory with deformation parameters is *exp/*, which have been derived from experimental information (spectroscopy, DWBA, etc.). For each isotope, we have stored Z, A, number of levels, type of collectivity, the type of parameter, nuclear symbol with the format (3i4,3x,a1,3x,a1,54x,i4,a2). The type of parameter can be D (deformation length δ_L) or B (deformation parameter β_L). The type of collectivity can be S (spherical), V (vibrational), R (rotational) and A (asymmetric rotational). Next, we read for each level the level number, the type of collectivity per level, the number of the vibrational band, multipolarity, magnetic quantum number, phonon number of the level, deformation parameter(s) with the format (i4,3x,a1,4i4,4f9.4). The type of collectivity per level can be either D (DWBA), V (vibrational) or R (rotational). In the case of levels that belong to a rotational band, only the level number and an 'R' are given. For the first level of the rotational band, the deformation parameter β_2 (and, if present, β_4 and β_6) is given. Also, for the first level of a vibrational band the deformation parameter is given. The vibration-rotational model is thus invoked if within the rotational model also states belonging to a vibrational band can be specified. The level of complexity of rotational or vibrational-rotational calculations can be specified with the **maxrot** (see page 156) and **maxband** (see page 156) keywords. For weakly coupled levels that can be treated with DWBA, the level number, a 'D' and the deformation parameter is given.

As an example, below are the deformation parameters for some even Ca isotopes, taken from *z020*. This file ensures that for a reaction on ^{40}Ca, a coupled-channels calculation with a vibrational model will automatically be invoked. Levels 2 (3^- at 3.737 MeV, with $\delta_3 = 1.34$), 3 (2^+ at 3.904 MeV, with $\delta_2 = 0.36$), 4 (5^- at 4.491 MeV, with $\delta_5 = 0.93$), will all be coupled individually as one-phonon states. There is an option to enforce a spherical OMP calculation through **spherical y** in the input, see page 156. In that case all levels will be treated with DWBA. The table below reveals that for the other Ca-isotopes the direct calculation will always be done with DWBA, but with deformation parameters β_L instead of deformation lengths δ_L.

```
  20  40   4   V   D                                                         40Ca
   0   V   0
   2   V   1   3       1  1.34000
   3   V   2   2       1  0.36000
   4   V   3   5       1  0.93000
```

```
 20  42   3   S   B                                                          42Ca
  0   V   0
  1   D                  0.24700
  9   D                  0.30264
 20  44   3   S   B                                                          44Ca
  0   V   0
  1   D                  0.25300
  8   D                  0.24012
 20  46   3   S   B                                                          46Ca
  0   V   0
  1   D                  0.15300
  6   D                  0.20408
 20  48   3   S   B                                                          48Ca
  0   V   0
  1   D                  0.10600
  4   D                  0.23003
```

As a second example, below is the info for ^{238}U from the *z092* file. The basis for the coupling scheme is a rotational model with deformation lengths $\delta_2 = 1.546$ and $\delta_4 = 0.445$, in which levels 1, 2, 3, 4, 7 and 20 can be coupled. In practice, we would include at least levels 1 and 2 (and if the results are important enough also levels 3 and 4) as rotational levels. There are 5 vibrational bands which can be included. By default we include no vibrational bands in a rotational model, but if e.g. **maxband 1** in the input, the levels 5, 6, 8 and 12 would be included with deformation length $\delta_3 = 0.9$.

```
 92 238  23   R   D                                                         238U
  0   R   0              1.54606  0.44508
  1   R   0
  2   R   0
  3   R   0
  4   R   0
  5   V   1   3   0      0.90000
  6   V   1
  7   R   0
  8   V   1
  9   V   2   4   0      0.20000
 10   V   3   3   1      0.10000
 11   V   3
 12   V   1
 13   V   2
 14   V   4   2   0      0.10000
 15   V   3
 16   V   4
 17   V   2
 19   V   5   2   2      0.10000
 20   R   0
 21   V   5
 23   V   4
 27   V   5
```

The other subdirectory with deformation parameters is *moller/*. It contains Möller's table with β_2 and β_4 deformation parameters (also included in the RIPL database). For each isotope, we have stored Z, A, β_2 and β_4, nuclear symbol with the format (2i4,1x,2f12.6,42x,i4,a2). Here is an example for various Fe-isotopes

```
  26  42    0.271000   -0.097000                                          42Fe
  26  43    0.221000   -0.072000                                          43Fe
  26  51    0.198000    0.023000                                          51Fe
  26  53    0.098000   -0.005000                                          53Fe
  26  57    0.189000   -0.003000                                          57Fe
  26  58    0.199000   -0.019000                                          58Fe
  26  59    0.219000   -0.048000                                          59Fe
  26  60    0.211000   -0.057000                                          60Fe
  26  61    0.200000   -0.069000                                          61Fe
  26  62    0.200000   -0.052000                                          62Fe
  26  63   -0.130000   -0.025000                                          63Fe
  26  64   -0.087000   -0.020000                                          64Fe
  26  65   -0.026000                                                      65Fe
```

These parameters are used when information in the *exp/* is not available.

5.6 Level density parameters

The level density parameters are stored in the *talys/structure/density/* directory. First, there are 2 subdirectories, *ground/* and *fission/*, for ground state and fission barrier level densities, respectively. In *ground/ctm/*, *ground/bfm/*, and *ground/gsm/*, phenomenological level density parameters are stored. When the level density parameter **a** is given, it is derived from a fit to the D_0 resonance spacing of the RIPL database. As an example, below are the parameters for the Zr-isotopes from *ground/bfm/z040*. For each isotope, we have stored Z, A, and then for both the effective and explicit collective model N_L, N_U, level density parameter a in MeV^{-1}, and pairing correction in MeV, nuclear symbol. The format is (2i4,2(2i4,2f12.5)4x,i4,a2).

```
  40  86   8  17     0.00000     0.51730   8  17     0.00000     1.04574    86Zr
  40  87   8  26     0.00000     0.15936   8  26     0.00000     0.65313    87Zr
  40  88   5  17     0.00000    -0.04425   5  17     0.00000     0.46704    88Zr
  40  89   2  15     0.00000     0.39230   2  15     0.00000     0.96543    89Zr
  40  90   8  16     0.00000     0.99793   8  16     0.00000     1.80236    90Zr
  40  91   3  17     9.57730     0.40553   3  17     5.13903     1.15428    91Zr
  40  92   3  16     9.94736    -0.03571   3  16     5.00387     0.39829    92Zr
  40  93   8  18    11.07918     0.50929   8  18     5.92169     1.07202    93Zr
  40  94   4  16    12.51538     0.28941   4  16     6.66540     0.60420    94Zr
  40  95   3  18    11.98832     0.83535   3  18     5.97084     1.28803    95Zr
  40  96   3  16     0.00000     0.64799   3  16     0.00000     1.06393    96Zr
  40  98   8  16     0.00000     0.32758   8  16     0.00000     0.67594    98Zr
  40  99   2  21     0.00000    -0.01325   2  21     0.00000     0.26100    99Zr
  40 100   8  17     0.00000    -0.25519   8  17     0.00000     0.00789   100Zr
  40 101   8  15     0.00000    -0.13926   8  15     0.00000     0.17608   101Zr
```

```
  40 102   8  17     0.00000    -0.37952   8  17     0.00000    -0.12167   102Zr
```

The second subdirectory *ground/goriely/*, contains the tabulated microscopic level densities of Goriely [134], also present in RIPL. For each isotope, there are first 4 comment lines, indicating the nucleus under consideration. Next, the excitation energy, temperature, number of cumulative levels, total level density, total state density and state density per spin are read in the format (f7.2,7.3,e10.2,31e9.2). Below is an example for the first energies of ^{42}Fe from *ground/goriely/z026.tab*

```
***************************************************************************
*  Z= 26 A= 42: Total and Spin-dependent Level Density [MeV-1] for Fe 42 *
***************************************************************************
 U[MeV]  T[MeV]  NCUMUL   RHOOBS   RHOTOT     J=0      J=1      J=2
   0.25  0.224  1.09E+00 7.33E-01 2.07E+00 2.44E-01 3.39E-01 1.26E-01
   0.50  0.302  1.33E+00 1.17E+00 4.14E+00 2.74E-01 4.83E-01 2.88E-01
   0.75  0.365  1.71E+00 1.86E+00 7.60E+00 3.45E-01 6.76E-01 4.95E-01
   1.00  0.419  2.29E+00 2.82E+00 1.31E+01 4.33E-01 9.05E-01 7.55E-01
```

Level densities for fission barriers are tabulated in *fission/goriely/*. There is an *inner/* and *outer/* subdirectory, for the inner and outer barrier, respectively. Here is an example for the first few energy/spin points of ^{230}U from *fission/goriely/inner/z090*. The format is the same as for the ground state, see above.

```
****************************************************************************
*  Z= 92 A=230: Total and Spin-dependent Level Density [MeV-1] at the inner
   saddle point c=  1.24 h=  0.00 a=  0.00 B=  3.80 MeV  *
****************************************************************************
 U[MeV]  T[MeV]  NCUMUL   RHOOBS   RHOTOT     J=0      J=1      J=2
   0.25  0.162  1.11E+00 8.86E-01 5.92E+00 6.44E-02 1.64E-01 1.98E-01
   0.50  0.190  1.51E+00 2.32E+00 1.81E+01 1.19E-01 3.20E-01 4.31E-01
   0.75  0.209  2.56E+00 6.10E+00 5.25E+01 2.54E-01 7.01E-01 9.85E-01
```

Similar tables can be found in the *hilaire/* subroutines.

5.7 Resonance parameters

Neutron resonance parameters are provided in the *talys/structure/resonances/* directory and stem from the the RIPL-2 database. As an example, below are the parameters for the Fe-isotopes from *resonances/z026*. For each isotope, we have stored Z, A, the experimental s-wave resonance spacing D_0 in keV, its uncertainty, the experimental s-wave strength function S_0 (x10^{-4}), its uncertainty, the experimental total radiative width in eV and its uncertainty, nuclear symbol. The format is (2i4,2e9.2,2f5.2,2f9.5,20x,i4,a2).

```
  26  55 1.80E+01 2.40E+00 6.90 1.80  1.80000  0.50000                      55Fe
  26  57 2.54E+01 2.20E+00 2.30 0.60  0.92000  0.41000                      57Fe
  26  58 6.50E+00 1.00E+00 4.70 1.10  1.90000  0.60000                      58Fe
  26  59 2.54E+01 4.90E+00 4.40 1.30  3.00000  0.90000                      59Fe
```

5.8 Gamma-ray parameters

The Giant Dipole Resonance (GDR) parameters, stored in the *talys/structure/gamma/gdr/* directory, originate from the Beijing GDR compilation, as present in the RIPL database. As an example, below are the GDR parameters for the U-isotopes from *z092*. For each isotope, we have stored Z, A, energy E_0 in MeV, strength σ_0 in mb, width of the GDR Γ_0 in MeV and, if present, another energy, strength and width for the second peak, nuclear symbol. The format is (2i4,6f8.2,18x,i4,a2).

```
92 233   11.08  221.00    1.94   13.86  433.00    5.47                      233U
92 234   11.13  371.00    2.26   13.94  401.00    4.46                      234U
92 235   10.90  328.00    2.30   13.96  459.00    4.75                      235U
92 236   10.92  271.00    2.55   13.78  415.00    4.88                      236U
92 238   10.77  311.00    2.37   13.80  459.00    5.13                      238U
```

The second subdirectory *gamma/hbfcs/*, contains the tabulated microscopic gamma ray strength functions of Goriely [21], calculated according to Hartree-Fock BCS theory. For each isotope, there is first a line indicating the nucleus under consideration, read in the format (2(4x,i3)). Next, one line with units is given after which comes a table of excitation energies and strength functions, in the format (f9.3,e12.3). Below is an example for the first energies of ^{110}Ba from *gamma/hfbcs/z056*

```
 Z=  56 A= 121 Ba
  U[MeV]  fE1[mb/MeV]
    0.100   5.581E-05
    0.200   2.233E-04
    0.300   5.028E-04
    0.400   8.947E-04
    0.500   1.400E-03
    0.600   2.018E-03
    0.700   2.752E-03
    0.800   3.601E-03
```

The third subdirectory *gamma/hbf/*, contains the tabulated microscopic gamma ray strength functions of Goriely [21], calculated according to Hartree-Fock QRPA theory. For each isotope, there is first a line indicating the nucleus under consideration, read in the format (2(4x,i3)). Next, one line with units is given after which comes a table of excitation energies and strength functions, in the format (f9.3,e12.3). Below is an example for the first energies of ^{110}Ba from *gamma/hfbcs/z056*

```
 Z=  56 A= 110
  U[MeV]  fE1[mb/MeV]
    0.100   8.463E-03
    0.200   9.116E-03
    0.300   9.822E-03
    0.400   1.058E-02
    0.500   1.139E-02
    0.600   1.226E-02
    0.700   1.318E-02
    0.800   1.416E-02
```

5.9 Thermal cross sections

In *talys/structure/thermal/*, the thermal cross sections for (n,γ), (n,p), (n,α) and (n,f) cross sections are stored. The values come from Kopecky, who has compiled this database for use in the EAF library. In TALYS, we use this to determine cross sections for non-threshold reactions at low energies. For each isotope, we read Z, A, target state (ground state or isomer), final state (ground state or isomer), the thermal (n,γ) cross section, its error, the thermal (n,p) cross section, its error, the thermal (n,α) cross section, its error, the thermal (n,f) cross section, its error, nuclear symbol. The format is (4i4,8e9.2,7x,i4,a2). As an example, below are the values for the Fe-isotopes from *z026*.

```
  26  54   0   0 2.70e+03 5.00e+02                   1.00e-02      ...       54Fe
  26  55   0   0 1.30e+04 2.00e+03                   1.70e+05      ...       55Fe
  26  56   0   0 2.60e+03 2.00e+02                                 ...       56Fe
  26  57   0   0 2.50e+03 5.00e+02                                 ...       57Fe
  26  58   0   0 1.30e+03 1.00e+02                                 ...       58Fe
  26  59   0   0 1.30e+04 3.00e+03                   1.00e+04      ...       59Fe
```

5.10 Optical model parameters

The optical model parameters are stored in the *talys/structure/optical/* directory. All the parameters are based on one and the same functional form, see Section 4.1. There are two subdirectories: *neutron/* and *proton/*. For each isotope, optical potential parameters can be given. Per isotope, we have stored Z, A, number of different optical potentials (2), character to determine coupled-channels potential, nuclear symbol with the format (3i4,3x,a1,58x,i4,a2). On the next line we read the OMP index (1: non-dispersive, 2: dispersive). Fermi energy and reduced Coulomb radius with the format (i4,f7.2,f8.3). On the next 3 lines we read the optical model parameters as defined in Section 4.1 with the following format

```
(2f8.3,f6.1,f10.4,f9.6,f6.1,f7.1) rv,av,v1,v2,v3,w1,w2
(2f8.3,f6.1,f10.4,f7.2) rvd,avd,d1,d2,d3
(2f8.3,f6.1,f10.4,f7.2,f6.1) rvso,avso,vso1,vso2,wso1,wso2
```

For neutrons, a dispersive potential may also be available. (These potentials have not (yet) been unpublished). In that case, another block of data is given per isotope, but now with an OMP index equal to 2, to denote the parameters for a dispersive potential. As an example, here are the parameters for the Fe-isotopes from *neutron/z026*.

```
  26  54   2                                                                 54Fe
   1 -11.34   0.000
   1.186   0.663  58.2    0.0071 0.000019  13.2   78.0
   1.278   0.536  15.4    0.0223  10.90
   1.000   0.580   6.1    0.0040  -3.1  160.0
   2 -11.34   0.000
   1.215   0.670  54.2    0.0077 0.000022   9.5   88.0
   1.278   0.536  15.4    0.0223  10.90
   1.000   0.580   6.1    0.0040  -3.1  160.0
```

```
 26  56   2                                                                     56Fe
  1  -9.42   0.000
  1.186   0.663  56.8    0.0071 0.000019  13.0   80.0
  1.282   0.532  15.3    0.0211  10.90
  1.000   0.580   6.1    0.0040  -3.1  160.0
  2  -9.42   0.000
  1.212   0.670  53.2    0.0079 0.000023  10.0   88.0
  1.282   0.532  15.3    0.0211  10.90
  1.000   0.580   6.1    0.0040  -3.1  160.0
```

5.11 Radial matter densities

For the calculation of the JLM OMP, both Stephane Goriely and Stephane Hilaire have provided radial matter densities from dripline to dripline. They are stored in *talys/structure/optical/jlm/*. As an example, below are the data of some of the Fe-isotopes as given in file *talys/structure/optical/jlm/goriely/z026*. First we give Z, A, number of radii (lines), incremental step between radii, all in fm, with the format (2i4,i5,f7.3). Next we give the radius, and the radial densities for different deformations, first for protons and then for neutrons, with the format (f8.3,10(e12.5)),

```
 26  56  200  0.100
  0.100 8.04162E-02 0.00000E+00 0.00000E+00 0.00000E+00 0.00000E+00 9.06018E-02
  0.200 8.02269E-02 0.00000E+00 0.00000E+00 0.00000E+00 0.00000E+00 9.05443E-02
  0.300 7.98895E-02 0.00000E+00 0.00000E+00 0.00000E+00 0.00000E+00 9.04407E-02
  0.400 7.94588E-02 0.00000E+00 0.00000E+00 0.00000E+00 0.00000E+00 9.03063E-02
  0.500 7.89124E-02 0.00000E+00 0.00000E+00 0.00000E+00 0.00000E+00 9.01315E-02
```

Note that only the spherical components in this database are non-zero. In the files of Hilaire, see *talys/structure/optical/jlm/hilaire/*, there are also deformed components, but they will only become relevant when deformed JLM calculations are included in TALYS.

5.12 Fission parameters

The fission parameters are stored in the *talys/structure/fission/* directory. There are various subdirectories: *barrier/*, *states/*, *brosa/*, *mamdouh/*, and *hfbpath/*.

First, the experimental fission parameter set can be found in directory *barrier/*. The directory *states/* includes headband transition states for even-even, even-odd, odd-odd, and odd-even nuclides. The parameters are the result of an extensive fit to many experimental fission cross sections, compiled by V. Maslov for the RIPL library. As an example we show the available parameters for the uranium isotopes which are present in the file *barrier/z092*. We have stored Z, A, a parameter specifying the symmetry of the inner barrier, height of the inner barrier, curvature of the inner barrier, a parameter specifying the symmetry of the outer barrier, height of the outer barrier, curvature of the outer barrier, the pairing correlation function at the barrier (which is not used in the calculation) and the nuclear symbol with the format (2i4,a5,2f8.3,a5,2f8.3,f9.4,15x,i4,a2).

```
 92 231   S     4.40    0.70   MA    5.50    0.50    0.869                231U
 92 232   S     4.90    0.90   MA    5.40    0.60    0.848                232U
```

```
  92 233   S      4.35    0.80   MA    5.55    0.50    0.946                     233U
  92 234   S      4.80    0.90   MA    5.50    0.60    0.889                     234U
  92 235   S      5.25    0.70   MA    6.00    0.50    0.803                     235U
  92 236   S      5.00    0.90   MA    5.67    0.60    0.833                     236U
  92 237   GA     6.40    0.70   MA    6.15    0.50    0.809                     237U
  92 238   GA     6.30    1.00   MA    5.50    0.60    0.818                     238U
  92 239   GA     6.45    0.70   MA    6.00    0.50    0.816                     239U
```

In *states*, we have stored files with default head band and class II-states for even-even, even-odd, odd-odd, and odd-even nuclides. An example of a file containing the head band transition states is given below for *states/hbstates.ee*. This file is used for even-even nuclides. We loop over the two barriers. On the first line one finds the barrier number, the number of head band states and the energy at which the continuum starts with the format(2i4,f8.3). Next we loop over the transition states, in which we read the level number, level energy in MeV, spin and parity with the format (i4,f11.6,f6.1,i5).

```
   1   8   0.800
   1   0.000000   0.0    1
   2   0.500000   2.0    1
   3   0.400000   0.0   -1
   4   0.400000   1.0   -1
   5   0.500000   2.0    1
   6   0.400000   2.0   -1
   7   0.800000   0.0    1
   8   0.800000   0.0    1
   2   4   0.500
   1   0.000000   0.0    1
   2   0.500000   2.0    1
   3   0.200000   0.0   -1
   4   0.500000   1.0   -1
```

We also include the possibility to incorporate the effect of class II states in the calculation. For this purpose we take four parameter sets with class II states for even-even, even-odd, odd-odd, and odd-even nuclides. As an example we show the file *states/class2states.ee*. This file contains the well number, and the number of class II states. Subsequent lines contain the level number, the level energy in MeV, spin and parity with the format (i4,f8.3,f9.1,i5).

```
   1  10
   1   2.700      0.0    1
   2   3.400      0.0   -1
   3   4.100      1.0   -1
   4   4.800      2.0   -1
   5   5.000      1.0    1
   6   5.200      0.0    1
   7   5.400      0.0   -1
   8   5.500      1.0   -1
   9   5.600      2.0   -1
  10   5.700      1.0    1
```

The directory *brosa/* contains three subdirectories: *barrier/*, *groundstate/*, and *prescission/*. In *brosa/barrier/* temperature-dependent fission barrier parameters per fission mode can be found. They are the results of calculations performed within the Brosa model. The extension in the filename reveals the fission mode: sl for superlong, st for standard I, and st2 for standard II. As an example, below are the superlong parameters for several U isotopes taken from *brosa/barrier/z092.sl*. Each line gives Z, A, temperature T in MeV, B_F in MeV, $\hbar\omega$ in MeV, and the barrier position in terms of the distance between the fragment centers d in fm. The format is (2i4,4f15.5).

```
 92 240        0.00000       11.40470        3.92020       10.37450
 92 240        0.30000       11.23440        4.18630       10.34980
 92 240        0.60000       11.64780        4.25390       10.44170
 92 240        0.90000        9.58680        2.58900       10.35970
 92 240        1.20000        7.88030        2.36520       10.53400
 92 240        1.60000        5.69890        1.58010       10.43420
 92 240        2.00000        4.17750        1.07010       10.28590
 92 240        2.50000        2.76320        0.47300        9.69080
 92 240        3.00000        1.84230        0.25520        8.57080
 92 238        0.00000       10.88450        4.67530       10.27930
 92 238        0.30000       10.97680        4.87110       10.27090
 92 238        0.60000       10.59680        4.44100       10.29590
 92 238        0.90000        9.31080        3.69600       10.37940
 92 238        1.20000        7.55620        2.32260       10.40990
 92 238        1.60000        5.46180        1.51320       10.33670
 92 238        2.00000        3.98050        0.82730       10.15860
 92 238        2.50000        2.74050        0.43440        9.43930
 92 238        3.00000        1.87030        0.34600        8.62610
```

The ground state energies as a function of temperature are stored in *brosa/barrier/groundstate/*. Each line has the same format: Z, A, T in MeV, and $E_{groundstate}$ in MeV (2i4,2f15.5). An example is included for U isotopes, see *brosa/barrier/groundstate/z092*.

```
 92 240        0.00000    -1811.82104
 92 240        0.30000    -1813.38599
 92 240        0.60000    -1818.06006
 92 240        0.90000    -1825.59497
 92 240        1.20000    -1836.26599
 92 240        1.60000    -1855.76294
 92 240        2.00000    -1881.23901
 92 240        2.50000    -1921.08105
 92 240        3.00000    -1969.60205
 92 238        0.00000    -1800.57996
 92 238        0.30000    -1802.16504
 92 238        0.60000    -1806.85205
 92 238        0.90000    -1814.34302
 92 238        1.20000    -1825.23596
 92 238        1.60000    -1844.68799
 92 238        2.00000    -1870.17004
 92 238        2.50000    -1910.02905
 92 238        3.00000    -1958.52405
```

The third directory, *brosa/barrier/prescission/*, contains parameters that fix the prescission shape of the nucleus in each fission mode. They mark the end of the fission path found in the same fission channel calculations that resulted in the Brosa barrier parameters. Again each line has the same format: Z, A, T in MeV, A_h the heavy fragment mass in amu, *l* the nucleus half length in fm, and $E_{prescission}$ in MeV (2i4,4f15.5). An example is included for prescission shape parameters in the superlong mode of U isotopes, see *brosa/barrier/prescission/z092.sl*,

```
 92 240         0.00000      120.45900        21.29700    -1840.84900
 92 240         0.30000      120.83730        21.48670    -1826.35022
 92 240         0.60000      120.83670        20.74300    -1831.38477
 92 240         0.90000      120.30430        20.21950    -1840.12256
 92 240         1.20000      120.65520        20.13060    -1854.43555
 92 240         1.60000      120.83060        19.56120    -1874.16174
 92 240         2.00000      120.74340        19.33610    -1902.75671
 92 240         2.50000      120.62800        18.38600    -1945.59497
 92 240         3.00000      120.78300        18.45000    -1998.50598
 92 238         0.00000      120.00730        21.40630    -1815.46497
 92 238         0.30000      119.64770        21.36200    -1816.33203
 92 238         0.60000      119.50730        20.50950    -1821.51123
 92 238         0.90000      119.27930        20.50120    -1830.13428
 92 238         1.20000      119.47550        19.91770    -1842.70630
 92 238         1.60000      123.00390        19.23990    -1864.13489
 92 238         2.00000      120.49580        19.24370    -1892.63281
 92 238         2.50000      119.62200        18.37100    -1935.14502
 92 238         3.00000      119.37600        18.38000    -1988.42395
```

The Mamdouh fission parameter set can be found in directory *mamdouh/*. This parameter set has been derived from Extended Thomas-Fermi plus Strutinsky Integral calculations and comprise double-humped fission barrier heights and curvatures for numerous isotopes. As an example we show the available parameters for the various U isotopes which are present in the file *mamdouh/z092*. We have stored Z, A, height of the inner barrier, height of the outer barrier in MeV and the nuclear symbol with the format (i3,i4,2(24x,f8.2),5x,i3,a2).

```
 92 230     1.24     0.00     0.00     3.80     1.77    -0.02     0.35     3.90      230U
 92 231     1.24     0.01     0.00     4.10     1.83     0.05     0.50     4.30      231U
 92 232     1.25     0.02     0.00     4.20     1.83     0.05     0.53     4.20      232U
 92 233     1.28     0.05     0.00     4.70     1.84     0.06     0.53     4.40      233U
 92 234     1.28     0.03     0.00     4.80     1.83     0.06     0.53     4.40      234U
 92 235     1.28     0.04     0.00     5.40     1.63     0.01     0.53     4.10      235U
 92 236     1.29     0.04     0.00     5.20     1.64     0.01     0.53     4.00      236U
 92 237     1.28     0.04     0.00     5.70     1.63     0.01     0.53     4.30      237U
 92 238     1.29     0.03     0.00     5.70     1.91     0.07     0.47     4.90      238U
 92 239     1.29     0.03     0.00     6.10     1.81    -0.07     0.35     5.50      239U
 92 240     1.29     0.03     0.00     6.00     1.90    -0.04     0.53     6.30      240U
 92 241     1.30     0.04     0.00     6.30     1.91    -0.03     0.55     5.70      241U
 92 242     1.30     0.04     0.00     5.90     1.90    -0.04     0.53     6.00      242U
```

If we use the WKB approximation to calculate fission transmission coefficients, **fismodel 5**, we need potential energy curves. They can be found in the directory *hfbpath/*. As an example, we show the data for ^{235}U as present in the file *hfbpath/z092*. We have stored Z, A, number of fission width values, total energy (not used) with the format (3i4,f12.3). Next, we give the values for the fission width and height with the format (f10.3,20x,f10.3),

```
 92 235 100   -1781.682
    0.269     0.000     0.152     0.000
    0.298     0.000     0.180     0.332
    0.326     0.000     0.189     1.047
    0.355     0.000     0.171     1.987
    0.383     0.000     0.216     2.846
    0.412     0.000     0.199     3.921
    0.440     0.000     0.194     4.695
    0.470     0.000     0.158     5.002
    0.501     0.000     0.136     5.391
    0.531     0.000     0.156     5.390
    0.563     0.000     0.173     5.186
```

Chapter 6

Input description

For the communication between TALYS and its users, we have constructed an input/output method which shields beginners from all the possible options for nuclear model parameters that can be specified in TALYS, while enabling at the same time maximal flexibility for experienced users.

An input file of TALYS consists of keywords and their associated values. Before we list all the input possibilities, let us illustrate the use of the input by the following example. It represents a minimum input file for TALYS:

```
projectile n
element    al
mass       27
energy     14.
```

This input file represents the simplest question that can be asked to TALYS: if a ^{27}Al nucleus is hit by 14 MeV neutrons, what happens? Behind this simple input file, however, there are more than a hundred default values for the various nuclear models, parameters, output flags, etc., that you may or may not be interested in. When you use a minimal input file like the one above, you leave it to the authors of TALYS to choose all the parameters and models for you, as well as the level of detail of the output file. If you want to use specific nuclear models other than the default, adjust parameters or want to have more specific information in the output file(s), more keywords are required. Obviously, more keywords means more flexibility and, in the case of adequate use, better results, though often at the expense of increasing the level of phenomenology. In this Chapter, we will first give the basic rules that must be obeyed when constructing an input file for TALYS. Next, we give an outline of all the keywords, which have been categorised in several groups. Finally, we summarize all keywords in one table.

6.1 Basic input rules

Theoretically, it would be possible to make the use of TALYS completely idiot-proof, i.e. to prevent the user from any input mistakes that possibly can be made and to continue a calculation with “assumed” values. Although we have invested a relatively large effort in the user-friendliness of TALYS, we have not taken such safety measures to the extreme limit and ask at least some minimal responsibility from the user. Once you have accepted that, only very little effort is required to work with the code. Successful execution of TALYS can be expected if you remember the following simple rules and possibilities of the input file:

1. One input line contains one keyword. Usually it is accompanied by only one value, as in the simple example given above, but some keywords for model parameters need to be accompanied by indices (usually Z and A) on the same line.
2. A keyword and its value(s) *must* be separated by at least 1 blank character.
3. The keywords can be given in arbitrary order. If, by mistake, you use the same keyword more than once, the value of the last one will be adopted. This does not hold for keywords with different Z and A indices, see below.
4. All characters can be given in either lowercase or uppercase. The exception concerns file names, as for e.g. the **optmod** keyword. These must be given in lowercase.
5. A keyword *must* be accompanied by a value. (There is one exception, the **rotational** keyword). To use default values, the keywords should simply be left out of the input file.
6. An input line starting with a # in column 1 is neglected. This is helpful for including comments in the input file or to temporarily deactivate keywords.
7. A minimal input file always consists of 4 lines and contains the keywords **projectile**, **element**, **mass** and **energy**. These 4 keywords *must* be given in any input file.
8. An input line may not exceed 80 characters.

As an example of rules 2, 3, 4 and 6, it can be seen that the following input file is completely equivalent to the one given in the beginning of this Chapter:

```
# Equivalent input file
energy              14.
projectile n
mass 27
Element AL
#outbasic y
```

In the following erroneous input file, only the first 2 lines are correct, while rules 2 and 5 are violated in the other lines.

```
 projectile n
element al
mass27
energy
```

In cases like this, TALYS will give an error message for the first encountered problem and the execution will be stopped. We like to believe that we have covered all such cases and that it is impossible to let TALYS crash (at least with our compilers, see also Chapter 7) without giving an appropriate error message, but you are of course invited to prove and let us know about the contrary (Sorry, no cash rewards). Typing errors in the input file will be spotted by TALYS, e.g. if you write **projjectile n**, it will tell you the keyword is not in our list.

6.2 Keywords

The four-line input file given above was an example of a minimum input file for TALYS. In general, you probably want to be more specific, as in the following example:

```
projectile   n
element      nb
mass         93
energy       1.
Ltarget      1
relativistic n
widthmode    2
outinverse   y
a 41 93 13.115
a 41 94 13.421
```

which will simulate the reaction of a 1 MeV neutron incident on ^{93}Nb, with the target in its first excited state (**Ltarget 1**, a 16-year isomer), using non-relativistic kinematics, the HRTW-model for width fluctuation corrections (**widthmode 2**) in the compound nucleus calculation, with the particle transmission coefficients and inverse reaction cross sections written on the output file (**outinverse y**) and with user-defined level density parameters at the binding energy **a** for ^{93}Nb and ^{94}Nb.

In this Section, we will explain all the possible keywords. We have classified according to their meaning and importance. For each keyword, we give an explanation, a few examples, the default value, and the theoretically allowed numerical range. As the input file above shows, there is usually one value per keyword. Often, however, in cases where several residual nuclides are involved, nuclear model parameters differ from nuclide to nuclide. Then, the particular nuclide under consideration must also be given in the input line. In general, for these model parameters, we read keyword, Z, A, a physical value and sometimes a possible further index (e.g. the fission barrier, index for the giant resonance, etc.), all separated by blanks. As the example above shows for the level density parameter a, the same keyword can appear more than once in an input file, to cover several different nuclides. Again, remember that all such keywords, if you don't specify them, have a default value from either the nuclear structure and model parameter database or from systematics. The usual reason to change them is to fit experimental data, to use new information that is not yet in the database, or simply because the user may not agree with our default values. A final important point to note is that some keywords induce defaults for other keywords. This may seem confusing, but in practice this is not so. As an example, for a ^{56}Fe target the **fission** keyword is automatically disabled whereas for ^{232}Th it is by default enabled. Hence, the default value of the **fission** keyword is mass dependent. In the input description that follows, you will find a few similar cases. Anyway, you can always find all adopted default values for all parameters at the top of the *output* file and overrule them in a new input file.

6.2.1 Four main keywords

As explained above there are 4 basic keywords that form the highest level of input. They determine the fundamental parameters for any nuclear reaction induced by a light particle.

projectile

Eight different symbols can be given as **projectile**, namely **n, p, d, t, h, a, g** representing neutron, proton, deuteron, triton, ^{3}He, alpha and gamma, respectively, and **0**, which is used if instead of a nuclear reaction (projectile + target) we start with an initial population of an excited nucleus.
Examples:

projectile n

projectile d

Range: **projectile** must be equal to **n, p, d, t, h, g** or **0**.
Default: None.

element

Either the nuclear symbol or the charge number Z of the target nucleus can be given. Possible values for **element** range from Li (3) to Ds (110).
Examples:

element pu

element 41

element V

Range: $\mathbf{3} \leq$ **element** $\leq \mathbf{110}$ or **Li** $\leq$ **element** $\leq$ **Ds**.
Default: None.

mass

The target mass number A. The case of a natural element can be specified by **mass 0**. Then, a TALYS calculation for each naturally occurring isotope will be performed (see also the **abundance** keyword, p. 143), after which the results will be properly weighted and summed.
Examples:

mass 239

mass 0

Range: **mass 0** or $\mathbf{5} <$ **mass** $\leq \mathbf{339}$. The extra condition is that the target nucleus, i.e. the combination of **mass** and **element** must be present in the mass database, which corresponds to all nuclei between the proton and neutron drip lines.
Default: None.

energy

The incident energy in MeV. The user has two possibilities: (1) A single incident energy is specified in the input as a real number, (2) A filename is specified, where the corresponding file contains a series of incident energies, with one incident energy per line. Any name can be given to this file, provided it starts with a character and it is present in your working directory. Option (2) is helpful for the calculation of excitation functions or for the creation of data libraries. Option (2) is mandatory if **projectile 0**, i.e., if instead of a nuclear reaction we start with a population of an excited nucleus (see below).
Examples:

energy 140.

energy 0.002

energy range

Range: $\mathbf{10^{-11}}$ MeV $\leq$ **energy** $<$ $\mathbf{250}$ MeV or a *filename*, whereby the corresponding file contains at least 1 and a maximum of **numenin** incident energies, where **numenin** is an array dimension specified in *talys.cmb*. Currently **numenin=125**.
Default: None.

Using the four main keywords

To summarize the use of the four basic keywords, consider the following input file

```
projectile n
element    pd
mass       110
energy range
```

The file *range* looks e.g. as follows

```
0.1
0.2
0.5
1.
1.5
2.
5.
8.
10.
15.
20.
```

In the source code, the number of incident energies, here 11, is known as **numinc**. For the four-line input given above, TALYS will simulate all open reaction channels for $n+{}^{110}$Pd for all incident energies given in the file *range*, using defaults for all models and parameters. The most important cross sections will automatically be written to the output file, see Chapter 7.

Special cases

There are two examples for which the **energy** keyword does not represent the incident energy of the projectile.

1. Populated initial nucleus If **projectile 0**, the user *must* give a filename for the **energy** keyword. This time however, the file does not consist of incident energies but of the excitation energy grid of the initial population, see Section 4.10. On the first line of the file we read the number of energies (lines), number of spins, and maximum excitation energy of the population. Next, the excitation energies that are read represent the middle values of the bins, and are followed by either (a) if the number of spins is zero, the total population in that bin, or (b) if the number of bins is not zero, the population per excitation energy bin and spin, using one column per spin. Hence, if we let TALYS determine the spin distribution (case (a)), an example of such as file is

```
    8    0   4.
0.25 0.1342
0.75 0.2176
1.25 0.3344
1.75 0.6522
2.25 0.6464
2.75 0.2897
3.25 0.1154
3.75 0.0653
```

and if we give the full spin-dependent population (case (b)) we could e.g. have

```
    8    3   4.
0.25 0.0334 0.0542 0.0112
0.75 0.0698 0.1043 0.0441
1.25 0.1131 0.2303 0.0971
1.75 0.1578 0.3333 0.1143
2.25 0.1499 0.3290 0.1212
2.75 0.1003 0.2678 0.0845
3.25 0.0844 0.1313 0.0661
3.75 0.0211 0.0889 0.0021
```

2. Astrophysical reaction rates If **astro y**, see page 143 for astrophysical reaction rate calculations, the incident energy as given in the input is overruled by a hardwired incident energy grid that is appropriate for the calculation of reaction rates. However, to avoid unnecessary programming complications, the **energy** keyword *must* still be given in the input, and it can have any value. Hence if **astro y** one could e.g. give **energy 1.** in the input file. The adopted incident energies that overrule this value will be given in the output.

Four main keywords: summary

The first four keywords are clearly the most important: they do *not* have a default value while they determine default values for some of the other keywords which, in other words, may be projectile-, energy-, element- or mass-dependent. All the keywords that follow now in this manual have default values and can hypothetically be left out of the input file if you are only interested in a minimal reaction specification. If you want to add keywords, you can enter them one by one in the format that will be described below. Another way is to go to the top of the output file that is generated by the simple input file given above. You will find all the keywords with their values as adopted in the calculation, either user-specified or as defaults. All nuclear model parameters per nucleus are printed in the file *parameters.dat*, provided **partable y** was set in the input. You can copy this part and paste it into the input file, after which the values can be changed.

6.2.2 Basic physical and numerical parameters

The keywords described in this subsection are rather general and do not belong to particular nuclear models. They determine the completeness and precision of the calculations and most of them can have a significant impact on the calculation time.

ejectiles

The outgoing particles that are considered in competing reaction channels. By default, all competing channels are included even if one is interested in only one type of outgoing particle. This is necessary since there is always competition with other particles that determines the outcome for the particle under study. Furthermore, reaction Q-values automatically keep channels closed at low incident energies. However, for diagnostic or time-economical purposes, or cases where e.g. one is only interested in high-energy (p, p') and (p, n) multi-step direct reactions, one may save computing time and output by skipping certain ejectiles as competing particles. For neutron-induced fission of actinides up to 20 MeV, setting **ejectiles g n** is a rather good approximation that saves time. Also comparisons with computer codes that do not include the whole range of particles will be facilitated by this keyword.
Examples:

ejectiles n

ejectiles g n p a

Range: **ejectiles** can be any combination of **g, n, p, d, t, h** and **a**.
Default: Include all possible outgoing particles, i.e. **ejectiles g n p d t h a**

Ltarget

The excited state of the target as given in the discrete level database. This keyword allows to compute cross sections for isomeric targets.
Examples:

Ltarget 2

Range: **0** $\leq$ **Ltarget** $\leq$ **numlev**, where **numlev** is specified in the file *talys.cmb*. Currently, **numlev=25**
Default: **Ltarget 0**, i.e. the target is in its ground state.

maxZ

The maximal number of protons away from the initial compound nucleus that is considered in a chain of nuclides. For example, if **maxZ 3**, then for a $n+{}^{56}$Fe (Z=26) reaction, the V-isotopes (Z=23) are the last to be considered for further particle evaporation in the multiple emission chain. **maxZ** is normally only changed for diagnostic purposes. For example, if you are only interested in the (n,n'), $(n,2n)$,...(n,xn) residual production cross sections, or the associated discrete gamma ray intensities, **maxZ 0** is appropriate. (Note that in this case, the competition of emission of protons up to alpha particles is *still* taken into account for all the nuclides along the (n,xn) chain, only the decay of the associated residual nuclides are not tracked further).
Examples:

maxZ 6

Range: **0** $\leq$ **maxZ** $\leq$ **numZ-2**, where we suggest **numZ=2+2*memorypar** is specified in the file *talys.cmb*, where **memorypar=5** for a computer with at least 256 Mb of memory.
Default: Continue until all possible reaction channels are closed or until the maximal possible value for **maxZ** is reached (which rarely occurs). By default **maxZ=numZ-2** where the parameter **numZ** is specified in the file *talys.cmb*. This parameter should be large enough to ensure complete evaporation of all daughter nuclei.

maxN

The maximal number of neutrons away from the initial compound nucleus that is considered in a chain of nuclides. For example, if **maxN 3**, then for a $n+{}^{56}$Fe (N=31) reaction, residual nuclei with N=28 (=31-3) are the last to be considered for further particle evaporation in the multiple emission chain. **maxN** is normally only changed for diagnostic or economical purposes.
Examples:

maxN 6

Range: **0** $\leq$ **maxN** $\leq$ **numN-2**, where we suggest **numN=4+4*memorypar** is specified in the file *talys.cmb*, where **memorypar=5** for a computer with at least 256 Mb of memory.
Default: Continue until all possible reaction channels are closed or until the maximal possible value for **maxN** is reached (which rarely occurs). By default **maxN=numN-2** where the parameter **numN** is specified in the file *talys.cmb*. This parameter should be large enough to ensure complete evaporation of all daughter nuclei.

bins

The number of excitation energy bins in which the continuum of the initial compound nucleus is divided for further decay. The excitation energy region between the last discrete level and the total excitation energy for the initial compound nucleus is divided into **bins** equidistant energy bins. The resulting bin width then also determines that for the neighboring residual nuclei, in the sense that for any residual nucleus we ensure that the bins fit exactly between the last discrete level and the maximal possible excitation energy. For residual nuclides far away from the target, a smaller number of bins is automatically

adopted. It is obvious that **bins** has a large impact on the computation time.
Examples:

bins 25

Range: **2** $\leq$ **bins** $\leq$ **numbins**, where **numbins** is specified in the file *talys.cmb*. Currently, **numbins=100**
Default: **bins 40**

segment

The number of segments to divide the standard emission energy grid. The basic emission energy grid we use for spectra and transmission coefficient calculations is:

```
  0.001, 0.002, 0.005    MeV
  0.01,  0.02,  0.05     MeV
  0.1-    2 MeV : dE= 0.1 MeV
  2  -    4 MeV : dE= 0.2 MeV
  4  -   20 MeV : dE= 0.5 MeV
 20  -   40 MeV : dE= 1.0 MeV
 40  - 250 MeV : dE= 2.0 MeV
```

This grid is divided into a finer grid by subdividing each interval by **segment**.
Examples:

segment 3

Range: **1** $\leq$ **segment** $\leq$ **4**. Extra conditions: **1** $\leq$ **segment** $\leq$ **3** if the maximum incident energy is larger than 20 MeV, **1** $\leq$ **segment** $\leq$ **2** if the maximum incident energy is larger than 40 MeV, **segment=1** if the maximum incident energy is larger than 100 MeV. (These rules are imposed due to memory limitations).
Default: **segment 1**

maxlevelstar

The number of included discrete levels for the *target* nucleus that is considered in Hauser-Feshbach decay and the gamma-ray cascade. For nuclides that do not have **maxlevelstar** available in the discrete level file, we take the last known level as the last discrete level in our calculation.
Examples:

maxlevelstar 0

maxlevelstar 12

Range: **0** $\leq$ **maxlevelstar** $\leq$ **numlev**, where **numlev** is specified in the file *talys.cmb*. Currently, **numlev=25**
Default: **maxlevelstar 20**

maxlevelsres

The number of included discrete levels for all *residual* nuclides that is considered in Hauser-Feshbach decay and the gamma-ray cascade. For nuclides that do not have **maxlevelsres** available in the discrete level file, we take the last known level as the last discrete level in our calculation. This keyword is overruled by **maxlevelsbin** and **maxlevelstar** for specified nuclides.
Examples:

maxlevelsres 0

maxlevelsres 12

Range: **0** $\leq$ **maxlevelsres** $\leq$ **numlev**, where **numlev** is specified in the file *talys.cmb*. Currently, **numlev=25**
Default: **maxlevelsres 10**

maxlevelsbin

The number of included discrete levels for the nuclides resulting from *binary* emission that is considered in Hauser-Feshbach decay and the gamma-ray cascade. For nuclides that do not have **maxlevelsbin** available in the discrete level file, we take the last known level as the last discrete level in our calculation. On the input line we read **maxlevelsbin**, the symbol of the ejectile and the number of levels of the associated residual nucleus.
Examples:

maxlevelsbin a 8

maxlevelsbin p 12

Range: **0** $\leq$ **maxlevelsbin** $\leq$ **numlev**, where **numlev** is specified in the file *talys.cmb*. Currently, **numlev=25**
Default: **maxlevelsbin g 10**, **maxlevelsbin n 10**, **maxlevelsbin p 10**, **maxlevelsbin d 5**, **maxlevelsbin t 5**, **maxlevelsbin h 5**, **maxlevelsbin a 10**. The value for the inelastic channel will however always be overruled by the **maxlevelstar** keyword, for the target nucleus, or the value for its default.

Nlevels

The number of included discrete levels for a *specific residual* nucleus that is considered in Hauser-Feshbach decay and the gamma-ray cascade. For nuclides that do not have **Nlevels** available in the discrete level file, we take the last known level as the last discrete level in our calculation. On the input line we read **Nlevels**, Z, A, and the number of levels.
Examples:

Nlevels 41 93 8

Range: **0** $\leq$ **Nlevels** $\leq$ **numlev**, where **numlev** is specified in the file *talys.cmb*. Currently, **numlev=25**
Default: **Nlevels** has the value specified by the defaults of **maxlevelstar**, **maxlevelsbin**, and **maxlevelsres**.

levelfile

File with discrete levels. The format of the file is exactly the same as that of the nuclear structure database *talys/structure/levels/*. In practice, the user can copy a file from this database, e.g. *z026*, to the working directory and change it. In this way, changes in the "official" database are avoided. Note that even if only changes for one isotope are required, the entire file needs to be copied if for the other isotopes the originally tabulated values are to be used. On the input line, we read **levelfile**, Z, filename.
Examples:

levelfile 26 z026.loc

Range: **levelfile** can be equal to any filename, provided it starts with a character and consists entirely of lowercase characters.
Default: If **levelfile** is not given in the input file, the discrete levels are taken from the *talys/structure/levels* database per nucleus.

massmodel

Model for nuclear masses. There are 3 theoretical mass models. They are only used when no experimental mass is available or when **expmass n**.
Examples:

massmodel 1: Möller

massmodel 2: Duflo-Zuker

massmodel 3: Goriely

Range: $\mathbf{1} \leq$ **massmodel** $\leq \mathbf{3}$
Default: **massmodel 3**

expmass

Flag for using the experimental nuclear mass when available. Use **expmass n** to overrule the experimental mass by the theoretical nuclear mass. This will then be done for all nuclides encountered in the calculation.
Examples:

expmass y

expmass n

Range: **y** or **n**
Default: **expmass y**

massnucleus

The mass of the nucleus in amu. Use **massnucleus** to overrule the value given in the mass table. On the input line, we read **massnucleus**, Z, A, value.
Examples:

massnucleus 41 93 92.12345

massnucleus 94 239 239.10101

Range: $\mathbf{A-0.5} \leq$ **massnucleus** $\leq$ **A+0.5**, where A is the mass number.
Default: **massnucleus 0.**, i.e. the nuclear mass is read from the mass table.

massexcess

The mass excess of the nucleus in MeV. Use **massexcess** to overrule the value given in the mass table. On the input line, we read **massexcess**, Z, A, value.
Examples:

massexcess 41 93 -45.678

massexcess 94 239 39.98765

Range: $\mathbf{-500.} \leq$ **massexcess** $\leq$ **500.**,
Default: **massexcess 0.**, i.e. the mass excess is read from the mass table.

isomer

The definition of an isomer in seconds. In the discrete level database, the lifetimes of most of the levels are given. With **isomer**, it can be specified whether a level is treated as an isomer or not. Use **isomer 0.** to treat all levels, with any lifetime, as isomer and use **isomer 1.e38**, or any other number larger than the longest living isomer present in the problem, to include no isomers at all.
Examples:

isomer 86400. (86400 sec.=one day)

Range: $\mathbf{0.} \leq$ **isomer** $\leq \mathbf{1.e38}$
Default: **isomer 1.** (second)

Elow

Lowest incident energy in MeV for which TALYS performs a full nuclear model calculation. Below this energy, cross sections result from inter- and extrapolation using the calculated values at **Elow** and tabulated values and systematics at thermal energy. This keyword should only be used in the case of several incident energies.
Examples:

Elow 0.001

Range: $\mathbf{1.e-6} \leq$ **Elow** $\leq \mathbf{1.}$
Default: **Elow**=D_0 for datafiles (**endf y**), **1.e-6** otherwise.

transpower

A limit for considering transmission coefficients in the calculation. Transmission coefficients T_{lj} smaller than $T_{0\frac{1}{2}} \times 10^{-transpower}/(2l+1)$ are not used in Hauser-Feshbach calculations, in order to reduce the computation time.
Examples:

transpower 12

Range: $\mathbf{2} \leq$ **transpower** $\leq \mathbf{20}$
Default: **transpower 5**

transeps

A limit for considering transmission coefficients in the calculation. Transmission coefficients smaller than **transeps** are not used in Hauser-Feshbach calculations, irrespective of the value of **transpower**, in order to reduce the computation time.
Examples:

transeps 1.e-12

Range: $\mathbf{0.} \leq$ **transeps** $\leq \mathbf{1.}$
Default: **transeps 1.e-8**

xseps

The limit for considering cross sections in the calculation, in mb. Reaction cross sections smaller than **xseps** are not used in the calculations, in order to reduce the computation time.
Examples:

xseps 1.e-10

Range: $\mathbf{0.} \leq$ **xseps** $\leq \mathbf{1000.}$
Default: **xseps 1.e-7**

popeps

The limit for considering population cross sections in the multiple emission calculation, in mb. Nuclides which, before their decay, are populated with a total cross section less than **popeps** are skipped, in order to reduce the computation time. From **popeps**, also the criteria for continuation of the decay per excitation energy bin (variable **popepsA**) and per (E_x, J, Π) bin (variable **popepsB**) in Hauser-Feshbach calculations are automatically derived.
Examples:

popeps 1.e-6

Range: $\mathbf{0.} \leq$ **popeps** $\leq \mathbf{1000.}$
Default: **popeps 1.e-3**

angles

Number of emission angles for reactions to discrete states.
Examples:

angles 18

Range: $\mathbf{1} \leq$ **angles** $\leq$ **numang**, where **numang** is specified in the file *talys.cmb*. Currently, **numang=90**
Default: **angles 90**

anglescont

Number of emission angles for reactions to the continuum.
Examples:

anglescont 18

Range: $\mathbf{1} \leq$ **anglescont** $\leq$ **numangcont**, where **numangcont** is specified in the file *talys.cmb*. Currently, **numangcont=36**
Default: **anglescont 36**

channels

Flag for the calculation and output of all exclusive reaction channel cross sections, e.g. $(n, 2n)$, $(n, 2npa)$, etc. The **channels** keyword can be used in combination with the keywords **outspectra** and **outangle** (see next Section) to give the exclusive spectra and angular distributions.
Examples:

channels y

channels n

Range: **y** or **n**
Default: **channels n**

maxchannel

Maximal number of outgoing particles in exclusive channel description, e.g. if **maxchannel 3**, then reactions up to 3 outgoing particles, e.g. $(n, 2np)$, will be given in the output. **maxchannel** is only active if **channels y**. We emphasize that, irrespective of the value of **maxchannel** and **channels**, all reaction chains are, by default, followed until all possible reaction channels are closed to determine composite particle production cross sections and residual production cross sections.
Examples:

maxchannel 2

Range: $\mathbf{0} \leq$ **maxchannel** $\leq \mathbf{8}$,
Default: **maxchannel 4**

relativistic

Flag for relativistic kinematics.
Examples:

relativistic y

relativistic n

Range: **y** or **n**
Default: **relativistic y**

reaction

Flag to disable nuclear reaction calculation. This may be helpful if one is e.g. only interested in a level density calculation.
Examples:

reaction y

reaction n

Range: **y** or **n**
Default: **reaction y**

recoil

Flag for the calculation of the recoils of the residual nuclides and the associated corrections to the light-particle spectra.
Examples:

recoil y

recoil n

Range: **y** or **n**
Default: **recoil n**

labddx

Flag for the calculation of double-differential cross sections in the LAB system. This is only active if **recoil y**. If **labddx n**, only the recoils of the nuclides are computed.
Examples:

labddx y

labddx n

Range: **y** or **n**
Default: **labddx n**

anglesrec

Number of emission angles for recoiling nuclides.
Examples:

anglesrec 4

Range: $1 \leq$ **anglesrec** $\leq$ **numangrec**, where **numangrec** is specified in the file *talys.cmb*. Currently, **numangrec=9**
Default: **anglesrec 9** if **labddx y**, **anglesrec 1** if **labddx n**

maxenrec

Number of emission energies for recoiling nuclides.
Examples:

maxenrec 4

Range: $1 \leq$ **maxenrec** $\leq$ **numenrec**, where **numenrec** is specified in the file *talys.cmb*. Currently, **numenrec=5*memorypar**, where we suggest **memorypar=5** for a computer with at least 256 Mb of memory.
Default: **maxenrec 10**

recoilaverage

Flag to consider only one average kinetic energy of the recoiling nucleus per excitation energy bin (instead of a full kinetic energy distribution). This approximation significantly decreases the calculation time.
Examples:

recoilaverage y

recoilaverage n

Range: **y** or **n**
Default: **recoilaverage n**

channelenergy

Flag to use the channel energy instead of the center-of-mass energy for the emission spectrum.
Examples:

channelenergy y

channelenergy n

Range: **y** or **n**
Default: **channelenergy n**

astro

Flag for the calculation of thermonuclear reaction rates for astrophysics. In the current implementation, only the ground state of the target nucleus is considered, i.e. there is not yet an averaging over all excited target states.
Examples:

astro y

astro n

Range: **y** or **n**
Default: **astro n**

astrogs

Flag for treating the target in the ground state only, for astrophysical reaction calculations. By default, an average between excited target states will be made.
Examples:

astrogs y

astrogs n

Range: **y** or **n**
Default: **astrogs n**

abundance

File with tabulated abundances. The **abundance** keyword is only active for the case of a natural target, i.e. if **mass 0**. By default, the isotopic abundances are read from the structure database, see Chapter 5. It can however be imagined that one wants to include only the most abundant isotopes of an element, to save some computing time. Also, **abundance** may be used to analyze experimental data for targets of a certain isotopic enrichment. On the input line, we read **abundance** and the filename. From each line of the file, TALYS reads Z, A and the isotopic abundance with the format (2i4,f11.6). An example of an abundance file, e.g. *abnew*, different from that of the database, is

```
  82 206  24.100000
  82 207  22.100000
  82 208  52.400000
```

where we have left out the “unimportant” ^{204}Pb (1.4%). TALYS automatically normalizes the abundances to a sum of 1, leading in the above case to 24.44 % of ^{206}Pb, 22.41 % of ^{207}Pb and 53.14 % of ^{208}Pb in the actual calculation.
Examples:

abundance abnew

Range: **abundance** can be equal to any filename, provided it consists entirely of lowercase characters, and must be present in the working directory.
Default: If **abundance** is not given in the input file, abundances are taken from *talys/structure/abundance* and calculations for all isotopes are performed.

partable

Flag to write the model parameters per nucleus on a separate file, *parameters.dat*. This can be a very powerful option when one wishes to vary any nuclear model parameter in the input. The file *parameters.dat* has the exact input format, so it can be easily copied and pasted into any input file. This is helpful for a quick look-up of all the parameters used in a calculation while we have used this for automatic (random) TALYS-input generators.
Examples:

partable y

partable n

Range: **y** or **n**
Default: **partable n**

nulldev

Path for the null device. The null device is a ”black hole” for output that is produced, but not of interest to the user. Some ECIS output files fall in this category. To ensure compatibility with Unix, Linux, Windows and other systems a null device string is used, of which the default setting is given in machine.f. With this keyword, extra flexibility is added. If the null device is properly set in machine.f, this keyword is not needed. On the input line, we read **nulldev**, filename.
Examples:

nulldev /dev/null

nulldev nul

Range: **nulldev** can be equal to any appropriate filename, provided it starts with a character and it is given entirely in lowercase.
Default: The default is set in subroutine *machine.f*.

strucpath

Path for the directory with nuclear structure information. With this keyword, extra flexibility is added. Nuclear structure databases other than the default can be invoked with this keyword. If the path name is properly set in machine.f, this keyword is not needed for standard use. On the input line, we read **strucpath**, filename.
Examples:

strucpath /home/raynal/mon-structure/

Range: **pathname** can be equal to any appropriate directory, provided it is given entirely in lowercase. The maximum length of the path is 60 characters.
Default: The default is set in subroutine *machine.f.*

6.2.3 Optical model

optmod

File with tabulated phenomenological optical model parameters as a function of energy. This can be helpful if one wishes to use an optical model parameterisation which is not hardwired in TALYS. One could write a driver to automatically generate a table with parameters. On the input line, we read **optmod**, Z, A, filename, particle type. From each line of the file, TALYS reads E, v, rv, av, w, rw, aw, vd, rvd, avd, wd, rwd, awd, vso, $rvso$, $avso$, wso, $rwso$, $awso$, and rc.
Examples:

optmod 40 90 ompzr90 d

optmod 94 239 omppu239

Range: **optmod** can be equal to any filename, provided it starts with a character and consists entirely of lowercase characters. The particle type must be equal to either **n, p, d, t, h** or **a**. A table of up to 500 incident energies (this is set by **numomp** in *talys.cmb*) and associated parameters can be specified.
Default: If the particle type is not given, as in the second example above, it is assumed it concerns neutrons. If **optmod** is not given in the input file, the optical model parameters are taken from the *talys/structure/optical* database per nucleus or, if not present there, from the global optical model.

optmodfileN

File with the neutron optical model parameters of Eq. (4.7). The format of the file is exactly the same as that of the nuclear structure database *talys/structure/optical/*. In practice, the user can copy a file from this database, e.g. *z026*, to the working directory and change it. In this way, changes in the "official" database are avoided. Note that even if only changes for one isotope are required, the entire file needs to be copied if for the other isotopes the originally tabulated values are to be used. On the input line, we read **optmodfileN**, Z, filename.
Examples:

optmodfileN 26 z026.loc

Range: **optmodfileN** can be equal to any filename, provided it starts with a character and consists entirely of lowercase characters.
Default: If **optmodfileN** is not given in the input file, the optical model parameters are taken from the *talys/structure/optical* database per nucleus or, if not present there, from the global optical model.

optmodfileP

File with the proton optical model parameters of Eq. (4.7). The format of the file is exactly the same as that of the nuclear structure database *talys/structure/optical/*. In practice, the user can copy a file from

this database, e.g. *z026*, to the working directory and change it. In this way, changes in the "official" database are avoided. Note that even if only changes for one isotope are required, the entire file needs to be copied if for the other isotopes the originally tabulated values are to be used. On the input line, we read **optmodfileP**, Z, filename.
Examples:

optmodfileP 26 z026.loc

Range: **optmodfileP** can be equal to any filename, provided it starts with a character and consists entirely of lowercase characters.
Default: If **optmodfileP** is not given in the input file, the optical model parameters are taken from the *talys/structure/optical* database per nucleus or, if not present there, from the global optical model.

localomp

Flag to overrule the local, nucleus-specific optical model by the global optical model. This may be helpful to study global mass-dependent trends.
Examples:

localomp n

Range: **y** or **n**
Default: **localomp y**, i.e. a nucleus-specific optical model, when available.

dispersion

Flag to invoke the dispersive optical model. These potentials are only available as tabulated neutron local potentials. If not available, TALYS will automatically resort to normal OMP's.
Examples:

dispersion n

Range: **y** or **n**
Default: **dispersion n**.

jlmomp

Flag to use the JLM microscopic optical model potential instead of the phenomenological optical model potential.
Examples:

jlmomp n

Range: **y** or **n**
Default: **jlmomp n**, i.e. to use the phenomenological OMP.

sysreaction

The types of particles for which the optical model reaction cross section is overruled by values obtained from systematics. The optical model transmission coefficients will be accordingly normalized.
Examples:

sysreaction p

sysreaction d a

Range: **sysreaction** can be any combination of **n, p, d, t, h** and **a**
Default: **sysreaction** is disabled for any particle.
Warning: setting e.g. **sysreaction p** will thus automatically disable the default setting. If this needs to be retained as well, set **sysreaction p d t h a**.

statepot

Flag for a different optical model parameterisation for each excited state in a DWBA or coupled-channels calculation. This may be appropriate if the emission energy of the ejectile, corresponding to a large excitation energy, differs considerably from the incident energy.
Examples:

statepot y

Range: **y** or **n**
Default: **statepot n**

optmodall

Flag for a new optical model calculation for each compound nucleus in the decay chain. In usual multiple Hauser-Feshbach decay, the transmission coefficients for the first compound nucleus are used for the whole decay chain. When a residual nucleus is far away from the initial compound nucleus, this approximation may become dubious. With **optmodall y**, new optical model calculations are performed for every compound nucleus that is depleted, for all types of emitted particles.
Examples:

optmodall y

Range: **y** or **n**
Default: **optmodall n**

autorot

Flag for automatic rotational coupled-channels calculations for $A > 150$. The discrete level file is scanned and the lowest rotational band is automatically identified. Deformation parameters are also read in from the database so automated coupled-channels calculations can be performed. This option is possible for the rare earth and actinide region.
Examples:

autorot y

Range: **y** or **n**
Default: **autorot n**

ecissave

Flag for saving ECIS input and output files. This has two purposes: (a) if the next calculation will be performed with already existing reaction cross sections and transmission coefficients. This is helpful for time-consuming coupled-channels calculations, (b) to study the ECIS input and output files in detail. **ecissave** *must* be set to **y**, if in the next run **inccalc n** or **eciscalc n** will be used. If not, an appropriate error message will be given and TALYS stops.
Examples:

ecissave y

ecissave n

Range: **y** or **n**
Default: **ecissave n**

eciscalc

Flag for the ECIS calculation of transmission coefficients and reaction cross sections for the inverse channels. If this calculation has already been performed in a previous run, it may be helpful to put **eciscalc n**, which avoids a new calculation. This saves time, especially in the case of coupled-channels calculations. We stress that it is the responsibility of the user to ensure that the first run of a particular problem is done with **ecissave y** and **eciscalc y**. If not, an appropriate error message will be given and TALYS stops. You also have to make sure that the same energy grid for inverse channels is used.
Examples:

eciscalc y

eciscalc n

Range: **y** or **n**
Default: **eciscalc y**

inccalc

Flag for the ECIS calculation of transmission coefficients and reaction cross sections for the incident channel. If this calculation has already been performed in a previous run, it may be helpful to put **inccalc n**, which avoids a new ECIS calculation. This saves time, especially in the case of coupled-channels calculations. We stress that it is the responsibility of the user to ensure that the first run of a particular problem is done with **eciscalc y** and **inccalc y**. If not, an appropriate error message will be given and TALYS stops. You also have to make sure that the same grid of incident energies is used.
Examples:

inccalc y

inccalc n

Range: **y** or **n**
Default: **inccalc y**

v1adjust

Multiplier to adjust the OMP parameter v1. On the input line, we read **v1adjust**, particle symbol, and value.
Examples:

v1adjust a 1.12

Range: $\mathbf{0.2} \leq$ **v1adjust** $\leq \mathbf{5}$.
Default: **v1adjust 1.**

v2adjust

Multiplier to adjust the OMP parameter v2. On the input line, we read **v2adjust**, particle symbol, and value.
Examples:

v2adjust n 0.96

Range: $\mathbf{0.2} \leq$ **v2adjust** $\leq \mathbf{5}$. This keyword does not apply to deuterons up to alpha's.
Default: **v2adjust 1.**

v3adjust

Multiplier to adjust the OMP parameter v3. On the input line, we read **v3adjust**, particle symbol, and value.
Examples:

v3adjust p 1.10

Range: $\mathbf{0.2} \leq$ **v3adjust** $\leq \mathbf{5}$. This keyword does not apply to deuterons up to alpha's.
Default: **v3adjust 1.**

v4adjust

Multiplier to adjust the OMP parameter v4. On the input line, we read **v4adjust**, particle symbol, and value.
Examples:

v4adjust n 0.98

Range: $\mathbf{0.2} \leq$ **v4adjust** $\leq \mathbf{5}$. This keyword does not apply to deuterons up to alpha's.
Default: **v4adjust 1.**

rvadjust

Multiplier to adjust the OMP parameter rv. On the input line, we read **rvadjust**, particle symbol, and value.
Examples:

rvadjust t 1.04

Range: $\mathbf{0.5} \leq$ **rvadjust** $\leq \mathbf{2}$.
Default: **rvadjust 1.**

avadjust

Multiplier to adjust the OMP parameter av. On the input line, we read **avadjust**, particle symbol, and value.
Examples:

avadjust d 0.97

Range: $\mathbf{0.5} \leq$ **avadjust** $\leq \mathbf{2}$.
Default: **avadjust 1.**

w1adjust

Multiplier to adjust the OMP parameter w1. On the input line, we read **w1adjust**, particle symbol, and value.
Examples:

w1adjust p 1.10

Range: $\mathbf{0.2} \leq$ **w1adjust** $\leq \mathbf{5}$.
Default: **w1adjust 1.**

w2adjust

Multiplier to adjust the OMP parameter w2. On the input line, we read **w2adjust**, particle symbol, and value.
Examples:

w2adjust n 0.80

Range: $\mathbf{0.2} \leq$ **w2adjust** $\leq \mathbf{5}$. This keyword does not apply to deuterons up to alpha's.
Default: **w2adjust 1.**

rvdadjust

Multiplier to adjust the OMP parameter rvd. On the input line, we read **rvdadjust**, particle symbol, and value.
Examples:

rvdadjust d 0.97

Range: $\mathbf{0.5} \leq$ **rvdadjust** $\leq \mathbf{2}$.
Default: **rvdadjust 1.**

avdadjust

Multiplier to adjust the OMP parameter avd. On the input line, we read **avdadjust**, particle symbol, and value.
Examples:

avdadjust d 0.97

Range: $\mathbf{0.5} \leq$ **avdadjust** $\leq \mathbf{2}$.
Default: **avdadjust 1.**

d1adjust

Multiplier to adjust the OMP parameter d1. On the input line, we read **d1adjust**, particle symbol, and value.
Examples:

d1adjust d 0.97

Range: $\mathbf{0.2} \leq$ **d1adjust** $\leq \mathbf{5}$.
Default: **d1adjust 1.**

d2adjust

Multiplier to adjust the OMP parameter d2. On the input line, we read **d2adjust**, particle symbol, and value.
Examples:

d2adjust n 1.06

Range: $\mathbf{0.2} \leq$ **d2adjust** $\leq \mathbf{5}$. This keyword does not apply to deuterons up to alpha's.
Default: **d2adjust 1.**

d3adjust

Multiplier to adjust the OMP parameter d3. On the input line, we read **d3adjust**, particle symbol, and value.
Examples:

d3adjust n 1.06

Range: $\mathbf{0.2} \leq$ **d3adjust** $\leq \mathbf{5}$. This keyword does not apply to deuterons up to alpha's.
Default: **d3adjust 1.**

vso1adjust

Multiplier to adjust the OMP parameter vso1. On the input line, we read **vso1adjust**, particle symbol, and value.
Examples:

vso1adjust d 1.15

Range: $\mathbf{0.2} \leq$ **vso1adjust** $\leq \mathbf{5}$.
Default: **vso1adjust 1.**

vso2adjust

Multiplier to adjust the OMP parameter vso2. On the input line, we read **vso2adjust**, particle symbol, and value.
Examples:

vso2adjust n 1.06

Range: $\mathbf{0.2} \leq$ **vso2adjust** $\leq \mathbf{5}$. This keyword does not apply to deuterons up to alpha's.
Default: **vso2adjust 1.**

wso1adjust

Multiplier to adjust the OMP parameter wso1. On the input line, we read **wso1adjust**, particle symbol, and value.
Examples:

wso1adjust d 1.15

Range: $\mathbf{0.2} \leq$ **wso1adjust** $\leq \mathbf{5}$.
Default: **wso1adjust 1.**

wso2adjust

Multiplier to adjust the OMP parameter wso2. On the input line, we read **wso2adjust**, particle symbol, and value.
Examples:

wso2adjust n 1.06

Range: $\mathbf{0.2} \leq$ **wso2adjust** $\leq \mathbf{5}$. This keyword does not apply to deuterons up to alpha's.
Default: **wso2adjust 1.**

rvsoadjust

Multiplier to adjust the OMP parameter rvso. On the input line, we read **rvsoadjust**, particle symbol, and value.
Examples:

rvsoadjust d 1.15

Range: $\mathbf{0.5} \leq$ **rvsoadjust** $\leq \mathbf{2}$.
Default: **rvsoadjust 1.**

avsoadjust

Multiplier to adjust the OMP parameter avso. On the input line, we read **avsoadjust**, particle symbol, and value.
Examples:

avsoadjust d 1.15

Range: $\mathbf{0.5} \leq$ **avsoadjust** $\leq \mathbf{2}$.
Default: **avsoadjust 1.**

rcadjust

Multiplier to adjust the OMP parameter rc. On the input line, we read **rcadjust**, particle symbol, and value.
Examples:

rcadjust d 1.15

Range: $\mathbf{0.5} \leq$ **rcadjust** $\leq \mathbf{2}$.
Default: **rcadjust 1.**

radialfile

File with radial matter densities. The format of the file is exactly the same as that of the nuclear structure database *talys/structure/optical/jlm/*. In practice, the user can copy a file from this database, e.g. *z026*, to the working directory and change it. In this way, changes in the "official" database are avoided. Note that even if only changes for one isotope are required, the entire file needs to be copied if for the other isotopes the originally tabulated values are to be used. On the input line, we read **radialfile**, Z, filename.
Examples:

radialfile 26 z026.loc

Range: **radialfile** can be equal to any filename, provided it starts with a character and consists entirely of lowercase characters.
Default: If **radialfile** is not given in the input file, the radial matter densities are taken from the *talys/structure/optical/jlm* database per nucleus.

lvadjust

Normalization factor for the real central potential for JLM calculations. On the input line, we read **lvadjust** and value.
Examples:

lvadjust 1.15

Range: $\mathbf{0.5} \leq$ **lvadjust** $\leq \mathbf{1.5}$
Default: **lvadjust 1.**

lwadjust

Normalization factor for the imaginary central potential for JLM calculations. On the input line, we read **lwadjust** and value.
Examples:

lwadjust 1.15

Range: $\mathbf{0.5} \leq$ **lwadjust** $\leq \mathbf{1.5}$
Default: **lwadjust 1.**

lv1adjust

Normalization factor for the real isovector potential for JLM calculations. On the input line, we read **lv1adjust** and value.
Examples:

lv1adjust 1.15

Range: $\mathbf{0.5} \leq$ **lv1adjust** $\leq \mathbf{1.5}$
Default: **lv1adjust 1.**

lw1adjust

Normalization factor for the imaginary isovector potential for JLM calculations. On the input line, we read **lw1adjust** and value.
Examples:

lw1adjust 1.15

Range: $\mathbf{0.5} \leq$ **lw1adjust** $\leq \mathbf{1.5}$
Default: **lw1adjust 1.**

lvsoadjust

Normalization factor for the real spin-orbit potential for JLM calculations. On the input line, we read **lvsoadjust** and value.
Examples:

lvsoadjust 1.15

Range: $\mathbf{0.5} \leq$ **lvsoadjust** $\leq \mathbf{1.5}$
Default: **lvsoadjust 1.**

lwsoadjust

Normalization factor for the imaginary spin-orbit potential for JLM calculations. On the input line, we read **lwsoadjust** and value.
Examples:

lwsoadjust 1.15

Range: $\mathbf{0.5} \leq$ **lwsoadjust** $\leq \mathbf{1.5}$
Default: **lwsoadjust 1.**

alphaomp

Some of our users need a very old alpha optical model potential for their applications, namely that of McFadden and Satchler[158]. Therefore, we included an option for that.
Examples:

alphaomp 1: Normal alpha potential

alphaomp 2: Alpha potential of McFadden and Satchler

Range: $\mathbf{1} \leq$ **alphaomp** $\leq$ **2**
Default: **alphaomp 1**

6.2.4 Direct reactions

rotational

Flag to enable or disable the rotational optical model for the various particles appearing in the calculation. This flag is to enable or disable coupled-channels calculations for the inverse channels provided a coupling scheme is given in the deformation database. Using no rotational model at all can be set with another keyword: **spherical y**.
Examples:

rotational n

rotational n p a

Range: **rotational** can be any combination of **n, p, d, t, h** and **a**
Default: **rotational n p**. Warning: setting e.g. **rotational a** will thus automatically disable the default setting. If this needs to be retained as well, set **rotational n p a**

spherical

Flag to enforce a spherical OMP calculation, regardless of the availability of a deformed OMP and a coupling scheme. Direct inelastic scattering will then be treated by DWBA.
Examples:

spherical n

Range: **y** or **n**
Default: **spherical n**

maxrot

Number of excited levels to be included in a rotational band. For example, use **maxrot 4** if the $0^+ - 2^+ - 4^+ - 6^+ - 8^+$ band needs to be included.
Examples:

maxrot 4

Range: **0** $\leq$ **maxrot** $\leq$ **10**
Default: **maxrot 2**

maxband

Maximum number of vibrational bands added to the rotational coupling scheme, regardless of the number of bands specified in the deformation database.
Examples:

maxband 4

Range: **0** $\leq$ **maxband** $\leq$ **100**
Default: **maxband 0**

deformfile

File with deformation parameters and coupling schemes. The format of the file is exactly the same as that of the nuclear structure database *talys/structure/deformation/*. In practice, the user can copy a file from this database, e.g. *z026*, to the working directory and change it. In this way, changes in the “official” database are avoided. Note that even if only changes for one isotope are required, the entire file needs to be copied if for the other isotopes the originally tabulated values are to be used. On the input line, we read **deformfile**, Z, filename.
Examples:

deformfile 26 z026.loc

Range: **deformfile** can be equal to any filename, provided it starts with a character and consists entirely of lowercase characters.
Default: If **deformfile** is not given in the input file, discrete levels are taken from *talys/structure/deformation*.

giantresonance

Flag for the calculation of giant resonance contributions to the continuum part of the spectrum. The GMR, GQR, LEOR and HEOR are included.
Examples:

giantresonance y

giantresonance n

Range: **y** or **n**
Default: **giantresonance y** for incident neutrons and protons, **giantresonance n** otherwise.

core

Integer to denote the even-even core for the weak-coupling model for direct scattering of odd-A nuclei. A value of -1 means the even-even core is determined by subtracting a nucleon from the target nucleus, while a value of +1 means a nucleon is added.
Examples:

core 1

Range: **-1** or **1**
Default: **core -1**

6.2.5 Compound nucleus

compound

Flag for compound nucleus calculation. This keyword can be used to disable compound nucleus evaporation if one is for example only interested in high-energy pre-equilibrium spectra.
Examples:

compound y

compound n

Range: **y** or **n**
Default: **compound y**

widthfluc

Enabling or disabling width fluctuation corrections in compound nucleus calculations. For **widthfluc**, the user has 3 possibilities: **y**, **n** or a value for the starting energy. The latter option is helpful in the case of a calculation with several incident energies. Then, the user may want to set the width fluctuation off as soon as the incident energy is high enough, in order to save computing time. We have taken care of this by the default, **widthfluc=S**, where S is the projectile separation energy ($\sim$ 8 MeV), of the target nucleus. This default is very safe, since in practice width fluctuation corrections are already negligible for incident energies above a few MeV, because the presence of many open channels reduces the correction to practically zero, i.e. the WFC factors to 1. Note that the disabling of width fluctuations for *any* incident energy can be accomplished by **widthfluc n**, which is equivalent to **widthfluc 0.** or any other energy lower than the (lowest) incident energy. Similarly, **widthfluc y**, equivalent to **widthfluc 20.**, will activate width fluctuations for any incident energy. To avoid numerical problems, width fluctuations are never calculated for incident energies beyond 20 MeV.
Examples:

widthfluc y

widthfluc n

widthfluc 4.5

Range: **y** or **n** or $0. \leq$ **widthfluc** $<$ **20.**
Default: **widthfluc** is equal to the projectile separation energy S, i.e. width fluctuation corrections are only used for incident energies below this value.

widthmode

Model for width fluctuation corrections in compound nucleus calculations.
Examples:

widthmode 0: no width fluctuation, i.e. pure Hauser-Feshbach model

widthmode 1: Moldauer model

widthmode 2: Hofmann-Richert-Tepel-Weidenmüller model

widthmode 3: GOE triple integral model

Range: **0** $\leq$ **widthmode** $\leq$ **3**
Default: **widthmode 1**

fullhf

Flag for Hauser-Feshbach calculation using the full j,l coupling. This keyword can be used to enable/disable the loop over total angular momentum of the ejectile j' in Eq. (4.164). If **fullhf n**, the transmission coefficients are averaged over j, reducing the calculation time of the full Hauser-Feshbach model. In practice, the difference with the results from the full calculation is negligible.
Examples:

fullhf y

fullhf n

Range: **y** or **n**
Default: **fullhf n**

eciscompound

Flag for compound nucleus calculation by ECIS-06, done in parallel with TALYS. This keyword is used for checking purposes only and does not influence the TALYS results. An ECIS input file is created that contains the same discrete levels, level density parameters etc., as the TALYS calculation. The compound nucleus results given by ECIS can be compared with the results from TALYS, but are not used in TALYS. The results are written on a separate ECIS output file.
Examples:

eciscompound y

eciscompound n

Range: **y** or **n**
Default: **eciscompound n**

6.2.6 Gamma emission

gammax

Maximum number of l-values for gamma multipolarity, whereby $l = 1$ stands for M1 and E1 transitions, $l = 2$ for M2 and E2 transitions, etc.
Examples:

gammax 1

Range: $\mathbf{1} \leq$ **gammax** $\leq \mathbf{6}$
Default: **gammax 2**

gnorm

Normalisation factor for gamma-ray transmission coefficient. This adjustable parameter can be used to scale e.g. the (n, γ) cross section.
Examples:

gnorm 1.6

Range: $0. \leq$ **gnorm** $\leq$ **100.**
Default: **gnorm** is given by the normalization factor of Eq. (4.69).

strength

Model for $E1$ gamma-ray strength function. There are four possibilities.
Examples:

strength 1 : Kopecky-Uhl generalized Lorentzian

strength 2 : Brink-Axel Lorentzian

strength 3 : Hartree-Fock BCS tables

strength 4 : Hartree-Fock-Bogolyubov tables

Range: **1 - 4**
Default: **strength 1**

electronconv

Flag for the application of an electron-conversion coefficient on the gamma-ray branching ratios from the discrete level file.
Examples:

electronconv y

electronconv n

Range: **y** or **n**
Default: **electronconv n**

egr

Energy of the giant dipole resonance in MeV. On the input line, we read **egr**, Z, A, value, type of radiation (the full symbol, i.e. M1, E1, E2, etc.), number of resonance (optional). If the number of the resonance is not given, it is assumed the keyword concerns the first Lorentzian.
Examples:

egr 41 93 16.2 E1

egr 94 239 13.7 E1 2

Range: $1. \leq$ **egr** $\leq$ **100.** The optional number of the resonance must be either 1 or 2.
Default: **egr** is read from the *talys/structure/gamma/* directory. If the value for the first resonance is not present in the directory, it is calculated from systematics, see Section 4.3. If no parameter for the second resonance is given, this term is omitted altogether.

sgr

Strength of the giant dipole resonance in millibarns. On the input line, we read **sgr**, Z, A, value, type of radiation (the full symbol, i.e. M1, E1, E2, etc.), number of resonance (optional). If the number of the resonance is not given, it is assumed the keyword concerns the first Lorentzian.
Examples:

sgr 41 93 221. E1

sgr 94 239 384. E1 2

Range: $\mathbf{0.} \leq$ **sgr** $\leq$ **10000.** The optional number of the resonance must be either 1 or 2.
Default: **sgr** is read from the *talys/structure/gamma/* directory. If the value for the first resonance is not present in the directory, it is calculated from systematics, see Section 4.3. If no parameter for the second resonance is given, this term is omitted altogether.

ggr

Width of the giant dipole resonance in MeV. On the input line, we read **ggr**, Z, A, value, type of radiation (the full symbol, i.e. M1, E1, E2, etc.), number of resonance (optional). If the number of the resonance is not given, it is assumed the keyword concerns the first Lorentzian.
Examples:

ggr 41 93 5.03 E1

ggr 94 239 4.25 E1 2

Range: $\mathbf{1.} \leq$ **ggr** $\leq$ **100.** The optional number of the resonance must be either 1 or 2.
Default: **ggr** is read from the *talys/structure/gamma/* directory. If the value for the first resonance is not present in the directory, it is calculated from systematics, see Section 4.3. If no parameter for the second resonance is given, this term is omitted altogether.

gamgam

The total radiative width, Γ_γ in eV. On the input line, we read **gamgam**, Z, A, value.
Examples:

gamgam 26 55 1.8

Range: $\mathbf{0.} \leq$ **gamgam** $\leq$ **10.**
Default: **gamgam** is read from the *talys/structure/resonances/* directory, or, if not present there, is taken from interpolation, see Section 4.3.

D0

The s-wave resonance spacing D_0 in keV. On the input line, we read **D0**, Z, A, value.
Examples:

D0 26 55 13.

Range: $\mathbf{1}.\mathrm{e}-\mathbf{6} \leq$ **D0** $\leq$ **10000.**
Default: **D0** is read from the *talys/structure/resonances/* directory.

S0

The s-wave strength function S_0 in units of 10^{-4}. On the input line, we read **S0**, Z, A, value.
Examples:

S0 26 55 6.90

Range: $\mathbf{0}. \leq$ **S0** $\leq$ **10.**
Default: **S0** is read from the *talys/structure/resonances/* directory.

etable

Constant E_{shift} of the adjustment function (4.67) for tabulated gamma strength functions densities, per nucleus. On the input line, we read **etable**, Z, A, value.
Examples:

etable 29 65 -0.6

Range: **-10.** $\leq$ **etable** $\leq$ **10.**
Default: **etable 0.**

ftable

Constant f^{nor} of the adjustment function (4.67) for tabulated gamma strength functions densities, per nucleus. On the input line, we read **ftable**, Z, A, value.
Examples:

ftable 29 65 1.2

Range: **0.1** $\leq$ **ftable** $\leq$ **10.**
Default: **ftable 1.**

6.2.7 Pre-equilibrium

preequilibrium

Enabling or disabling the pre-equilibrium reaction mechanism. For **preequilibrium**, the user has 3 possibilities: **y**, **n** or a value for the starting energy. The latter option is helpful in the case of a calculation with several incident energies. Then, the user may want to set pre-equilibrium contributions on as soon as the incident energy is high enough. We have taken care of this by the default, **preequilibrium=Ex(Nm)**, where Ex(Nm) is the excitation energy of the last discrete level Nm of the target nucleus. This default is very safe, since in practice the pre-equilibrium contribution becomes only sizable for incident energies several MeV higher than Ex(Nm). Note that the disabling of pre-equilibrium for *any* incident energy can be accomplished by **preequilibrium n**. Similarly, **preequilibrium y**, equivalent to **preequilibrium 0.**, will enable pre-equilibrium for any incident energy.
Examples:

preequilibrium y

preequilibrium n

preequilibrium 4.5

Range: **y** or **n** or 0. ≤ **preequilibrium** < **250.**
Default: **preequilibrium** is equal to Ex(NL), i.e. pre-equilibrium calculations are included for incident energies above the energy of the last discrete level of the target nucleus.

preeqmode

Model for pre-equilibrium reactions. There are four possibilities.
Examples:

preeqmode 1: Exciton model: Analytical transition rates with energy-dependent matrix element.

preeqmode 2: Exciton model: Numerical transition rates with energy-dependent matrix element.

preeqmode 3: Exciton model: Numerical transition rates with optical model for collision probability.

preeqmode 4: Multi-step direct/compound model

Range: **1** ≤ **preeqmode** ≤ **4**
Default: **preeqmode 2**

multipreeq

Enabling or disabling multiple pre-equilibrium reaction mechanism. For **multipreeq**, the user has 3 possibilities: **y**, **n** or a value for the starting energy. The latter option is helpful in the case of a calculation with several incident energies. Then, the user may want to set multiple pre-equilibrium contributions on as soon as the incident energy is high enough. We have taken care of this by the default, **multipreeq 20.**. This default is very safe, since in practice the multiple pre-equilibrium contribution becomes only sizable for incident energies a few tens of MeV higher than the default. Note that the disabling of multiple pre-equilibrium for *any* incident energy can be accomplished by **multipreeq n**. Similarly, **multipreeq y**, equivalent to **multipreeq 0.**, will activate multiple pre-equilibrium for any incident energy.
Examples:

multipreeq y

multipreeq n

multipreeq 40.

Range: **y** or **n** or 0. ≤ **multipreeq** < **250.**
Default: **multipreeq 20.**, i.e. multiple pre-equilibrium calculations are included for incident energies above this value. TALYS always sets **multipreeq n** if **preequilibrium n**.

mpreeqmode

Model for multiple pre-equilibrium reactions. There are two possibilities, see Section 4.6.2 for an explanation.
Examples:

mpreeqmode 1: Multiple exciton model

mpreeqmode 2: Transmission coefficient method

Range: $\mathbf{1} \leq$ **mpreeqmode** $\leq \mathbf{2}$
Default: **mpreeqmode 1**

preeqspin

Flag to use the pre-equilibrium (y) or compound nucleus (n) spin distribution for the pre-equilibrium population of the residual nuclides.
Examples:

preeqspin y

preeqspin n

Range: **y** or **n**
Default: **preeqspin n**

preeqsurface

Flag to use surface corrections in the exciton model.
Examples:

preeqsurface y

preeqsurface n

Range: **y** or **n**
Default: **preeqsurface y**

Esurf

Effective well depth for surface effects in MeV in the exciton model, see Eq. (4.87).
Examples:

Esurf 25.

Range: $\mathbf{0.} \leq$ **Esurf** $\leq \mathbf{Efermi}$, where **Efermi** = 38 MeV is the Fermi well depth.
Default: **Esurf** is given by Eq. (4.87).

preeqcomplex

Flag to use the Kalbach model for pickup, stripping and knockout reactions, in addition to the exciton model, in the pre-equilibrium region.
Examples:

preeqcomplex y

preeqcomplex n

Range: **y** or **n**
Default: **preeqcomplex y**

twocomponent

Flag to use the two-component (y) or one-component (n) exciton model.
Examples:

twocomponent y

twocomponent n

Range: **y** or **n**
Default: **twocomponent y**

pairmodel

Model for pairing correction for pre-equilibrium model.
Examples:

pairmodel 1: Fu's pairing energy correction

pairmodel 2: Compound nucleus pairing correction

Range: $\mathbf{1} \leq$ **pairmodel** $\leq \mathbf{2}$
Default: **pairmodel 1**

M2constant

Overall constant for the matrix element, or the optical model strength, in the exciton model. The parameterisation of the matrix element is given by Eq. (4.122) for the one-component model, and by Eq. (4.102) for the two-component model. **M2constant** is also used to scale the MSD cross section (preeqmode 4).
Examples:

M2constant 1.22

Range: $0. \leq$ **M2constant** $\leq 100.$
Default: **M2constant 1.**

M2limit

Constant to scale the asymptotic value of the matrix element in the exciton model. The parameterisation of the matrix element is given by Eq. (4.122) for the one-component model, and by Eq. (4.102) for the two-component model.
Examples:

M2limit 1.22

Range: $0. \leq$ **M2limit** ≤ 100.
Default: **M2limit 1.**

M2shift

Constant to scale the energy shift of the matrix element in the exciton model. The parameterisation of the matrix element is given by Eq. (4.122) for the one-component model, and by Eq. (4.102) for the two-component model.
Examples:

M2shift 1.22

Range: $0. \leq$ **M2shift** ≤ 100.
Default: **M2shift 1.**

Rnunu

Neutron-neutron ratio for the matrix element in the two-component exciton model, see Eq. (4.100).
Examples:

Rnunu 1.6

Range: $0. \leq$ **Rnunu** ≤ 100.
Default: **Rnunu 1.5**

Rnupi

Neutron-proton ratio for the matrix element in the two-component exciton model, see Eq. (4.100).
Examples:

Rnupi 1.6

Range: $0. \leq$ **Rnupi** ≤ 100.
Default: **Rnupi 1.**

Rpipi

Proton-proton ratio for the matrix element in the two-component exciton model, see Eq. (4.100).
Examples:

Rpipi 1.6

Range: $0. \leq$ **Rpipi** $\leq 100.$
Default: **Rpipi 1.**

Rpinu

Proton-neutron ratio for the matrix element in the two-component exciton model, see Eq. (4.100).
Examples:

Rpinu 1.6

Range: $0. \leq$ **Rpinu** $\leq 100.$
Default: **Rpinu 1.**

Rgamma

Adjustable parameter for pre-equilibrium gamma decay.
Examples:

Rgamma 1.22

Range: $0. \leq$ **Rgamma** $\leq 100.$
Default: **Rgamma 2.**

Cstrip

Adjustable parameter for the stripping or pick-up process, to scale the complex-particle pre-equilibrium cross section per outgoing particle. On the input line, we read **Cstrip**, particle symbol, and value.
Examples:

Cstrip d 1.3

Cstrip a 0.4

Range: $0. \leq$ **Cstrip** $\leq 10.$
Default: **Cstrip 1.**

Cknock

Adjustable parameter for the knock-out process, to scale the complex-particle pre-equilibrium cross section per outgoing particle. In practice, for nucleon-induced reactions this parameter affects only alpha-particles. This parameter is however also used as scaling factor for break-up reactions (such as (d,p) and (d,n)). On the input line, we read **Cknock**, particle symbol, and value.
Examples:

Cknock a 0.4

Range: $0. \leq$ **Cknock** $\leq 10.$
Default: **Cknock 1.**

ecisdwba

Flag for DWBA calculations for multi-step direct calculations. If this calculation has already been performed in a previous run, it may be helpful to put **ecisdwba n**, which avoids a new calculation and thus saves time. We stress that it is the responsibility of the user to ensure that the first run of a particular problem is done with **ecisdwba y**. If not, an appropriate error message will be given and TALYS stops.
Examples:

ecisdwba y

ecisdwba n

Range: **y** or **n**
Default: **ecisdwba y**

onestep

Flag for inclusion of *only* the one-step direct contribution in the continuum multi-step direct model. This is generally enough for incident energies up to about 14 MeV, and thus saves computing time.
Examples:

onestep y

onestep n

Range: **y** or **n**
Default: **onestep n**

msdbins

The number of emission energy points for the DWBA calculation for the multi-step direct model.
Examples:

msdbins 8

Range: **2** $\leq$ **msdbins** $\leq$ **numenmsd/2-1**, where **numenmsd** is specified in the file *talys.cmb*. Currently, **numenmsd=18**
Default: **msdbins 6**

Emsdmin

The minimal emission energy in MeV for the multi-step direct calculation.
Examples:

Emsdmin 8.

Range: $0. \leq$ **Emsdmin**
Default: **Emsdmin** is equal to **eninc/5.** where **eninc** is the incident energy.

6.2.8 Level densities

ldmodel

Model for level densities. There are 3 phenomenological level density models and 2 options for microscopic level densities.
Examples:

ldmodel 1: Constant temperature + Fermi gas model

ldmodel 2: Back-shifted Fermi gas model

ldmodel 3: Generalised superfluid model

ldmodel 4: Microscopic level densities from Goriely's table

ldmodel 5: Microscopic level densities from Hilaire's table

Range: **1** $\leq$ **ldmodel** $\leq$ **5**
Default: **ldmodel 1**

colenhance

Flag to enable or disable explicit collective enhancement of the level density, using the K_{rot} and K_{vib} factors. This keyword can be used in combination with the **ldmodel** keyword. For fission, if **colenhance n**, collective effects for the ground state are included implicitly in the intrinsic level density, and collective effects on the barrier are determined relative to the ground state.
Examples:

colenhance y

Range: **y** or **n**
Default: **colenhance n**

ctmglobal

Flag to enforce global formulae for the Constant Temperature Model (CTM). By default, if enough discrete levels are available the CTM will always make use of them for the estimation of the level density at low energies. For an honest comparison with other level density models, and also to test the predictive power for nuclides for which no discrete levels are known, we have included the possibility to perform a level density calculation with a truly global CTM. In practice it means that the matching energy E_M is always determined from the empirical formula (4.264), while T and E_0 are determined from E_M through Eqs.(4.258) and (4.255), respectively. This flag is only relevant if **ldmodel 1**.
Examples:

ctmglobal y

Range: **y** or **n**
Default: **ctmglobal n**

spincutmodel

Model for spin cut-off parameter for the ground state level densities. There are 2 expressions.
Examples:

spincutmodel 1: $\sigma^2 = c\frac{a}{\tilde{a}}\sqrt{\frac{U}{a}}$

spincutmodel 2: $\sigma^2 = c\sqrt{\frac{U}{a}}$

Range: **1** $\leq$ **spincutmodel** $\leq$ **2**
Default: **spincutmodel 1**

asys

Flag to use all level density parameters from systematics by default, i.e. to neglect the connection between a and D_0, even if an experimental value is available for the latter.
Examples:

asys y

Range: **y** or **n**
Default: **asys n**

parity

Flag to enable or disable non-equiparity level densities. At present, this option only serves to average tabulated parity-dependent level densities (**ldmodel 5**) over the two parities (using **parity n**), for comparison purposes.
Examples:

parity y

Range: **y** or **n**
Default: **parity n** for **ldmodel 1-4**, **parity y** for **ldmodel 5**.

a

The level density parameter **a** at the neutron separation energy in MeV^{-1}. On the input line, we read **a**, Z, A, value.
Examples:

a 41 93 11.220

a 94 239 28.385

Range: $1. \leq$ **a** $\leq$ **100.**
Default: **a** is read from the *talys/structure/density/* directory or, if not present, is calculated from systematics, see Eq. (4.231).

alimit

The asymptotic level density parameter $\tilde{a}$, for a particular nucleus, in MeV^{-1}, see Eq. (4.231). On the input line, we read **alimit**, Z, A, value.
Examples:

alimit 41 93 10.8

alimit 94 239 28.010

Range: $1. \leq$ **alimit** $\leq$ **100.**
Default: **alimit** is determined from the systematics given by Eq. (4.232).

alphald

Constant for the global expression for the asymptotic level density parameter $\tilde{a}$, see Eq. (4.232).
Examples:

alphald 0.054

Range: $0.01 \leq$ **alphald** $\leq$ **0.2**
Default: **alphald** is determined from the systematics given by Table 4.3, depending on the used level density model.

betald

Constant for the global expression for the asymptotic level density parameter $\tilde{a}$, see Eq. (4.232).
Examples:

betald 0.15

Range: $-0.5 \leq$ **betald** $\leq$ **0.5** with the extra condition that if **betald** $<$ **0.** then **abs(betald)** $<$ **alphald** (to avoid negative **a** values).
Default: **betald** is determined from the systematics given by Table 4.3, depending on the used level density model.

gammald

The damping parameter for shell effects in the level density parameter, for a particular nucleus, in MeV^{-1}, see Eq. (4.231). On the input line, we read **gammald**, Z, A, value.
Examples:

gammald 41 93 0.051

Range: $0. \leq$ **gammald** $\leq$ **1.**
Default: **gammald** is determined from either Eq. (4.233) or (4.239).

gammashell1

Constant for the global expression for the damping parameter for shell effects in the level density parameter γ, see Eq. (4.233).
Examples:

gammashell1 0.5

gammashell1 0.

Range: $0. \leq$ **gammashell1** $\leq$ **1.**
Default: **gammashell1** is determined from the systematics given by Table 4.3.

gammashell2

Constant for the global expression for the damping parameter for shell effects in the level density parameter γ, see Eq. (4.233).
Examples:

gammashell2 0.054

gammashell1 0.

Range: $0. \leq$ **gammashell2** $\leq$ **0.2**
Default: **gammashell2=0.**

shellmodel

Model for liquid drop expression for nuclear mass, to be used to calculate the shell correction. There are 2 expressions.
Examples:

shellmodel 1: Myers-Siatecki

shellmodel 2: Goriely

Range: **1** $\leq$ **shellmodel** $\leq$ **2**
Default: **shellmodel 1**

kvibmodel

Model for the vibrational enhancement of the level density. There are 2 expressions.
Examples:

kvibmodel 1: Eq. (4.303)

kvibmodel 2: Eq. (4.297)

Range: $\mathbf{1} \leq$ **kvibmodel** $\leq \mathbf{2}$
Default: **kvibmodel 2**

pairconstant

Constant for the pairing energy expression in MeV.
Examples:

pairconstant 11.3

Range: $\mathbf{0.} \leq$ **pairconstant** $\leq$ **30.**
Default: **pairconstant=12.**

pair

The pairing correction in MeV. On the input line, we read **pair**, Z, A, value.
Examples:

pair 94 239 0.76

Range: $\mathbf{0.} \leq$ **pair** $\leq$ **10.**
Default: **pair** is determined from Eq. (4.268).

deltaW

Shell correction of the mass in MeV, see Eq. (4.231). On the input line, we read **deltaW**, Z, A, value, the ground state or fission barrier to which it applies (optional). If the fission barrier is not given or is equal to 0, it concerns the ground state of the nucleus.
Examples:

deltaW 41 93 0.110

deltaW 94 239 -0.262 1

Range: $-\mathbf{20.} \leq$ **deltaW** $\leq$ **20.**
Default: **deltaW** is determined from Eq. (4.234).

Nlow

Lower level to be used in the temperature matching problem of the Gilbert and Cameron formula. On the input line, we read **Nlow**, Z, A, value, the ground state or fission barrier to which it applies (optional). If the fission barrier is not given or equal to 0, it concerns the ground state of the nucleus.
Examples:

Nlow 41 93 4

Nlow 94 239 2 1

Range: $\mathbf{0 \leq}$ **Nlow** $\mathbf{\leq 200}$
Default: **Nlow 2**

Ntop

Upper level to be used in the temperature matching problem of the Gilbert and Cameron formula. On the input line, we read **Ntop**, Z, A, value, the ground state or fission barrier to which it applies (optional). If the fission barrier is not given or equal to 0, it concerns the ground state of the nucleus.
Examples:

Ntop 41 93 14

Ntop 94 239 20 1

Range: $\mathbf{0 \leq}$ **Ntop** $\mathbf{\leq 200}$
Default: **Ntop** is read from the *talys/structure/density/nmax* directory. If not present there, **Ntop** is equal to the last discrete level used for the Hauser-Feshbach calculation.

Exmatch

The matching energy between the constant temperature and Fermi gas region in MeV, see Eq. (4.254). On the input line, we read **Exmatch**, Z, A, value, the ground state or fission barrier to which it applies (optional). If the fission barrier is not given or is equal to 0, it concerns the ground state of the nucleus.
Examples:

Exmatch 41 93 4.213

Exmatch 94 239 5.556 2

Range: $\mathbf{0.1 \leq}$ **Exmatch** $\mathbf{\leq 20.}$
Default: **Exmatch** is determined from Eq. (4.261).

T

The temperature of the Gilbert-Cameron formula in MeV, see Eq. (4.258). On the input line, we read **T**, Z, A, value, the ground state or fission barrier to which it applies (optional). If the fission barrier is not given or is equal to 0, it concerns the ground state of the nucleus.
Examples:

T 41 93 0.332

T 94 239 0.673 1

Range: $0.001 \leq$ **T** $\leq$ **10.**
Default: **T** is determined from Eq. (4.258).

E0

The ”back-shift” energy of the four-component formula in MeV, see Eq. (4.255). On the input line, we read **E0**, Z, A, value, the ground state or fission barrier to which it applies (optional). If the fission barrier is not given or is equal to 0, it concerns the ground state of the nucleus.
Examples:

E0 41 93 0.101

E0 94 239 -0.451 1

Range: $-10. \leq$ **E0** $\leq$ **10.**
Default: **E0** is determined from Eq. (4.255).

Pshift

An extra pairing shift for adjustment of the Fermi Gas level density, in MeV. On the input line, we read **Pshift**, Z, A, value.
Examples:

Pshift 60 142 0.26

Range: $-10. \leq$ **Pshift** $\leq$ **10.**
Default: **Pshift** is determined from Eqs. (4.250), (4.268), or (4.282), depending on the level density model.

Pshiftconstant

Global constant for the adjustable pairing shift in MeV.
Examples:

Pshiftconstant 1.03

Range: $-5. \leq$ **Pshiftconstant** $\leq$ **5.**
Default: **Pshiftconstant=1.09** for **ldmodel 3** and **Pshiftconstant=0.** otherwise.

Ufermi

Constant U_f of the phenomenological function (4.309) for damping of collective effects, in MeV.
Examples:

Ufermi 45.

Range: $0. \leq$ **Ufermi** $\leq$ **1000.**
Default: **Ufermi 30.**

cfermi

Width C_f of the phenomenological Fermi distribution (4.309) for damping of collective effects, in MeV.
Examples:

cfermi 16.

Range: $0. \leq$ **cfermi** $\leq$ **1000.**
Default: **cfermi 10.**

Ufermibf

Constant U_f of the phenomenological function (4.309) for damping of collective effects on the fission barrier, in MeV.
Examples:

Ufermibf 90.

Range: $0. \leq$ **Ufermibf** $\leq$ **1000.**
Default: **Ufermibf 45.**

cfermibf

Width C_f of the phenomenological Fermi distribution (4.309) for damping of collective effects on the fission barrier, in MeV.
Examples:

cfermibf 16.

Range: $0. \leq$ **cfermibf** $\leq$ **1000.**
Default: **cfermibf 10.**

Rspincut

Adjustable constant for spin cut-off parameter. Eq. (4.244) is multiplied by **Rspincut**.
Examples:

Rspincut 0.8

Range: **0.** $\leq$ **Rspincut** $\leq$ **10.**
Default: **Rspincut 1.**

beta2

Deformation parameter for moment of inertia for the ground state or fission barrier, see Eq. (4.305). On the input line, we read **beta2**, Z, A, value, fission barrier. If the number of the fission barrier is not given or is equal to 0, it concerns the ground state.
Examples:

beta2 90 232 0.3

beta2 94 239 1.1 2

Range: $0. \leq$ **beta2** $<$ **1.5**
Default: **beta2 0.** for the ground state, **beta2 0.6** for the first barrier, **beta2 0.8** for the second barrier, and **beta2 1.** for the third barrier.

Krotconstant

Normalization constant for rotational enhancement for the ground state or fission barrier, to be multiplied with the r.h.s. of Eq. (4.306). On the input line, we read **Krotconstant**, Z, A, value, fission barrier. If the number of the fission barrier is not given or is equal to 0, it concerns the ground state.
Examples:

Krotconstant 90 232 0.4

Krotconstant 94 239 1.1 2

Range: $0.01 \leq$ **Krotconstant** $\leq$ **100.**
Default: **Krotconstant 1.**

ctable

Constant c of the adjustment function (4.314) for tabulated level densities, per nucleus. On the input line, we read **ctable**, Z, A, value.
Examples:

ctable 29 65 2.8

Range: **-10.** $\leq$ **ctable** $\leq$ **10.**
Default: **ctable 0.**

ptable

Constant δ of the adjustment function (4.314) for tabulated level densities, per nucleus. On the input line, we read **ptable**, Z, A, value.
Examples:

ptable 29 65 -0.6

Range: **-10.** $\leq$ **ptable** $\leq$ **10.**
Default: **ptable 0.**

cglobal

Constant c of the adjustment function (4.314) for tabulated level densities, applied for all nuclides at the same time. Individual cases can be overruled by the **ctable** keyword. On the input line, we read **cglobal**, value.
Examples:

cglobal 1.5

Range: **-10.** $\leq$ **cglobal** $\leq$ **10.**
Default: **cglobal 0.**

pglobal

Constant δ of the adjustment function (4.314) for tabulated level densities, applied for all nuclides at the same time. Individual cases can be overruled by the **ptable** keyword. On the input line, we read **pglobal**, value.
Examples:

pglobal 0.5

Range: **-10.**
eq **pglobal** $\leq$ **10**
Default: **pglobal 0.**

Kph

Value for the constant of the single-particle level density parameter, i.e. $g = A/K_{ph}$, or $g_\pi = Z/K_{ph}$ and $g_\nu = N/K_{ph}$
Examples:

Kph 12.5

Range: $\mathbf{1.} \leq$ **Kph** $\leq$ **100.**
Default: **Kph 15.**

g

The single-particle level density parameter **g** in MeV^{-1}. On the input line, we read **g**, Z, A, value.
Examples:

g 41 93 7.15

g 94 239 17.5

Range: $\mathbf{0.1} \leq$ **g** $\leq$ **100.**
Default: $g = A/Kph$

gp

The single-particle proton level density parameter g_π in MeV^{-1}. On the input line, we read **gp**, Z, A, value.
Examples:

gp 41 93 3.15

gp 94 239 7.2

Range: $0.1 \leq$ **gp** $\leq$ **100.**
Default: $gp = Z/Kph$

gn

The single-particle neutron level density parameter g_ν in MeV^{-1}. On the input line, we read **gn**, Z, A, value.
Examples:

gn 41 93 4.1

gn 94 239 11.021

Range: $0.1 \leq$ **gn** $\leq$ **100.**
Default: $gn = N/Kph$

gshell

Flag to include the damping of shell effects with excitation energy in single-particle level densities. The Ignatyuk parameterisation for total level densities is also applied to the single-particle level density parameters.
Examples:

gshell y

gshell n

Range: **y** or **n**
Default: **gshell n**

6.2.9 Fission

fission

Flag for the enabling or disabling of fission. By default **fission** is enabled if the target mass is above 209. Hence, for lower masses, it is necessary to set **fission y** manually at high incident energies (subactinide fission).
Examples:

fission y

fission n

Range: **y** or **n**. Fission is not allowed for $A \leq 56$
Default: **fission y** for $A > 209$, **fission n** for $A \leq 209$. The default enabling or disabling of fission is thus mass dependent.

fismodel

Model for fission barriers. **fismodel** is only active if **fission y**. There are 5 possibilities:
Examples:

fismodel 1: experimental fission barriers

fismodel 2: theoretical fission barriers, Mamdouh table

fismodel 3: theoretical fission barriers, Sierk model

fismodel 4: theoretical fission barriers, rotating liquid drop

fismodel 5: WKB approximation for fission path model

Range: **1** $\leq$ **fismodel** $\leq$ **5**
Default: **fismodel 1**

fismodelalt

"Back-up" model for fission barriers, for the case that the parameters of the tables used in **fismodel 1-2** are not available. There are two possibilities:
Examples:

fismodelalt 3 : theoretical fission barriers, Sierk model

fismodelalt 4 : theoretical fission barriers, rotating liquid drop model

Range: **3** $\leq$ **fismodelalt** $\leq$ **4**
Default: **fismodelalt 4**

axtype

Type of axiality of the fission barrier. There are five options:

1: axial symmetry

2: left-right asymmetry

3: triaxial and left-right asymmetry

4: triaxial no left-right asymmetry

5: no symmetry

On the input line, we read **axtype**, Z, A, value, fission barrier. If the number of the fission barrier is not given or is equal to 0, it concerns the first barrier.
Examples:

axtype 90 232 3

axtype 94 239 1 2

Range: $\mathbf{1} \leq$ **axtype** $\leq \mathbf{5}$
Default: **axtype 2** for the second barrier and $N > 144$, **axtype 3** for the first barrier and $N > 144$, **axtype 1** for the rest.

fisbar

Fission barrier in MeV. On the input line, we read **fisbar**, Z, A, value, fission barrier. This keyword overrules the value given in the nuclear structure database. If the number of the fission barrier is not given or is equal to 0, it concerns the first barrier.
Examples:

fisbar 90 232 5.6

fisbar 94 239 6.1 2

Range: $\mathbf{0.} \leq$ **fisbar** $\leq$ **100.**
Default: **fisbar** is read from the *talys/structure/fission/* directory, or determined by systematics according to the choice of **fismodel**.

fishw

Fission barrier width in MeV. On the input line, we read **fishw**, Z, A, value, fission barrier. This keyword overrules the value given in the nuclear structure database. If the number of the fission barrier is not given or is equal to 0, it concerns the first barrier.
Examples:

fishw 90 232 0.8

fishw 94 239 1.1 2

Range: $\mathbf{0.01} \leq$ **fishw** $\leq$ **10.**
Default: **fishw** is read from the *talys/structure/fission/* directory or determined by systematics, according to the choice of **fismodel**.

Rtransmom

Normalization constant for moment of inertia for transition states, see Eq. (4.305). On the input line, we read **Rtransmom**, Z, A, value, fission barrier. If the number of the fission barrier is not given or is equal to 0, it concerns the first barrier.
Examples:

Rtransmom 90 232 1.15

Rtransmom 94 239 1.1 2

Range: $0.1 \leq$ **Rtransmom** $\leq$ **10.**
Default: **Rtransmom 0.6** for the first barrier, **Rtransmom 1.0** for the other barriers.

hbtransfi le

File with head band transition states. The format of the file is exactly the same as that of the nuclear structure database *talys/structure/fission/barrier/*. In practice, the user can copy a file from this database, e.g. *z092*, to the working directory and change it. In this way, changes in the "official" database are avoided. Note that one file in the working directory can only be used for one isotope. On the input line, we read **hbtransfile**, Z, A, filename.
Examples:

hbtransfile 92 238 u238.hb

Range: **hbtransfile** can be equal to any filename, provided it starts with a character and consists entirely of lowercase characters.
Default: If **hbtransfile** is not given in the input file, the head band transition states are taken from the *talys/structure/fission/states* database.

class2

Flag for the enabling or disabling of class II/III states in fission. **class2** is only active if **fission y**.
Examples:

class2 y

class2 n

Range: **y** or **n**
Default: **class2 n**

Rclass2mom

Normalization constant for moment of inertia for class II/III states, see Eq. (4.305). On the input line, we read **Rclass2mom**, Z, A, value, fission barrier. If the number of the fission barrier is not given or is equal to 0, it concerns the first barrier well.
Examples:

Rclass2mom 90 232 1.15

Rclass2mom 94 239 1.1 2

Range: $0.1 \leq$ **Rclass2mom** $\leq$ **10.**
Default: **Rclass2mom 1.**

class2width

Width of class II/III states. On the input line, we read **class2width**, Z, A, value, fission barrier. If the number of the fission barrier is not given or is equal to 0, it concerns the first barrier well.
Examples:

class2width 90 232 0.35

class2width 94 239 0.15 2

Range: $0.01 \leq$ **class2width** $\leq$ **10.**
Default: **class2width 0.2**

class2file

File with class II/III transition states. The format of the file is exactly the same as that of the nuclear structure database *talys/structure/fission/states/*. In practice, the user can copy a file from this database, e.g. *z092*, to the working directory and change it. In this way, changes in the "official" database are avoided. Note that one file in the working directory can only be used for one isotope. On the input line, we read **class2file**, Z, A, filename.
Examples:

class2file 92 238 u238.c2

Range: **class2file** can be equal to any filename, provided it starts with a character and consists entirely of lowercase characters.
Default: If **class2file** is not given in the input file, the head band transition states are taken from the *talys/structure/fission/states* database.

betafiscor

Factor to adjust the width of the WKB fission path. (only applies for **fismodel 5**). On the input line, we read **betafiscor**, Z, A, value.
Examples:

betafiscor 92 239 1.2

Range: **0.1** $\leq$ **betafiscor** $\leq$ **10.**
Default: **betafiscor 1.**

vfiscor

Factor to adjust the height of the WKB fission path. (only applies for **fismodel 5**). On the input line, we read **vfiscor**, Z, A, value.
Examples:

vfiscor 92 239 0.9

Range: **0.1** $\leq$ **vfiscor** $\leq$ **10.**
Default: **vfiscor 1.**

Rfiseps

Ratio for limit for fission cross section per nucleus. This parameter determines whether the mass distribution for a residual fissioning nucleus will be calculated. Cross sections smaller than **Rfiseps** times the fission cross section are not used in the calculations, in order to reduce the computation time.
Examples:

Rfiseps 1.e-5

Range: $\mathbf{0}.$ $\leq$ **Rfiseps** $\leq$ $\mathbf{1}.$
Default: **Rfiseps 1.e-3**

massdis

Flag for the calculation of the fission-fragment mass distribution with the Brosa model.
Examples:

massdis y

massdis n

Range: **y** or **n**
Default: **massdis n**

ffevaporation

Flag to enable phenomenological correction for evaporated neutrons from fission fragments with the Brosa model.
Examples:

ffevaporation y

ffevaporation n

Range: **y** or **n**
Default: **ffevaporation n**

6.2.10 Output

The output can be made as compact or as extensive as you like. This can be specified by setting the following keywords. We especially wish to draw your attention to the several keywords that start with "**file**", at the end of this section. They can be very helpful if you directly want to have specific results available in a single file. Note that if you perform calculations with several incident energies, the files produced with these "**file**" keywords are incremented *during* the calculation. In other words, you can already plot intermediate results before the entire calculation has finished.

outmain

Flag for the main output. The header of TALYS is printed, together with the input variables and the automatically adopted default values. Also the most important computed cross sections are printed.
Examples:

outmain y

outmain n

Range: **y** or **n**
Default: **outmain y**

outbasic

Flag for the output of *all* basic information needed for the nuclear reaction calculation, such as level/bin populations, numerical checks, optical model parameters, transmission coefficients, inverse reaction cross sections, gamma and fission information, discrete levels and level densities. If **outbasic** is set to **y** or **n**, the keywords **outpopulation**, **outcheck**, **outlevels**, **outdensity**, **outomp**, **outdirect**, **outdiscrete**, **outinverse**, **outgamma** and **outfission** (see below for their explanation) will all be set to the same value automatically. Setting **outbasic y** is generally not recommended since it produces a rather large output file. Less extensive output files can be obtained by enabling some of the aforementioned keywords individually.
Examples:

outbasic y

outbasic n

Range: **y** or **n**
Default: **outbasic n**

outpopulation

Flag for the output of the population, as a function of excitation energy, spin and parity, of each compound nucleus in the reaction chain before it decays.
Examples:

outpopulation y

outpopulation n

Range: **y** or **n**
Default: the same value as **outbasic**: **outpopulation n**

outcheck

Flag for the output of various numerical checks. This is to check interpolation schemes for the transformation from the emission grid to the excitation energy grid and vice versa, and to test the WFC method by means of flux conservation in the binary compound nucleus calculation. Also, the emission spectra integrated over energy are compared with the partial cross sections, and summed exclusive channel cross sections are checked against total particle production cross sections and residual production cross sections.
Examples:

outcheck y

outcheck n

Range: **y** or **n**
Default: the same value as **outbasic**: **outcheck n**

outlevels

Flag for the output of discrete level information for each nucleus. All level energies, spins parities, branching ratios and lifetimes will be printed.
Examples:

outlevels y

outlevels n

Range: **y** or **n**
Default: the same value as **outbasic**: **outlevels n**

outdensity

Flag for the output of level density parameters and level densities for each residual nucleus.
Examples:

outdensity y

outdensity n

Range: **y** or **n**
Default: the same value as **outbasic**: **outdensity n**

outomp

Flag for the output of optical model parameters for each particle and energy.
Examples:

outomp y

outomp n

Range: **y** or **n**
Default: the same value as **outbasic**: **outomp n**

outdirect

Flag for the output of the results from the direct reaction calculation of ECIS (DWBA, giant resonances and coupled-channels).
Examples:

outdirect y

outdirect n

Range: **y** or **n**
Default: the same value as **outbasic**: **outdirect n**

outinverse

Flag for the output of particle transmission coefficients and inverse reaction cross sections.
Examples:

outinverse y

outinverse n

Range: **y** or **n**
Default: the same value as **outbasic**: **outinverse n**

outtransenergy

Flag for the output of transmission coefficients sorted per energy (**y**) or per angular momentum (**n**). **outtransenergy** is only active if **outinverse y**.
Examples:

outtransenergy y

outtransenergy n

Range: **y** or **n**
Default: **outtransenergy y**

outecis

Flag for keeping the various ECIS output files produced during a TALYS run. This is mainly for diagnostic purposes.
Examples:

outecis y

outecis n

Range: **y** or **n**
Default: **outecis n**

outgamma

Flag for the output of gamma-ray parameters, strength functions, transmission coefficients and reaction cross sections.
Examples:

outgamma y

outgamma n

Range: **y** or **n**
Default: the same value as **outbasic**: **outgamma n**

outpreequilibrium

Flag for the output of pre-equilibrium parameters and cross sections. **outpreequilibrium** is only active if **preequilibrium y**.
Examples:

outpreequilibrium y

outpreequilibrium n

Range: **y** or **n**
Default: **outpreequilibrium n**

outfission

Flag for the output of fission parameters, transmission coefficients and partial cross sections. **outfission** is only active if **fission y**.
Examples:

outfission y

outfission n

Range: **y** or **n**
Default: the same value as **outbasic**: **outfission n**

outdiscrete

Flag for the output of cross sections to each individual discrete state. This is given for both the direct and the compound component.
Examples:

outdiscrete y

outdiscrete n

Range: **y** or **n**
Default: the same value as **outbasic**: **outdiscrete n**

adddiscrete

Flag for the addition of energy-broadened non-elastic cross sections for discrete states to the continuum spectra. **adddiscrete** is only active if **outspectra y**.
Examples:

adddiscrete y

adddiscrete n

Range: **y** or **n**
Default: **adddiscrete y**

addelastic

Flag for the addition of energy-broadened elastic cross sections to the continuum spectra. This case is treated separately from **adddiscrete**, since sometimes the elastic contribution is already subtracted from the experimental spectrum. **addelastic** is only active if **outspectra y**.
Examples:

addelastic y

addelastic n

Range: **y** or **n**
Default: the same value as **adddiscrete**: **addelastic y**

outspectra

Flag for the output of angle-integrated emission spectra.
Examples:

outspectra y

outspectra n

Range: **y** or **n**
Default: **outspectra y** if only one incident energy is given in the input file, and **outspectra n** for more than one incident energy.

elwidth

Width of elastic peak in MeV. For comparison with experimental angle-integrated and double-differential spectra, it may be helpful to include the energy-broadened cross sections for discrete states in the high-energy tail of the spectra. **elwidth** is the width of the Gaussian spreading that takes care of this. **elwidth** is only active if **outspectra y** or if **ddxmode 1, 2** or **3**.
Examples:

elwidth 0.2

Range: $\mathbf{1.e-6} \leq$ **elwidth** ≤ 100
Default: **elwidth 0.5**

outangle

Flag for the output of angular distributions for scattering to discrete states.
Examples:

outangle y

outangle n

Range: **y** or **n**
Default: **outangle n**

outlegendre

Flag for the output of Legendre coefficients for the angular distributions for scattering to discrete states. **outlegendre** is only active if **outangle y**.
Examples:

outlegendre y

outlegendre n

Range: **y** or **n**
Default: **outlegendre n**

ddxmode

Option for the output of double-differential cross sections. There are 4 possibilities.
Examples:

ddxmode 0: No output.

ddxmode 1: Output per emission energy as a function of angle (angular distributions).

ddxmode 2: Output per emission angle as a function of energy (spectra).

ddxmode 3: Output per emission energy and per emission angle.

Range: **0** $\leq$ **ddxmode** $\leq$ **3**
Default: **ddxmode 0**. If there is a **fileddxe** keyword, see p. 194, in the input file, **ddxmode 1** will be set automatically . If there is a **fileddxa** keyword, see p. 195, in the input file, **ddxmode 2** will be set automatically. If both **fileddxe** and **fileddxa** are present, **ddxmode 3** will be set automatically.

outdwba

Flag for the output of DWBA cross sections for the multi-step direct model.
Examples:

outdwba y

outdwba n

Range: **y** or **n**
Default: **outdwba n**

outgamdis

Flag for the output of discrete gamma-ray intensities. All possible discrete gamma transitions for all nuclei are followed. In the output they are given in tables per nuclide and for each decay from state to state.
Examples:

outgamdis y

outgamdis n

Range: **y** or **n**
Default: **outgamdis n**

outexcitation

Flag for the output of excitation functions, i.e. cross sections as a function of incident energy, such as residual production cross sections, inelastic cross sections, etc.
Examples:

outexcitation y

outexcitation n

Range: **y** or **n**
Default: **outexcitation y** if only one incident energy is given in the input file, and **outexcitation n** for more than one incident energy.

endf

Flag for the creation of various output files needed for the assembling of an ENDF-6 formatted file. Apart from the creation of various files that will be discussed for the following keywords, a file *endf.tot* is created which contains the reaction, elastic and total cross sections (calculated by ECIS) on a fine energy grid. Also a file *decay.X* will be created, with X the ejectile symbol in (a1) format, that contains the discrete gamma decay probabilities for the binary residual nuclides. This will be used for gamma-ray production from discrete binary levels. In addition to all the output detailed below, the continuum gamma-ray spectra per residual nucleus and incident energy will be stored in files *gamZZZA-AAEYYY.YYY.tot*, where where ZZZ is the charge number and AAA is the mass number in (i3.3) format, and YYY.YYY is the incident energy in (f7.3) format. Setting **endf y** will automatically enable many of the "**file**" keywords given below. All these specific files will be written to output if **endfdetail y**, see the next keyword.
Examples:

endf y

endf n

Range: **y** or **n**
Default: **endf n**

endfdetail

Flag for detailed ENDF-6 information. Certain ENDF-6 data files, usually those for incident charged particles, only require lumped cross sections, spectra etc. and not all the exclusive channels. The **endfdetail** keyword enables to choose between this. For incident neutrons and photons, it is generally assumed that detailed ENDF-6 info, such as exclusive channels for all separate MT numbers, is required.
Examples:

endfdetail y

endfdetail n

Range: **y** or **n**
Default: **endfdetail y** for incident neutrons and photons, **endfdetail n** for incident charged particles.

fi ledensity

Flag to write the level density and associated parameters on a separate file *ldZZZAAA.tot*, where ZZZ is the charge number and AAA is the mass number in (i3.3) format. **filedensity** is only active if **outdensity y**.
Examples:

filedensity y

filedensity n

Range: **y** or **n**
Default: **filedensity n**

fileelastic

Flag to write the elastic angular distribution on a separate file *XXYYY.YYYang.L00*, where XX is the particle symbol in (2a1) format (e.g. *nn* for elastic scattering), and YYY.YYY the incident energy in (f7.3) format. The file contains the angle, and 3 columns containing the total, shape elastic, and compound elastic angular distribution, respectively. If in addition **outlegendre y**, the elastic scattering Legendre coefficients will be written on a file *XXYYY.YYYleg.L00*. This file contains the L-value, and 4 columns containing the total, direct, compound and normalized Legendre coefficient. **fileelastic** is only active if **outangle y**.
Examples:

> **fileelastic y**, giving files *nn014.000ang.L00*, and (if **outlegendre y**) *nn014.000leg.L00*, for an incident energy of 14 MeV.
>
> **fileelastic n**

Range: **y** or **n**
Default: **fileelastic n**

fileangle

Designator for the output of the non-elastic angular distribution of one specific level on a separate file *PXYYY.YYYang.LMM*, where P and X are the particle symbols in (a1) format for the projectile and ejectile, respectively, YYY.YYY is the incident energy in (f7.3) format, and MM is the level number in (i2.2) format. The file contains the angle and 3 columns with the total inelastic, direct inelastic and compound inelastic angular distribution to the specified level. On the input line we read the level number. The **fileangle** keyword can appear more than once in an input file, one for each level that one is interested in. It will automatically produce files for all ejectiles. If in addition **outlegendre y**, the non-elastic scattering Legendre coefficients will be written on a file *PXYYY.YYYleg.LMM*. This file contains the L-value, and 4 columns containing the total, direct, compound and normalized Legendre coefficient. **fileangle** is only active if **outdiscrete y** and **outangle y**.
Examples:

> **fileangle 2**, giving files *np014.000ang.L02* and (**outlegendre y**) *np014.000leg.L02*, for the (n, p) reaction to the second discrete level and an incident energy of 14 MeV, and similarly for the other ejectiles.

Range: **0** $<$ **fileangle** $<$ **numlev**. Currently, **numlev=25**
Default: **fileangle** not active.

filechannels

Flag to write the exclusive channel cross sections as a function of incident energy on separate files. The files will be called *xsNPDTHA.tot*, where N is the neutron number of the exclusive channel, P the proton number, etc., in (a1) format. For example *xs210000.tot* contains the excitation function for $\sigma(n, 2np)$, if the incident particle was a neutron. The files contain the incident energy and 3 columns

with the exclusive cross section, the associated gamma-ray production cross section, and the fraction of this cross section relative to the total residual production cross section. If in addition isomers can be produced, files called *xsNPDTHA.LMM* will be created with MM the isomeric level number in (i2.2) format. If **filechannels y**, the exclusive binary continuum cross sections, such as continuum inelastic scattering, will also be written to files *PX.con*, where P and X are the particle symbols in (a1) format for the projectile and ejectile, respectively. If *outspectra y*, the exclusive channel spectra will be written on files *spNPDTHAEYYY.YYY.tot* where YYY.YYY is the incident energy in (f7.3) format. The files contain the incident energy and 6 columns, with the spectra per outgoing particle type. **filechannels** is only active if **channels y**.
Examples:

filechannels y

filechannels n

Range: **y** or **n**
Default: **filechannels n**

filespectrum

Designator for the output of the composite particle spectrum for a specific particle type on a separate file. On the input line we read the particle symbols. This will result in files *XspecYYY.YYY.tot*, where X is the outgoing particle symbol in (a1) format, and YYY.YYY the incident energy in (f7.3) format. The file contains the emission energy and 5 columns with the total, direct, pre-equilibrium, multiple pre-equilibrium and compound spectrum, respectively. **filespectrum** is only active if **outspectra y**.
Examples:

filespectrum n p a, giving files *nspec014.000.tot*, *pspec014.000.tot* and *aspec014.000.tot*, for an incident energy of 14 MeV.

Range: **n p d t h a**
Default: **filespectrum** not active.

fileddxe

Designator for the output of double-differential cross sections per emission energy for a specific particle type. On the input line we read the particle type and the emission energy. This will result in files *XddxYYY.Y.mev*, where X is the particle symbol in (a1) format and YYY.Y the emission energy in (f5.1) format. The file contains the emission angle and 5 columns with the total, direct, pre-equilibrium, multiple pre-equilibrium and compound spectrum, respectively. The **fileddxe** keyword can appear more than once in an input file, one for each outgoing energy that one is interested in. If there is at least one **fileddxe** keyword in the input **ddxmode**, see p. 190, will automatically be enabled.
Examples:

fileddxe n 60. (giving a file *nddx060.0.mev*).

Range: **n p d t h a** for the particles and **0.** - E_{inc} for outgoing energies.
Default: **fileddxe** not active.

fileddxa

Designator for the output of double-differential cross sections per emission angle for a specific particle type. On the input line we read the particle type and the emission angle. This will result in files *XddxYYY.Y.deg*, where X is the particle symbol in (a1) format and YYY.Y the emission angle in (f5.1) format. The file contains the emission energy and 5 columns with the total, direct, pre-equilibrium, multiple pre-equilibrium and compound spectrum, respectively. The **fileddxa** keyword can appear more than once in an input file, one for each outgoing angle that one is interested in. If there is at least one **fileddxa** keyword in the input **ddxmode**, see p. 190, will automatically be enabled.
Examples:

fileddxa n 30. (giving a file *nddx030.0.deg*).

Range: **n p d t h a** for the particles and **0. - 180.** for outgoing angles.
Default: **fileddxa** not active.

filegamdis

Flag to write the discrete gamma-ray intensities as a function of incident energy to separate files. This will result in files *gamZZZAAALYYLMM.tot*, where ZZZ is the charge number and AAA is the mass number in (i3.3) format, YY is the number of the initial discrete state and MM the number of the final discrete state. **filegamdis** is only active if **outgamdis y**.
Examples:

filegamdis y

filegamdis n

Range: **y** or **n**
Default: **filegamdis n**

filetotal

Flag to write all the total cross sections as a function of incident energy on a separate file *total.tot*. The file contains the incident energy, and 9 columns containing the non-elastic, total elastic, total, compound elastic, shape elastic, reaction, compound non-elastic, direct and pre-equilibrium cross section. In addition, the total particle production cross sections will be written on files *Xprod.tot*, with X the particle symbol in (a1) format. Finally, separate x-y tables will be made for the total cross section, on *totalxs.tot*, the total elastic cross section, on *elastic.tot*, and the total nonelastic cross section, on *nonelastic.tot*. **filetotal** is only active if **outexcitation y** or **endf y**.
Examples:

filetotal y

filetotal n

Range: **y** or **n**
Default: **filetotal n**

fi leresidual

Flag to write all the residual production cross sections as a function of incident energy on separate files. The files for the total (i.e. the sum over ground state + isomers) residual production cross sections have the name *rpZZZAAA.tot* where ZZZ is the charge number and AAA is the mass number in (i3.3) format. If a residual nuclide contains one or more isomeric states, there are additional files *rpZZZAAA.LMM*, where MM is the number of the isomer (ground state=0) in (i2.2) format. The files contain the incident energy and the residual production cross section. **fileresidual** is only active if **outexcitation y** or **endf y**.
Examples:

fileresidual y

fileresidual n

Range: **y** or **n**
Default: **fileresidual n**

fi lerecoil

Flag to write the recoil spectra of the residual nuclides as a function of incident energy on separate files. The files for the recoil spectra have the name *recZZZAAAspecYYY.YYY.tot* where ZZZ is the charge number and AAA is the mass number in (i3.3) format and YYY.YYY the incident energy in (f7.3) format. If in addition **flagchannels y**, there are additional files *spNPDTHAEYYY.YYY.rec*, where N is the neutron number of the exclusive channel, P the proton number, etc. The files contain the incident energy and the recoil.
Examples:

filerecoil y

filerecoil n

Range: **y** or **n**
Default: **filerecoil n**

fi lefi ssion

Flag to write all the fission cross sections as a function of incident energy on a separate file *fission.tot*. The file contains the incident energy and the total fission cross section. If in addition *filechannels y*, the exclusive fission cross sections will be written to files *fisNPDTHA.tot*, where N is the neutron number of the exclusive channel, P the proton number, etc., in (a1) format. For example, *fis200000.tot* contains the excitation function for $\sigma(n, 2nf)$, also known as the third chance fission cross section. **filefission** is only active if **fission y**.
Examples:

filefission y

filefission n

Range: **y** or **n**
Default: **filefission n**

<u>fi lediscrete</u>

Designator for the output of the excitation function of one specific non-elastic level on a separate file *PX.LMM*, where P and X are the particle symbols in (a1) format for the projectile and ejectile, respectively, and MM is the level number in (i2.2) format. The file contains the incident energy and 3 columns with the total inelastic, direct inelastic and compound inelastic cross section to the specified level. On the input line we read the level number. The **filediscrete** keyword can appear more than once in an input file, one for each level that one is interested in. It automatically produces a file for each ejectile. **filediscrete** is only active if **outdiscrete y**.
Examples:

> **filediscrete 2** , giving files *nn.L02*, *np.L02*, etc. for the excitation functions of (inelastic and other) neutron scattering to the second discrete level.

Range: **0** $<$ **filediscrete** $<$ **numlev**. Currently, **numlev=25**
Default: **filediscrete** not active.

6.2.11 Input parameter table

From all the keywords given above you can see that certain default values depend on mass, energy or other parameters. In table 6.1 we summarize all these dependencies and give the full table of keywords including their relation with each other.

Table 6.1: The keywords of TALYS.

Keyword	Range	Default	Page
a	1. - 100.	table or systematics	171
abundance	filename	no default	143
adddiscrete	y,n	y	189
addelastic	y,n	y	189
alimit	1. - 100.	systematics	171
alphald	0.01 - 0.2	systematics	171
alphaomp	1 - 2	1	155
angles	1-numang (90)	90	140
anglescont	1-numangcont (36)	36	140
anglesrec	1-numangrec (9)	9	142
astro	y,n	n	143
astrogs	y,n	n	143
asys	y,n	n	170
autorot	y,n	n	147
avadjust	0.5 - 2.	1.	150
avdadjust	0.5 - 2.	1.	151
avsoadjust	0.5 - 2.	1.	153
axtype	1-5	1 and 2,3 for $N > 144$	180
Pshift	-10. - 10.	systematics	175
Pshiftconstant	-5. - 5.	0. or 1.09	175
beta2	0. - 1.5	0.-1. (barrier dep.)	176
betafiscor	0.1 - 10.	1.	183
betald	0. - 0.5	systematics	171
bins	2 - numbins (100)	40	134
cglobal	-10. - 10.	1.	178
cfermi	0. - 1000.	10.	176
cfermibf	0. - 1000.	10.	176
channelenergy	y,n	n	142
channels	y,n	n	140
Cknock	0. - 10.	1.	167
class2	y,n	n	182
class2file	filename	no default	183
class2width	0.01 - 10.	0.2	183
colenhance	y,n	n	169
compound	y,n	y	157
core	-1,1	-1	157
Cstrip	0. - 10.	1.	167
ctable	-10. - 10.	1.	177
ctmglobal	y,n	n	170

Continuation of **Table 6.1.**

Keyword	Range	Default	Page
D0	1.e-6 - 10000.	table	161
d1adjust	0.2 - 5.	1.	151
d2adjust	0.2 - 5.	1.	151
d3adjust	0.2 - 5.	1.	152
ddxmode	0 - 3	0	190
deformfile	filename	no default	157
deltaW	-20. - 20.	calculated	173
dispersion	y,n	n	146
E0	-10. - 10.	calculated	175
eciscalc	y,n	y	148
eciscompound	y,n	n	159
ecisdwba	y,n	y	168
ecissave	y,n	n	148
egr	1. - 100.	table or systematics	160
ejectiles	g n p d t h a	g n p d t h a	133
electronconv	y,n	n	160
element	3 - 109 or Li - Mt	no default	130
Elow	1.e-6 - 1.	D_0	138
elwidth	1.e-6 - 100.	0.5	190
Emsdmin	>0.	Eninc/5.	169
endf	y,n	n	192
endfdetail	y,n	y for n,g; n otherwise	192
energy	1.e-11 - 250.	no default	131
Esurf	0. - 38.	systematics	164
etable	-10. - 10.	0.	162
Exmatch	0.1 - 20.	calculated	174
expmass	y,n	y	137
ffevaporation	y,n	n	184
fileangle	0 - numlev(25)	no default	193
filechannels	y,n	n	193
fileddxa	n,...,a 0. - 180.	no default	195
fileddxe	n,...,a 0. - energy	no default	194
filedensity	y,n	n	192
filediscrete	0 - numlev(25)	no default	197
fileelastic	y,n	n	193
filefission	y,n	n	196
filegamdis	y,n	n	195
filerecoil	y,n	n	196
fileresidual	y,n	n	196

Continuation of **Table 6.1.**

Keyword	Range	Default	Page
filespectrum	g n p d t h a	no default	194
filetotal	y,n	n	195
fisbar	0. - 100.	table or systematics	181
fishw	0.01 - 10.	table or systematics	181
fismodel	1 - 5	1	180
fismodelalt	3 - 4	4	180
fission	y,n,$A \geq 56$	y for mass$>$ 209, n for mass$\leq$ 209	179
ftable	0.1 - 10.	1.	162
fullhf	y,n	n	159
g	0.1-100.	systematics	178
gamgam	0. - 10.	table or systematics	161
gammald	0.01 - 1.	systematics	172
gammashell1	0. - 1.	systematics	172
gammashell2	0. - 0.2	0.	172
gammax	1 - 6	2	159
ggr	1. - 100.	table or systematics	161
giantresonance	y,n	y for n,p; n otherwise	157
gn	0.1 - 100.	systematics	179
gnorm	0. - 100.	calculated	159
gp	0.1 - 100.	systematics	179
gshell	y,n	n	179
hbtransfile	filename	no default	182
inccalc	y,n	y	148
isomer	0. - 1.e38	1.	138
jlmomp	y,n	n	146
Kph	1. - 100.	15.	178
Krotconstant	0.01 - 100.	1.	177
kvibmodel	1 - 2	2	173
labddx	y,n	n	141
ldmodel	1 - 5	1	169
levelfile	filename	no default	137
localomp	y,n	y	146
Ltarget	0 - numlev (25)	0	133
lvadjust	0.5 - 1.5	1.	154
lv1adjust	0.5 - 1.5	1.	154
lvsoadjust	0.5 - 1.5	1.	155
lwadjust	0.5 - 1.5	1.	154
lw1adjust	0.5 - 1.5	1.	155

Continuation of **Table 6.1.**

Keyword	Range	Default	Page
lwsoadjust	0.5 - 1.5	1.	155
M2constant	0. - 100.	1.	165
M2limit	0. - 100.	1.	166
M2shift	0. - 100.	1.	166
mass	0, 5 - 339	no default	130
massdis	y,n	n	184
massexcess	-500. - 500.	mass table	138
massmodel	1 - 3	3	137
massnucleus	A-0.5 - A+0.5	mass table	138
maxband	0 - 100	0	156
maxchannel	0 - 8	4	140
maxenrec	0 - numenrec (25)	10	142
maxlevelsbin	0 - numlev (25)	10 (g,n,p,a) and 5 (d,t,h)	136
maxlevelsres	0 - numlev (25)	10	136
maxlevelstar	0 - numlev (25)	20	135
maxN	0 - numN-2 (22)	22	134
maxrot	0 - 10	2	156
maxZ	0 - numZ-2 (10)	10	134
mpreeqmode	1 - 2	1	164
msdbins	2 - numenmsd/2-1 (8)	6	168
multipreeq	y,n or 0.001 - 250.	20.	163
Nlevels	0 - numlev (25)	equal to maxlevelsres	136
Nlow	0 - 200	2	174
Ntop	0 - 200	table or equal to Nlevels	174
nulldev	filename	no default	144
onestep	y,n	n	168
optmod	filename	no default	145
optmodall	y,n	n	147
optmodfileN	filename	no default	145
optmodfileP	filename	no default	145
outangle	y,n	y for one energy, n for many	190
outbasic	y,n	n	185
outcheck	y,n	equal to outbasic	186
outdensity	y,n	equal to outbasic	186
outdirect	y,n	equal to outbasic	187
outdiscrete	y,n	equal to outbasic	189
outdwba	y,n	n	191
outecis	y,n	n	188

Continuation of **Table 6.1.**

Keyword	Range	Default	Page
outexcitation	y,n	n for one energy, y for many	191
outfission	y,n	equal to outbasic	188
outgamdis	y,n	n	191
outgamma	y,n	equal to outbasic	188
outinverse	y,n	equal to outbasic	187
outlegendre	y,n	n	190
outlevels	y,n	equal to outbasic	186
outmain	y,n	y	185
outomp	y,n	equal to outbasic	187
outpopulation	y,n	equal to outbasic	185
outpreequilibrium	y,n	n	188
outspectra	y,n	y for one energy, n for many	189
outtransenergy	y,n	y	187
pair	0. - 10.	systematics	173
pairconstant	0. - 30.	12.	173
pairmodel	1 - 2	1	165
parity	y,n	n	170
partable	y,n	n	144
pglobal	-10. - 10.	0.	178
popeps	0. - 1000.	1.e-3	139
preeqcomplex	y,n	y	165
preeqmode	1 - 4	2	163
preeqspin	y,n	n	164
preeqsurface	y,n	y	164
preequilibrium	y,n or 0.001 - 250.	Ex(NL)	162
projectile	n,p,d,t,h,a,g,0	no default	130
ptable	-10. - 10.	0.	177
radialfile	filename	no default	154
rcadjust	0.5 - 2.	1.	153
Rclass2mom	0.1 - 10.	1.	182
reaction	y,n	y	141
recoil	y,n	n	141
recoilaverage	y,n	n	142
relativistic	y,n	y	141
Rfiseps	0. - 1.	1.e-3	184
Rgamma	0. - 100.	2.	167
Rnunu	0. - 100.	1.	166
Rnupi	0. - 100.	1.	166

Continuation of **Table 6.1.**

Keyword	Range	Default	Page
rotational	n p d t h a	n p	156
Rpinu	0. - 100.	1.	167
Rpipi	0. - 100.	1.	167
Rspincut	0. - 10.	1.	176
Rtransmom	0.1 - 10.	1.	182
rvadjust	0.5 - 2.	1.	150
rvdadjust	0.5 - 2.	1.	151
rvsoadjust	0.5 - 2.	1.	153
S0	0. - 10.	table	162
segment	1 - 4	1	135
sgr	0. - 10000.	table or systematics	161
shellmodel	1 - 2	1	172
spherical	y,n	n	156
spincutmodel	1 - 2	1	170
statepot	y,n	n	147
strength	1 - 4	1	160
strucpath	filename	no default	144
sysreaction	n p d t h a	d t h a	147
T	0.001 - 10.	calculated	174
transeps	0. - 1.	1.e-8	139
transpower	2 - 20	5	139
twocomponent	y,n	n	165
Ufermi	0. - 1000.	30.	175
Ufermibf	0. - 1000.	45.	176
v1adjust	0.2 - 5.	1.	149
v2adjust	0.2 - 5.	1.	149
v3adjust	0.2 - 5.	1.	149
v4adjust	0.2 - 5.	1.	149
vfiscor	0.1 - 10.	1.	184
vso1adjust	0.2 - 5.	1.	152
vso2adjust	0.2 - 5.	1.	152
w1adjust	0.2 - 5.	1.	150
w2adjust	0.2 - 5.	1.	150
wso1adjust	0.2 - 5.	1.	152
wso2adjust	0.2 - 5.	1.	153
widthfluc	y,n or 0.001 - 20.	S(n)	158
widthmode	0 - 3	1	158
xseps	0. - 1000.	1.e-7	139

Chapter 7

Verification and validation, sample cases and output

TALYS has been tested both formally (”computational robustness”) and by comparison of calculational results with experimental data. This will be described in the present Chapter. Also a description of the output will be given.

7.1 Robustness test with DRIP

One way to test a nuclear model code is to let it calculate results for a huge number of nuclides, and the whole range of projectiles and energies. We have written a little code DRIP, not included in the release, that launches TALYS for complete calculations for all nuclides, from dripline to dripline. Besides checking whether the code crashes, visual inspection of many curves simultaneously, e.g. (n,2n) excitation functions for 50 different targets, may reveal non-smooth behaviour. Various problems, not only in the TALYS source code itself, but also in the nuclear structure database, were revealed with this approach in the initial development stages.

7.2 Robustness test with MONKEY

Chapter 6 contains a description of the more than 200 keywords that can be used in a problem for TALYS. Some of them are flags which can only be set to **y** or **n**. Other keywords can be set to a few or several integer values and there are also keywords whose values may cover a quasi-continuous range between the minimum and maximum possible value that we allow for them. Strictly speaking, the total number of possible input files for TALYS is huge (though theoretically finite, because of the finite precision of a computer), and obviously only a small subset of them corresponds to physically meaningful cases. Indeed, as with any computer code it is not too difficult to bring a TALYS calculation to a formally successful end, i.e. without crashing, with an input file that represents a completely unphysical case. Obviously, there is no way to prevent this - the user is supposed to have full responsibility for what she or he is doing - and we can never anticipate what input files are made by other users. Nevertheless, to test the robustness of our code, we wrote a little program called MONKEY which remotely simulates

TALYS in the hands of an evil user: It creates an input file for TALYS, using all the keywords, with *random* values, and starts a run with it. Each keyword in this input file has a value that remains within the allowed (and very broad) range as specified in Chapter 6. If TALYS is compiled with all checking options (i.e. array out-of-bounds problems, divisions by zero, other over/underflow errors, etc.) enabled and completes many cases without crashing, we can at least say we have tested *computational* robustness to some extent, and that we *may* have probed every corner of the code. We realize that this is not a full-proof method to test TALYS formally on the Fortran level (if there exists such a test!), but MONKEY has helped us to discover a few bugs during development which otherwise would have come to the surface sooner or later. We think it is better that *we* find them first. The ideal result of this procedure would be that TALYS never crashes or stops without giving an appropriate error message. We emphasize that this test alone does obviously not guarantee any physical quality of the results. For that, much more important are the input files that *are* physically meaningful. These are discussed in the next Section.

7.3 Validation with sample cases

With this manual, we hope to convince you that a large variety of nuclear reaction calculations can be handled with TALYS. To strengthen this statement, we will discuss many different sample cases. In each case, the TALYS input file, the relevant output and, if available, a graphical comparison with experimental data will be given. The description of the first sample case is the longest, since the output of TALYS will be discussed in complete detail. Obviously, that output description is also applicable to the other sample cases. The entire collection of sample cases serves as (a) verification of TALYS: the sample output files should coincide, apart from numerical differences of insignificant order, with the output files obtained on your computer, and (b) validation of TALYS: the results should be comparable to experimental data for a widely varying set of nuclear reactions. Table 7.1 tells you what to expect in terms of computer time, and this shows that it thus may take a while (about one hour on a PC) before all sample cases have finished. Running the *verify* script will be worth the wait, since a successful execution of all sample cases will put you on safer ground for your own calculations. In general, we will explain the keywords again as they appear in the input files below. If not, consult Table 6.1, which will tell you where to find the explanation of a keyword.

Sample case	Time
1a	0 m 3.02 sec
1b	0 m 3.19 sec
1c	0 m 5.14 sec
1d	0 m 3.06 sec
1e	0 m 3.29 sec
1f	0 m 5.14 sec
1g	0 m 3.03 sec
1h	0 m 5.37 sec
1i	0 m 2.90 sec
2	1 m 38.93 sec
3a	0 m 0.72 sec
3b	0 m 0.76 sec
3c	0 m 0.73 sec
3d	6 m 21.21 sec
4a	0 m 42.81 sec
4b	0 m 28.32 sec
5	16 m 51.29 sec
6a	0 m 45.99 sec
6b	0 m 46.12 sec
7	0 m 51.25 sec
8	9 m 15.40 sec
9	0 m 4.89 sec
10a	0 m 20.04 sec
10b	1 m 14.46 sec
11	1 m 53.14 sec
12	0 m 11.86 sec
13	1 m 59.75 sec
14	0 m 00.00 sec
15	0 m 13.06 sec
16a	0 m 28.87 sec
16b	0 m 28.83 sec
16c	0 m 29.01 sec
16d	0 m 30.55 sec
17a	0 m 59.22 sec
17b	1 m 0.83 sec
17c	0 m 59.01 sec
18a	0 m 7.54 sec
18b	3 m 28.29 sec

Table 7.1: Computation time for the sample cases, run on a 3GHz Pentium processor, and TALYS compiled with the Lahey/Fujitsu f95 compiler under Linux Red Hat-9.

7.3.1 Sample 1: All results for 14 MeV n + ^{93}Nb

We have included 9 different versions of this sample case, in order to give an impression of the various types of information that can be retrieved from TALYS. Most, but not all, output options will be described, while the remaining will appear in the other sample cases. We have chopped the sample output after column 80 to let it fit within this manual. We suggest to consult the output files in the *samples/* directory for the full results.

Case 1a: The simplest input file

The first sample problem concerns the simplest possible TALYS calculation. Consider the following input file that produces the results for a 14 MeV neutron on ^{93}Nb:

```
#
# General
#
projectile n
element nb
mass 93
energy 14.
```

where the purpose of the lines starting with a "#" is purely cosmetical. This input file called *input* can simply be run as follows:

talys < **input** > **output**

An output file of TALYS consists of several blocks. Whether these blocks are printed or not depends on the status of the various keywords that were discussed in Chapter 6. By default, the so-called main output is always given (through the default **outmain y**), and we discuss this output in the present sample case. For a single incident energy, a default calculation gives the most important cross sections only. "Most important" is obviously subjective, and probably every user has an own opinion on what should always appear by default in the output. We will demonstrate in the other sample problems how to extract all information from TALYS. The output file starts with a display of the version of TALYS you are using, the name of the authors, and the Copyright statement. Also the physics dimensions used in the output are given:

```
    TALYS-1.0      (Version: December 21, 2007)

 Copyright (C) 2007  A.J. Koning, S. Hilaire and M.C. Duijvestijn
                          NRG          CEA               NRG

 Dimensions - Cross sections: mb, Energies: MeV, Angles: degrees
```

The next output block begins with:

```
########## USER INPUT ##########
```

Here, the first section of the output is a print of the keywords/input parameters. This is done in two steps: First, in the block

```
USER INPUT FILE

#
# General
#
projectile n
element nb
mass 93
energy 14.
```

an exact copy of the input file as given by the user is returned. Next, in the block

```
USER INPUT FILE + DEFAULTS

Keyword           Value   Variable     Explanation

#
# Four main keywords
#
projectile          n     ptype0       type of incident particle
element            Nb     Starget      symbol of target nucleus
mass               93     mass         mass number of target nucleus
energy             14.000 eninc        incident energy in MeV
#
# Basic physical and numerical parameters
#
ejectiles  g n p d t h a  outtype      outgoing particles
.............
```

a table with all keywords is given, not only the ones that you have specified in the input file, but also all the defaults that are set automatically. The corresponding Fortran variables are also printed, together with a short explanation of their meaning. This table can be helpful as a guide to change further input parameters for a next run. You may also copy and paste the block directly into your next input file.

In the next output block

```
########## BASIC REACTION PARAMETERS ##########

Projectile           : neutron     Mass in a.m.u.      :   1.008665
Target               :  93Nb       Mass in a.m.u.      :  92.906378

Included channels:
                    gamma
                    neutron
                    proton
                    deuteron
```

```
                    triton
                    helium-3
                    alpha

1 incident energy (LAB):

    14.000

Q-values for binary reactions:

Q(n,g):  7.22755
Q(n,n):  0.00000
Q(n,p):  0.69112
Q(n,d): -3.81879
Q(n,t): -6.19635
Q(n,h): -7.72313
Q(n,a):  4.92559
```

we print the main parameters that characterize the nuclear reaction: the projectile, target and their masses and the outgoing particles that are included as competitive channels. The incident energy or range of incident energies in the LAB system is given together with the binary reaction Q-values.

The block with final results starts with

```
########## RESULTS FOR E= 14.00000 ##########

Energy dependent input flags

Width fluctuations (flagwidth)      : n
Preequilibrium (flagpreeq)          : y
Multiple preequilibrium (flagmulpre): n
```

with no further information for the present sample case since no further output was requested. When all nuclear model calculations are done, the most important cross sections are summarized in the main part of the output, in which we have printed the center-of-mass energy, the main (total) cross sections. the inclusive binary cross sections $\sigma^{inc,bin}_{n,k}$, see Eq. (3.19), the total particle production cross sections $\sigma_{n,xn}$ of Eq. (3.20) and the multiplicities Y_n of Eq. (3.22), and the residual production cross sections. The latter are given first per produced nuclide and isomer. Next, nuclides with the same mass are summed to give mass yield curves. Also, the sum over all the residual cross sections is compared with the non-elastic cross section. Obviously, these two values should be approximately equal.

```
 ########### REACTION SUMMARY FOR E= 14.000 ###########

 Center-of-mass energy:  13.849

 1. Total (binary) cross sections

 Total           = 3.98195E+03
   Shape elastic   = 2.21132E+03
```

```
  Reaction        = 1.77063E+03
    Compound elastic= 5.91922E-04
    Non-elastic     = 1.77063E+03
      Direct          = 4.15966E+01
      Pre-equilibrium = 4.15821E+02
      Giant resonance = 6.97499E+01
      Compound non-el = 1.24346E+03
    Total elastic   = 2.21132E+03

2. Binary non-elastic cross sections (non-exclusive)

gamma   = 2.23665E+00
neutron = 1.68950E+03
proton  = 3.79183E+01
deuteron= 1.04112E+01
triton  = 6.70826E-01
helium-3= 2.35820E-08
alpha   = 2.98966E+01

3. Total particle production cross sections

gamma   = 2.24031E+03    Multiplicity= 1.26526E+00
neutron = 3.06135E+03    Multiplicity= 1.72896E+00
proton  = 4.03049E+01    Multiplicity= 2.27630E-02
deuteron= 1.04112E+01    Multiplicity= 5.87995E-03
triton  = 6.70826E-01    Multiplicity= 3.78863E-04
helium-3= 2.35820E-08    Multiplicity= 1.33184E-11
alpha   = 3.05269E+01    Multiplicity= 1.72407E-02

4. Residual production cross sections

  a. Per isotope

  Z   A  nuclide    total     level   isomeric    isomeric    lifetime
              cross section       cross section  ratio

  41  94 ( 94Nb) 1.18344E+00    0    5.75062E-01  0.48592
                                1    6.08379E-01  0.51408   3.76000E+02 sec.
  41  93 ( 93Nb) 3.27555E+02    0    2.75161E+02  0.84005
                                1    5.23933E+01  0.15995   5.09000E+08 sec.
  40  93 ( 93Zr) 2.96183E+01    0    2.96183E+01  1.00000
  41  92 ( 92Nb) 1.35998E+03    0    8.46105E+02  0.62215
                                1    5.13872E+02  0.37785   8.77000E+05 sec.
  40  92 ( 92Zr) 2.10977E+01    0    2.10977E+01  1.00000
  40  91 ( 91Zr) 6.70822E-01    0    6.70822E-01  1.00000
  39  90 ( 90Y ) 2.73781E+01    0    1.35362E+01  0.49442
                                2    1.38420E+01  0.50558   1.15000E+04 sec.
  39  89 ( 89Y ) 3.14870E+00    0    1.27418E+00  0.40467
```

```
                                            1    1.87452E+00  0.59533   1.57000E+01 sec.

   b. Per mass

   A  cross section

   94 1.18344E+00
   93 3.57173E+02
   92 1.38108E+03
   91 6.70822E-01
   90 2.73781E+01
   89 3.14870E+00

 Total residual production cross section:  1770.62939
 Non-elastic cross section              :  1770.62939
```

At the end of the output, the total calculation time is printed, followed by a message that the calculation has been successfully completed:

```
Execution time:  0 hours  0 minutes  3.15 seconds

The TALYS team congratulates you with this successful calculation.
```

Case 1b: Discrete state cross sections and spectra

As a first extension to the simple input/output file given above, we will request the output of cross sections per individual discrete level of the residual nuclides. Also, the cumulated angle-integrated and double-differential particle spectra are requested. This is obtained with the following input file:

```
#
# General
#
projectile n
element nb
mass 93
energy 14.
#
# Output
#
outdiscrete y
outspectra y
ddxmode 2
filespectrum n p a
fileddxa n 30.
fileddxa n 60.
fileddxa a 30.
fileddxa a 60.
```

In addition to the information printed for case 1a, the cross sections per discrete state for each binary channel are given, starting with the (n,γ) channel,

```
 5. Binary reactions to discrete levels and continuum

   (n,g)   cross sections:

 Inclusive:

 Level Energy    E-out      J/P       Direct     Compound      Total     Origin

  0   0.00000  21.07609    6.0+     0.00000     0.00000     0.00000    Preeq
  1   0.04090  21.03519    3.0+     0.00000     0.00000     0.00000    Preeq
...............................
```

after which the inelastic cross section to every individual discrete state of the target nucleus is printed, including the separation in direct and compound, see Eq. (3.16). These are summed, per contribution, to the total discrete inelastic cross section, see Eq. (3.15). To these cross sections, the continuum inelastic cross sections of Eq. (3.17) are added to give the total inelastic cross section (3.14). Finally, the $(n,\gamma n)$ cross section is also printed. This output block looks as follows

```
 Inelastic cross sections:

 Inclusive:

 Level Energy    E-out      J/P       Direct     Compound      Total     Origin

  1   0.03077  13.81777    0.5-     0.00670     0.00013     0.00683    Direct
  2   0.68709  13.16145    1.5-     0.01311     0.00025     0.01336    Direct
  3   0.74386  13.10468    3.5+     4.28791     0.00048     4.28839    Direct
  4   0.80849  13.04005    2.5+     0.08705     0.00037     0.08741    Direct
  5   0.81025  13.03829    2.5-     3.20756     0.00036     3.20792    Direct
  6   0.94982  12.89872    6.5+     7.43461     0.00065     7.43526    Direct
  7   0.97000  12.87854    1.5-     0.02590     0.00024     0.02614    Direct
  8   0.97891  12.86963    5.5+     6.36403     0.00062     6.36465    Direct
  9   1.08257  12.76597    4.5+     5.27768     0.00056     5.27823    Direct
 10   1.12676  12.72178    2.5+     0.31992     0.00036     0.32028    Direct
 11   1.28440  12.56414    0.5+     0.01591     0.00012     0.01603    Direct
 12   1.29000  12.55854    1.5-     0.24336     0.00024     0.24360    Direct
 13   1.29715  12.55139    4.5+     0.26629     0.00055     0.26684    Direct
 14   1.31515  12.53339    2.5-     0.02135     0.00035     0.02170    Direct
 15   1.33000  12.51854    1.5+     0.03001     0.00024     0.03025    Direct
 16   1.33516  12.51338    8.5+     0.96835     0.00060     0.96895    Direct
 17   1.36400  12.48454    3.5-     0.42107     0.00044     0.42152    Direct
 18   1.36970  12.47884    1.5+     0.03173     0.00024     0.03197    Direct
 19   1.39510  12.45344    2.5+     0.08954     0.00035     0.08990    Direct
 20   1.45420  12.39434    0.5+     0.10706     0.00012     0.10718    Direct
                                  ---------   ---------   ---------
```

```
Discrete  Inelastic:              29.21914     0.00727    29.22641
Continuum Inelastic:             428.71729  1231.55090  1660.26819
                                 ---------   ---------   ---------
Total     Inelastic:             457.93640  1231.55823  1689.49597

(n,gn) cross section:     1.05107
```

This is repeated for the (n, p) and other channels,

```
  (n,p)   cross sections:

Inclusive:

Level Energy    E-out     J/P       Direct    Compound      Total     Origin

 0   0.00000  14.53966    2.5+     0.33165     0.00026     0.33191    Preeq
 1   0.26688  14.27278    1.5+     1.10724     0.00017     1.10741    Preeq
 2   0.94714  13.59252    0.5+     0.85027     0.00008     0.85035    Preeq
 3   1.01800  13.52166    0.5+     0.24244     0.00008     0.24252    Preeq
...........................
```

The last column in these tables specifies the origin of the direct contribution to the discrete state. “Direct” means that this is obtained with coupled-channels, DWBA or, as in this case, weak coupling, whereas “Preeq” means that the pre-equilibrium cross section is collapsed onto the discrete states, as an approximate method for more exact direct reaction approaches for charge-exchange and pick-up reactions. We note here that the feature of calculating, and printing, the inelastic cross sections for a specific state is of particular interest in the case of excitations, i.e. to obtain this particular cross section for a whole range of incident energies. This will be handled in another sample case.

Since **outspectra y** was specified in the input file, the composite particle spectra for the continuum are also printed. Besides the total spectrum, the division into direct (i.e. smoothed collective effects and giant resonance contributions), pre-equilibrium, multiple pre-equilibrium and compound is given. First we give the photon spectrum,

```
7. Composite particle spectra

Spectra for outgoing gamma

 Energy   Total       Direct    Pre-equil.  Mult. preeq  Compound

  0.001 1.10530E+01 0.00000E+00 2.22494E-13 0.00000E+00 1.10530E+01
  0.002 1.11348E+01 0.00000E+00 2.17671E-12 0.00000E+00 1.11348E+01
  0.005 1.13792E+01 0.00000E+00 2.99265E-11 0.00000E+00 1.13792E+01
  0.010 1.17873E+01 0.00000E+00 2.25661E-10 0.00000E+00 1.17873E+01
  0.020 1.26069E+01 0.00000E+00 1.71084E-09 0.00000E+00 1.26069E+01
  0.050 1.54725E+01 0.00000E+00 2.42110E-08 0.00000E+00 1.54725E+01
  0.100 3.27488E+01 0.00000E+00 1.71082E-07 0.00000E+00 3.27488E+01
...........................
```

followed by the neutron spectrum

```
 Spectra for outgoing neutron

  Energy   Total       Direct    Pre-equil.  Mult. preeq  Compound

   0.001 1.77195E+01 7.72138E-03 9.45985E-02 0.00000E+00 1.76172E+01
   0.002 3.53846E+01 7.73366E-03 1.42810E-01 0.00000E+00 3.52340E+01
   0.005 8.83650E+01 7.77059E-03 2.69012E-01 0.00000E+00 8.80882E+01
   0.010 1.45726E+02 7.83249E-03 4.82712E-01 0.00000E+00 1.45236E+02
   0.020 2.71007E+02 7.95765E-03 9.71034E-01 0.00000E+00 2.70028E+02
   0.050 5.46087E+02 8.34413E-03 2.85497E+00 0.00000E+00 5.43223E+02
   0.100 8.71934E+02 9.02631E-03 6.72888E+00 0.00000E+00 8.65196E+02
...........................
```

and the spectra for the other outgoing particles. Depending on the value of **ddxmode**, the double-differential cross sections are printed as angular distributions or as spectra per fixed angle. For the present sample case, **ddxmode 2**, which gives

```
 9. Double-differential cross sections per outgoing angle

 DDX for outgoing neutron  at   0.000 degrees

   E-out    Total      Direct     Pre-equil. Mult. preeq   Compound

   0.001 1.41397E+00 1.50567E-03 1.05321E-02 0.00000E+00 1.40193E+00
   0.002 2.82124E+00 1.50806E-03 1.59003E-02 0.00000E+00 2.80383E+00
   0.005 7.04130E+00 1.51527E-03 2.99548E-02 0.00000E+00 7.00983E+00
   0.010 1.16128E+01 1.52734E-03 5.37603E-02 0.00000E+00 1.15575E+01
   0.020 2.15979E+01 1.55174E-03 1.08185E-01 0.00000E+00 2.14882E+01
   0.050 4.35484E+01 1.62711E-03 3.18426E-01 0.00000E+00 4.32283E+01
   0.100 6.96037E+01 1.76013E-03 7.51868E-01 0.00000E+00 6.88501E+01
................................
```

followed by the other angles and other particles. A final important feature of the present input file is that some requested information has been written to separate output files, i.e. besides the standard output file, TALYS also produces the ready-to-plot files

```
aspec014.000.tot
nspec014.000.tot
pspec014.000.tot
```

containing the angle-integrated neutron, proton and alpha spectra, and

```
addx030.0.deg
addx060.0.deg
nddx030.0.deg
nddx060.0.deg
```

containing the double-differential neutron and alpha spectra at 30 and 60 degrees.

Case 1c: Exclusive channels and spectra

As another extension of the simple input file we can print the exclusive cross sections at one incident energy and the associated exclusive spectra. This is accomplished with the input file

```
#
# General
#
projectile n
element nb
mass 93
energy 14.
#
# Output
#
channels y
outspectra y
```

Contrary to the previous sample case, in this case no double-differential cross sections or results per separate file are printed (since it only concerns one incident energy). The exclusive cross sections are given in one table, per channel and per ground or isomeric state. It is checked whether the exclusive cross sections add up to the non-elastic cross section. Note that this sum rule, Eq. (3.25), is only expected to hold if we include enough exclusive channels in the calculation. If **maxchannel 4**, this equality should always hold for incident energies up to 20 MeV. This output block looks as follows:

```
 6. Exclusive cross sections
 6a. Total exclusive cross sections
     Emitted particles     cross section reaction         level    isomeric    i
    n   p   d   t   h   a                                        cross section
    0   0   0   0   0   0    1.18344E+00  (n,g)
                                                              0     5.75062E-01
                                                              1     6.08379E-01
    1   0   0   0   0   0    3.26664E+02  (n,n')
                                                              0     2.74409E+02
                                                              1     5.22550E+01
    0   1   0   0   0   0    2.96168E+01  (n,p)
    0   0   1   0   0   0    1.04112E+01  (n,d)
    0   0   0   1   0   0    6.70822E-01  (n,t)
    0   0   0   0   0   1    2.73777E+01  (n,a)
                                                              0     1.35359E+01
                                                              2     1.38418E+01
    2   0   0   0   0   0    1.35982E+03  (n,2n)
                                                              0     8.46000E+02
                                                              1     5.13817E+02
    1   1   0   0   0   0    1.06861E+01  (n,np)
    1   0   0   0   0   1    3.14862E+00  (n,na)
                                                              0     1.27412E+00
                                                              1     1.87450E+00
```

```
   0   1   0   0   0   1    1.49401E-05  (n,pa)

 Sum over exclusive channel cross sections:  1769.57593
 (n,gn) + (n,gp) +...(n,ga) cross sections:     1.05321
 Total                                    :  1770.62915
 Non-elastic cross section                :  1770.62939
```

Note that the (n, np) and (n, d) cross sections add up to the residual production cross section for ^{92}Zr, as given in the first sample case.

Since **outspectra y**, for each exclusive channel the spectrum per outgoing particle is given. This output block begins with:

```
 6b. Exclusive spectra

     Emitted particles     cross section reaction      gamma cross section
   n   p   d   t   h   a
   1   0   0   0   0   0    3.26664E+02  (n,n')            1.00870E+03

  Outgoing spectra

  Energy  gamma       neutron     proton      deuteron    triton      helium-3

   0.001 4.06619E+00 2.14250E-03 0.00000E+00 0.00000E+00 0.00000E+00 0.00000E+00
   0.002 4.08311E+00 4.22497E-03 0.00000E+00 0.00000E+00 0.00000E+00 0.00000E+00
   0.005 4.13354E+00 1.04500E-02 0.00000E+00 0.00000E+00 0.00000E+00 0.00000E+00
   0.010 4.21777E+00 2.08288E-02 0.00000E+00 0.00000E+00 0.00000E+00 0.00000E+00
   0.020 4.38694E+00 4.16553E-02 0.00000E+00 0.00000E+00 0.00000E+00 0.00000E+00
   0.050 4.92328E+00 1.04608E-01 0.00000E+00 0.00000E+00 0.00000E+00 0.00000E+00
   0.100 6.46225E+00 2.10358E-01 0.00000E+00 0.00000E+00 0.00000E+00 0.00000E+00
..................................
     Emitted particles     cross section reaction      gamma cross section
   n   p   d   t   h   a
   1   1   0   0   0   0    1.06861E+01  (n,np)            1.97965E+01

  Outgoing spectra

  Energy  gamma       neutron     proton      deuteron    triton      helium-3

   0.001 6.35050E-02 1.87485E-01 0.00000E+00 0.00000E+00 0.00000E+00 0.00000E+00
   0.002 6.94942E-02 3.74836E-01 0.00000E+00 0.00000E+00 0.00000E+00 0.00000E+00
   0.005 8.74445E-02 9.36836E-01 0.00000E+00 0.00000E+00 0.00000E+00 0.00000E+00
   0.010 1.17368E-01 1.88679E+00 0.00000E+00 0.00000E+00 0.00000E+00 0.00000E+00
   0.020 1.77238E-01 3.89497E+00 0.00000E+00 0.00000E+00 0.00000E+00 0.00000E+00
   0.050 3.57037E-01 6.03595E+00 0.00000E+00 0.00000E+00 0.00000E+00 0.00000E+00
   0.100 6.57333E-01 8.96107E+00 0.00000E+00 0.00000E+00 0.00000E+00 0.00000E+00
   0.200 1.58990E+00 1.04045E+01 0.00000E+00 0.00000E+00 0.00000E+00 0.00000E+00
   0.300 1.88712E+00 9.88185E+00 0.00000E+00 0.00000E+00 0.00000E+00 0.00000E+00
   0.400 2.01034E+00 9.03657E+00 0.00000E+00 0.00000E+00 0.00000E+00 0.00000E+00
```

```
   0.500 1.41701E+00 8.28305E+00 0.00000E+00 0.00000E+00 0.00000E+00 0.00000E+00
   0.600 5.68786E+00 7.59201E+00 0.00000E+00 0.00000E+00 0.00000E+00 0.00000E+00
   0.700 8.64822E+00 6.60600E+00 0.00000E+00 0.00000E+00 0.00000E+00 0.00000E+00
   0.800 4.28359E+00 5.86945E+00 0.00000E+00 0.00000E+00 0.00000E+00 0.00000E+00
   0.900 2.37448E+00 5.09628E+00 0.00000E+00 0.00000E+00 0.00000E+00 0.00000E+00
   1.000 2.20641E+00 4.19745E+00 1.23263E-07 0.00000E+00 0.00000E+00 0.00000E+00
.................................
```

Note, as explained in Section 3.3.2, the (n,np) cross section is characterized by both a neutron and a proton spectrum.

Case 1d: Nuclear structure

It is possible to have all the nuclear structure information in the output file. The simplest way is to set **outbasic y**, which means that about everything that can be printed, will be printed. This may be a bit overdone if one is only interested in e.g. discrete levels or level densities. If the keywords **outlevels** and/or **outdensity** are set to **y**, discrete level and level density information will always be given for the target nucleus and the primary compound nucleus. With **outgamma y**, photon strength function information is also given. If we would set, in addition, **outpopulation y**, this info will also be given for all the other residual nuclides that are reached in the reaction chain. The input file for this sample case is

```
#
# General
#
projectile n
element nb
mass 93
energy 14.
#
# Output
#
outlevels y
outdensity y
outgamma y
```

In addition to the output of case 1a, the separation energies for the six light particles are printed.

```
 NUCLEAR STRUCTURE INFORMATION FOR Z= 41 N= 52 ( 93Nb)
 Separation energies:
 Particle        S
 neutron      8.83126
 proton       6.04337
 deuteron    12.45360
 triton      13.39081
 helium-3    15.65202
 alpha        1.93144
```

In the next output block, the discrete level scheme is printed for the first **maxlevelstar** levels. The discrete level info contains level number, energy, spin, parity, branching ratios and lifetimes of possible isomers. It is also indicated whether the spin (J) or parity (P) of a level is experimentally known or whether a value was assigned to it (see Section 5.4). The "string" of the original ENSDF database is also given, so that the user can learn about possible alternative choices for spin and parity. This output block begins with:

```
 Discrete levels of Z= 41 N= 52 ( 93Nb)

 Number  Energy Spin Parity  Branching  Ratio (%) Lifetime(sec) Assignment

   0     0.0000  4.5   +
   1     0.0308  0.5   -                                   5.090E+08
                               --->  0  100.0000
   2     0.6871  1.5   -
                               --->  1  100.0000
   3     0.7439  3.5   +
                               --->  0  100.0000
   4     0.8085  2.5   +
                               --->  0   96.1951
                               --->  3    3.8049
....................................
```

Since **outdensity y**, we print all the level density parameters that are involved, as discussed in Section 4.7: the level density parameter at the neutron separation energy $a(S_n)$, the experimental and theoretical average resonance spacing D_0, the asymptotic level density parameter $\tilde{a}$, the shell damping parameter γ, the pairing energy Δ, the shell correction energy δW, the matching energy E_x, the last discrete level, the levels for the matching problem, the temperature T, the back-shift energy E_0, the discrete state spin cut-off parameter σ and the spin cut-off parameter at the neutron separation energy. Next, we print a table with the level density parameter a, the spin cut-off parameter and the level density itself, all as a function of the excitation energy. This output block begins with:

```
 Level density parameters for Z= 41 N= 52 ( 93Nb)

 Model: Gilbert-Cameron
 Collective enhancement: no

 a(Sn)           :  12.33543
 Experimental D0 :             0.00 eV +-        0.00000
 Theoretical D0  :            77.69 eV
 Asymptotic a    :  12.24515
 Damping gamma   :   0.09559
 Pairing energy  :   1.24434
 Shell correction:   0.10845
 Last disc. level:        20
 Nlow            :         5
 Ntop            :        15
 Matching Ex     :   7.63849
 Temperature     :   0.86816
```

```
 E0              :  -1.36134
 Adj. pair shift :   0.00000
 Discrete sigma  :   2.78158
 Sigma (Sn)      :   4.57840
 Level density per parity for ground state
 (Total level density summed over parity)
    Ex     a    sigma   total   JP=  0.5  JP=  1.5  JP=  2.5  JP=  3.5  JP=  4.5

   0.25 12.372  2.782 3.685E+00 4.465E-01 7.356E-01 7.987E-01 6.774E-01 4.734E-0
   0.50 12.372  2.782 4.915E+00 5.955E-01 9.810E-01 1.065E+00 9.035E-01 6.313E-0
   0.75 12.372  2.782 6.555E+00 7.942E-01 1.308E+00 1.421E+00 1.205E+00 8.420E-0
   1.00 12.372  2.782 8.742E+00 1.059E+00 1.745E+00 1.895E+00 1.607E+00 1.123E+0
....................................
```

Finally, a comparison of the total level density with the cumulative number of discrete levels is given,

```
 Discrete levels versus total level density

   Energy Level   N_cumulative

   0.9498   6       7.125
   0.9700   7       7.462
   0.9789   8       7.614
   1.0826   9       9.491
   1.1268  10      10.363
   1.2844  11      13.856
   1.2900  12      13.992
   1.2972  13      14.167
....................................
```

Note also that, since **outdensity y** by default implies **filedensity y**, the files *ld041093.tot* and *ld041094.tot* have been created. They contain all level density parameters and a comparison between cumulated discrete levels and the integrated level density.

With **outgamma y** the gamma-ray information is printed. First, all relevant parameters are given: the total radiative width Γ_Γ, the s-wave resonance spacing D_0, the s-wave strength function S_0 and the normalization factor for the gamma-ray strength function. Second, we print the giant resonance information. For each multipolarity, we print the strength of the giant resonance σ_0, its energy and its width. Next, the gamma-ray strength function and transmission coefficients for this multipolarity and as a function of energy are printed. This output block begins with:

```
 ########## GAMMA STRENGTH FUNCTIONS, TRANSMISSION COEFFICIENTS AND CROSS SECTIO

 Gamma-ray information for Z= 41 N= 53 ( 94Nb)

 S-wave strength function parameters:

 Exp. total radiative width=   0.14500 eV +/- 0.01000 Theor. total radiative wid
 Exp. D0                   =     80.00 eV +/-   10.00 Theor. D0
```

```
 Exp. S-wave strength func.=   0.45000E-4 +/- 0.07000 Theor. S-wave strength fun
 Normalization factor      =   0.70061

 Gamma-ray strength function model for E1: Kopecky-Uhl

 Normalized gamma-ray strength functions and transmission coefficients for l= 1

 Giant resonance parameters :

 sigma0(M1) =   2.515       sigma0(E1) = 192.148
      E(M1) =   9.017            E(E1) =  16.523
  gamma(M1) =   4.000        gamma(E1) =   5.515
      k(M1) =   8.67373E-08      k(E1) =   8.67373E-08

     E       f(M1)        f(E1)        T(M1)        T(E1)

   0.001  0.00000E+00  1.36200E-08  0.00000E+00  8.55769E-17
   0.002  7.39798E-13  1.36205E-08  3.71863E-20  6.84642E-16
   0.005  1.84950E-12  1.36221E-08  1.45259E-18  1.06988E-14
   0.010  3.69900E-12  1.36248E-08  2.32415E-17  8.56071E-14
   0.020  7.39805E-12  1.36301E-08  3.71867E-16  6.85126E-13
   0.050  1.84960E-11  1.36461E-08  1.45267E-14  1.07176E-11
   0.100  3.69981E-11  1.36725E-08  2.32466E-13  8.59069E-11
....................................
```

which is repeated for each l-value. Finally, the photoabsorption cross section is printed:

```
 Photoabsorption cross sections

    E      reaction

   0.001  2.2413E-04
   0.002  5.5010E-04
   0.005  1.2228E-03
   0.010  2.3445E-03
   0.020  4.5901E-03
   0.050  1.1345E-02
   0.100  2.2662E-02
   0.200  4.5515E-02
   0.300  6.8659E-02
   0.400  9.2090E-02
   0.500  1.1581E-01
....................................
```

Case 1e: Detailed pre-equilibrium information

The single- and double-differential spectra have already been covered in sample 1b. In addition to this, the contribution of the pre-equilibrium mechanism to the spectra and cross sections can be printed in more detail with the **outpreequilibrium** keyword. With the input file

```
#
# General
#
projectile n
element nb
mass 93
energy 14.
#
# Output
#
outpreequilibrium   y
outspectra          y
ddxmode             2
```

we obtain, in addition to the aforementioned output blocks, a detailed outline of the pre-equilibrium model used, in this case the default: the two-component exciton model. First, the parameters for the exciton model are printed, followed by the matrix elements as a function of the exciton number:

```
 ########## PRE-EQUILIBRIUM ##########

 ++++++++++ TWO-COMPONENT EXCITON MODEL ++++++++++

 1. Matrix element for E=  21.076

 Constant for matrix element :   1.000
 p-p ratio for matrix element:   1.000
 n-n ratio for matrix element:   1.500
 p-n ratio for matrix element:   1.000
 n-p ratio for matrix element:   1.000

 p(p) h(p) p(n) h(n)     M2pipi      M2nunu      M2pinu      M2nupi

  0    0    1    0    2.63420E-05 3.95131E-05 2.63420E-05 2.63420E-05
  0    0    2    1    1.08884E-04 1.63327E-04 1.08884E-04 1.08884E-04
  1    1    1    0    1.08884E-04 1.63327E-04 1.08884E-04 1.08884E-04
  0    0    3    2    1.76643E-04 2.64964E-04 1.76643E-04 1.76643E-04
  1    1    2    1    1.76643E-04 2.64964E-04 1.76643E-04 1.76643E-04
....................................
```

Next, the emission rates are printed: first as function of particle type and particle-hole number, and in the last column summed over particles:

```
 2. Emission rates or escape widths

 A. Emission rates ( /sec)

 p(p) h(p) p(n) h(n)    gamma       neutron      proton      deuteron    triton

  0    0    1    0    2.16570E+18 0.00000E+00 0.00000E+00 0.00000E+00 0.00000E+0
```

```
  0    0    2    1    5.29285E+17 1.63578E+21 0.00000E+00 0.00000E+00 0.00000E+0
  1    1    1    0    5.58040E+17 8.15540E+20 2.32728E+20 2.79804E+19 0.00000E+0
  0    0    3    2    1.26381E+17 4.52770E+20 0.00000E+00 0.00000E+00 0.00000E+0
  1    1    2    1    1.08464E+17 3.04371E+20 1.11136E+19 3.36637E+18 9.21406E+1
.....................................
```

Also, the alternative representation in terms of the escape widths, see Eqs. (4.127) and (4.128), is given,

```
 B. Escape widths (MeV)

 p(p) h(p) p(n) h(n)    gamma       neutron     proton      deuteron    triton

  0    0    1    0    1.42549E-03 0.00000E+00 0.00000E+00 0.00000E+00 0.00000E+0
  0    0    2    1    3.48382E-04 1.07669E+00 0.00000E+00 0.00000E+00 0.00000E+0
  1    1    1    0    3.67309E-04 5.36798E-01 1.53184E-01 1.84170E-02 0.00000E+0
  0    0    3    2    8.31858E-05 2.98019E-01 0.00000E+00 0.00000E+00 0.00000E+0
  1    1    2    1    7.13921E-05 2.00341E-01 7.31511E-03 2.21578E-03 6.06481E-0
  2    2    1    0    9.92804E-05 8.90114E-02 1.26899E-02 1.26325E-03 0.00000E+0
.....................................
```

The internal transition rates such as those of Eq. (4.93) and the associated damping and total widths are given next,

```
 3. Internal transition rates or damping widths, total widths

 A. Internal transition rates ( /sec)

 p(p) h(p) p(n) h(n)     lambdapiplus   lambdanuplus    lambdapinu     lambdanup

  0    0    1    0       1.45456E+21    1.74977E+21    0.00000E+00    0.00000E+0
  0    0    2    1       3.18197E+21    3.67047E+21    0.00000E+00    1.62232E+2
  1    1    1    0       1.74347E+21    3.78846E+21    1.30118E+20    0.00000E+0
  0    0    3    2       3.26507E+21    3.59251E+21    0.00000E+00    7.12888E+2
  1    1    2    1       2.35211E+21    3.64486E+21    1.72552E+20    2.29011E+2
.....................................
```

The lifetimes, $t(p,h)$ of Eq. (4.116) and the depletion factors $D_{p,h}$ of Eq. (4.117), are printed next,

```
 4. Lifetimes
 p(p) h(p) p(n) h(n)      Strength

  0    0    1    0       3.11867E-22
  0    0    2    1       6.41109E-23
  1    1    1    0       6.88639E-23
  0    0    3    2       3.09624E-23
  1    1    2    1       7.50433E-23
  2    2    1    0       2.43181E-23
.....................................
```

The partial state densities are printed for the first particle-hole combinations as a function of excitation energy. We also print the exciton number-dependent spin distributions and their sum, to see whether we have exhausted all spins. This output block is as follows

```
 ++++++++++ PARTIAL STATE DENSITIES ++++++++++

 Particle-hole state densities

    Ex    P(n=3)   gp     gn                          Configuration p(p) h(p) p
                              1 1 0 0   0 0 1 1   1 1 1 0   1 0 1 1   2 1 0 0

   1.000  0.000  2.733  3.533 7.471E+00 1.248E+01 9.728E+00 1.139E+01 0.000E+00
   2.000  0.000  2.733  3.533 1.494E+01 2.497E+01 4.559E+01 5.633E+01 8.212E+00
   3.000  0.000  2.733  3.533 2.241E+01 3.745E+01 1.078E+02 1.354E+02 2.627E+01
   4.000  0.000  2.733  3.533 2.988E+01 4.994E+01 1.965E+02 2.486E+02 5.453E+01
   5.000  0.000  2.733  3.533 3.736E+01 6.242E+01 3.116E+02 3.959E+02 9.301E+01
   6.000  0.000  2.733  3.533 4.483E+01 7.491E+01 4.530E+02 5.774E+02 1.417E+02
.....................................
 Particle-hole spin distributions

   n     J= 0        J= 1        J= 2        J= 3        J= 4        J= 5

   1  1.7785E-02  4.3554E-02  4.8369E-02  3.6832E-02  2.1025E-02  9.3136E-03  3.
   2  6.3683E-03  1.7261E-02  2.3483E-02  2.4247E-02  2.0773E-02  1.5284E-02  9.
   3  3.4812E-03  9.7603E-03  1.4208E-02  1.6237E-02  1.5926E-02  1.3878E-02  1.
   4  2.2659E-03  6.4613E-03  9.7295E-03  1.1698E-02  1.2277E-02  1.1642E-02  1.
   5  1.6234E-03  4.6764E-03  7.1862E-03  8.9070E-03  9.7354E-03  9.7128E-03  8.
.....................................
```

We print a table with the pre-equilibrium cross sections per stage and outgoing energy, for each outgoing particle. At the end of each table, we give the total pre-equilibrium cross sections per particle. Finally the total pre-equilibrium cross section summed over outgoing particles is printed,

```
 ++++++++++ TOTAL PRE-EQUILIBRIUM CROSS SECTIONS ++++++++++

 Pre-equilibrium cross sections for gamma

    E      Total        p=1         p=2         p=3         p=4         p=5        p

   0.001 2.2249E-13 9.1810E-14 5.0384E-14 3.8551E-14 4.1750E-14 0.0000E+00 0.000
   0.002 2.1767E-12 8.9578E-13 4.9358E-13 3.7794E-13 4.0941E-13 0.0000E+00 0.000
   0.005 2.9926E-11 1.2218E-11 6.8126E-12 5.2280E-12 5.6681E-12 0.0000E+00 0.000
   0.010 2.2566E-10 9.0941E-11 5.1690E-11 3.9811E-11 4.3221E-11 0.0000E+00 0.000
   0.020 1.7108E-09 6.7253E-10 3.9631E-10 3.0739E-10 3.3461E-10 0.0000E+00 0.000
   0.050 2.4211E-08 8.9017E-09 5.7581E-09 4.5550E-09 4.9961E-09 0.0000E+00 0.000
   0.100 1.7108E-07 5.7425E-08 4.1833E-08 3.4050E-08 3.7774E-08 0.0000E+00 0.000
.....................................
  19.000 1.3505E-01 1.3040E-01 4.3802E-03 2.6369E-04 4.8448E-06 0.0000E+00 0.000
```

```
  19.500 1.2227E-01 1.1875E-01 3.4007E-03 1.2338E-04 6.6196E-07 0.0000E+00 0.000
  20.000 1.1171E-01 1.0895E-01 2.7321E-03 3.1776E-05 0.0000E+00 0.0000E+00 0.000
  21.000 0.0000E+00 0.0000E+00 0.0000E+00 0.0000E+00 0.0000E+00 0.0000E+00 0.000
  22.000 0.0000E+00 0.0000E+00 0.0000E+00 0.0000E+00 0.0000E+00 0.0000E+00 0.000

         1.2864E+00 1.1291E+00 1.2096E-01 2.6279E-02 1.0140E-02 0.0000E+00 0.000

 Integrated:     1.28644


 Pre-equilibrium cross sections for neutron

    E      Total        p=1        p=2        p=3        p=4        p=5        p

   0.001 9.4598E-02 0.0000E+00 2.6248E-02 2.5416E-02 2.0231E-02 1.4060E-02 8.642
   0.002 1.4281E-01 0.0000E+00 3.9637E-02 3.8373E-02 3.0539E-02 2.1220E-02 1.304
   0.005 2.6901E-01 0.0000E+00 7.4728E-02 7.2301E-02 5.7513E-02 3.9941E-02 2.453
   0.010 4.8271E-01 0.0000E+00 1.3428E-01 1.2979E-01 1.0316E-01 7.1572E-02 4.391
   0.020 9.7103E-01 0.0000E+00 2.7090E-01 2.6131E-01 2.0733E-01 1.4358E-01 8.790
.....................................
  17.500 2.5293E-01 0.0000E+00 0.0000E+00 0.0000E+00 0.0000E+00 0.0000E+00 0.000
  18.000 0.0000E+00 0.0000E+00 0.0000E+00 0.0000E+00 0.0000E+00 0.0000E+00 0.000
  18.500 0.0000E+00 0.0000E+00 0.0000E+00 0.0000E+00 0.0000E+00 0.0000E+00 0.000
  19.000 0.0000E+00 0.0000E+00 0.0000E+00 0.0000E+00 0.0000E+00 0.0000E+00 0.000

         2.6727E+01 0.0000E+00 0.0000E+00 0.0000E+00 1.0326E-02 1.1088E-02 4.974

 Integrated:    26.72690

 Total pre-equilibrium cross section:   415.82114
```

Case 1f: Discrete direct cross sections and angular distributions

More specific information on the characteristics of direct reactions can be obtained with the following input file,

```
#
# General
#
projectile n
element nb
mass 93
energy 14.
#
# Output
#
outdiscrete         y
outangle            y
outlegendre         y
```

```
outdirect          y
outspectra         y
```

Now we obtain, through **outdirect y**, the direct cross sections from inelastic collective scattering and giant resonances. The output block begins with

```
 ++++++++++ DIRECT CROSS SECTIONS ++++++++++
 Direct inelastic cross sections
 Level  Energy   E-out      J/P   Cross section  Def. par.
   1   0.03077  13.81777    0.5-     0.00670     B  0.00239
   2   0.68709  13.16145    1.5-     0.01311     B  0.00338
   3   0.74386  13.10468    3.5+     4.28791     B  0.04699
   4   0.80849  13.04005    2.5+     0.08705     B  0.00873
   5   0.81025  13.03829    2.5-     3.20756     B  0.04070
   6   0.94982  12.89872    6.5+     7.43461     B  0.06216
.....................................
  92  12.99300   0.85554    0.5+     0.01342     B  0.01008
  93  13.09000   0.75854    3.5-     0.00194     B  0.00797
  94  13.54200   0.30654    2.5-     0.00680     B  0.00730
  95  13.58100   0.26754    1.5+     0.00089     B  0.00437

 Discrete direct inelastic cross section:    29.21914   Level 1- 20
 Collective cross section in continuum  :    45.69146
```

which for the case of ^{93}Nb gives the results of the weak-coupling model. For every level, the angular distribution is given, since **outangle y** was specified:

```
 Direct inelastic angular distributions

 Angle Ex= 0.031   Ex= 0.687   Ex= 0.744   Ex= 0.808   Ex= 0.810   Ex= 0.950   E
        JP= 0.5-    JP= 1.5-    JP= 3.5+    JP= 2.5+    JP= 2.5-    JP= 6.5+

   0.0 1.06392E-03 2.02551E-03 1.31400E+00 1.33822E-02 9.82438E-01 2.27460E+00 1
   2.0 1.06611E-03 2.03034E-03 1.30995E+00 1.34149E-02 9.79407E-01 2.26757E+00 1
   4.0 1.07266E-03 2.04477E-03 1.29828E+00 1.35125E-02 9.70673E-01 2.24731E+00 1
   6.0 1.08348E-03 2.06854E-03 1.28032E+00 1.36731E-02 9.57224E-01 2.21608E+00 1
   8.0 1.09840E-03 2.10115E-03 1.25797E+00 1.38933E-02 9.40465E-01 2.17707E+00 1
  10.0 1.11708E-03 2.14179E-03 1.23324E+00 1.41675E-02 9.21900E-01 2.13374E+00 1
.....................................
```

The table with total giant resonance results is given next,

```
 ++++++++++ GIANT RESONANCES ++++++++++

      Cross section   Exc. energy Emis. energy   Width    Deform. par.

 GMR  :     0.00000    16.37500    -2.52646     3.00000     0.02456
 GQR  :     0.00000    14.34671    -0.49817     4.14092     0.14081
 LEOR :    24.05840     6.84228     7.00626     5.00000     0.15788
```

```
HEOR :     0.00000    25.38264   -11.53410     7.36250     0.13210

Total:    24.05840
```

followed, since **outspectra y**, by the associated spectra,

```
Giant resonance spectra

 Energy   Total       GMR        GQR       LEOR       HEOR     Collective

  0.001 7.7214E-03 0.0000E+00 0.0000E+00 7.7214E-03 0.0000E+00 0.0000E+00
  0.002 7.7337E-03 0.0000E+00 0.0000E+00 7.7337E-03 0.0000E+00 0.0000E+00
  0.005 7.7706E-03 0.0000E+00 0.0000E+00 7.7706E-03 0.0000E+00 0.0000E+00
  0.010 7.8325E-03 0.0000E+00 0.0000E+00 7.8325E-03 0.0000E+00 0.0000E+00
  0.020 7.9577E-03 0.0000E+00 0.0000E+00 7.9577E-03 0.0000E+00 0.0000E+00
  0.050 8.3441E-03 0.0000E+00 0.0000E+00 8.3441E-03 0.0000E+00 0.0000E+00
....................................
```

The total, i.e. direct + compound cross section per discrete level of each residual nucleus was already described for sample 1b. In addition, we have now requested the angular distributions and the associated Legendre coefficients. First, the angular distribution for elastic scattering, separated by direct and compound contribution, is given. Since **outlegendre y** it is given first in terms of Legendre coefficients. This output block begins with:

```
8. Discrete state angular distributions

8a1. Legendre coefficients for elastic scattering

  L       Total           Direct         Compound       Normalized

  0     1.75971E+02     1.75971E+02     4.71035E-05     7.95776E-02
  1     1.55728E+02     1.55728E+02     0.00000E+00     7.04232E-02
  2     1.39720E+02     1.39720E+02     1.86062E-06     6.31840E-02
  3     1.21488E+02     1.21488E+02     0.00000E+00     5.49390E-02
  4     1.02659E+02     1.02659E+02     3.25580E-07     4.64241E-02
....................................
```

where the final column means division of the Legendre coefficients by the cross section. This is followed by the associated angular distribution. This output block begins with:

```
8a2. Elastic scattering angular distribution

Angle         Total           Direct          Compound

  0.0     6.69554E+03     6.69554E+03     6.12260E-05
  2.0     6.62134E+03     6.62134E+03     6.11570E-05
  4.0     6.40317E+03     6.40317E+03     6.09526E-05
  6.0     6.05390E+03     6.05390E+03     6.06204E-05
```

```
   8.0     5.59369E+03     5.59369E+03     6.01725E-05
  10.0     5.04824E+03     5.04824E+03     5.96247E-05
  12.0     4.44657E+03     4.44657E+03     5.89949E-05
.....................................
```

Next, the Legendre coefficients for inelastic scattering to each discrete level, separated by the direct and compound contribution, is given. This output block begins with:

```
 8b1. Legendre coefficients for inelastic scattering

    Level  1

   L       Total          Direct         Compound       Normalized

   0     5.43660E-04     5.33254E-04     1.04057E-05     7.95775E-02
   1     1.86109E-04     1.86109E-04     0.00000E+00     2.72415E-02
   2     6.20916E-05     6.21244E-05    -3.27812E-08     9.08857E-03
   3     1.66523E-05     1.66523E-05     0.00000E+00     2.43746E-03
   4    -1.37214E-05    -1.35853E-05    -1.36110E-07    -2.00846E-03
   5    -1.90397E-05    -1.90397E-05     0.00000E+00    -2.78691E-03
   6    -1.61471E-05    -1.61584E-05     1.12224E-08    -2.36352E-03
.....................................
```

which is also followed by the associated angular distributions. This output block begins with:

```
 8b2. Inelastic angular distributions

    Level  1

 Angle       Total         Direct       Compound

   0.0    1.07320E-03    1.06392E-03    9.28143E-06
   2.0    1.07540E-03    1.06611E-03    9.28519E-06
   4.0    1.08196E-03    1.07266E-03    9.29647E-06
   6.0    1.09280E-03    1.08348E-03    9.31533E-06
   8.0    1.10774E-03    1.09840E-03    9.34185E-06
  10.0    1.12646E-03    1.11708E-03    9.37618E-06
  12.0    1.14844E-03    1.13902E-03    9.41848E-06
.....................................
```

Finally, the same is given for the (n, p) and the other channels.

Case 1g: Discrete gamma-ray production cross sections

The gamma-ray intensity for each mother and daughter discrete level appearing in the reaction can be obtained with the following input file,

```
#
# General
```

```
#
projectile n
element nb
mass 93
energy 14.
#
# Output
#
outgamdis           y
```

For all discrete gamma-ray transitions, the intensity is printed. For each nucleus, the initial level and the final level is given, the associated gamma energy and the cross section. This output block begins with:

```
 10. Gamma-ray intensities

 Nuclide:  94Nb

     Initial level          Final level     Gamma Energy  Cross section

  no.  J/Pi    Ex          no.  J/Pi    Ex

   2   4.0+  0.0587  --->  1   3.0+  0.0409    0.01780    2.11853E-01
   3   6.0+  0.0787  --->  0   6.0+  0.0000    0.07867    2.12745E-01
   4   5.0+  0.1134  --->  0   6.0+  0.0000    0.11340    8.56884E-02
   4   5.0+  0.1134  --->  2   4.0+  0.0587    0.05470    3.36955E-02
   5   2.0-  0.1403  --->  1   3.0+  0.0409    0.09941    2.43882E-01
   6   2.0-  0.3016  --->  5   2.0-  0.1403    0.16126    5.42965E-02
   7   4.0+  0.3118  --->  2   4.0+  0.0587    0.25311    5.48060E-02
....................................
```

When we discuss multiple incident energy runs in the other sample cases, we will see how the excitation functions for gamma production cross sections per level are accumulated and how they can be written to separate files for easy processing.

Case 1h: The full output file

In this sample case we print basically everything that can be printed in the main output file for a single-energy reaction on a non-fissile nucleus. The input file is

```
#
# General
#
projectile n
element nb
mass 93
energy 14.
#
# Output
```

```
#
outbasic            y
outpreequilibrium   y
outspectra          y
outangle            y
outlegendre         y
ddxmode             2
outgamdis           y
partable            y
```

resulting in an output file that contains all nuclear structure information, all partial results, and moreover all intermediate results of the calculation, as well as results of intermediate checking. Note that basically all flags in the "Output" block on top of the output file are set to **y**, the only exceptions being irrelevant for this sample case. In addition to the output that is already described, various other output blocks are present. First, since **outbasic y** automatically means **outomp y**, a block with optical model parameters is printed. The optical model parameters for all included particles are given as a function of incident energy. This output block begins with:

```
 ######### OPTICAL MODEL PARAMETERS ##########

           neutron  on  93Nb

  Energy    V     rv    av    W     rw    aw    Vd   rvd   avd    Wd   rwd   awd

   0.001  51.02 1.215 0.663  0.14 1.215 0.663  0.00 1.274 0.534  3.32 1.274 0.53
   0.002  51.02 1.215 0.663  0.14 1.215 0.663  0.00 1.274 0.534  3.32 1.274 0.53
   0.005  51.02 1.215 0.663  0.14 1.215 0.663  0.00 1.274 0.534  3.32 1.274 0.53
   0.010  51.02 1.215 0.663  0.14 1.215 0.663  0.00 1.274 0.534  3.33 1.274 0.53
   0.020  51.02 1.215 0.663  0.14 1.215 0.663  0.00 1.274 0.534  3.33 1.274 0.53
....................................
```

In the next part, we print general quantities that are used throughout the nuclear reaction calculations, such as transmission coefficients and inverse reaction cross sections. The transmission coefficients as a function of energy are given for all particles included in the calculation. Depending upon whether **outtransenergy y** or **outtransenergy n**, the transmission coefficient tables will be grouped per energy or per angular momentum, respectively. The latter option may be helpful to study the behavior of a particular transmission coefficient as a function of energy. The default is **outtransenergy n**, leading to the following output block,

```
 ########## TRANSMISSION COEFFICIENTS AND INVERSE REACTION CROSS SECTIONS ######

 Transmission coefficients for incident neutron  at   0.00101 MeV

   L   T(L-1/2,L)   T(L+1/2,L)    Tav(L)

   0  0.00000E+00  8.82145E-03  8.82145E-03
   1  1.45449E-04  2.56136E-04  2.19240E-04
```

```
 Transmission coefficients for incident neutron  at   0.00202 MeV

   L   T(L-1/2,L)   T(L+1/2,L)    Tav(L)

   0  0.00000E+00  1.24534E-02  1.24534E-02
   1  4.11628E-04  7.24866E-04  6.20454E-04
   2  2.55785E-08  1.88791E-08  2.15588E-08

 Transmission coefficients for incident neutron  at   0.00505 MeV

   L   T(L-1/2,L)   T(L+1/2,L)    Tav(L)

   0  0.00000E+00  1.96205E-02  1.96205E-02
   1  1.62890E-03  2.86779E-03  2.45483E-03
   2  2.52135E-07  1.86214E-07  2.12582E-07
.....................................
```

which is repeated for each included particle type. Next, the (inverse) reaction cross sections is given for all particles on a LAB energy grid. For neutrons also the total elastic and total cross section on this energy grid is printed for completeness. This output block begins with:

```
 Total cross sections for neutron

     E        total      reaction    elastic   OMP reaction

   0.00101  1.1594E+04  6.2369E+03  5.3566E+03  6.2369E+03
   0.00202  1.0052E+04  4.7092E+03  5.3430E+03  4.7092E+03
   0.00505  8.8645E+03  3.5518E+03  5.3127E+03  3.5518E+03
   0.01011  8.4660E+03  3.1918E+03  5.2741E+03  3.1918E+03
   0.02022  8.4357E+03  3.2208E+03  5.2148E+03  3.2208E+03
   0.05054  8.9304E+03  3.8249E+03  5.1055E+03  3.8249E+03
   0.10109  9.6344E+03  4.5808E+03  5.0536E+03  4.5808E+03
   0.20217  1.0198E+04  5.0370E+03  5.1609E+03  5.0370E+03
   0.30326  1.0068E+04  4.7878E+03  5.2799E+03  4.7878E+03
   0.40434  9.6390E+03  4.3377E+03  5.3013E+03  4.3377E+03
   0.50543  9.1158E+03  3.8893E+03  5.2264E+03  3.8893E+03
   0.60651  8.5881E+03  3.5056E+03  5.0825E+03  3.5056E+03
   0.70760  8.0915E+03  3.1968E+03  4.8946E+03  3.1968E+03
.....................................
```

The final column "OMP reaction" gives the reaction cross section as obtained from the optical model. This is not necessary the same as the adopted reaction cross section of the middle column, since sometimes (especially for complex particles) this is overruled by systematics, see the **sysreaction** keyword, page 147. For the incident energy, we separately print the OMP parameters, the transmission coefficients and the shape elastic angular distribution,

```
+++++++++ OPTICAL MODEL PARAMETERS FOR INCIDENT CHANNEL ++++++++++
```

```
          neutron  on  93Nb

  Energy    V     rv    av    W     rw    aw    Vd   rvd   avd    Wd   rwd   awd

  14.000  46.11 1.215 0.663  0.98 1.215 0.663  0.00 1.274 0.534  6.84 1.274 0.53

 Optical model results

 Total cross section   : 3.9819E+03 mb
 Reaction cross section: 1.7706E+03 mb
 Elastic cross section : 2.2113E+03 mb

 Transmission coefficients for incident neutron  at  14.000 MeV

  L    T(L-1/2,L)   T(L+1/2,L)    Tav(L)

   0  0.00000E+00  7.46404E-01  7.46404E-01
   1  8.02491E-01  7.78050E-01  7.86197E-01
   2  7.77410E-01  8.08483E-01  7.96054E-01
   3  7.75550E-01  6.94249E-01  7.29092E-01
   4  9.15115E-01  9.53393E-01  9.36381E-01
   5  6.01374E-01  6.19435E-01  6.11226E-01
   6  7.00430E-01  4.72026E-01  5.77443E-01
   7  1.15102E-01  1.90743E-01  1.55444E-01
   8  1.59959E-02  1.88919E-02  1.75291E-02
   9  2.36267E-03  2.49532E-03  2.43249E-03
  10  3.55525E-04  3.61442E-04  3.58625E-04
  11  5.38245E-05  5.39431E-05  5.38864E-05
  12  8.20113E-06  8.17260E-06  8.18630E-06
  13  1.26174E-06  1.25428E-06  1.25788E-06

 Shape elastic scattering angular distribution

 Angle    Cross section

   0.0     6.69554E+03
   2.0     6.62134E+03
   4.0     6.40317E+03
   6.0     6.05390E+03
   8.0     5.59369E+03
  10.0     5.04824E+03
  12.0     4.44657E+03
  14.0     3.81867E+03
  16.0     3.19323E+03
  18.0     2.59561E+03
  20.0     2.04638E+03
.....................................
```

At some point during a run, TALYS has performed the direct reaction calculation and the pre-equilibrium calculation. A table is printed which shows the part of the reaction population that is left for the formation of a compound nucleus. Since the pre-equilibrium cross sections are calculated on an emission energy grid, there is always a small numerical error when transferring these results to the excitation energy grid. The pre-equilibrium spectra are therefore normalized. The output block looks as follows

```
########## POPULATION CHECK ##########

Particle Pre-equilibrium Population

gamma        1.28644     1.27794
neutron    428.71729   410.91696
proton      25.24361    25.20203
deuteron     3.50197     3.49032
triton       0.09480     0.09451
helium-3     0.00000     0.00000
alpha       26.72690    26.64193

++++++++++ Normalization of reaction cross section ++++++++++

Reaction cross section          : 1770.63000 (A)
Sum over T(j,l)                 : 1770.62537 (B)
Compound nucleus formation c.s. : 1243.46240 (C)
Ratio C/B                       :    0.70227
```

After the compound nucleus calculation, the results from the binary reaction are printed. First, the binary cross sections for the included outgoing particles are printed, followed by, if **outspectra y**, the binary emission spectra. If also **outcheck y**, the integral over the emission spectra is checked against the cross sections. The printed normalization factor has been applied to the emission spectra. This output block begins with:

```
########## BINARY CHANNELS ###########

++++++++++ BINARY CROSS SECTIONS ++++++++++

gamma    channel to Z= 41 N= 53 ( 94Nb): 2.23665E+00
neutron  channel to Z= 41 N= 52 ( 93Nb): 1.68950E+03
proton   channel to Z= 40 N= 53 ( 93Zr): 3.79183E+01
deuteron channel to Z= 40 N= 52 ( 92Zr): 1.04112E+01
triton   channel to Z= 40 N= 51 ( 91Zr): 6.70826E-01
helium-3 channel to Z= 39 N= 52 ( 91Y ): 2.35820E-08
alpha    channel to Z= 39 N= 51 ( 90Y ): 2.98966E+01

Binary emission spectra

 Energy   gamma       neutron     proton      deuteron    triton      helium-3

   0.001 1.14462E-06 1.89788E+00 0.00000E+00 0.00000E+00 0.00000E+00 0.00000E+0
```

```
    0.002 2.28923E-06 3.74165E+00 0.00000E+00 0.00000E+00 0.00000E+00 0.00000E+0
    0.005 5.72311E-06 9.25456E+00 0.00000E+00 0.00000E+00 0.00000E+00 0.00000E+0
    0.010 1.14464E-05 1.84461E+01 0.00000E+00 0.00000E+00 0.00000E+00 0.00000E+0
    0.020 2.28940E-05 3.68901E+01 0.00000E+00 0.00000E+00 0.00000E+00 0.00000E+0
    0.050 5.72550E-05 9.26411E+01 0.00000E+00 0.00000E+00 0.00000E+00 0.00000E+0
    0.100 1.14633E-04 1.86293E+02 0.00000E+00 0.00000E+00 0.00000E+00 0.00000E+0
    0.200 2.30055E-04 3.28686E+02 2.64905E-30 1.35926E-43 0.00000E+00 0.00000E+0
    0.300 7.48114E-04 4.14446E+02 3.56019E-23 9.99027E-34 9.03852E-41 0.00000E+0
    0.400 1.81798E-03 4.97986E+02 5.12047E-19 1.48517E-27 3.14528E-33 0.00000E+0
    0.500 2.88939E-03 5.48371E+02 3.42302E-16 1.47275E-23 2.43692E-28 0.00000E+0
    0.600 3.96241E-03 5.39365E+02 4.07677E-14 1.28871E-20 9.22918E-25 0.00000E+0
    0.700 5.03710E-03 5.29973E+02 1.64259E-12 2.45195E-18 5.46266E-22 0.00000E+0
.....................................
 ++++++++++ CHECK OF INTEGRATED BINARY EMISSION SPECTRA ++++++++++

             Continuum cross section  Integrated spectrum  Compound normalizatio

 gamma             2.19555E+00           2.19555E+00           1.00011E+00
 neutron           1.66025E+03           1.64343E+03           1.01805E+00
 proton            3.43220E+01           3.43220E+01           1.00226E+00
 deuteron          3.51689E+00           3.51689E+00           1.02829E+00
 triton            9.54471E-02           9.54471E-02           1.01145E+00
 helium-3          2.86109E-10           2.86109E-10           0.00000E+00
 alpha             2.86177E+01           2.86176E+01           9.99189E-01
```

Since **outpopulation y**, the population that remains in the first set of residual nuclides after binary emission is printed,

```
 ++++++++++ POPULATION AFTER BINARY EMISSION ++++++++++

 Population of Z= 41 N= 53 ( 94Nb) after binary gamma    emission: 2.23665E+00
 Maximum excitation energy:  21.076 Discrete levels: 10 Continuum bins: 40 Conti

 bin    Ex    Popul.    J= 0.0-   J= 0.0+   J= 1.0-   J= 1.0+   J= 2.0-   J= 2.0

   0   0.000 3.206E-07 0.000E+00 0.000E+00 0.000E+00 0.000E+00 0.000E+00 0.000E+
   1   0.041 1.889E-07 0.000E+00 0.000E+00 0.000E+00 0.000E+00 0.000E+00 0.000E+
   2   0.059 2.525E-07 0.000E+00 0.000E+00 0.000E+00 0.000E+00 0.000E+00 0.000E+
   3   0.079 1.528E-03 0.000E+00 0.000E+00 0.000E+00 0.000E+00 0.000E+00 0.000E+
   4   0.113 3.443E-03 0.000E+00 0.000E+00 0.000E+00 0.000E+00 0.000E+00 0.000E+
   5   0.140 1.051E-02 0.000E+00 0.000E+00 0.000E+00 0.000E+00 1.051E-02 0.000E+
   6   0.302 9.579E-03 0.000E+00 0.000E+00 0.000E+00 0.000E+00 9.579E-03 0.000E+
   7   0.312 1.818E-03 0.000E+00 0.000E+00 0.000E+00 0.000E+00 0.000E+00 0.000E+
   8   0.334 4.717E-03 0.000E+00 0.000E+00 0.000E+00 0.000E+00 0.000E+00 0.000E+
   9   0.396 6.486E-03 0.000E+00 0.000E+00 0.000E+00 0.000E+00 0.000E+00 0.000E+
  10   0.450 3.014E-03 0.000E+00 0.000E+00 0.000E+00 0.000E+00 0.000E+00 0.000E+
  11   0.708 3.665E-02 2.036E-04 1.520E-04 1.592E-03 1.152E-03 3.293E-03 2.540E-
  12   1.224 5.702E-02 2.592E-04 1.935E-04 2.065E-03 1.494E-03 4.428E-03 3.415E-
.....................................
```

where in this case bins 0-10 concern discrete levels and bins 11-50 concern continuum bins.

After this output of the binary emission, we print for each nuclide in the decay chain the population as a function of excitation energy, spin and parity *before* it decays. This loop starts with the initial compound nucleus and the nuclides formed by binary emission. When all excitation energy bins of the nucleus have been depleted, the final production cross section (per ground state/isomer) is printed. The feeding from this nuclide to all its daughter nuclides is also given. If in addition **outspectra y**, the emission spectra for all outgoing particles from this nucleus are printed. At high incident energies, when generally **multipreeq y**, the result from multiple pre-equilibrium emission is printed (not included in this output). If **outcheck y**, it is checked whether the integral over the emission spectra from this nucleus is equal to the corresponding feeding cross section. This output block begins with:

```
 ########## MULTIPLE EMISSION ##########

 Population of Z= 41 N= 53 ( 94Nb) before decay: 3.58813E+00
 Maximum excitation energy:  21.076 Discrete levels: 10 Continuum bins: 40 Conti

 bin    Ex     Popul.    J= 0.0    J= 1.0    J= 2.0    J= 3.0    J= 4.0    J= 5.0

   0   0.000 1.050E-06 0.000E+00 0.000E+00 0.000E+00 0.000E+00 0.000E+00 0.000E+
   1   0.041 6.181E-07 0.000E+00 0.000E+00 0.000E+00 6.181E-07 0.000E+00 0.000E+
   2   0.059 8.266E-07 0.000E+00 0.000E+00 0.000E+00 0.000E+00 8.266E-07 0.000E+
   3   0.079 1.525E-03 0.000E+00 0.000E+00 0.000E+00 0.000E+00 0.000E+00 0.000E+
   4   0.113 3.436E-03 0.000E+00 0.000E+00 0.000E+00 0.000E+00 0.000E+00 3.436E-
   5   0.140 1.049E-02 0.000E+00 0.000E+00 1.049E-02 0.000E+00 0.000E+00 0.000E+
   6   0.302 9.558E-03 0.000E+00 0.000E+00 9.558E-03 0.000E+00 0.000E+00 0.000E+
   7   0.312 1.814E-03 0.000E+00 0.000E+00 0.000E+00 0.000E+00 1.814E-03 0.000E+
   8   0.334 4.706E-03 0.000E+00 0.000E+00 0.000E+00 4.706E-03 0.000E+00 0.000E+
   9   0.396 6.472E-03 0.000E+00 0.000E+00 0.000E+00 6.472E-03 0.000E+00 0.000E+
  10   0.450 3.008E-03 0.000E+00 0.000E+00 0.000E+00 3.008E-03 0.000E+00 0.000E+
  11   0.708 3.657E-02 1.517E-04 1.150E-03 2.536E-03 3.531E-03 3.593E-03 2.702E-
  12   1.224 5.693E-02 1.939E-04 1.497E-03 3.419E-03 5.023E-03 5.489E-03 4.513E-
  13   1.739 6.580E-02 1.843E-04 1.443E-03 3.395E-03 5.210E-03 6.036E-03 5.335E-
  14   2.255 7.347E-02 1.744E-04 1.381E-03 3.323E-03 5.274E-03 6.390E-03 5.973E-
.....................................
 Emitted flux per excitation energy bin of Z= 41 N= 53 ( 94Nb):

 bin    Ex       gamma       neutron      proton      deuteron    triton      heli

   0   0.000 0.00000E+00 0.00000E+00 0.00000E+00 0.00000E+00 0.00000E+00 0.00000
   1   0.041 0.00000E+00 0.00000E+00 0.00000E+00 0.00000E+00 0.00000E+00 0.00000
   2   0.059 2.11853E-01 0.00000E+00 0.00000E+00 0.00000E+00 0.00000E+00 0.00000
   3   0.079 2.12745E-01 0.00000E+00 0.00000E+00 0.00000E+00 0.00000E+00 0.00000
   4   0.113 1.19384E-01 0.00000E+00 0.00000E+00 0.00000E+00 0.00000E+00 0.00000
   5   0.140 2.43882E-01 0.00000E+00 0.00000E+00 0.00000E+00 0.00000E+00 0.00000
   6   0.302 5.42965E-02 0.00000E+00 0.00000E+00 0.00000E+00 0.00000E+00 0.00000
.....................................
 Emission cross sections to residual nuclei from Z= 41 N= 53 ( 94Nb):
```

```
 gamma    channel to Z= 41 N= 53 ( 94Nb): 2.66180E+00
 neutron  channel to Z= 41 N= 52 ( 93Nb): 1.05107E+00
 proton   channel to Z= 40 N= 53 ( 93Zr): 1.67352E-03
 deuteron channel to Z= 40 N= 52 ( 92Zr): 1.07608E-06
 triton   channel to Z= 40 N= 51 ( 91Zr): 2.06095E-08
 helium-3 channel to Z= 39 N= 52 ( 91Y ): 1.07027E-16
 alpha    channel to Z= 39 N= 51 ( 90Y ): 4.69800E-04

 Emission spectra from Z= 41 N= 53 ( 94Nb):

  Energy   gamma       neutron     proton      deuteron    triton      helium-3

    0.001 1.14218E-02 5.11503E-03 0.00000E+00 0.00000E+00 0.00000E+00 0.00000E+0
    0.002 1.19276E-02 1.10501E-02 0.00000E+00 0.00000E+00 0.00000E+00 0.00000E+0
    0.005 1.34434E-02 3.25383E-02 0.00000E+00 0.00000E+00 0.00000E+00 0.00000E+0
    0.010 1.59698E-02 7.24291E-02 0.00000E+00 0.00000E+00 0.00000E+00 0.00000E+0
    0.020 2.10227E-02 1.27402E-01 0.00000E+00 0.00000E+00 0.00000E+00 0.00000E+0
    0.050 4.45166E-02 2.33433E-01 0.00000E+00 0.00000E+00 0.00000E+00 0.00000E+0
.....................................
 ++++++++++ CHECK OF INTEGRATED EMISSION SPECTRA ++++++++++

            Cross section   Integrated spectrum  Average emission energy

 gamma        2.66180E+00     2.66180E+00            1.776
 neutron      1.05107E+00     1.05107E+00            1.174
 proton       1.67352E-03     1.67334E-03            5.377
 deuteron     1.07608E-06     7.97929E-07            5.635
 triton       2.06095E-08     0.00000E+00            0.000
 helium-3     1.07027E-16     0.00000E+00            0.000
 alpha        4.69800E-04     4.69563E-04           10.831

 Final production cross section of Z= 41 N= 53 ( 94Nb):

 Total       : 1.18344E+00
 Ground state: 5.75062E-01
 Level  1    : 6.08379E-01
```

Note that once a new nucleus is encountered in the reaction chain, all nuclear structure information for that nucleus is printed as well.

Case 1i: No output at all

It is even possible to have an empty output file. With the following input file,

```
#
# General
#
projectile n
element nb
```

```
mass 93
energy 14.
#
# Output
#
outmain n
```

it is specified that even the main output should be suppressed. The sample output file should be empty. This can be helpful when TALYS is invoked as a subroutine from other programs and the output from TALYS is not required (if the communication is done e.g. through shared arrays or subroutine variables). We have not yet used this option ourselves.

7.3.2 Sample 2: Excitation functions: ^{208}Pb (n,n'), (n,2n), (n,p) etc.

Often we are not interested in only one incident energy, but in excitation functions of the cross sections. If more than one incident energy is given in the file specified by the **energy** keyword, it is helpful to have the results, for each type of cross section, in a table as a function of incident energy. TALYS will first calculate all quantities that remain equal for all incident energy calculations, such as the transmission coefficients. Next, it will calculate the results for each incident energy. When the calculation for the last incident energy has been completed, the cross sections are collected and printed as excitation functions in the output if **outexcitation y** (which is the default if there is more than one incident energy). Moreover, we can provide the results in separate files: one file per reaction channel. Consider the following input file

```
#
# General
#
projectile n
element pb
mass 208
energy energies
#
# Parameters
#
gnorm 0.35
Rgamma 2.2
gn 81 208 9.4
gp 81 208 6.2
egr     82 209 12.0    E1 1
optmodfileN 82 pb.omp
#
# Output
#
channels y
filechannels y
filetotal y
fileresidual y
outdiscrete y
```

which provides all partial cross sections for neutrons incident on ^{208}Pb for 46 incident energies, from 1 to 30 MeV, as given in the file *energies* that is present in this sample case directory. In the main output file, first the results per incident energy are given. At the end of the output file, there is an output block that begins with:

```
########## EXCITATION FUNCTIONS ###########
```

The first table contains the most important total cross sections as a function of incident energy. This output block begins with:

```
 1. Total (binary) cross sections
```

```
   Energy    Non-elastic  Elastic     Total    Comp. el.  Shape el.  Reaction

  1.000E+00   5.4614E-01 4.8367E+03 4.8372E+03 1.7271E+03 3.1096E+03 1.7276E+03
  1.200E+00   6.0181E-01 4.7812E+03 4.7818E+03 1.8195E+03 2.9618E+03 1.8201E+03
  1.400E+00   6.7627E-01 4.9406E+03 4.9413E+03 1.9485E+03 2.9921E+03 1.9492E+03
  1.600E+00   7.6416E-01 5.2462E+03 5.2469E+03 2.1039E+03 3.1423E+03 2.1046E+03
  1.800E+00   8.6914E-01 5.6345E+03 5.6353E+03 2.2653E+03 3.3692E+03 2.2662E+03
  2.000E+00   1.0015E+00 6.0464E+03 6.0474E+03 2.4110E+03 3.6354E+03 2.4120E+03
.....................................
```

Next, the binary cross sections are printed. This output block begins with:

```
 2. Binary non-elastic cross sections (non-exclusive)

   Energy     gamma      neutron    proton     deuteron   triton     helium-3

  1.000E+00   1.9672E-01 0.0000E+00 0.0000E+00 0.0000E+00 0.0000E+00 0.0000E+00
  1.200E+00   2.4416E-01 0.0000E+00 0.0000E+00 0.0000E+00 0.0000E+00 0.0000E+00
  1.400E+00   3.0773E-01 0.0000E+00 0.0000E+00 0.0000E+00 0.0000E+00 0.0000E+00
  1.600E+00   3.8879E-01 0.0000E+00 0.0000E+00 0.0000E+00 0.0000E+00 0.0000E+00
  1.800E+00   4.9418E-01 0.0000E+00 0.0000E+00 0.0000E+00 0.0000E+00 0.0000E+00
  2.000E+00   6.3274E-01 0.0000E+00 0.0000E+00 0.0000E+00 0.0000E+00 0.0000E+00
.....................................
```

Next, the total particle production cross sections are printed. Parts of this output block look as follows:

```
 3. Total particle production cross sections

 gamma    production

 Energy   Cross section Multiplicity

  1.000E+00 2.47648E-01 1.43346E-04
  1.200E+00 3.14552E-01 1.72825E-04
  1.400E+00 4.06594E-01 2.08595E-04
  1.600E+00 5.23101E-01 2.48546E-04
  1.800E+00 6.76670E-01 2.98596E-04
  2.000E+00 8.80247E-01 3.64945E-04
  2.200E+00 1.14449E+00 4.52788E-04
  2.400E+00 1.48925E+00 5.70753E-04
.....................................
 neutron  production

 Energy   Cross section Multiplicity

  1.000E+00 4.26190E-03 2.46692E-06
  1.200E+00 9.15765E-03 5.03151E-06
  1.400E+00 1.71089E-02 8.77738E-06
```

```
  1.600E+00 3.18516E-02 1.51339E-05
  1.800E+00 5.42068E-02 2.39200E-05
  2.000E+00 8.89349E-02 3.68719E-05
  2.200E+00 1.41778E-01 5.60908E-05
  2.400E+00 2.20738E-01 8.45971E-05
  2.600E+00 3.30648E-01 1.24267E-04
  2.800E+00 3.16809E+02 1.17802E-01
.....................................
```

Next in the output are the residual production cross sections. The output block begins with:

```
 4. Residual production cross sections

 Production of Z= 82 A=209 (209Pb) - Total

 Q-value    =   3.937307
 E-threshold=   0.000000

 Energy   Cross section

  1.000E+00 1.92452E-01
  1.200E+00 2.35002E-01
  1.400E+00 2.90625E-01
  1.600E+00 3.56940E-01
  1.800E+00 4.39971E-01
  2.000E+00 5.43801E-01
  2.200E+00 6.70818E-01
  2.400E+00 8.26660E-01
  2.600E+00 1.02344E+00
.....................................
```

and the remaining isotopes follow in decreasing order of mass and isotope.

The final part of the output, for this input file at least, concerns the exclusive reaction cross sections. This output block begins with:

```
 6. Exclusive cross sections

     Emitted particles     reaction
   n   p   d   t   h   a
   0   0   0   0   0   0       (n,g)

 Q-value    =   3.937307
 E-threshold=   0.000000

 Energy   Cross section Gamma c.s. c.s./res.prod.cs

  1.000E+00 1.92452E-01 3.48872E-01 1.00000E+00
  1.200E+00 2.35002E-01 4.35691E-01 1.00000E+00
  1.400E+00 2.90625E-01 5.54769E-01 1.00000E+00
```

```
  1.600E+00 3.56940E-01 6.97846E-01 1.00000E+00
  1.800E+00 4.39971E-01 8.82793E-01 1.00000E+00
  2.000E+00 5.43801E-01 1.12074E+00 1.00000E+00
...................................
     Emitted particles     reaction
   n   p   d   t   h   a
   1   1   0   0   0   0       (n,np)

 Q-value    =  -8.003758
 E-threshold=   8.042576


 Energy   Cross section Gamma c.s. c.s./res.prod.cs

  1.000E+00 0.00000E+00 0.00000E+00 0.00000E+00
  1.200E+00 0.00000E+00 0.00000E+00 0.00000E+00
  1.400E+00 0.00000E+00 0.00000E+00 0.00000E+00
  1.600E+00 0.00000E+00 0.00000E+00 0.00000E+00
  1.800E+00 0.00000E+00 0.00000E+00 0.00000E+00
  2.000E+00 0.00000E+00 0.00000E+00 0.00000E+00
  2.200E+00 0.00000E+00 0.00000E+00 0.00000E+00
...................................
  2.000E+01 3.12374E+00 2.18877E+00 5.08526E-01
  2.200E+01 8.55243E+00 8.69348E+00 6.06418E-01
  2.400E+01 1.70454E+01 2.30865E+01 6.79074E-01
  2.600E+01 2.70534E+01 4.51648E+01 7.31295E-01
  2.800E+01 3.62134E+01 6.92506E+01 7.66934E-01
  3.000E+01 4.31314E+01 9.02171E+01 7.89711E-01
```

For plotting data, or processing into ENDF-6 data files, it is more practical to have the data in individual output files. Note that, since **filechannels y**, several files with names as e.g. *xs200000.tot* have been created in your working directory. These files contain the entire excitation function per reaction channel. Besides these exclusive cross sections, residual production cross section files are produced (**fileresidual y**). Note that for this reaction, *rp082207.tot* and *xs200000.tot* obviously have equal contents.

We illustrate this sample case with various comparisons with measurements. Since **filetotal y**, a file *total.tot* is created with, among others, the total cross section. The resulting curves are shown in Figs. 7.1 and 7.2.

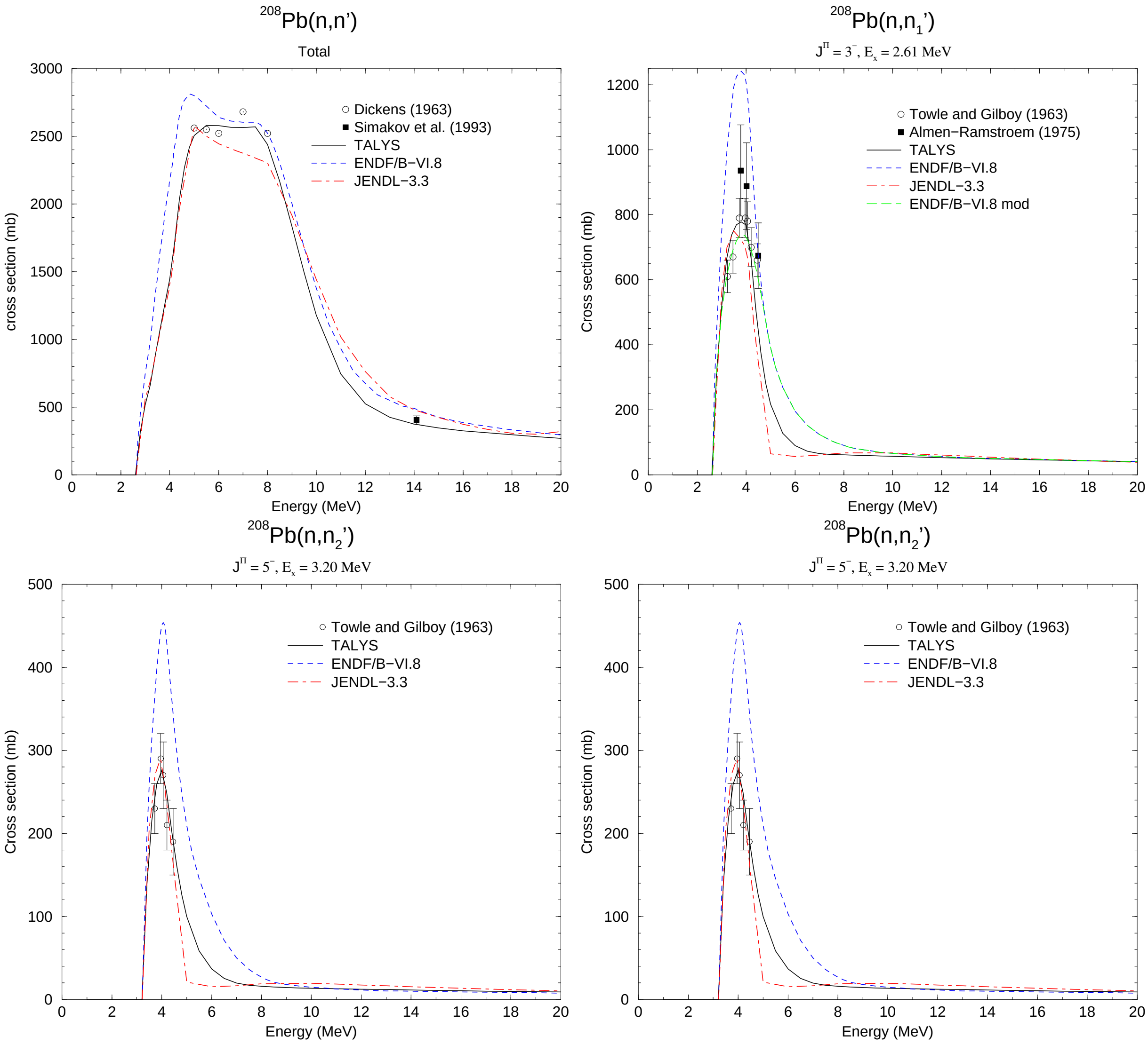

Figure 7.1: Partial cross sections for neutrons incident on ^{208}Pb.

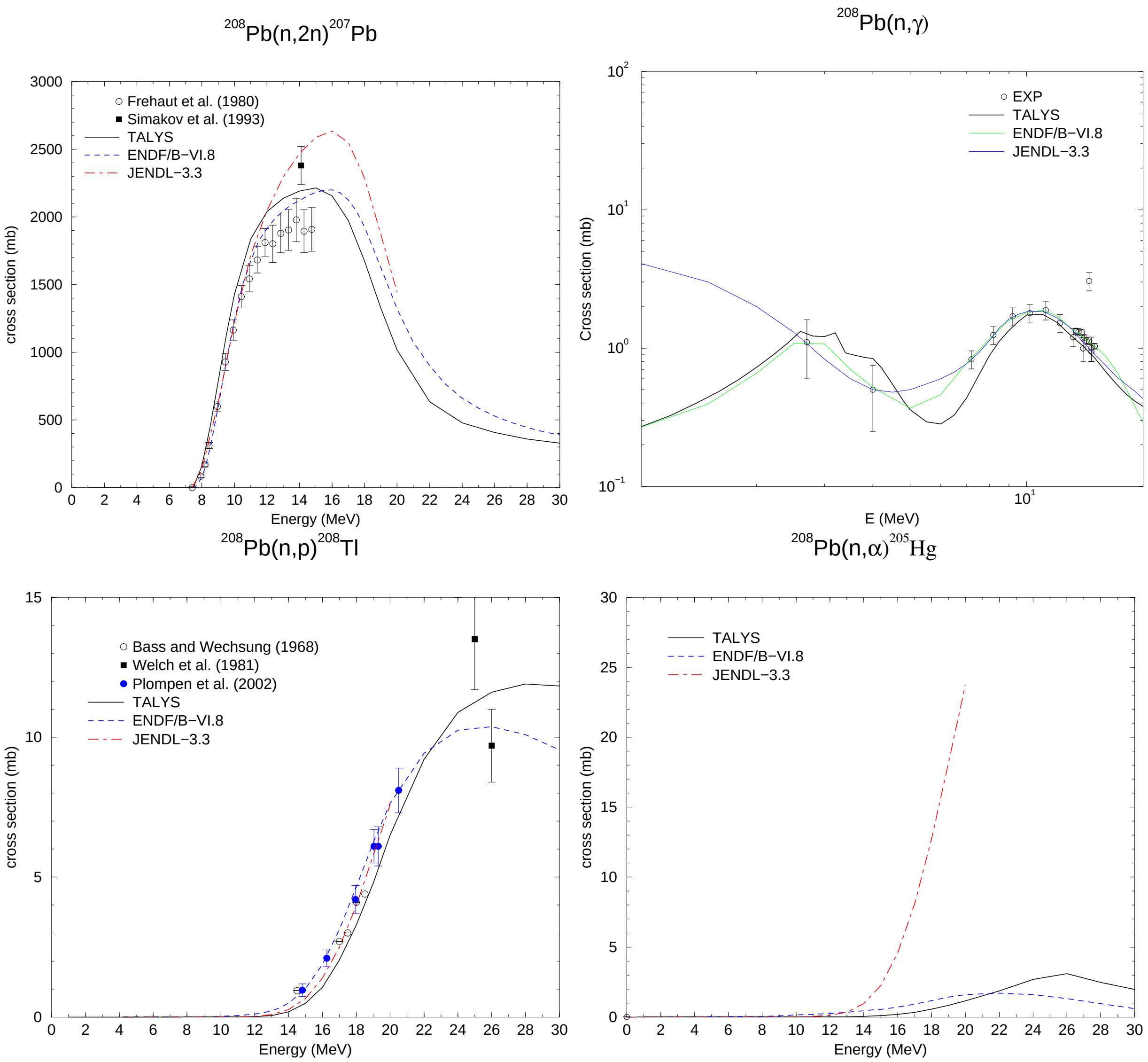

Figure 7.2: Partial cross sections for neutrons incident on ^{208}Pb.

7.3.3 Sample 3: Comparison of compound nucleus WFC models: 10 keV n + ^{93}Nb

In this sample case, we demonstrate the difference between the various models for the width fluctuation correction in compound nucleus reactions, as discussed extensively in Ref. [25]. As sample case, we take 10 keV neutrons incident on ^{93}Nb and we ask for various compound nucleus models to calculate cross sections and angular distributions (**outangle y**), and to put the result for the elastic scattering angular distribution on a separate file, called *nn000.010ang.L00*. Since the GOE calculation (**widthmode 3**) is rather time-consuming, we reduce the number of bins to 20 for all cases. We wish to check whether the flux is conserved in the compound nucleus model for the various WFC models, so we set **outcheck y**. This means that for each set of quantum numbers, unitarity is checked by means of Eq. (4.179).

Case 3a: Hauser-Feshbach model

The following input file is used

```
#
# General
#
projectile n
element nb
mass 93
energy 0.01
#
# Parameters
#
bins 20
widthmode 0
#
# Output
#
outcheck y
outangle y
fileelastic y
```

This only new output block, i.e. not discussed before, is

```
 ++++++++++ CHECK OF FLUX CONSERVATION OF TRANSMISSION COEFFICIENTS ++++++++++
 Hauser-Feshbach model

 Parity=-  J= 3.0  j= 1.5  l= 1  T(j,l)= 7.98822E-03  Sum over outgoing channels
 Parity=-  J= 4.0  j= 0.5  l= 1  T(j,l)= 4.54100E-03  Sum over outgoing channels
 Parity=-  J= 4.0  j= 1.5  l= 1  T(j,l)= 7.98822E-03  Sum over outgoing channels
 Parity=-  J= 5.0  j= 0.5  l= 1  T(j,l)= 4.54100E-03  Sum over outgoing channels
 Parity=-  J= 5.0  j= 1.5  l= 1  T(j,l)= 7.98822E-03  Sum over outgoing channels
 Parity=-  J= 6.0  j= 1.5  l= 1  T(j,l)= 7.98822E-03  Sum over outgoing channels
....................................
```

in which the aforementioned unitarity is checked.

Model	$\sigma^{comp-el}$
Hauser-Feshbach	2410.89 mb
Moldauer	2617.22 mb
HRTW	2752.25 mb
GOE	2617.12 mb

Table 7.2: Compound elastic cross section for 4 different compound nucleus models for 10 keV neutrons incident on ^{93}Nb.

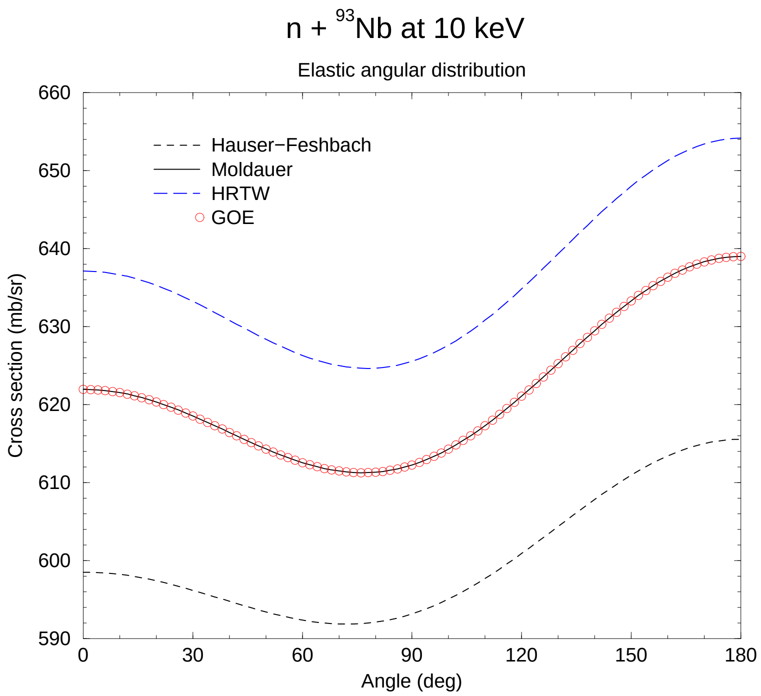

Figure 7.3: Total elastic angular distribution for 4 different compound nucleus models for 10 keV neutrons incident on ^{93}Nb.

Case 3b: Moldauer model

As for case a, but now with **widthmode 1** in the input file.

Case 3c: HRTW model

As for case a, but now with **widthmode 2** in the input file.

Case 3d: GOE model

As for case a, but now with **widthmode 3** in the input file.

Table 7.2 lists the obtained compound nucleus elastic cross section for the 4 cases.

Fig. 7.3 displays the elastic angular distribution for the 4 models. Results like these made us conclude in Ref. [25] that Moldauer's model, which is closest to the exact GOE result, is the one to use in practical applications, especially when considering the calculation times as printed in Table 7.1. Obviously, this sample case can be extended to one with various incident energies, so that the differences between excitation functions can be studied, see also Ref. [25].

7.3.4 Sample 4: Recoils: 20 MeV n + ^{28}Si

In this sample case, we calculate the recoils of the residual nuclides produced by 20 MeV neutrons incident on ^{28}Si reaction. Two methods are compared.

Case 4a: "Exact" approach

In the exact approach, each excitation energy bin of the population of each residual nucleus is described by a full distribution of kinetic recoil energies. The following input file is used

```
#
# General
#
projectile n
element si
mass 28
energy 20.
#
# Parameters
#
m2constant 0.70
sysreaction p d t h a
spherical y
#
# Output
#
recoil y
filerecoil y
```

For increasing incident energies, this calculation becomes quickly time-expensive. The recoil calculation yields separate files with the recoil spectrum per residual nucleus, starting with *rec*, followed by the Z, A and incident energy, e.g. *rec012024spec020.000.tot*. Also following additional output block is printed:

```
 8. Recoil spectra

 Recoil Spectrum for  29Si

  Energy   Cross section

   0.018 0.00000E+00
   0.053 0.00000E+00
   0.088 0.00000E+00
....................................
   0.676 3.21368E+00
   0.720 3.22112E+00
   0.763 3.21215E+00
   0.807 3.10619E+00
   0.851 2.60156E+00
   0.894 2.30919E-01
```

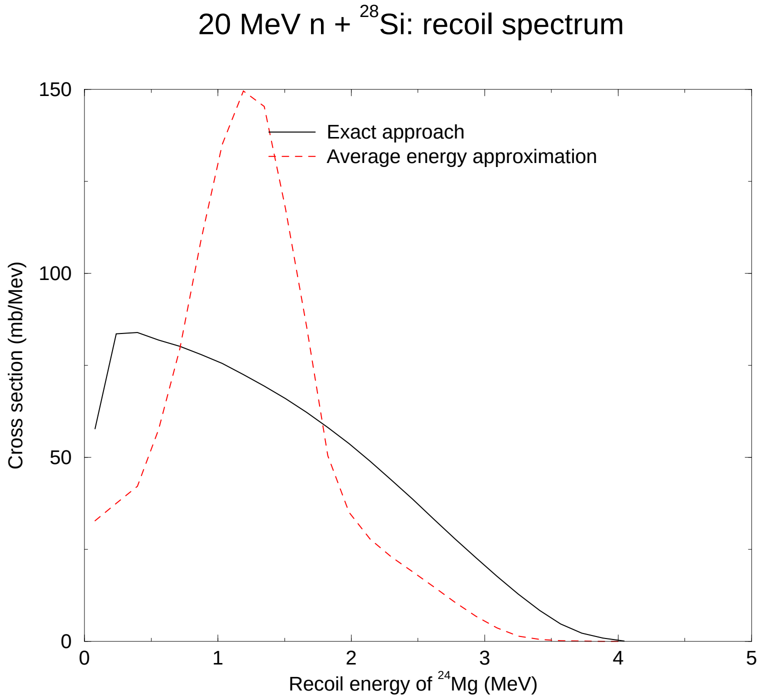

Figure 7.4: Recoil energy distribution of ^{24}Mg for 20 MeV n + ^{28}Si according to the exact and approximative approach.

```
Integrated recoil spectrum       :  1.04358E+00
Residual production cross section:  9.71110E-01
```

Case 4b: Approximative approach

As an approximation, each excitation energy bin of the population of each residual nucleus is described by a an average kinetic recoil energy. For this, we add one line to the input file above,

```
recoilaverage y
```

The results, together with those of case (a), are compared in Fig. 7.4.

7.3.5 Sample 5: Fission cross sections: n + ^{241}Am

Due to time constraints, we have not been able to include a sample case for fission for TALYS-1.0. This requires a new fit of the total fission cross section (as the level density and fission description has been improved since the previous release) and this has not been accomplished for the present release. Again this shows that a systematic approach for fission is still lacking. Hence, **the results given below for this sample case are not reproduced by the actual calculation as stored in the sample case directory**, but we include it to give an idea of the complexity of an input file for fission. It is possible to obtain very satisfactory fits to fission data with TALYS, but at the expense of using many adjustable input parameters. At the time of this writing, we are performing extensive model calculations to bring somewhat more structure in the collection of fitting parameters. In the meantime, we include a sample case for the description of the fission cross section. As sample case for TALYS validation, we only run the case up to 3 MeV. However, you are invited to enter directory *5/org/high/* where we have stored our input files for a calculation up to 30 MeV. You may want to perform that calculation, but we warn you that such a calculation, due to the coupling scheme of 4 rotational and one vibrational level, may take several hours. The plots in this section are from that calculation. In general, for long calculations involving OMP coupling schemes, we strongly suggest to do a first run with the input file like the one given below, and if one wants to adjust non-OMP related parameters in the next run, to put **eciscalc y** and **inccalc y**. We use the following input file,

```
#
# General
#
projectile n
element am
mass 241
energy energies
#
# Models and output
#
channels y
filechannels y
ecissave y
eciscalc y
inccalc y
fileresidual y
outdiscrete y
filediscrete 1
filediscrete 2
filediscrete 3
filediscrete 4
filediscrete 5
filediscrete 6
filediscrete 7
filediscrete 8
outgamdis y
filegamdis y
filefission y
fismodel 1
fismodelalt 3
```

```
ldmodel 1
spincutmodel 1
maxband 1
maxrot 4
optmod 95 241 omp241am.neu n
#
# Parameters
#
m2constant             0.94259
# 242Am
a         95 242      19.54423
fisbar    95 242       6.76515  1
fishw     95 242       0.71169  1
fisbar    95 242       5.53502  2
fishw     95 242       0.50403  2
pshift    95 242       0.27568  0
pshift    95 242       0.18933  1
pshift    95 242       0.80609  2
deltaW    95 242       1.94748  0
deltaW    95 242       2.45131  1
deltaW    95 242       2.41161  2
# 241Am
a         95 241      19.12652
fisbar    95 241       5.43611  1
fishw     95 241       0.61974  1
fisbar    95 241       4.80241  2
fishw     95 241       0.64878  2
pshift    95 241       0.04567  0
pshift    95 241      -0.36236  1
pshift    95 241      -0.08312  2
deltaW    95 241       1.40262  0
deltaW    95 241      -0.49979  1
deltaW    95 241       3.04138  2
# 240Am
a         95 240      19.29563
fisbar    95 240       5.43115  1
fishw     95 240       0.96134  1
fisbar    95 240       5.14247  2
fishw     95 240       0.63210  2
pshift    95 240      -0.31820  0
pshift    95 240       0.19744  1
pshift    95 240      -0.02710  2
deltaW    95 240       3.95835  0
deltaW    95 240      -0.47697  1
deltaW    95 240      -1.99853  2
# 239Am
a         95 239      17.
fisbar    95 239       4.50  1
```

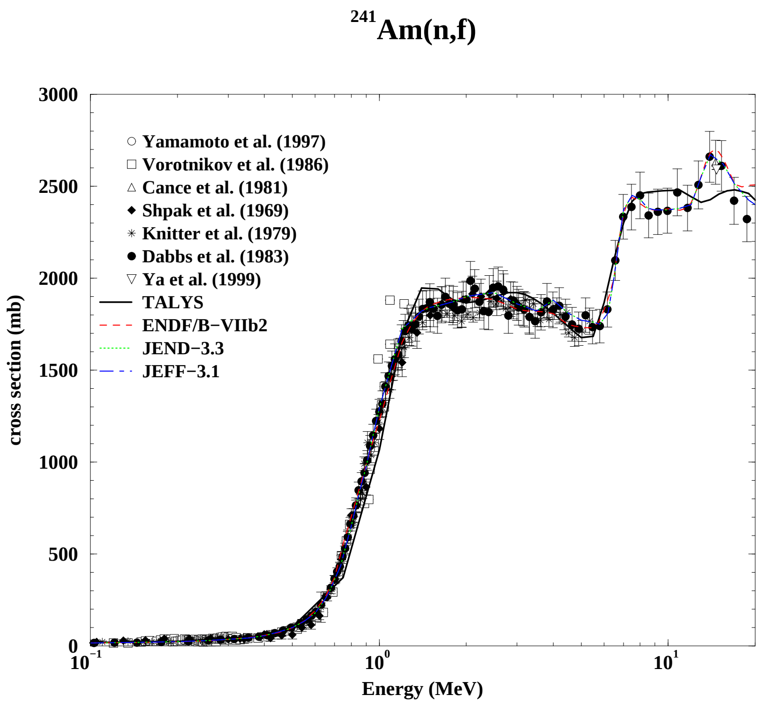

Figure 7.5: Neutron induced fission cross section of ^{241}Am compared with experimental data and some major nuclear data libraries.

```
fishw     95 239         0.80  1
fisbar    95 239         4.10  2
fishw     95 239         0.63  2
# 238Am
a         95 238        19.
fisbar    95 238         4.50  1
fishw     95 238         0.80  1
fisbar    95 238         4.10  2
fishw     95 238         0.63  2
```

which has been obtained from an automated fitting procedure. The optical model file *omp241am.neu* contains the parameters of a recent deformed OMP by Pascal Romain. The keyword **filefission y** ensures that the total fission cross section appear in the file *fission.tot*, and this is plotted together with experimental data in Fig. 7.5.

Due to the presence of **outfission y** in the input file, all nuclear structure related to the fission process is given in the output for the target and the compound nucleus

```
 Fission information for Z= 95 N=146 (241Am)

 Number of fission barriers           :  2

 Parameters for fission barrier  1

 Type of axiality                     :  2 (tri-axial)
```

```
 Height of fission barrier 1          :   5.436
 Width of fission barrier 1           :   0.620
 Rtransmom                            :   0.600
 Moment of inertia                    :  93.398
 Number of head band transition states:  4
 Start of continuum energy            :   0.180

 Head band transition states

  no.    E    spin    parity

    1   0.000   1.5   -
    2   0.140   2.5   +
    3   0.180   3.5   -
    4   0.180   2.5   -

 Rotational bands

  no.    E    spin    parity

    1   0.000   1.5   -
    2   0.027   2.5   -
    3   0.064   3.5   -
    4   0.112   4.5   -
    5   0.140   2.5   +
    6   0.171   5.5   -
    7   0.177   3.5   +
    8   0.180   3.5   -
    9   0.180   2.5   -

 Parameters for fission barrier  2

 Type of axiality                     :  1 (axial)
 Height of fission barrier 2          :   4.802
 Width of fission barrier 2           :   0.649
 Rtransmom                            :   1.000
 Moment of inertia                    : 164.311
 Number of head band transition states:  8
 Start of continuum energy            :   0.050
.............
```

Moreover, the corresponding fission transmission coefficients are printed for all excitation energies encountered in the calculation

```
 Fission transmission coefficients for Z= 95 N=147 (242Am) and an excitation ene

   J      T(J,-)      T(J,+)

  0.0   4.44954E-04 4.44954E-04
  1.0   1.26309E-03 1.19865E-03
```

```
  2.0   1.67128E-03 1.61140E-03
  3.0   1.70432E-03 1.63567E-03
  4.0   0.00000E+00 0.00000E+00
  5.0   0.00000E+00 0.00000E+00
  6.0   0.00000E+00 0.00000E+00
  7.0   0.00000E+00 0.00000E+00
  8.0   0.00000E+00 0.00000E+00
  9.0   0.00000E+00 0.00000E+00
 10.0   0.00000E+00 0.00000E+00
 11.0   0.00000E+00 0.00000E+00
 12.0   0.00000E+00 0.00000E+00
.............
```

The fission information for all residual nuclides can be obtained in the output file as well by adding *outpopulation y* to the input file.

7.3.6 Sample 6: Continuum spectra at 63 MeV for Bi(n,xp)...Bi(n,xα)

In this sample case, we calculate angle-integrated and double-differential particle spectra for 63 MeV neutrons on ^{209}Bi, see Ref. [43].

Case 6a: Default calculation

The following input file is used

```
#
# General
#
projectile n
element bi
mass 209
energy 63.
#
# Output
#
ddxmode 2
filespectrum n p d t h a
fileddxa p 20.
fileddxa p 70.
fileddxa p 110.
fileddxa d 20.
fileddxa d 70.
fileddxa d 110.
fileddxa t 20.
fileddxa t 70.
fileddxa t 110.
fileddxa h 20.
fileddxa h 70.
fileddxa h 110.
fileddxa a 20.
fileddxa a 70.
fileddxa a 110.
```

Note that we request that angle-integrated spectra for all particles are written on separate files through *filespectrum n p d t h a*. At 20, 70 and 110 degrees, we also ask for the double-differential spectrum for protons up to alpha-particles. The resulting files *pspec063.000.tot*, *pddx020.0.deg*, etc. are presented, together with experimental data, in Figs. 7.6 and 7.7.

Case 6b: Adjusted matrix element

The default results of case (a) for the proton spectra are a bit high. Therefore, as a second version of this sample case, we adjust a pre-equilibrium parameter and add the following to the input above:

```
#
```

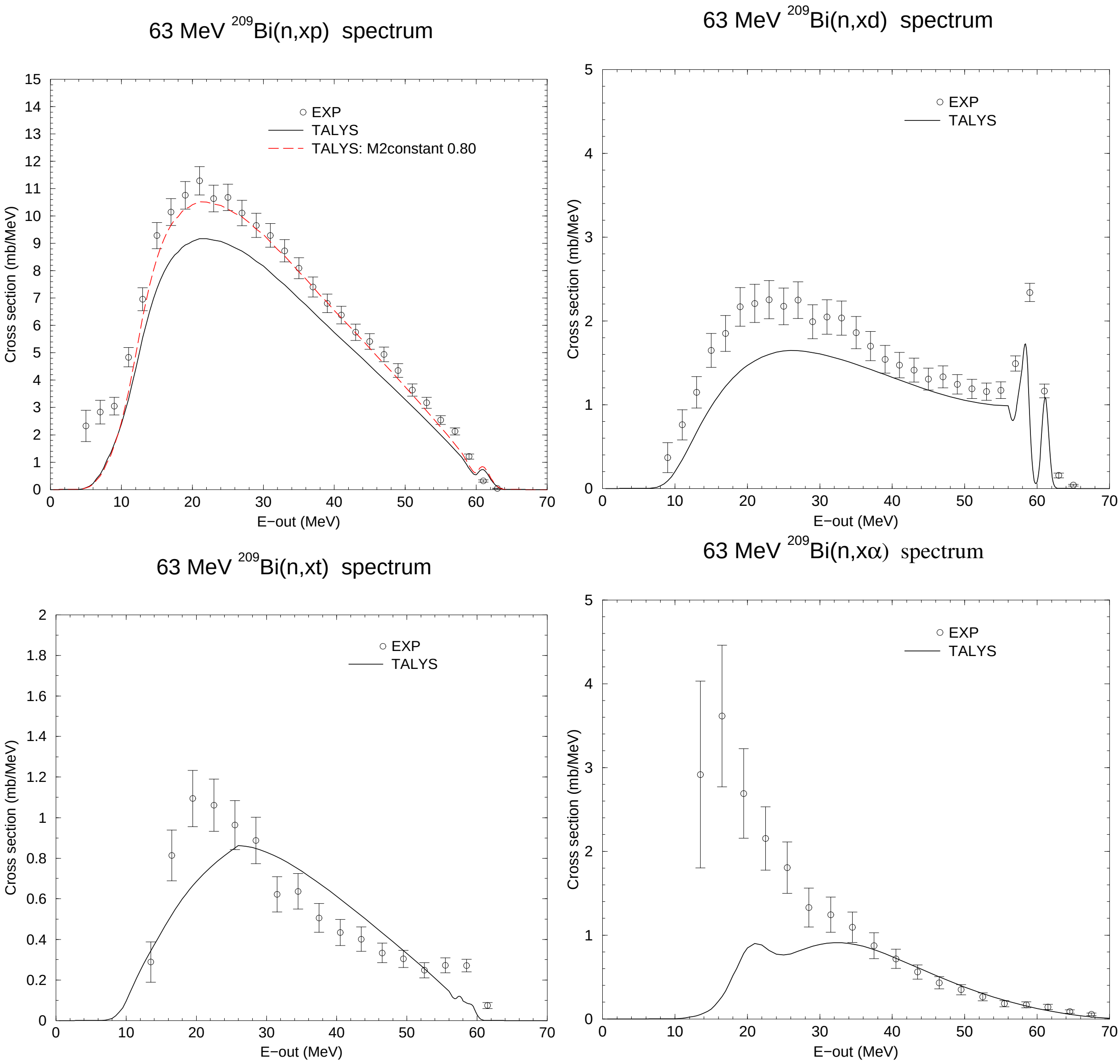

Figure 7.6: Angle-integrated proton, deuteron, triton and alpha emission spectra for 63 MeV neutrons on ^{209}Bi. The experimental data are from [43].

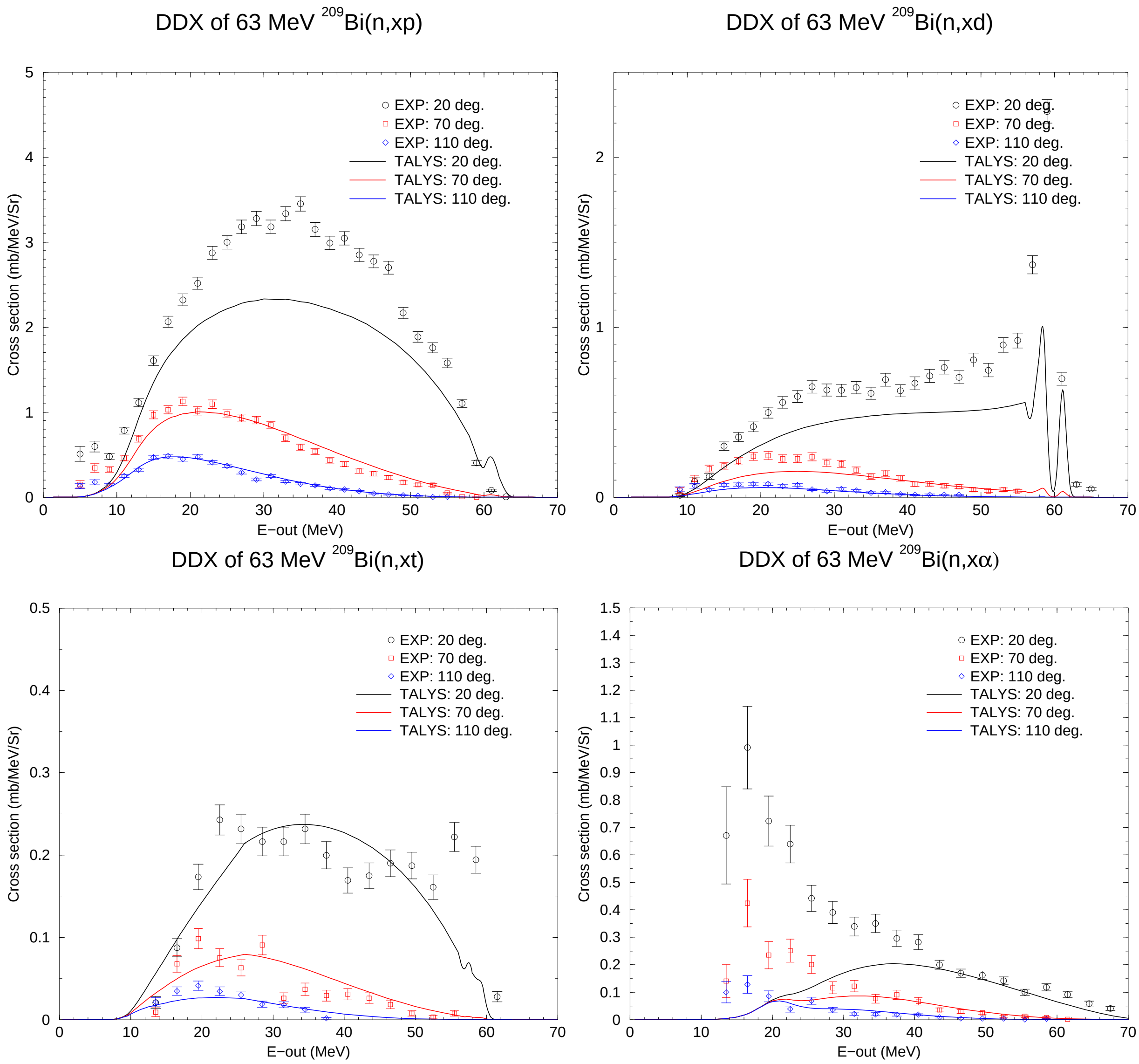

Figure 7.7: Double-differential proton, deuteron, triton and alpha emission spectra for 63 MeV neutrons on ^{209}Bi. The experimental data are from [43].

```
# Parameters
#
M2constant 0.80
```

By decreasing **M2constant** by 20% (which is a common and acceptable deviation from the average), we favor the pre-equilibrium emission rate over the rate rate, leading to a harder spectrum. The result is shown in Fig. 7.6 for the proton spectrum.

7.3.7 Sample 7: Pre-equilibrium angular dist. and multiple pre-equilibrium emission

At high incident energies, multiple pre-equilibrium reactions play a significant role. In this sample case, we show the results for this mechanism in the output file. Also, as an alternative to the previous sample case, we present another way of producing double-differential cross sections, namely as a function of angle at a fixed outgoing energy. With the following input file, the reaction of 120 MeV protons incident on ^{90}Zr is simulated:

```
#
# General
#
projectile p
element zr
mass 90
energy 120.
#
# Output
#
outpopulation y
ddxmode 1
filespectrum n p
fileddxe p 20.
fileddxe p 40.
fileddxe p 60.
fileddxe p 80.
fileddxe p 100.
```

The results are presented in Figs. 7.8 and 7.9. For this sample case, since **outpopulation y**, after each print of the population for each residual nucleus (as already described in the first sample case), a block with multiple pre-equilibrium decay information is printed. This output block begins with

```
 Multiple preequilibrium emission from Z= 41 N= 49 ( 90Nb):

                                                                          Feeding terms from

 bin    Ex  Mpe ratio  neutron   proton   1 1 0 0   0 0 1 1   1 0 0 1   0 1 1 0
                      emission  emission

  11   2.208 0.00000 0.000E+00 0.000E+00 0.000E+00 0.000E+00 5.287E-01 0.000E+00
  12   4.980 0.00000 0.000E+00 0.000E+00 0.000E+00 0.000E+00 1.249E+00 0.000E+00
  13   7.752 0.00000 0.000E+00 0.000E+00 0.000E+00 0.000E+00 1.961E+00 0.000E+00
  14  10.524 0.00001 0.000E+00 4.343E-05 0.000E+00 0.000E+00 2.645E+00 0.000E+00
  15  13.296 0.00555 3.214E-04 1.999E-02 0.000E+00 0.000E+00 3.300E+00 0.000E+00
  16  16.067 0.04999 5.901E-03 2.049E-01 0.000E+00 0.000E+00 3.928E+00 0.000E+00
  17  18.839 0.10870 2.305E-02 5.024E-01 0.000E+00 0.000E+00 4.527E+00 0.000E+00
  18  21.611 0.17335 5.014E-02 8.952E-01 0.000E+00 0.000E+00 5.098E+00 0.000E+00
.....................................
```

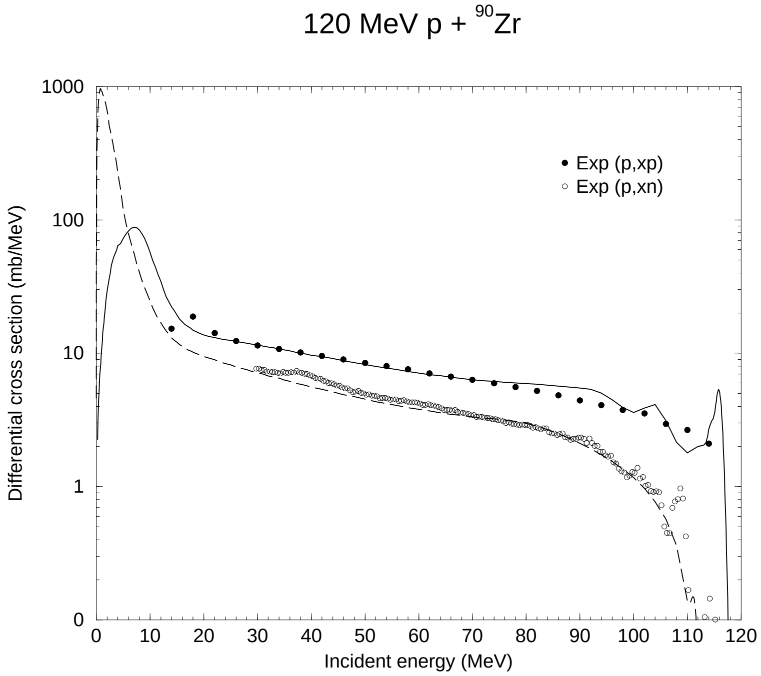

Figure 7.8: Angle-integrated (p,xn) and (p,xp) spectra for 120 MeV protons on ^{90}Zr. Experimental data are taken from [159, 160]

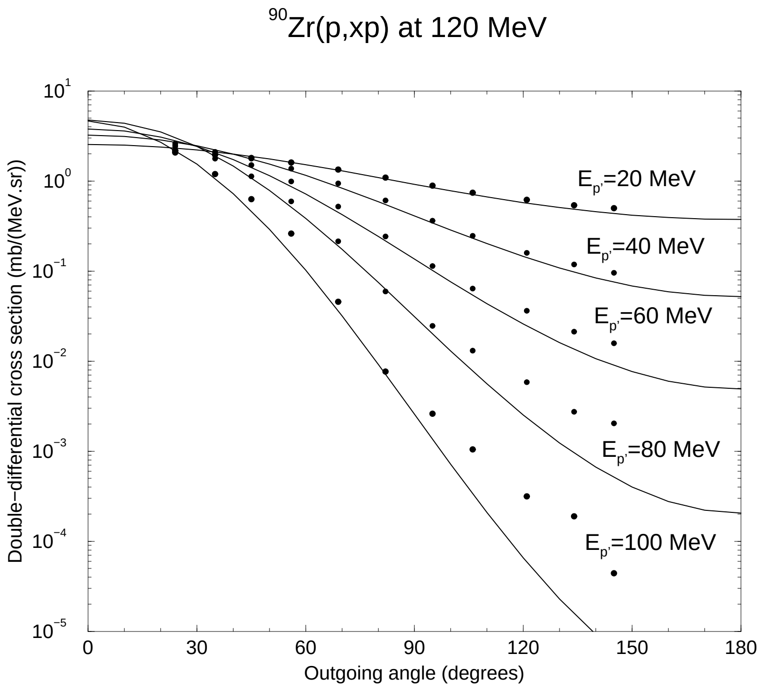

Figure 7.9: Double-differential (p,xp) spectra for 120 MeV protons on ^{90}Zr. Experimental data are taken from [159]

For each continuum bin, with excitation energy E_x, we print the fraction of the population that is emitted as multiple pre-equilibrium. Also the total neutron and proton emission per residual nucleus is printed, as well as the feeding terms from previous particle-hole configurations. With this input file, files *nspec120.000.tot* and *pspec120.000.tot* are created through the *filespectrum n p* keyword. The results are displayed in Fig. 7.8. Also, the combination of **ddxmode 1** and the various **fileddxe** keywords generate the *pddx100.0.mev*, etc. files that are compared with experimental data in Fig. 7.9.

7.3.8 Sample 8: Residual production cross sections: p + ^{nat}Fe up to 100 MeV

In this sample case, we calculate the residual production cross sections for protons on ^{nat}Fe for incident energies up to 100 MeV. A calculation for a natural target is launched, meaning that successive TALYS calculations for each isotope are performed, after which the results are weighted with the natural abundance. We restrict ourselves to a calculation with all nuclear model parameters set to their default values. The following input file is used:

```
#
# General
#
projectile p
element fe
mass 0
energy energies
#
# Output
#
fileresidual        y
```

The file *energies* contains 34 incident energies between 1 and 100 MeV. Obviously, this sample case can be extended to more incident energies, e.g. up to 200 MeV, by simply adding numbers to the *energies* file. In that case, we recommend to include more energy bins in the calculation, (e.g. **bins 80**) to avoid numerical fluctuations, although this will inevitably take more computer time. Note that we have enabled the **fileresidual** keyword, so that a separate cross sections file for each final product is produced. The results from the files *rp027056.tot*, *rp027055.tot*, *rp025054.tot* and *rp025052.tot* are presented, together with experimental data, in Fig. 7.10.

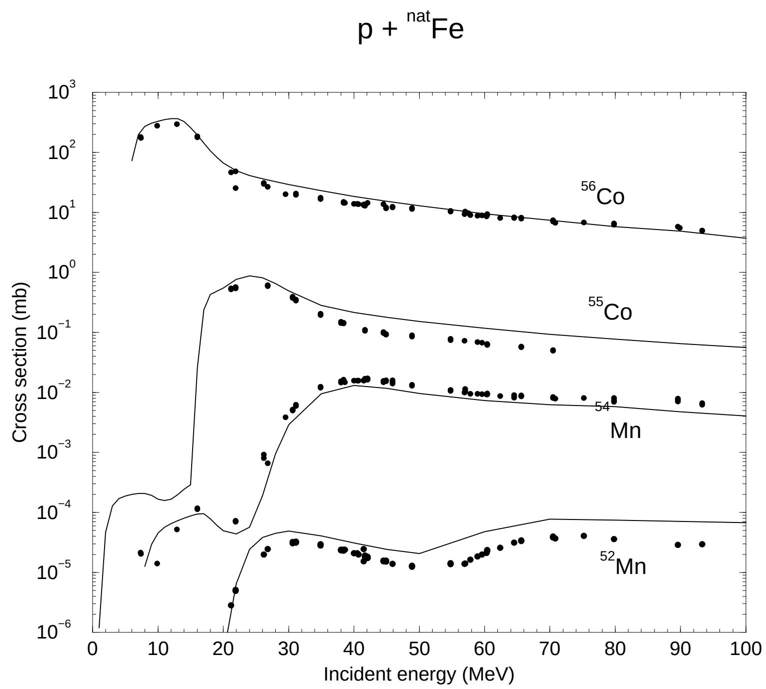

Figure 7.10: Residual production cross sections for protons incident on ^{nat}Fe. Experimental data are obtained from [161].

7.3.9 Sample 9: Spherical optical model and DWBA: n + ^{208}Pb

Three types of optical model calculations are included in the set of sample cases. In this first one, we treat ^{208}Pb as a spherical nucleus and request calculations for the elastic angular distributions and inelastic angular distributions at a few incident energies. This is accomplished with the input file

```
#
# General
#
projectile n
element pb
mass 208
energy energies
#
# Avoid unnecessary calculations and output
#
ejectiles n
preequilibrium n
compound n
maxZ 0
maxN 0
bins 5
fileresidual n
filetotal n
#
```

```
# Output
#
outangle y
fileelastic y
fileangle 1
fileangle 2
```

where the file *energies* consists of the energies 11., 13.7, 20., 22., and 25.7 MeV (for which experimental data exists). The keyword *fileelastic y* has created the files *nn011.000ang.L00*, etc. which contain the elastic scattering angular distribution and are compared with experimental data in Fig. 7.11. With **fileangle 1** and **fileangle 2** we have created the files *nn010.000ang.L01*, etc. with the inelastic scattering angular distribution to the first and second discrete state. These are also plotted in Figs. 7.11. Note that the keywords in the middle block (**ejectiles n** up to **filetotal n**) have been added to avoid a full calculation of all the cross sections. For the present sample case we assume that only elastic scattering and DWBA angular distributions are of interest, so we economize on output options, number of bins, ejectiles and nuclides that can be reached. Obviously, for reliable results for all observables this middle block would have to be deleted. See also sample case (1f) for obtaining more specific information from the output.

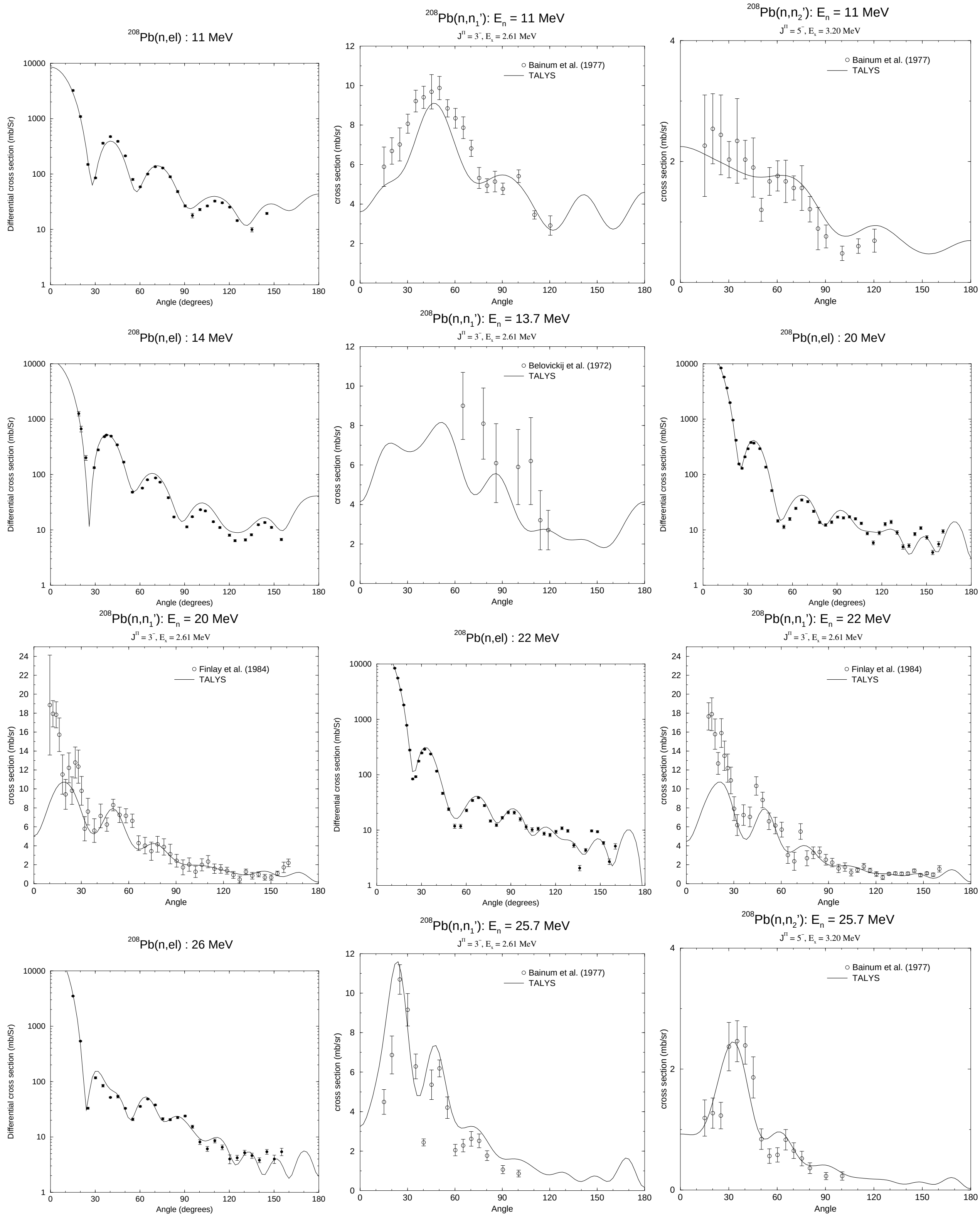

Figure 7.11: Elastic and inelastic scattering angular distributions between 11 and 26 MeV for ^{208}Pb.

7.3.10 Sample 10: Coupled-channels rotational model: n + ^{28}Si

In this sample case, we consider spherical OMP and rotational coupled-channels calculations for the deformed nucleus ^{28}Si.

Case 10a: Spherical optical model

In the first case, we treat ^{28}Si as a spherical nucleus and include the first (2^+), second (4^+) and sixth (3^-) level as weakly coupled levels, i.e. the cross sections are calculated with DWBA. The input file is

```
#
# General
#
projectile n
element si
mass 28
energy energies
#
# Parameters
#
spherical y
#
# Output
#
channels y
filechannels y
```

For the default calculation, TALYS will look in the *deformation/exp* database to see whether a coupling scheme is given. Since this is the case for ^{28}Si, we have to put **spherical y** to enforce a spherical calculation.

Case 10b: Symmetric rotational model

In the second case, we include the first and second level of the ground state rotational band and the 3^- state in the coupling scheme. This is accomplished with the input file

```
#
# General
#
projectile n
element si
mass 28
energy energies
#
# Output
#
channels y
filechannels y
```

In Fig. 7.12, the calculated total inelastic scattering for cases a and b are plotted.

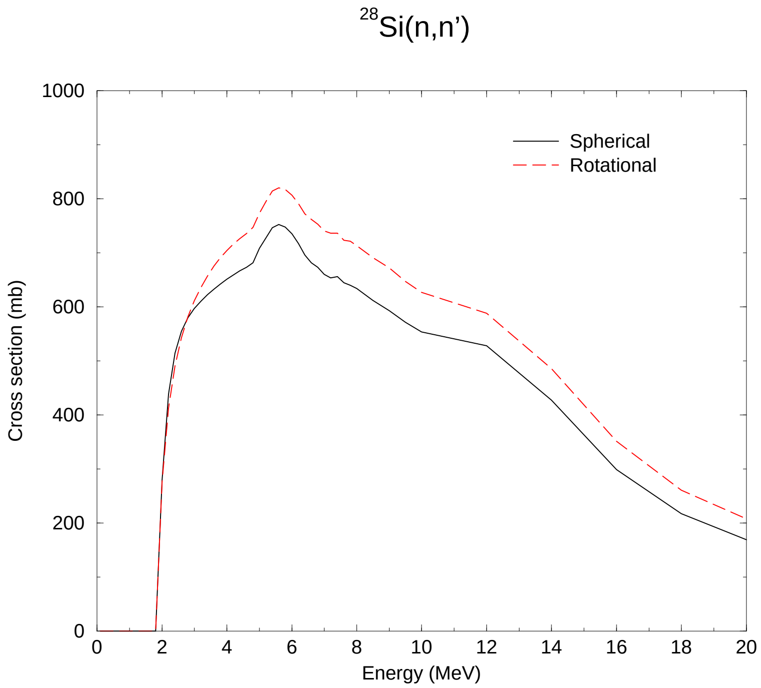

Figure 7.12: Total inelastic neutron scattering off ^{28}Si for a spherical and a deformed OMP.

7.3.11 Sample 11: Coupled-channels vibrational model: n + ^{74}Ge

In this sample case we consider a neutron-induced reaction on the vibrational nucleus ^{74}Ge which consists of a one-phonon state (2^+) followed by a $(0^+, 2^+, 4^+)$ triplet of two-phonon states, and a 3^- phonon state. The coupling scheme as stored in *structure/deformation/exp/z032* is automatically adopted. The following input file is used:

```
#
# General
#
projectile n
element ge
mass 74
energy energies
#
# Output
#
outexcitation n
outdiscrete y
filediscrete 1
```

In Fig. 7.13, the calculated inelastic scattering to the first discrete state is plotted.

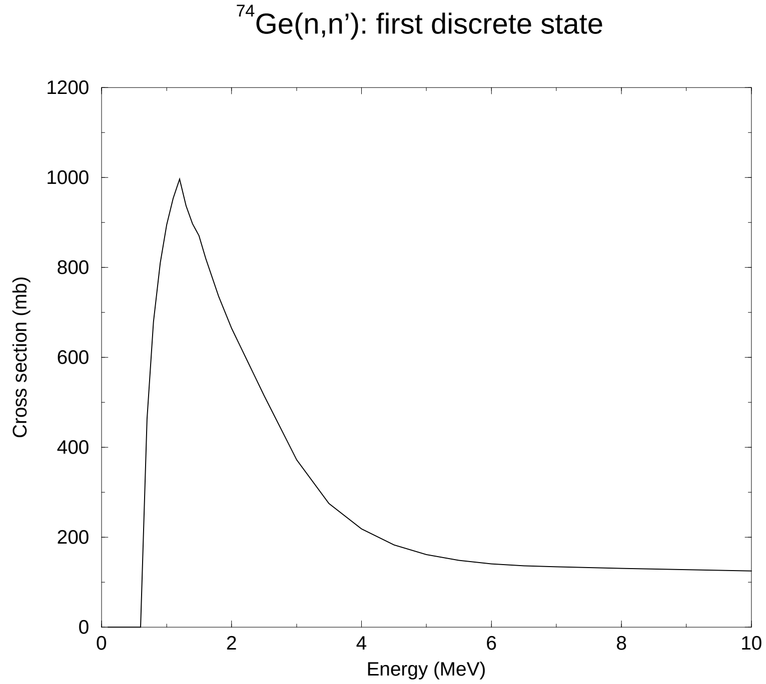

Figure 7.13: Inelastic scattering to the first discrete state of ^{74}Ge.

7.3.12 Sample 12: Inelastic spectra at 20 MeV: Direct + Preeq + GR + Compound

For pre-equilibrium studies, it may be worthwhile to distinguish between the various components of the emission spectrum. This was already mentioned in sample case (1c). As an extra sample case, we compare the calculated ^{209}Bi(n,xn) spectrum at 20 MeV with experimental data. This is accomplished with the following input file,

```
#
# General
#
projectile n
element bi
mass 209
energy 20.
#
# Parameters
#
ddxmode 2
filespectrum n
```

The various components of the spectrum, and the total, as present in the file *nspec020.000.tot*, are plotted in Fig. 7.14.

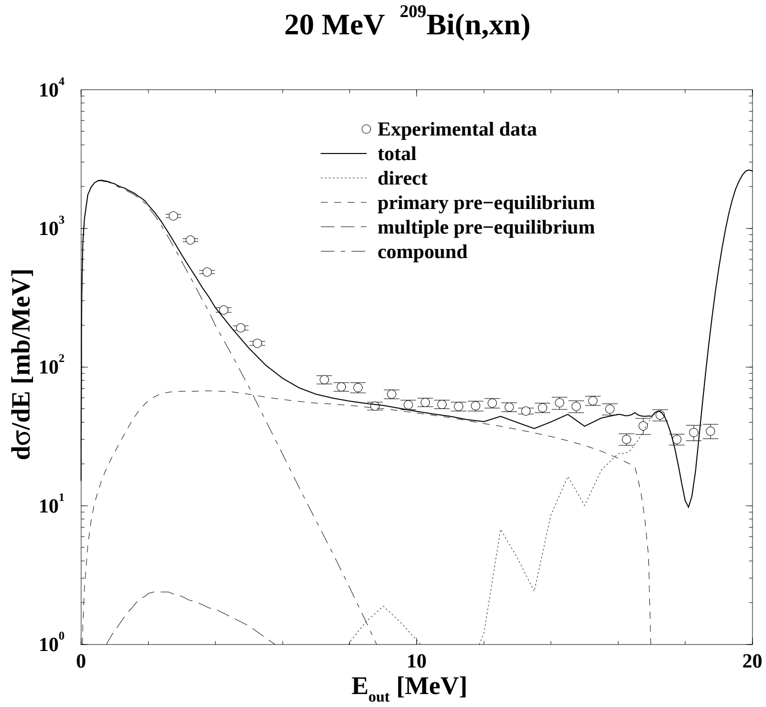

Figure 7.14: ^{209}Bi (n,xn) spectrum at 20 MeV. Experimental data are obtained from [163].

7.3.13 Sample 13: Gamma-ray intensities: ^{208}Pb$(n, n\gamma)$ and ^{208}Pb$(n, 2n\gamma)$

This feature could simply have been included in the sample case on excitation functions for ^{208}Pb, but in order not to overburden the description of that sample case we include it here. With the input file

```
#
# General
#
projectile n
element pb
mass 208
energy energies
#
# Parameters
#
isomer 1.e-4
maxZ 0
gnorm 0.35
Rgamma 2.2
egr     82 209 12.0    E1 1
optmodfileN 82 pb.omp
#
# Output
#
channels y
```

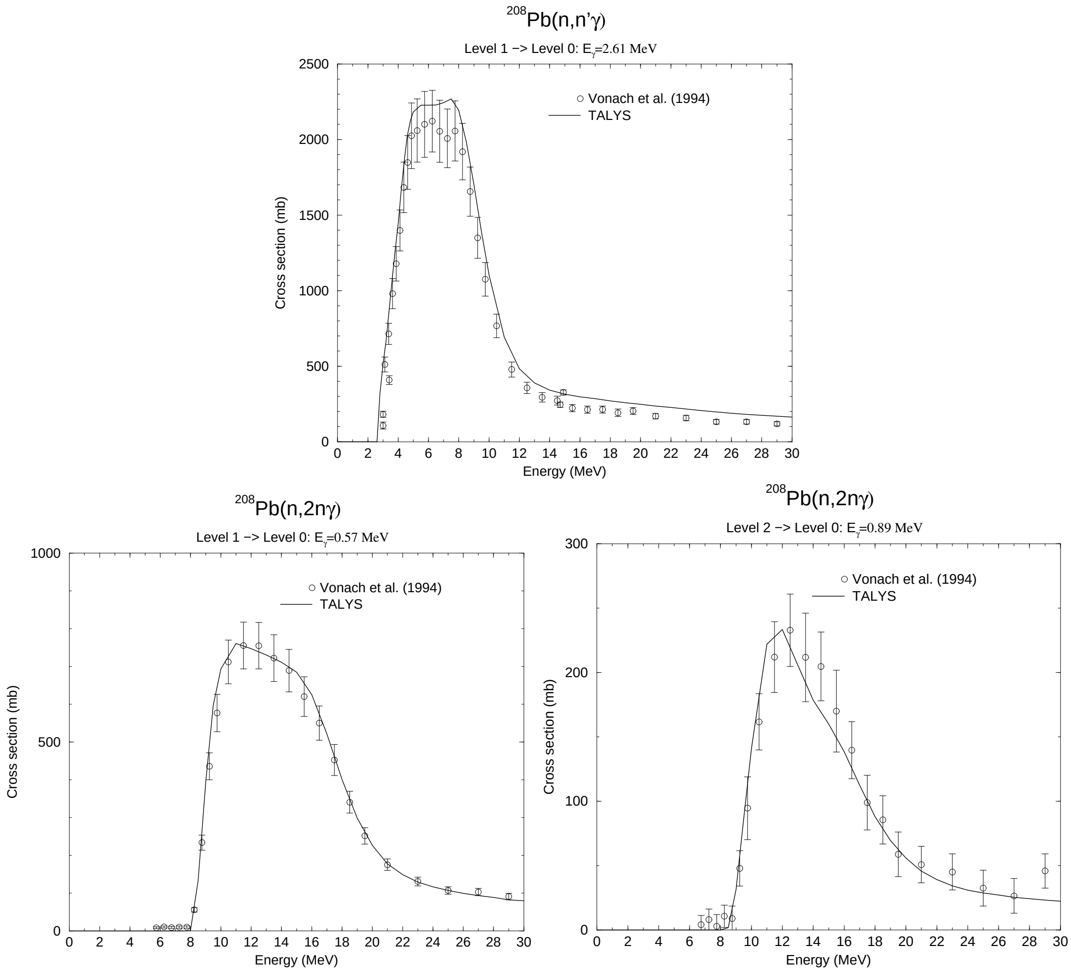

Figure 7.15: Gamma-ray production lines for a few transitions in ^{208}Pb(n,n') and ^{208}Pb(n,2n) reactions. The experimental data are from [164].

```
filechannels y
fileresidual y
outgamdis y
```

all discrete gamma lines are printed and stored in separate files. To avoid the production of too many data files, we have put **maxZ 0** so that only the gamma-ray production files for Pb-chain are created. Also, we include a special OMP with the file *pb.omp* and we set **isomer 1.e-4** to allow for gamma decay of some rather short-lived levels. Experimental data exists for the $^{208}\text{Pb}(n, n'\gamma)$ cross section for level 1 to level 0 and the $^{208}\text{Pb}(n, 2n'\gamma)$ cross section for level 2 to level 0 and for level 1 to level 0. These data have been plotted together with the results of the calculated files *gam082208L01L00.tot*, *gam082207L02L00.tot* and *gam082207L01L00.tot*, in Fig. 7.15.

7.3.14 Sample 14: Fission yields for ^{238}U

Due to time constraints, we have not been able to include a sample case for ^{238}U fission yields for TALYS-1.0. This requires a new fit of the total fission cross section (as the level density and fission description has been improved since the previous release) and this has not been accomplished for the present release. To compute the fission fragment/product mass/isotope yields it is required to obtain a good description of the fission cross section as e.g. in Sample 5. Next the following two keywords can be added to the input file:

```
massdis y
ffevaporation y
```

For completeness, we show the results for ^{238}U we obtained with TALYS-0.64 for incident energies of 1, 1.6, 3.5, 5.5, 7.5 and 10 MeV. The TALYS results for the pre-neutron emission mass yields can be found in *yield001.600.fis* and *yield005.500.fis* and are given in the upper plot of Fig. 7.16. The two other plots show a comparison of the normalized yields with experimental data [154].

Since we have added the keyword *ffevaporation y* to the input, we have also calculated the fission product isotope yields. Fig. 7.17 contains the result for the production of the fission products ^{115}Cd and ^{140}Ba. The left plot shows the cumulative yield (obtained after adding the calculated independent yields of all beta-decay precursors). The normalized cumulative yields are compared to experimental data [155, 156] in the other two plots.

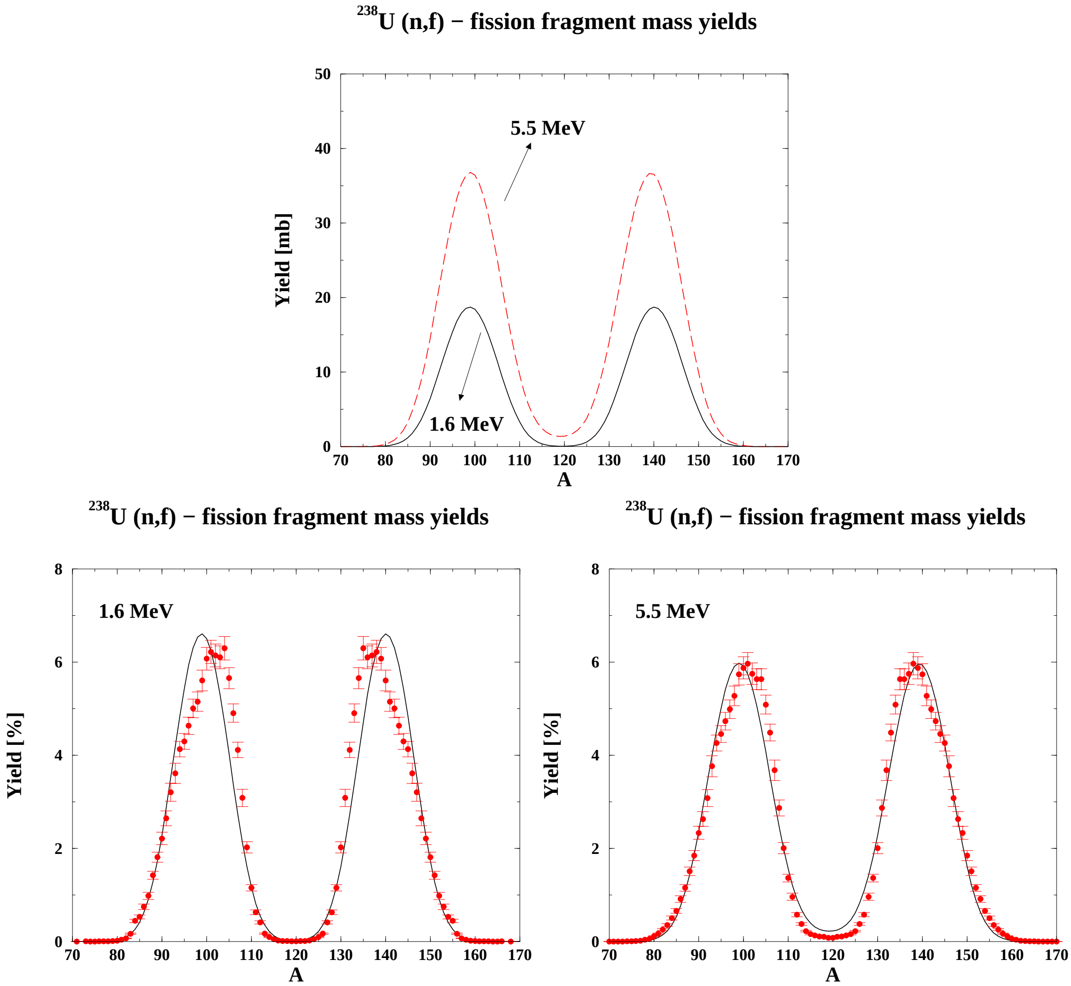

Figure 7.16: Fission fragment mass yield curves as function of the mass number A, produced by 1.6 MeV and 5.5 MeV neutrons on ^{238}U. The upper curve shows the results as they are produced by TALYS and the other two plots contain the comparison with experimental data in terms of normalized yields [154].

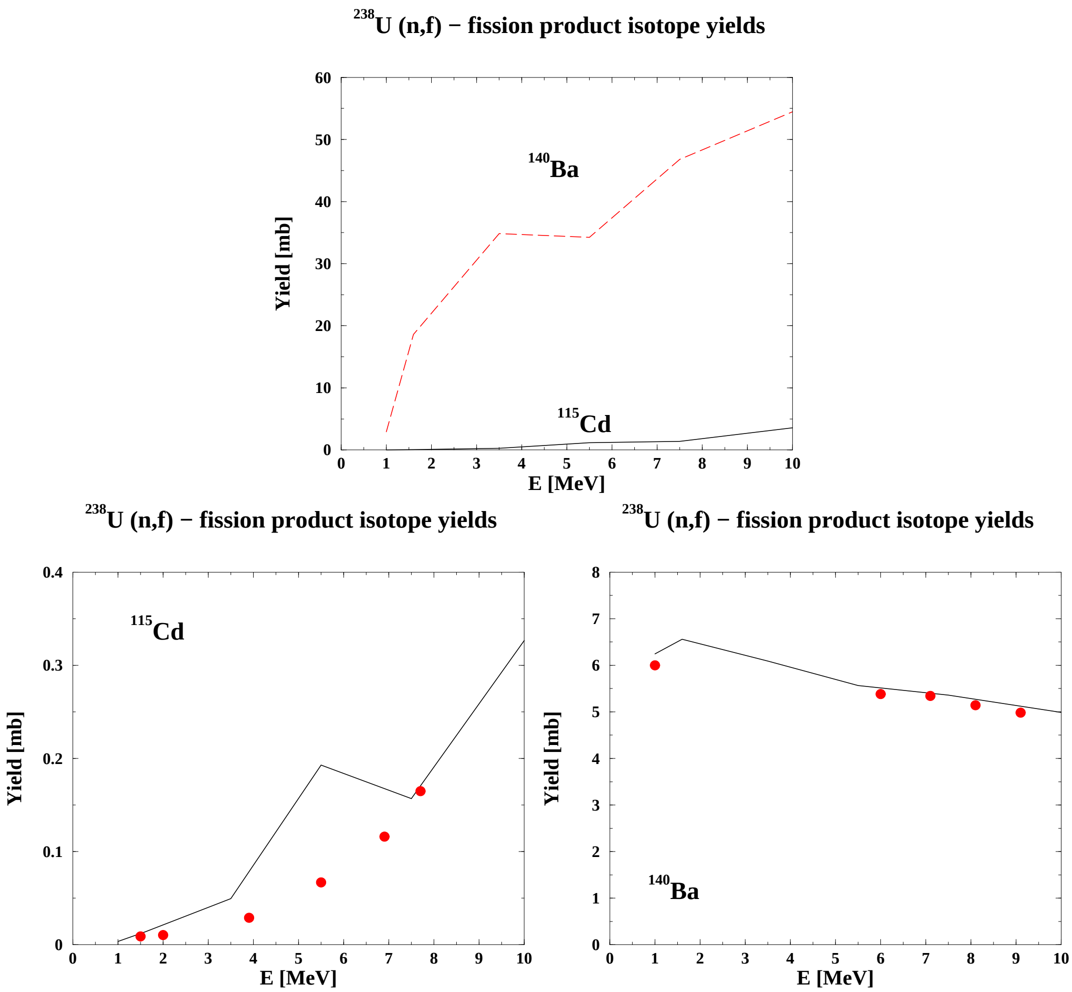

Figure 7.17: Fission product isotope yields produced by neutrons on ^{238}U as function of the mass number A. The upper plot shows the results for ^{115}Cd and ^{140}Ba as they are produced by TALYS-0.64 and the other two plots contain the comparison with experimental data in terms of normalized yields [155, 156].

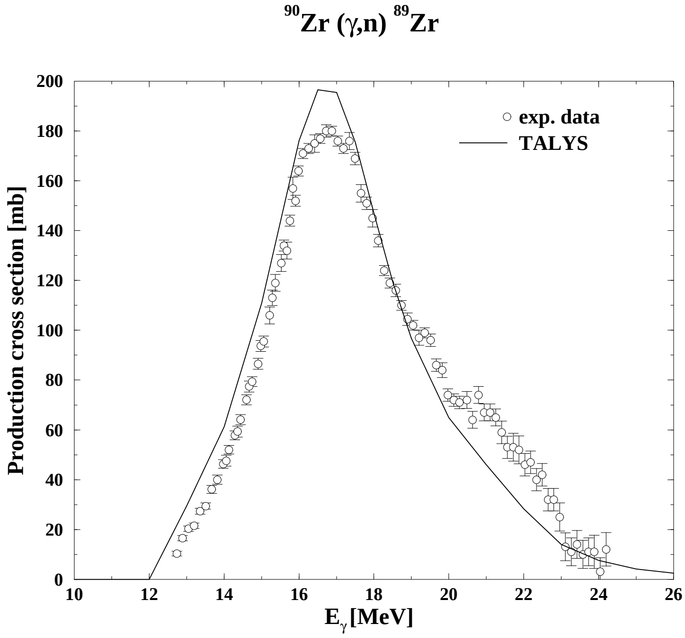

Figure 7.18: Photonuclear reaction on ^{90}Zr. Experimental data are obtained from [162].

7.3.15 Sample 15: Photonuclear reactions: g + ^{90}Zr

This sample case illustrates the capabilities of TALYS to treat photonuclear reactions. We calculate the (γ,n) reaction on ^{90}Zr as a function of incident energy, with default model parameters, and compare the result to experimental data. The following input file is used

```
#
# General
#
projectile g
element zr
mass 90
energy energies
```

Fig. 7.18 displays the resulting production cross section of ^{89}Zr, as obtained in file *rp040089.tot*.

7.3.16 Sample 16: Different optical models : n + ^{120}Sn

To demonstrate the variety of optical models that we have added recently to TALYS, we include a sample case in which 4 OMP's for neutrons on ^{120}Sn are compared. The results are given in Fig. 7.19 for the total cross section and in Fig.7.20 for the total inelastic cross section.

Case 16a: Koning-Delaroche local potential

The input file is

```
#
# General
#
projectile n
element    sn
mass       120
energy     energies
```

This is the default calculation: TALYS will find a local OMP in the structure database and will use it.

Case 16b: Koning-Delaroche global potential

The input file is

```
#
# General
#
projectile n
element    sn
mass       120
energy     energies
#
# Parameters
#
localomp n
```

Case 16c: Koning-Delaroche local dispersive potential

The input file is

```
#
# General
#
projectile n
element    sn
mass       120
energy     energies
#
# Parameters
#
dispersion y
```

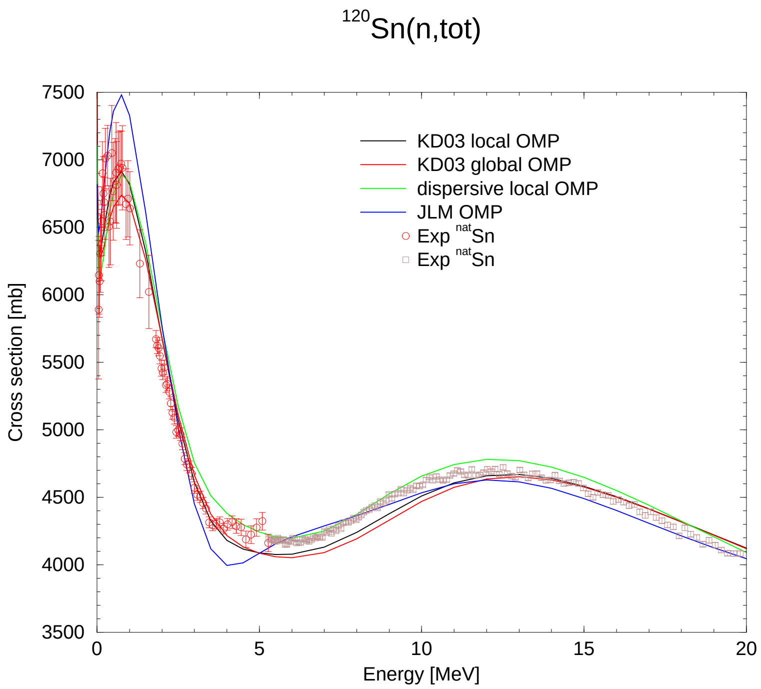

Figure 7.19: Total cross section for neutrons incident on ^{120}Sn for different optical model potentials.

Case 16d: Bauge-Delaroche JLM potential

The input file is

```
#
# General
#
projectile n
element    sn
mass       120
energy     energies
#
# Parameters
#
jlmomp y
```

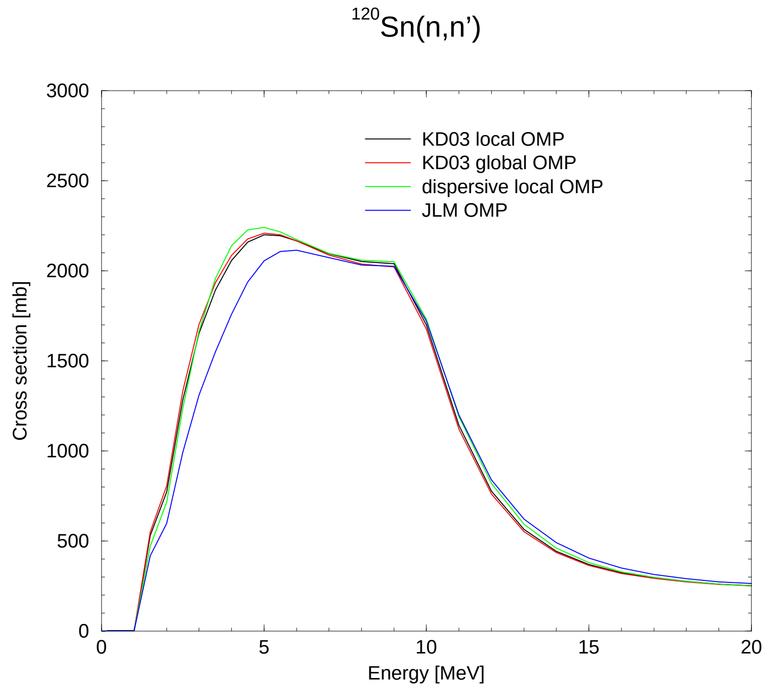

Figure 7.20: Total inelastic cross section for neutrons incident on ^{120}Sn for different optical model potentials.

7.3.17 Sample 17: Different level density models : n + ^{99}Tc

To demonstrate the variety of level density models that we have added recently to TALYS, we include a sample case in which 3 different models are compared. The results are given in Fig. 7.21 for the cumulative number of discrete levels and in Fig.7.22 for the (n,p) cross section.

Case 17a: Constant Temperature Model

The input file is

```
#
# General
#
projectile n
element tc
mass 99
energy energies
#
# Parameters
#
outdensity y
filedensity y
ldmodel 1
```

This is the default calculation: TALYS use the local CTM level density for its calculations

Case 17b: Back-shifted Fermi gas Model

The input file is

```
#
# General
#
projectile n
element tc
mass 99
energy energies
#
# Parameters
#
outdensity y
filedensity y
ldmodel 2
```

Case 17c: Hartree-Fock Model

The input file is

```
#
# General
#
projectile n
element tc
mass 99
energy energies
#
# Parameters
#
outdensity y
filedensity y
ldmodel 5
```

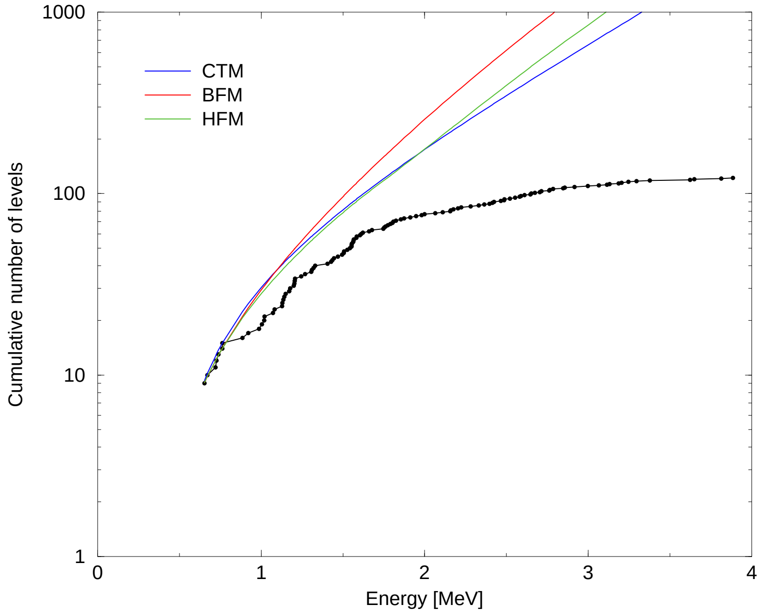

Figure 7.21: Cumulative number of discrete levels of ^{99}Tc for different level density models.

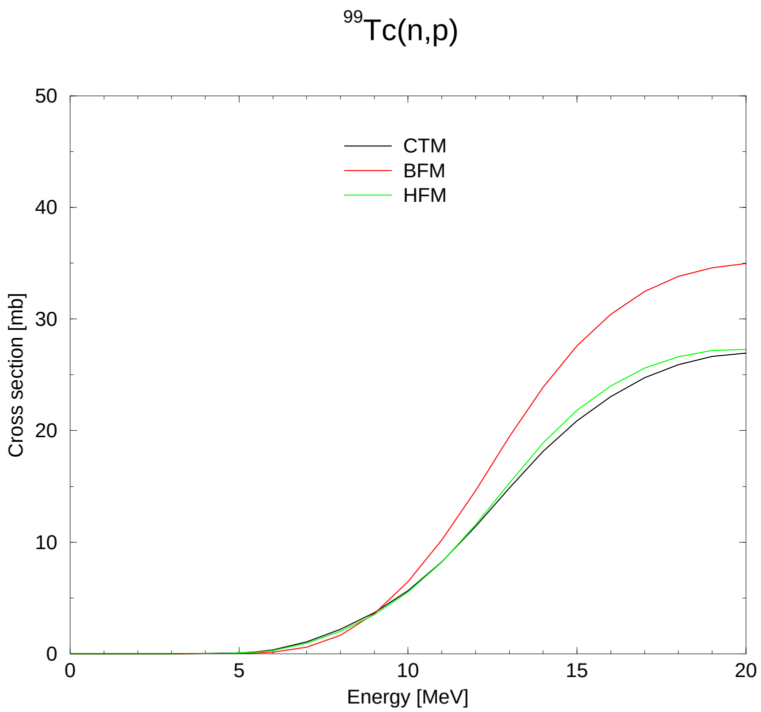

Figure 7.22: ^{99}Tc(n,p) cross section for different level density models.

7.3.18 Sample 18: Astrophysical reaction rates : n + ^{187}Os

With TALYS-1.0, astrophysical reaction rates can be calculated, see section 4.11. As sample case, we took the work done in Ref.[49] where the ^{187}Os(n,γ) was studied for the derivation of the age of the galaxy withing the Re-Os cosmochronology.

Case 18a: ^{187}Os(n,γ) cross section

First, the calculated ^{187}Os(n,γ) was compared with experimental data, using the following input file

```
#
# General
#
projectile n
element    os
mass       187
energy   energies
#
# Parameters
#
ldmodel   5
asys n
strength 2
gnorm 0.27
```

where obviously **gnorm** was used as adjustment parameter. The results are given in Fig.7.23.

Case 18b: ^{187}Os(n,γ) astrophysical reaction rate

Next, the astrophysical reaction rates for neutrons on ^{187}Os are computed with the following input file

```
#
# General
#
projectile n
element    os
mass       187
energy   energies
#
# Parameters
#
ldmodel   5
asys n
strength 2
gnorm 0.27
astro y
astrogs n
```

which produces various output files in which the reaction rates as function of temperature are given. The (n, γ) rate as given in the output file is

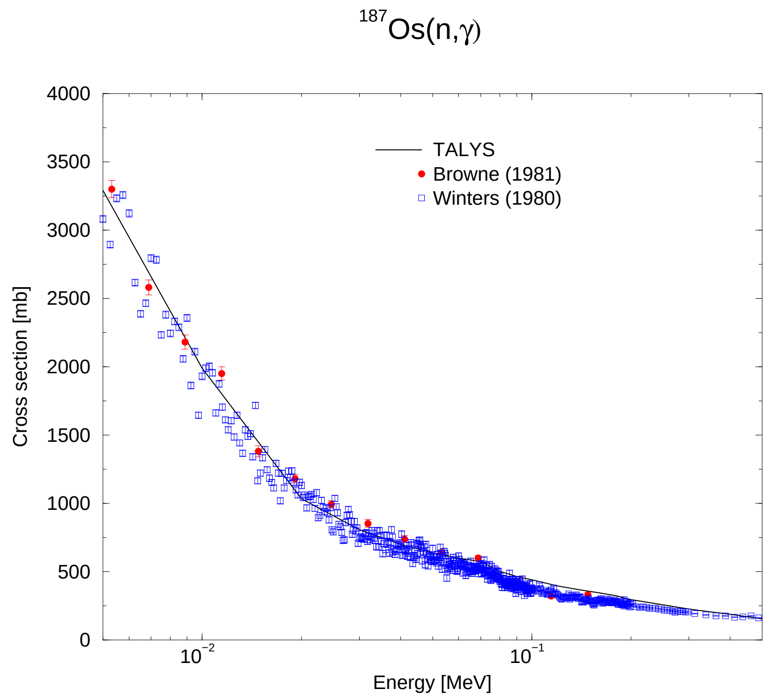

Figure 7.23: ^{187}Os(n,γ) cross section.

```
 8. Thermonuclear reaction rates
 Reaction rate for Z= 76 A=188 (188Os)
    T          G(T)         Rate
   0.0001 1.00000E+00 5.46242E+08
   0.0005 1.00000E+00 4.96512E+08
   0.0010 1.00000E+00 4.45882E+08
   0.0050 1.00000E+00 3.52813E+08
   0.0100 1.00002E+00 3.01755E+08
   0.0500 1.20827E+00 2.03467E+08
   0.1000 1.64630E+00 1.87256E+08
   0.1500 1.95860E+00 1.82416E+08
   0.2000 2.21894E+00 1.80436E+08
   0.2500 2.48838E+00 1.79690E+08
   0.3000 2.79031E+00 1.79474E+08
   0.4000 3.49874E+00 1.79716E+08
   0.5000 4.31540E+00 1.80165E+08
   0.6000 5.20597E+00 1.80375E+08
   0.7000 6.15215E+00 1.80187E+08
   0.8000 7.14759E+00 1.79580E+08
   0.9000 8.19300E+00 1.78579E+08
   1.0000 9.29313E+00 1.77221E+08
....................................
```

The same numbers can be found in the separate file *astrorate.g*. In *astrorate.tot* the rates for all reactions can be found.

Chapter 8

Computational structure of TALYS

8.1 General structure of the source code

The source of TALYS-1.0 is written in Fortran77, and we assume it can be successfully compiled with any f77 or f90/f95 compiler. We have aimed at a setup that is as modular as Fortran77 allows it to be, using programming procedures that are consistent throughout the whole code. In total, there are 273 Fortran subroutines, which are connected through one file, *talys.cmb*, in which all global variables are declared and stored in common blocks. This adds up to a total of more than 40000 lines, of which about 45% are comments. These numbers do not include the *ecis06t* subroutine (23761 lines), see below. On a global level, the source of TALYS consists of 3 main parts: Input, initialisation and reaction calculation. This structure can easily be recognized in the main program, *talys*, which consists merely of calls to the following 5 subroutines:

```
TALYS
|--machine
|--constants
|--talysinput
|--talysinitial
|--talysreaction
|--natural
```

8.1.1 machine

In this subroutine, the database is set for the directories with nuclear structure information and possible other operating system dependent settings. Only this subroutine should contain the machine-dependent statements.

8.1.2 constants

In this subroutine the fundamental constants are defined. First, in the block data module **constants0** the nuclear symbols and the fundamental properties of particles are defined. Also, the magic numbers, character strings for the two possible parity values and a few fundamental constants are initialized. From these constants, other constants that appear in various reaction formulae are directly defined in subroutine *constants*. Examples are $2\pi/\hbar$, $\hbar c$, $1/\pi^2\hbar^2c^2$, $1/\pi^2\hbar^3c^2$ and $amu/\pi^2\hbar^3c^2$. In the initialisation, they are directly defined in units of MeV and mb. Also, a few other constants are set.

8.1.3 talysinput

Subroutine for the user input of keywords and their defaults.

8.1.4 talysinitial

Subroutine for the initialisation of nuclear structure and other basic parameters.

8.1.5 talysreaction

Subroutine with reaction models.

8.1.6 natural

For calculations of reactions on natural elements a fifth subroutine may be called, namely a subroutine to handle natural elements as target. In this subroutine, another loop over *talysinput*, *talysinitial* and *talysreaction* is performed, for each isotope of the element.

8.1.7 ecis06t

Another integral part of TALYS that should explicitly be mentioned is Raynal's multi-disciplinary reaction code ECIS-06, which we have included as a subroutine. It is called several times by TALYS for the calculation of basic reaction cross sections, angular distributions and transmission coefficients, for either spherical or deformed nuclei. To enable the communication between ECIS-06 and the rest of TALYS, a few extra lines were added to the original ECIS code. In the source *ecis06t.f* our modifications, not more than 30 lines, can be recognized by the extension *ak000000* in columns 73-80.

We will now describe the main tasks of the three main subroutines mentioned above. We will start with the calling sequence of the subroutines, followed by an explanation of each subroutine. A subroutine will only be explained the first time it appears in the calling tree. Moreover, if a subtree of subroutines has already been described before in the text, we put a "$>$" behind the name of the subroutine, indicating it can be found in the text above.

8.2 Input: talysinput

The subroutine *talysinput* deals with the user input of keywords and their defaults and consists of calls to the following subroutines:

```
talysinput
|--readinput
|--input1
   |--getkeywords
```

```
   |--abundance
|--input2
   |--getkeywords
|--input3
   |--getkeywords
|--input4
   |--getkeywords
|--input5
   |--getkeywords
|--input6
   |--getkeywords
|--checkkeyword
   |--getkeywords
|--checkvalue
```

8.2.1 readinput

This subroutine reads in all the lines from the user input file as character strings and transfers them to lower case, for uniformity. The actual reading of the keywords from these lines is done in the next six subroutines.

8.2.2 input1

In *input1*, the four main keywords **projectile, element, mass** and **energy** are read and it is determined whether there is only one incident energy (directly given as a number in the input file) or a range of incident energies (given in an external file), after which the energy or range of energies are read in. The maximal incident energy is determined, the incident particle is identified, and the numerical Z, N and A values for the target are set. The keywords are read from the input line using the following subroutine,

getkeywords

With *getkeywords*, all separate words are read from each input line. From each input line we retrieve the keyword, the number of values, and the values themselves. These are all stored in strings to enable an easy setting of variables in the input subroutines.

For natural targets, *input1* also calls the following subroutine,

abundance

In *abundance*, the isotopic abundances are read from the database or from a user input file, if present.

8.2.3 input2, input3, input4, input5, input6

In the other 5 subroutines, all other keywords that can be present in the input file are identified. Most of them are first set to their default values at the beginning of the subroutine, after which these values can be overwritten by means of a read statement. In all input subroutines, checks are built in for the most flagrant input errors. For example, if a character string is read from the input file where a numerical value is expected, TALYS warns the user and gracefully stops. Subroutine *input2* deals with general physical parameters, *input3* deals with choices for nuclear models, *input4* deals with choices for the output, *input5* deals with nuclear model parameters, and *input6* deals with output to be written to specific files. The order of these subroutines, and the information in them, is important since sometimes defaults are set according to previously set flags.

8.2.4 checkkeyword

In this subroutine, we check whether all keywords given by the user are valid. If for example the wrongly typed keyword **projjectile** appears in the input, TALYS stops after giving an error message.

8.2.5 checkvalue

This subroutine performs a more intelligent check on erroneous input values. Values of parameters which are out of the ranges that were specified in Chapter 6, and are thus beyond physically reasonable values, are detected here. In such cases the program also gives an error message and stops. Sufficiently wide ranges are set, i.e. the input values have to be really ridiculous before TALYS stops.

8.3 Initialisation: talysinitial

In subroutine *talysinitial*, nuclear structure and other basic parameters are initialised. It consists of calls to the following subroutines:

```
talysinitial
|--particles
|--nuclides
|--grid
|--mainout
|--timer
```

8.3.1 particles

In *particles*, it is determined, on the basis of the **ejectiles** keyword (page 133), which particles are included and which are skipped as competing particles in the calculation. The default is to include all particles from photons to alpha's as competing channels. If specific outgoing particles in the input are given, only those will be included as competing channels. This sets the two logical variables **parinclude** and **parskip**, which are each others' opposite and are used throughout TALYS.

8.3.2 nuclides

In *nuclides* the properties of the involved nuclides are set. The following subroutines are called:

```
nuclides
|--strucinitial
|--masses
|--separation
```

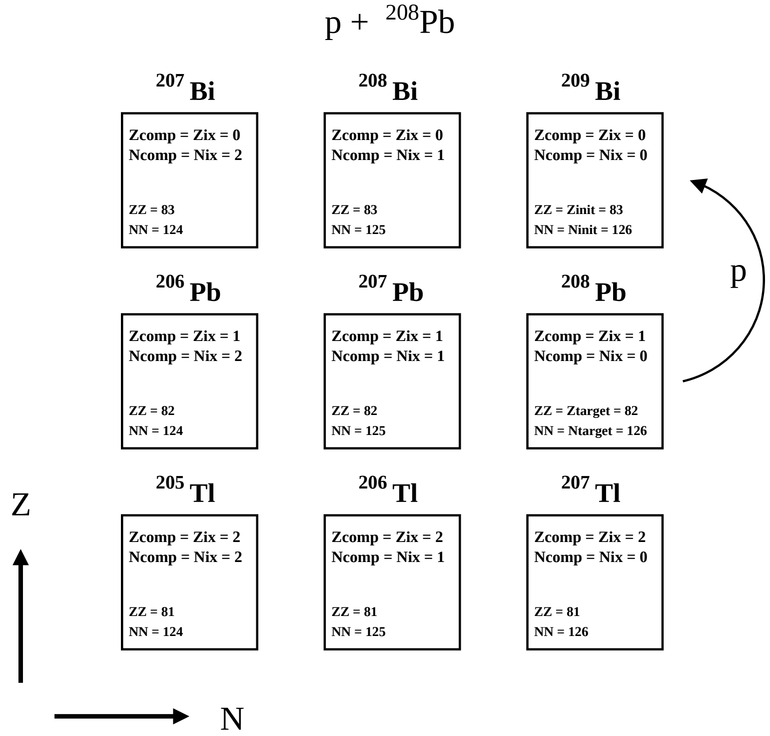

Figure 8.1: Illustration of the various nuclide designators used throughout TALYS.

```
|--structure
|--weakcoupling
|--radwidtheory
|--sumrules
|--kalbachsep
|--egridastro
```

First, in *nuclides* we assign the Z, N, and A of all possible residual nuclei. In TALYS we make use of both absolute and relative designators to describe the nuclides. This is illustrated in Fig. 8.1.

ZZ, NN, AA, Zinit, Ninit, Ainit, Ztarget, Ntarget, Atarget, represent true values of the charge, neutron and mass number. The extension 'init' indicates the initial compound nucleus and 'target' corresponds to the target properties. Zix, Nix, Zcomp and Ncomp are indices relative to the initial compound nucleus. The initial compound nucleus (created by projectile + target) has the indices (0,0). The first index represents the number of protons and the second index the number of neutrons away from the initial compound nucleus. Example: For the reaction p + ^{208}Pb, the set (0,0) represents ^{209}Bi and the set (1,2) represents ^{206}Pb. In the calculation Zix and Nix are used in loops over daughter nuclides and Zcomp and Ncomp are used in loops over decaying mother nuclides. In addition, TALYS makes use of the arrays Zindex and Nindex, which are the first two indices of many other arrays. At any point in the reaction calculation, given the indices of the mother nucleus Zcomp, Ncomp and the particle type, these relative nuclide designators will be directly known through the arrays we initialize in this subroutine.

As an example for the ^{56}Fe(n,p)^{56}Mn reaction: Ztarget=26, Ntarget=30, Zcomp=0 (primary compound nucleus), Ncomp=0 (primary compound nucleus), Zindex=1, Nindex=0, Zinit=26, Ninit=31, ZZ=25, NN=31. Next, many structure and model parameters are set. This is done by calling the subroutines mentioned above. Nuclear structure properties for the target, Q-values and the Coulomb barriers are also set in *nuclides*. Finally, some set-off energies for pre-equilibrium and width fluctuation corrections are set here. The subroutines called are:

strucinitial

This subroutine merely serves to initialize a lot of arrays. Also, the energy grid for tabulated level densities are set.

masses

In *masses* the nuclear masses are read from the mass table. The following subroutines are called:

```
masses
|--duflo
```

We read both the experimental masses, of Audi-Wapstra, and the theoretical masses from the mass table. The experimental nuclear mass is adopted, when available. We also read the experimental and theoretical mass excess, to enable a more precise calculation of separation energies. If a residual nucleus is not in the experimental/theoretical mass table, we use the analytical formula of Duflo-Zuker. Finally, the so-called reduced and specific masses are calculated for every nucleus.

duflo

Subroutine with the analytical mass formula of Duflo-Zuker.

separation

In *separation*, the separation energies for all light particles on all involved nuclides are set. For consistency, separation energies are always calculated using two nuclear masses of the same type, i.e. both experimental or both theoretical. Hence if nucleus A is in the experimental part of the table but nucleus B is not, for both nuclides the theoretical masses are used.

structure

This is a very important subroutine. In *structure*, for each nuclide that can be reached in the reaction chain the nuclear structure properties are read in from the nuclear structure and model database. If the nuclear parameters are not available in tabular form they are determined using models or systematics. TALYS is written such that a call to *structure* only occurs when a new nuclide is encountered in the reaction chain. First, it is called for the binary reaction. Later on, in *multiple*, the call to *structure* is repeated for nuclides that can be reached in multiple emission. The full calling tree is as follows:

```
structure
|--levels
|--gammadecay
```

```
|--deformpar
|--resonancepar
|--gammapar
|--omppar
|--radialtable
|--fissionpar
|--densitypar
|--densitytable
|--densitymatch
|--d0theory
|--partable
```

levels

In *levels*, the discrete level information is read. First, for any nuclide, we assign a 0+ ground state to even-even and odd-odd nuclei and a 1/2+ ground state to odd nuclei. Of course, if there is information in the discrete level file, this will be overwritten by the full discrete level info. The amount of information that is read in is different for the first several levels and higher lying levels. For the discrete levels that explicitly appear in the multiple Hauser-Feshbach decay (typically the first 20 levels), we need all information, i.e. the energy, spin, parity, lifetime and branching ratio's. We also read extra levels which are used only for the level density matching problem or for direct reactions (deformation parameters) in the continuum. The branching ratios and lifetimes are not read for these higher levels. In *levels*, it is also determined whether the target nucleus is in an excited state, in which case the level properties are read in.

gammadecay

For ENDF-6 data files, specific information on gamma-ray branching ratios, namely the cumulated flux originating from a starting level, needs to be handled. This is performed in *gammadecay*.

deformpar

In *deformpar*, the deformation parameters or deformation lengths are read, together with the associated coupling scheme for the case of coupled-channels calculations. In the case of vibrational nuclides, simple systematical formulae are used for the first few excited states if no experimental information is available. Spherical (S), vibrational (V) or rotational (R) coupled-channels calculations are automated. Finally, the deformation parameter for rotational enhancement of fission barrier level densities is read in from the nuclear structure database.

resonancepar

The experimental values from the resonance parameter file, D_0, Γ_γ, and S_0 are read here. A simple systematics for Γ_γ derived by Kopecky (2002), is provided in the block data module **gamdata** for nuclides not present in the table.

gammapar

In *gammapar*, the default giant dipole resonance parameters for gamma-ray strength functions are read from the database. Also the default values for M1, E1, E2 etc., are set using systematics if no value is present in the database [56]. Also, Goriely's microscopic gamma ray strength functions can be read in this subroutine.

omppar

The optical model parameters for nucleons are read from the database. If there are no specific parameters for a nuclide, they are determined by a global optical model for neutrons and protons. Also possible user-supplied input files with optical model parameters are read here.

radialtable

The radial matter densities for protons and neutrons are read from the database, to perform semi-microscopic OMP calculations. Also possible user-supplied input files with radial matter densities are read here.

fissionpar

In *fissionpar*, the fission barrier parameters are read, using the following subroutines:

```
fissionpar
|--barsierk
   |--plegendre
|--rldm
|--wkb
|--rotband
|--rotclass2
```

Several databases with fission barrier parameters can be read. There are also calls to two subroutines, *barsierk* and *rldm*, which provide systematical predictions for fission barrier parameters from Sierk's model and the rotating liquid drop model, respectively. As usual, it is also possible to overrule these parameters with choices from the user input. If *fismodel 1*, also the head band states and possible class II states are read in this subroutine. If *fismodel 5*, the WKB approximation as implemented in *wkb.f* is used. Finally, rotational bands are built on transition and class II states. Note that next to the chosen fission model (**fismodel**), there is always an alternative fission model (**fismodelalt**) which comes into play if fission parameters for the first choice model are not available.

barsierk

Using the rotating finite range model, the l-dependent fission barrier heights are estimated with A.J. Sierk's method. This subroutine returns the fission barrier height in MeV. It is based on calculations using yukawa-plus-exponential double folded nuclear energy, exact Couloumb diffuseness corrections, and diffuse-matter moments of inertia [139]. The implementation is analogous to the subroutine "asierk" written by A.J. Sierk (LANL, 1984). This subroutine makes use of the block data module *fisdata*.

plegendre

This function calculates the Legendre polynomial.

rldm

Using the rotating liquid drop model [140], the fission barrier heights are estimated. This subroutine returns the fission barrier height in MeV and is based on the subroutine FISROT incorporated in ALICE-91 [52]. This subroutine makes use of the block data module *fisdata*.

wkb

This subroutines computes fission transmission coefficients according to the WKB approximation. The subroutine itself calls various other subroutines and functions.

rotband

Here, the rotational bands are built from the head band transition states, for fission calculations.

rotclass2

Here, the rotational bands are built from the class II states. For this, the maximum energy of class II states is first determined.

densitypar

In *densitypar*, parameters for the level density are set, or read from the database. The following subroutines are called:

```
densitypar
|--mliquid1
|--mliquid2
```

The N_L and N_U of the discrete level region where the level density should match are read or set. Next the spin cut-off parameter for the discrete energy region is determined. All parameters of the Ignatyuk formula are determined, either from systematics or from mutual relations, for the level density model under consideration. Pairing energies and, for the generalized superfluid model, critical functions that do not depend on energy, are set. There are many input possibilities for the energy-dependent level density parameter of the Ignatyuk formula. The required parameters are alev, alimit, gammald and deltaW. The Ignatyuk formula implies that these parameters can not *all* be given at the same time in the input file, or in a table. All possibilities are handled in this subroutine. Also, the single-particle state density parameters are set.

mliquid1

Function to calculate the Myers-Swiatecki liquid drop mass for spherical nuclei.

mliquid2

Function to calculate the Goriely liquid drop mass for spherical nuclei.

densitytable

This subroutine reads in the tabulated level densities from Goriely.

densitymatch

The following subroutines are called:

```
densitymatch
|--ignatyuk
|--colenhance
|--fermi
|--matching
|--pol1
```

In *densitymatch*, the matching levels for the temperature and Fermi gas level densities are determined, and the level density matching problem is solved for both ground-state level densities and level densities on fission barriers. The matching problem is solved by calling *matching*.

ignatyuk

The level density parameter as function of excitation energy is calculated here.

colenhance

In *colenhance*, the collective (vibrational and rotational) enhancement for fission level densities is calculated. Here, a distinction is made between (a) **colenhance n**: collective effects for the ground state are included implicitly in the intrinsic level density, and collective effects on the barrier are determined relative to the ground state, and (b) **colenhance y**: both ground state and barrier collective effects are included explicitly. The calling tree is:

```
colenhance
|--ignatyuk
```

fermi

In *fermi*, the Fermi gas level density is calculated. The calling tree is:

```
fermi
|--spincut
```

spincut

In *spincut*, the spin cut-off parameter is calculated. Above the matching energy, this is done by an energy-dependent systematical formula. Below the matching energy, the value for the spin cut-off parameter is interpolated from the value at the continuum energy and the value from the discrete energy region. For the generalized superfluid model, the spin cut-off parameter is related to its value at the critical energy.

matching

In *matching*, the matching problem of Eq. (4.261) is solved. First, we determine the possible region of the roots of the equation, then we determine the number of solutions and finally we choose the solution for our problem. The calling tree is:

```
matching
|--ignatyuk
|--zbrak
|--rtbis
|--match
   |--pol1
```

zbrak

This subroutine finds the region in which the matching equation has a root ("bracketing" a function).

rtbis

This function finds the roots of a function.

match

This function represents Eq. (4.261).

pol1

Subroutine for interpolation of first order.

d0theory

Subroutine to calculate the theoretical average resonance spacing D_0 from the level density. The following subroutines are called:

```
d0theory
|--levels
|--density
```

density

This is the function for the level density. It is calculated as a function of the excitation energy, spin, parity, fission barrier and model identifier. On the basis of **ldmodel**, the level density model is chosen. The following subroutines are called:

```
density
|--ignatyuk
|--densitytot
|--spindis
|--locate
```

densitytot

This is the function for the total level density. It is calculated as a function of the excitation energy, fission barrier and model identifier. On the basis of **ldmodel**, the level density model is chosen. The following subroutines are called:

```
densitytot
|--ignatyuk
|--colenhance >
|--gilcam
   |--fermi >
|--bsfgmodel
   |--fermi >
   |--spincut >
|--superfluid
   |--fermi >
   |--spincut >
|--locate
```

spindis

In *spindis*, the Wigner spin distribution is calculated. The calling tree is:

```
spindis
|--spincut >
```

locate

Subroutine to find a value in an ordered table.

gilcam

In *gilcam*, the Gilbert-Cameron level density formula is calculated with the constant temperature and the Fermi gas expression.

bsfgmodel

In *bsfgmodel*, the Back-shifted Fermi gas formula is calculated with the Grossjean-Feldmeier approximation at low energy.

superfluid

In *superfluid*, the generalized superfluid model level density is calculated.

partable

Subroutine to write model parameters per nucleus to a separate output file.

weakcoupling

Subroutine *weakcoupling* is only called for odd target nuclides. The even-even core is determined and its deformation parameters, if any, are retrieved. These are then re-distributed over the levels of the odd-nucleus, so that later on DWBA calculations with the even core can be made. The selection of the odd-nucleus levels is automatic, and certainly not full proof. The following subroutines are called:

```
weakcoupling
|--deformpar >
|--levels >
```

radwidtheory

Subroutine for the calculation of the theoretical total radiative width, using gamma-ray strength functions and level densities. The following subroutines are called:

```
radwidtheory
|--levels >
|--density >
```

sumrules

Using sum rules for giant resonances, the collective strength in the continuum is determined. The deformation parameters of the collective low lying states are subtracted from the sum, so that the final GR deformation parameters can be determined.

kalbachsep

In *kalbachsep*, the separation energies for the Kalbach systematics are computed. We use the Myers-Swiatecki parameters as used by Kalbach [106].

egridastro

Subroutine to calculate the default incident energy grid for astrophysical rates. For astrophysical calculations, no use is made of an incident energy as supplied by the user, but instead is hardwired.

8.3.3 grid

In subroutine *grid*, the outgoing energy grid to be used for spectra and the transmission coefficients and inverse reaction cross section calculation is fixed. This non-equidistant grid ensures that the calculation for outgoing energies of a few MeV (around the evaporation peak) is sufficiently precise, whereas at higher energies a somewhat coarser energy grid can be used. For the same reason, this energy grid is used for the calculation of transmission coefficients. The begin and end of the energy grid for charged particles is set. The energy grid for which TALYS uses extrapolation (basically from thermal energies up to the first energy where we believe in a nuclear model code) is set. Also a few parameters for the angular grid, the transmission coefficient numerical limit, and temperatures for astrophysical calculations are set here. The following subroutines are called:

```
grid
|--energies
   |--locate
|--locate
```

energies

This subroutine is called for each new incident energy. The center-of-mass energy and the wave number are calculated (relativistic and non-relativistic), the upper energy limit for the energy grid is set, as well as the outgoing energies that belong to discrete level scattering. Finally, several incident energy-dependent flags are disabled and enabled.

8.3.4 mainout

Subroutine *mainout* takes care of the first part of the output. The output of general information such as date, authors etc., is printed first. Next, the basic reaction parameters are printed. The following subroutines are called:

```
mainout
|--inputout
   |--yesno
|--levelsout
|--densityout
   |--aldmatch
   |--spincut >
   |--ignatyuk
   |--colenhance >
   |--densitytot >
   |--density >
|--fissionparout
```

inputout

In this subroutine, the (default) values of all input keywords are written. This will appear at the top of the output file.

yesno

Function to assign the strings 'y' and 'n' to the logical values .true. and .false..

levelsout

In *levelsout*, all discrete level information for the nucleus under consideration is printed.

densityout

In *densityout*, all level density parameters are written, together with a table of the level density itself. For fissile nuclides, also the level densities on top of the fission barriers are printed. Cumulative level densities are calculated and written to files.

aldmatch

For fission, the effective level density parameter, which we only show for reference purposes, is obtained in three steps: (1) create the total level density in Fermi gas region, (2) apply a rotational enhancement to the total level density (3) determine the effective level density parameter by equating the rotational enhanced level density by a new effective total level density. The calling tree is:

```
aldmatch
|--ignatyuk
|--fermi >
|--spindis >
|--colenhance >
|--spincut >
```

fissionparout

In this subroutine, we write the main fission parameters, such as barrier heights and widths, and the head band transition states, rotational band transition states and class II states.

8.3.5 timer

Subroutine for the output of the execution time and a congratulation for the successful calculation.

8.4 Nuclear models: talysreaction

The main part of TALYS, *talysreaction*, contains the implementation of all the nuclear reaction models. First it calls *basicxs*, for the calculation of transmission coefficients, inverse reaction cross sections, etc. which are to be calculated only once (i.e. regardless of the number of incident energies). Next, for either one or several incident energies, subroutines for the nuclear reaction models are called according to the flags set by default or by input. During these nuclear model calculations, information such as cross sections, spectra, angular distributions, and nuclide populations, is collected and stored. At the end, all results are collected and transferred to the requested output. Finally, a message that the calculation was successful should be printed. The following subroutines are called:

```
talysreaction
|--basicxs
|--preeqinit
|--excitoninit
|--compoundinit
|--astroinit
|--energies >
|--reacinitial
|--incident
|--exgrid
|--recoilinit
|--direct
|--preeq
|--population
|--compnorm
|--comptarget
|--binary
|--angdis
|--multiple
|--channels
|--totalxs
|--spectra
|--massdis
|--residual
|--totalrecoil
|--thermal
|--output
|--finalout
|--astro
|--endf
|--timer
```

8.4.1 basicxs

The transmission coefficients and inverse reaction cross sections for the outgoing energy grid need to be calculated only once for all particles and gamma's, for energies up to the maximal incident energy. The following subroutines are called:

```
basicxs
|--basicinitial
|--inverse
|--gamma
```

basicinitial

In *basicinitial*, all arrays that appear in this part of the program are initialized.

inverse

Subroutine *inverse* organises the calculation of total, reaction and elastic cross sections and transmission coefficients for all outgoing particles and the whole emission energy grid (the inverse channels). The following subroutines are called:

```
inverse
|--inverseecis
|--inverseread
|--inversenorm
|--inverseout
```

inverseecis

In this subroutine the loop over energy and particles is performed for the basic ECIS calculations. For each particle and energy, the optical model parameters are determined by calling *optical*. The subroutine *ecisinput* is called for the creation of the ECIS input files. At the end of this subroutine, *ecis06t* is called to perform the actual ECIS calculation. The following subroutines are called:

```
inverseecis
|--ecisinput
   |--optical
   |--mom
|--optical
|--ecis06t >
```

ecisinput

This subroutine creates a standard ECIS input file for spherical or coupled-channels calculations.

optical

This is the main subroutine for the determination of optical model parameters. The following subroutines are called:

```
optical
|--opticaln
   |--soukhovitskii
|--opticalp
   |--soukhovitskii
|--opticald
   |--opticaln
   |--opticalp
|--opticalt
   |--opticaln
   |--opticalp
|--opticalh
   |--opticaln
```

```
   |--opticalp
|--opticala
   |--opticaln
   |--opticalp
```

opticaln, opticalp

Subroutines for the neutron and proton optical model parameters. If an optical model file is given with the **optmod** keyword, see page 145, we interpolate between the tabulated values. In most cases, the general energy-dependent form of the optical potential is applied, using parameters per nucleus or from the global optical model, both from subroutine *omppar*.

soukhovitskii

Subroutine for the global optical model for actinides by Soukhovitskii et al. [79].

opticald, opticalt, opticalh, opticala

Subroutines for deuteron, triton, helion and alpha optical potentials. In the current version of TALYS, we use the Watanabe method [61] to make a composite particle potential out of the proton and neutron potential.

mom

Subroutine for the semi-microscopic JLM optical model. This is basically Eric Bauge's MOM code turned into a TALYS subroutine. Inside this subroutine, there are many calls to other local subroutines. It also uses the file *mom.cmb*, which contains all common blocks and declarations for *mom.f*.

inverseread

In this subroutine the results from ECIS are read. For every particle and energy we first read the reaction (and for neutrons the total and elastic) cross sections. Next, the transmission coefficients are read into the array Tjl, which has four indices: particle type, energy, spin and l-value. For spin-1/2 particles, we use the array indices -1 and 1 for the two spin values. For spin-1 particles, we use -1, 0 and 1 and for spin-0 particles we use 0 only. For rotational nuclei, we transform the rotational transmission coefficients into their spherical equivalents for the compound nucleus calculation. Also, transmission coefficients averaged over spin are put into separate arrays. For each particle and energy, the maximal l-value is determined to constrain loops over angular momentum later on in the code.

inversenorm

In *inversenorm*, a semi-empirical formula for the reaction cross section can be invoked to overrule the results from the optical model. This is sometimes appropriate for complex particles. The normalization is only performed if the option for semi-empirical reaction cross sections is enabled. The semi-empirical results have a too sharp cut-off at low energies. Therefore, for the lowest energies the optical model results are normalized with the ratio at the threshold. The following subroutines are called:

```
inversenorm
|--tripathi
   |--radius
```

tripathi

Function for semi-empirical formula for the reaction cross section by Tripathi et al.. The original coding (which is hard to understand) does not coincide with the formulae given in Ref. [74] though the results seem to agree with the plotted results.

radius

Function for the radius, needed for the Tripathi systematics.

inverseout

This subroutine takes care of the output of reaction cross sections and transmission coefficients. Depending on the **outtransenergy** keyword, see page 187, the transmission coefficients are grouped per energy or per angular momentum.

gamma

This subroutine deals with calculations for gamma cross sections, strength functions and transmission coefficients. The following subroutines are called:

```
gamma
|--gammanorm
|--gammaout
```

gammanorm

In this subroutine, we normalize the gamma-ray strength functions by imposing the condition that the transmission coefficients integrated from zero up to neutron separation energy are equal to the ratio of the experimental mean gamma width and mean level spacing for s-wave neutrons. The gamma transmission coefficients are generated through calls to the strength function *fstrength*. The gamma-ray cross sections are also normalized. The following subroutines are called:

```
gammanorm
|--density >
|--fstrength
|--gammaxs
   |--fstrength
```

fstrength

In *fstrength*, the gamma-ray strength functions according to Kopecky-Uhl or Brink-Axel are calculated, or are interpolated from Goriely's HFB or HFBCS tables.

gammaxs

In *gammaxs*, the photo-absorption cross sections are calculated. They consist of a GDR part and a quasi-deuteron part.

gammaout

In *gammaout*, the gamma-ray strength functions, transmission coefficients and cross sections are written to output. The following subroutines are called:

```
gammaout
|--fstrength
```

8.4.2 preeqinit

General quantities needed for pre-equilibrium calculations are set, such as factorials, spin distribution functions and Pauli correction factors. The following subroutines are called:

```
preeqinit
|--bonetti
  |--mom >
  |--optical >
```

bonetti

In this subroutine, the average imaginary volume potential for the internal transition rates is calculated.

8.4.3 excitoninit

Quantities needed for exciton model calculations are set, such as preformation factors, factors for the emission rates and charge conserving Q-factors.

8.4.4 compoundinit

Quantities needed for compound nucleus model calculations are set, such as factors for width fluctuation and angular distribution calculations. The following subroutines are called:

```
compoundinit
|--gaulag
|--gauleg
```

8.4.5 astroinit

Quantities needed for astrophysical reaction calculations are initialized.

gaulag

This subroutine is for Gauss-Laguerre integration.

gauleg

This subroutine is for Gauss-Legendre integration.

8.4.6 reacinitial

In *reacinitial*, all arrays that appear in the nuclear reaction model part of the program are initialized.

8.4.7 incident

Subroutine *incident* handles the calculation of total, reaction, elastic cross section, transmission coefficients and elastic angular distribution for the incident energy. Also, some main parameters for the current incident energy are set. The following subroutines are called:

```
incident
|--yesno
|--incidentecis
   |--optical    >
   |--mom    >
   |--ecisinput  >
|--incidentread
|--incidentnorm
   |--tripathi   >
|--incidentgamma
   |--fstrength
   |--gammaxs    >
|--spr
|--incidentout
```

incidentecis

In this subroutine the basic ECIS calculation for the incident particle and energy is performed for either a spherical or a deformed nucleus. The optical model parameters are determined by calling *optical*. The subroutine *ecisinput* is called for the creation of the ECIS input files. At the end of this subroutine, *ecis06t* is called to perform the actual ECIS calculation.

incidentread

In this subroutine the results from ECIS are read for the incident particle and energy. We first read the reaction (and for neutrons the total and elastic) cross section. Next, the transmission coefficients are read into the array Tjlinc, which has has four indices: particle type, energy, spin and l-value. For spin-1/2 particles, we use the indices -1 and 1 for the two spin values. For spin-1 particles, we use -1, 0 and 1 and for spin-0 particles we use 0 only. For rotational nuclei, we transform the rotational transmission coefficients into their spherical equivalents for the compound nucleus calculation. Also, transmission coefficients averaged over spin are put into separate arrays. The maximal l-value is determined to constrain loops over angular momentum later on in the code. The direct reaction Legendre coefficients and angular distribution are also read in. For coupled-channels calculations, we also read the discrete inelastic angular distributions and cross sections.

incidentnorm

In *incidentnorm*, the transmission coefficients can be normalized with values obtained from semi-empirical systematics for the reaction cross section, if required.

incidentgamma

Here, the transmission coefficients for the incident gamma channel, in the case of photo-nuclear reactions, are generated.

spr

In *spr*, the S, P and R resonance parameters for low incident neutron energies are calculated and, if requested, written to file.

incidentout

In this subroutine the basic cross sections, transmission coefficients and possible resonance parameters for the incident channel are written to output.

8.4.8 exgrid

In *exgrid*, the possible routes to all reachable residual nuclei are followed, to determine the maximum possible excitation energy for each nucleus, given the incident energy. From this, the equidistant excitation energy grid for each residual nucleus is determined. The first NL values of the excitation energy grid Ex correspond to the discrete level excitation energies of the residual nucleus. The NL+1th value corresponds to the first continuum energy bin. The continuum part of the nuclides are then divided into equidistant energy bins. The Q-values for the residual nuclides are also determined. Finally, the calculation of level densities in TALYS can be done outside many loops of various quantum numbers performed in other subroutines. Therefore, in *exgrid* we store the level density as function of residual nucleus, excitation energy, spin and parity. The following subroutines are called:

```
exgrid
|--density >
|--spincut >
```

8.4.9 recoilinit

In this subroutine the basic recoil information is initialized. Various arrays are initialized and the maximum recoil energies for all residual nuclides are determined. Recoil energy and angular bins are determined.

8.4.10 direct

Subroutine *direct* takes care of the calculation of direct cross sections to discrete states that have not already been covered as coupled-channels for the incident channel, such as DWBA and giant resonance cross sections. The following subroutines are called:

```
direct
|--directecis
   |--ecisinput >
|--directread
|--giant
|--directout
```

directecis

In this subroutine the basic DWBA calculation for a spherical nucleus is performed. The subroutine *ecisinput* is called for the creation of the ECIS input files. At the end of this subroutine, *ecis06t* is called to perform the actual ECIS calculation.

directread

In this subroutine the results from ECIS are read for the DWBA calculation. We first read the direct cross section for the collective discrete states. The direct reaction Legendre coefficients and angular distribution are also read in. The procedure is repeated for the giant resonance states.

giant

In *giant*, the DWBA cross sections for the continuum are smeared into spectra. The same is done for other collective states that are in the continuum.

directout

In this subroutine the direct cross sections for discrete states and giant resonances are written to output.

8.4.11 preeq

Subroutine *preeq* is the general module for pre-equilibrium reactions. Particle-hole numbers for the reaction under consideration are initialized. Depending on the chosen pre-equilibrium model, the following subroutines may be called:

```
preeq
|--surface
|--exciton
|--excitonout
|--exciton2
|--exciton2out
|--msd
```

```
|--msdplusmsc
|--preeqcomplex
|--preeqcorrect
|--preeqtotal
|--preeqang
|--preeqout
```

surface

This function evaluates the effective well depth for pre-equilibrium surface effects.

exciton

This is the main subroutine for the one-component exciton model. For each exciton number, we subsequently calculate the emission rates and the lifetime of the exciton state according to the never-come-back approximation. There is also a possibility to create J-dependent pre-equilibrium cross sections using the spin distribution. As an alternative (which is the default), the Hauser-Feshbach spin distribution is adopted. The following subroutines are called:

```
exciton
|--emissionrate
  |--ignatyuk
  |--preeqpair
  |--phdens
     |--finitewell
|--lifetime
  |--lambdaplus
     |--matrix
     |--ignatyuk
     |--preeqpair
     |--finitewell
     |--phdens     >
```

emissionrate

This subroutine delivers the particle and photon emission rates (4.111), (4.115), (4.132) for the one-component exciton model.

preeqpair

In this subroutine, the pre-equilibrium pairing correction according to either Fu, see Eq. 4.81, or to the compound nucleus value is calculated.

phdens

The function *phdens* computes the one-component particle-hole state density (4.113).

finitewell

The function *finitewell* computes the finite well function (4.86).

lifetime

In this subroutine, the lifetime of the exciton state (4.116) is calculated, according to the never-come-back approximation.

lambdaplus

The function *lambdaplus* delivers the transition rates (4.119) in either analytical or numerical form, for the one-component exciton model based on matrix elements or on the optical model.

matrix

This function computes the matrix element (4.122) for the one-component model, and (4.102) for the two-component model.

excitonout

In *excitonout* all information of the one-component exciton model, such as matrix elements, emission rates and lifetimes, is written.

exciton2

This is the main subroutine for the two-component exciton model. For each exciton number, we subsequently calculate the emission rates and exchange terms (both in subroutine exchange2) and the lifetime of the exciton state. There is also a possibility to create J-dependent pre-equilibrium cross sections using the spin distribution. As an alternative (which is the default), the Hauser-Feshbach spin distribution is adopted. The following subroutines are called:

```
exciton2
|--exchange2
  |--emissionrate2
     |--ignatyuk
     |--preeqpair
     |--phdens2
        |--finitewell
  |--lambdapiplus
     |--matrix
     |--ignatyuk
     |--preeqpair
     |--finitewell
     |--phdens2    >
  |--lambdanuplus
     |--matrix
```

```
      |--ignatyuk
      |--preeqpair
      |--finitewell
      |--phdens2    >
   |--lambdapinu
      |--matrix
      |--ignatyuk
      |--preeqpair
      |--finitewell
      |--phdens2    >
   |--lambdanupi
      |--matrix
      |--ignatyuk
      |--preeqpair
      |--finitewell
      |--phdens2    >
|--lifetime2
```

exchange2

In *exchange2*, the probabilities (4.91) for the strength of the exciton state are calculated.

phdens2

The function *phdens2* computes the two-component particle-hole state density (4.80).

emissionrate2

This subroutine delivers the particle and photon emission rates for the two-component exciton model.

lambdapiplus, lambdanuplus

The function *lambdapiplus* delivers the proton transition rates (4.93) in either analytical or numerical form, for the two-component exciton model based on matrix elements or the optical model. Similarly for *lambdanuplus*.

lambdapinu, lambdanupi

The function *lambdapinu* delivers the proton-neutron transition rates (4.93) in either analytical or numerical form, for the two-component exciton model based on matrix elements or the optical model. Similarly for *lambdanupi*.

lifetime2

In this subroutine, the lifetime of the exciton state through the quantity of Eq. (4.90) is calculated.

exciton2out

In *exciton2out* all information of the two-component exciton model, such as matrix elements, emission rates and lifetimes, is written.

msd

This subroutine calculates pre-equilibrium cross sections according to the macroscopic multi-step direct (MSD) model. The MSD model is implemented for neutrons and protons only. The following subroutines are called:

```
msd
|--msdinit
  |--interangle
|--dwbaecis
  |--ecisdwbamac
     |--optical    >
  |--dwbaread
  |--dwbaout
  |--dwbaint
  |--onecontinuumA
     |--ignatyuk
     |--omega
        |--phdens      >
  |--onestepA
     |--ignatyuk
     |--omega      >
     |--locate
     |--pol2
|--msdcalc
  |--onestepB
     |--cmsd
  |--onecontinuumB
  |  |--cmsd
  |--multistepA
  |--multistepB
  |  |--locate
  |  |--pol2
|--msdtotal
|--msdout
```

msdinit

This subroutine initializes various arrays for the multi-step direct calculation, such as the MSD energy grid and the intermediate angles through a call to *interangle*.

interangle

Subroutine *interangle* produces the intermediate angles for MSD model, by the addition theorem. For multi-step reactions, this is necessary to transform the ingoing angle of the second step and link it with the outgoing angle of the first step.

dwbaecis

This subroutine takes care of all the ECIS calculations that need to be performed for the various steps of the multi-step reaction. Subsequently, DWBA calculations are performed for the first exchange one-step reaction, the inelastic one-step reaction and the second exchange one-step reaction. For this, various subroutines are called.

dwbaecis

Subroutine *ecisdwbamac* creates the ECIS input file for a macroscopic DWBA calculation. Potentials for the incident, transition and outgoing channel are calculated.

dwbaread

In this subroutine the results from ECIS are read. For every energy and spin we read the total DWBA cross section and the angle-differential DWBA cross section.

dwbaread

This subroutine takes care of the output of the DWBA cross sections.

dwbaint

In *dwbaint*, the DWBA cross sections are interpolated on the appropriate energy grid.

onecontinuumA

In *onecontinuumA*, the continuum one-step cross sections to be used in multi-step calculations are calculated by multiplying the DWBA cross sections by particle-hole state densities.

omega

This is a function of the particle-hole state density per angular momentum.

onestepA

In *onestepA*, the unnormalized one-step direct cross sections for the outgoing energy grid are calculated (these will be normalized in subroutine onestepB).

pol2

Subroutine for interpolation of second order.

msdcalc

This is the general subroutine for the final MSD calculations.

onestepB

In *onestepB*, the one-step direct cross sections are calculated using a final normalization.

onecontinuumB

In *onecontinuumB*, the final one-step direct cross sections for use in the multi-step calculations are computed using the final normalization.

multistepA

In *multistepA*, the multi-step direct cross sections (second and higher steps) are calculated using a final normalization.

multistepB

In *multistepB*, the multi-step direct cross sections are interpolated on the final outgoing energy grid.

msdtotal

In *msdtotal*, the total multi-step direct cross sections are calculated.

msdout

In *msdout*, the multi-step direct cross sections are written to output.

msdplusmsc

In this subroutine, the MSD cross sections are put in the general pre-equilibrium cross sections.

preeqcomplex

Subroutine *preeqcomplex* handles pre-equilibrium complex particle emission. The implemented complex particle emission model is described in Section 4.4.4. Note that several purely empirical fixes to the model were needed to prevent divergence of certain cross section estimates. The subroutine consists of two main parts: One for stripping/pickup and one for alpha knock-out reactions. The following subroutines are called:

```
preeqcomplex
|--phdens2    >
```

preeqcorrect

This subroutine handles the correction of pre-equilibrium cross sections for direct discrete cross sections. If the cross sections for discrete states have *not* been calculated by a direct reaction model, we collapse the continuum pre-equilibrium cross sections in the high-energy region on the associated discrete states. After this, the pre-equilibrium cross sections in the discrete energy region are set to zero. The following subroutines are called:

```
preeqcorrect
|--locate
```

preeqtotal

In *preeqtotal*, the total pre-equilibrium cross sections are calculated. The pre-equilibrium spectra and spectra per exciton number are summed to total pre-equilibrium cross sections. Special care is taken for the continuum bin with the highest outgoing energy, i.e. the one that overlaps with the energy corresponding to the last discrete state. In line with unitarity, the summed direct + pre-equilibrium cross section may not exceed the reaction cross section. In these cases, we normalize the results. Also, the discrete pre-equilibrium contribution is added to the discrete state cross sections.

preeqang

In *preeqang*, the pre-equilibrium angular distribution is calculated. Also here, there is a correction of the pre-equilibrium cross sections for direct discrete angular distributions. If the angular distributions for discrete states have *not* been calculated by a direct reaction model, we collapse the continuum pre-equilibrium angular distributions in the high energy region on the associated discrete states. For the exciton model, the pre-equilibrium angular distributions are generated with the Kalbach systematics. The following subroutines are called:

```
preeqang
|--kalbach
```

kalbach

This is the function for the Kalbach systematics [106].

preeqout

In *preeqout*, the output of pre-equilibrium cross sections is handled. The following subroutines are called:

```
preeqout
|--ignatyuk
|--phdens     >
|--phdens2    >
```

8.4.12 population

In *population*, the pre-equilibrium spectra are processed into population bins. The pre-equilibrium cross sections have been calculated on the emission energy grid. They are interpolated on the excitation energy grids of the level populations (both for the total and the spin/parity-dependent cases) to enable further decay of the residual nuclides. also, the pre-equilibrium population cross section are normalized. Due to interpolation, the part of the continuum population that comes from pre-equilibrium is not exactly equal to the total pre-equilibrium cross section. The normalization is done over the whole excitation energy range. The following subroutines are called:

```
population
|--locate
|--pol1
```

8.4.13 compnorm

There is a small difference between the reaction cross section as calculated by ECIS and the sum over transmission coefficients. We therefore normalize the level population accordingly in this subroutine. The compound nucleus formation cross section xsflux and the associated normalization factors are created.

8.4.14 comptarget

In *comptarget*, the compound reaction for the initial compound nucleus is calculated. First, the level densities and transmission coefficients are prepared before the nested loops over all quantum numbers are performed. Next the following nested loops are performed:

- compound nucleus parity
- total angular momentum J of compound nucleus
- j of incident channel
- l of incident channel
- outgoing particles and gammas
- outgoing excitation energies
- residual parity
- residual spin
- j of outgoing channel
- l of outgoing channel

There are two possible types of calculation for the initial compound nucleus. If either width fluctuation corrections or compound nucleus angular distributions are wanted, we need to sum explicitly over all possible quantum numbers before we calculate the width fluctuation or angular factor. If not, the sum over j and l of the transmission coefficients can be lumped into one factor, which decreases the calculation time. In the latter case, the partial decay widths enumhf are calculated in subroutine *compprepare*.

In order to get do-loops running over integer values, certain quantum numbers are multiplied by 2, which can be seen from a 2 present in the corresponding variable names. For each loop, the begin and end point is determined from the triangular rule.

For every J and P (parity), first the denominator (total width) denomhf for the Hauser-Feshbach formula is constructed in subroutine compprepare. Also width fluctuation variables that only depend on J and P and not on the other angular momentum quantum numbers are calculated in subroutine *widthprepare*. For the width fluctuation calculation, all transmission coefficients need to be placed in one sequential array. Therefore, a counter tnum needs to be followed to keep track of the proper index for the transmission coefficients.

Inside the nested loops listed above, compound nucleus calculations for photons, particles and fission are performed. In the middle of all loops, we determine the index for the width fluctuation calculation and call the subroutine that calculates the correction factor. Also, compound angular distributions, i.e. the Legendre coefficients, for discrete states are calculated.

The following subroutines are called:

```
comptarget
|--densprepare
|--tfission
|--compprepare
|--widthprepare
|--widthfluc
|--clebsch
|--racah
|--tfissionout
|--raynalcomp
```

densprepare

In *densprepare*, we prepare the energy grid, level density and transmission coefficient information for the compound nucleus and its residual nuclides. For various types of decay (continuum to discrete, continuum to continuum, etc.) we determine the energetically allowed transitions. These are then taken into account for the determination of integrated level densities. To get the transmission coefficients on the excitation energy grid from those on the emission energy grid, we use interpolation of the second order. Finally, the fission level densities are calculated.

The following subroutines are called:

```
densprepare
|--fstrength
|--locate
|--pol2
|--density    >
```

tfission

In this subroutine, the fission transmission coefficients are calculated. The fission transmission coefficients decrease very rapidly with excitation energy. Therefore, we calculate them at the end points and at the middle of each excitation energy bin. With this information, we can do logarithmic integration. Calls to subroutine *t1barrier* are done for 1, 2 and 3 barriers. Also transmission coefficients corrected for the presence of class II states are calculated.

The following subroutines are called:

```
tfission
|--t1barrier
   |--thill
```

t1barrier

Subroutine *t1barrier* handles the fission transmission coefficient for one barrier. Both discrete states and the continuum are taken into account.

thill

Function for the Hill-Wheeler formula.

compprepare

In *compprepare*, information for the initial compound nucleus is prepared. The transmission coefficients are put in arrays for possible width fluctuation calculations. Also the total width denomhf appearing in the denominator of the compound nucleus formula is created. Note that the complete subroutine is performed inside the loop over compound nucleus spin J and parity P in subroutine comptarget.

widthprepare

In this subroutine, the preparation of width fluctuation calculations is done. All width fluctuation variables that only depend on J and P and not on the other angular momentum quantum numbers are calculated. The following subroutines are called:

```
widthprepare
|--molprepare
|--hrtwprepare
|--goeprepare
   |--prodm
   |--prodp
```

molprepare

This subroutine takes care of the preparation of the Moldauer width fluctuation correction (information only dependent on J and P).

hrtwprepare

This subroutine takes care of the preparation of the HRTW width fluctuation correction (information only dependent on J and P).

goeprepare

This subroutine takes care of the preparation of the GOE triple integral width fluctuation correction (information only dependent on J and P).

prodm, prodp

Functions to calculate a product for the GOE calculation.

widthfluc

General subroutine for width fluctuation corrections. The following subroutines are called:

```
widthfluc
|--moldauer
|--hrtw
|--goe
   |--func1
```

moldauer

Subroutine for the Moldauer width fluctuation correction.

hrtw

Subroutine for the HRTW width fluctuation correction.

goe

Subroutine for the GOE width fluctuation correction.

clebsch

Function for the calculation of Clebsch-Gordan coefficients.

racah

Function for the calculation of Racah coefficients.

tfissionout

Subroutine *tfissionout* takes care of the output of fission transmission coefficients.

raynalcomp

Using subroutine *raynalcomp*, a compound nucleus run by ECIS can be performed, in addition to the calculation by TALYS. The results as calculated by ECIS will however not be used for TALYS but are just for comparison. The following subroutines are called:

```
raynalcomp
|--eciscompound
   |--optical    >
```

eciscompound

In *eciscompound*, an ECIS input file for a compound nucleus calculation is prepared.

8.4.15 binary

In *binary*, the binary reaction cross section are accumulated. The direct and pre-equilibrium cross sections are processed into population arrays. Binary feeding channels, necessary for exclusive cross sections, are determined. Also the population after binary emission is printed. The following subroutines are called:

```
binary
|--ignatyuk
|--spindis    >
|--binaryspectra
   |--binemission
      |--locate
      |--pol1
|--binaryrecoil
```

binaryspectra

Subroutine to interpolate decay, from one bin to another, on the emission spectrum. The binary and compound emission spectra are constructed.

binemission

In *binemission*, the decay from the primary compound nucleus to residual nuclei is converted from the excitation energy grid to emission energies. Due to interpolation errors, there is always a small difference between the binary continuum cross section and the integral of the spectrum over the continuum. The spectrum is accordingly normalized. The interpolation is performed for both inclusive and exclusive channels.

binaryrecoil

Subroutine *binaryrecoil* calculates the recoil and ejectile spectra in the LAB frame from the ejectile spectra calculated in the CM frame. The following subroutines are called:

```
binaryrecoil
|--cm2lab
|--labsurface
   |--belongs
   |--binsurface
      |--intri
         |--sideline
      |--intersection
         |--belongs
      |--invect
      |--belongs
```

cm2lab

Subroutine *cm2lab* performs the classical kinematical transformation from the center of mass frame to the LAB frame. For massive ejectiles the CM emission energy is converted into a CM emission velocity and is then vectorially coupled with the CM velocity to deduce the LAB velocity. No coupling is performed for photons. The same subroutine is used to calculate the recoil velocities.

labsurface

Subroutine *labsurface* is used to calculate the way the area of a triangle defined by three points is distributed in a given bidimensional grid.

belongs

This function tests if a real number is inside or outside a given bin.

binsurface

This subroutine returns the area of a given bidimensional bin covered by a triangle.

intri

This function tests if a point is inside or outside a triangle.

sideline

This function tells if a point is on one side or on the other side of a given line.

intersection

Subroutine *intersection* determines the intersection points of a straight line with a given bidimensional bin.

invect

This function tests if a point is within a segment or not.

8.4.16 angdis

In *angdis*, angular distributions for discrete states are calculated. This is done through Legendre polynomials for direct, compound and the total contribution per discrete state. The following subroutines are called:

```
angdis
|--plegendre
|--angdisrecoil
```

angdisrecoil

Subroutine *angdisrecoil* calculates the recoil and ejectile spectra in the LAB frame from the ejectile spectra calculated in the CM frame. The following subroutines are called:

```
angdisrecoil
|--cm2lab
|--labsurface >
```

8.4.17 multiple

This is the subroutine for multiple emission. We loop over all residual nuclei, starting with the initial compound nucleus (Zcomp=0, Ncomp=0), and then according to decreasing Z and N. For each encountered residual nuclide in the chain, we determine its nuclear structure properties. In total, the following nested loops are performed for multiple Hauser-Feshbach decay:

- compound nuclides Zcomp,Ncomp
- mother excitation energy bins
- compound nucleus parity
- total angular momentum J of compound nucleus
- (in *compound*) outgoing particles and gammas
- (in *compound*) outgoing excitation energies
- (in *compound*) residual parity
- (in *compound*) residual spin
- (in *compound*) j of outgoing channel
- (in *compound*) l of outgoing channel

Before the *compound subroutine* is entered there is a call to the multiple pre-equilibrium subroutine *multipreeq(2)* to deplete the flux if enough fast-particle flux is present. The following subroutines are called:

```
multiple
|--excitation
|--structure  >
|--exgrid     >
|--basicxs    >
|--levelsout
|--densityout >
|--fissionparout
|--cascade
|--densprepare >
|--multipreeq2
|--multipreeq
|--tfission   >
|--compound
|--tfissionout
|--compemission
|--kalbach
```

excitation

Subroutine for initial population of a nucleus. If there is no nuclear reaction specified, buth the starting condition is a populated nucleus, in this subroutine the initial population is redistributed over the excitation energy bins.

cascade

Subroutine for the gamma-ray cascade. The discrete gamma line intensities are stored.

multipreeq2

Subroutine for the two-component multiple preequilibrium model. A loops over all possible particle-hole excitations of the mother bin is performed. From each configuration, a new exciton model calculation is launched (**mpreeqmode 1**) or a simple transmission coefficient method is used (**mpreeqmode 2**). The particle-hole configurations of all residual nuclides are populated with the emitted pre-equilibrium flux. The depletion factor to be used for multiple compound emission is determined. The following subroutines are called:

```
multipreeq2
|--ignatyuk
|--phdens2    >
|--exchange2
|--lifetime2
|--locate
```

multipreeq

Subroutine for the one-component multiple preequilibrium model. A loops over all possible particle-hole excitations of the mother bin is performed. From each configuration, a new exciton model calculation is launched (**mpreeqmode 1**) or a simple transmission coefficient method is used (**mpreeqmode 2**). The particle-hole configurations of all residual nuclides are populated with the emitted pre-equilibrium flux. The depletion factor to be used for multiple compound emission is determined. The following subroutines are called:

```
multipreeq
|--ignatyuk
|--phdens     >
|--emissionrate >
|--lifetime >
|--locate
```

compound

Subroutine with the Hauser-Feshbach model for multiple emission. the nested loops are the same as those described for *comptarget*, with the exception of j and l of the incident channel, since we start from an excitation energy bin with a J, P value. In order to get do-loops running over integer values, certain quantum numbers are multiplied by 2, which can be seen from a 2 present in the corresponding variable names. For each loop, the begin and end point is determined from the triangular rule.

For every J and P (parity), first the denominator (total width) denomhf for the Hauser-Feshbach formula is constructed. Inside the nested loops, compound nucleus calculations for photons, particles and fission are performed.

compemission

In *compemission*, the compound nucleus emission spectra are determined from the multiple Hauser-Feshbach decay scheme. The decay from compound to residual nuclei is converted from the excitation energy grid to emission energies. The spectrum is obtained by spreading the decay over the mother bin and, in the case of continuum-continuum transitions, the residual bin. For each mother excitation energy bin, we determine the highest possible excitation energy bin for the residual nuclei. As reference, we take the top of the mother bin. The maximal residual excitation energy is obtained by subtracting the separation energy from this. Various types of decay are possible:

- Decay from continuum to continuum. For most residual continuum bins, no special care needs to be taken and the emission energy that characterizes the transition is simply the average between the highest energetic transition that is possible and the lowest.

- Decay from continuum to discrete. The lowest possible mother excitation bin can not entirely decay to the discrete state. For the residual discrete state, it is checked whether the mother excitation bin is such a boundary case. This is done by adding the particle separation energy to the excitation energy of the residual discrete state.

When the decay type has been identified, the decay from the population is distributed over the emission energy bins. All possible end point problems are taken into account. The following subroutines are called:

```
compemission
|--locate
|--comprecoil
```

comprecoil

If **recoil y**, the recoil and/or light particle spectra in the LAB frame are calculated in *comprecoil*. The following subroutines are called:

```
comprecoil
|--kalbach
|--cm2lab
|--labsurface >
```

8.4.18 channels

In *channels*, the exclusive reaction cross sections and spectra as outlined in Section 3.2.2 are calculated. A loop over all residual nuclides is performed and it is determined whether the residual nucleus under consideration can be reached by a certain particle combination. The associated gamma-ray production and isomeric exclusive cross sections are also computed. Finally, numerical checks with the total cross sections are performed. The following subroutines are called:

```
channels
|--specemission
   |--locate
```

specemission

In *specemission*, the exclusive emission spectra are computed. The procedure is analogous to that of *compemission*.

8.4.19 totalxs

In this subroutine, a few total cross sections are cumulated, such as the continuum exclusive cross section, the total particle production cross section and the total fission cross section.

8.4.20 spectra

In *spectra*, smoothed discrete cross sections are added to the emission spectra. A more precise energy grid at the high-energy tail is created to account for the structure of discrete states. This is done for both angle-integrated and double-differential spectra. The following subroutines are called:

```
spectra
|--locate
```

8.4.21 massdis

In *massdis* the fission fragment and product yields are calculated. A loop over all fissioning systems is performed. Some of the excitation energy bins are lumped into larger energy bins to save computation time. The fission yields per fissioning system are weighted with the fission cross section and added to form the total yield. The following subroutines are called:

```
massdis
|--brosafy
   |--spline
   |--ignatyuk
   |--trans
      |--funcfismode
         |--ignatyuk
         |--splint
         |--density    >
      |--trapzd
         |--funcfismode
   |--splint
   |--neck
      |--bdef
         |--fcoul
         |--fsurf
      |--ignatyuk
      |--fmin
      |--rpoint
         |--vr2
      |--vr1
      |--vr2
      |--vr3
      |--rtbis
      |--evap
         |--bdef
      |--sform
      |--rhodi
      |--fidi
         |--vr1
         |--vr2
         |--vr3
```

brosafy

In this subroutine the fission fragment and product mass yields are determined per fissioning system. The relative contribution of each fission mode is calculated. Subsequently, the fission yields per fission mode are calculated and summed with the fission mode weight.

spline

This subroutine performs a spline fit to the fission mode barrier parameters and the deformation parameters used in the subroutine *neck*.

trans

This subroutine calculates the fission transmission coefficient per fission mode to determine the relative contribution of each fission mode.

funcfismode

This function corresponds to the expression of the fission transmission coefficient.

splint

This subroutine uses the spline fit obtained in the subroutine *spline* to interpolate.

neck

In this subroutine the actual fission fragment and product mass yield per fission mode is computed based on the Random-neck Rupture model.

bdef

This subroutine computes the binding energy of a deformed nucleus with an eccentricity by the droplet model without shell corrections.

fcoul

This function contains the form factor for the Coulomb self energy.

fsurf

This function contains the form factor for the surface energy.

fmin

This subroutine searches the minimal value of a function.

rpoint

This subroutine is used to calculate the rupture point *zriss* for a given nucleon number hidden in the left-hand side of the dinuclear complex.

vr1

This function gives the volume of the projectile-like section.

vr2

This function gives the volume of the neck.

vr3

This function gives the volume of the target-like section.

evap

This function is used to determine the number of evaporated neutrons for a given fission fragment.

sform

This function determines the form factor for the coulomb interaction energy between two spheroids.

rhodi

This function computes the shape of the dinuclear system.

fidi

This function determines the exact shape of the dinuclear complex.

8.4.22 residual

In *residual*, the residual production cross sections, both total and isomeric, are stored in arrays.

8.4.23 totalrecoil

In this subroutine, the total recoil results are assembled.

8.4.24 thermal

In *thermal*, the cross sections down to thermal energies are estimated. For non-threshold channels, the cross sections are extrapolated down to 1.e-5 eV. Capture values at thermal energies are used. For energies up to 1 eV, the 1/sqrt(E) law is used. Between 1 eV and the first energy at which TALYS performs the statistical model calculation, we use logarithmic interpolation. The following subroutines are called:

```
thermal
|--pol1
```

8.4.25 output

Subroutine *output* handles the output of all cross sections, spectra, angular distributions, etc. per incident energy. The following subroutines are called:

```
output
|--totalout
|--binaryout
|--productionout
|--residualout
|--fissionout
|--discreteout
|--channelsout
|--spectraout
|--recoilout
|--angleout
|--ddxout
   |--locate
|--gamdisout
```

totalout

Subroutine for the output of total cross sections, such as total, non-elastic, pre-equilibrium, direct, etc.

binaryout

Subroutine for the output of the binary cross sections.

productionout

Subroutine for the output of particle production cross sections and total fission cross section.

residualout

Subroutine for the output of residual production cross sections.

fissionout

Subroutine for the output of fission cross sections per fissioning nuclide.

discreteout

Subroutine for the output of cross sections for discrete states for inelastic and other non-elastic channels.

channelsout

Subroutine for the output of exclusive channel cross sections and spectra, including ground state and isomer production and fission.

spectraout

Subroutine for the output of angle-integrated particle spectra.

recoilout

Subroutine for the output of recoil information.

angleout

Subroutine for the output of angular distributions for elastic scattering, inelastic scattering to discrete states and non-elastic scattering to other discrete states.

ddxout

Subroutine for the output of double-differential cross sections.

gamdisout

Subroutine for the output of discrete gamma-ray production.

8.4.26 finalout

In *finalout*, all results are printed as a function of incident energy, i.e. all excitation functions. This information appears in the main output file and/or in separate output files per reaction channel. Also, general nuclear model parameters are written to the parameter file.

8.4.27 astro

Subroutine for astrophysical reaction rates. The following subroutines are called:

```
|--stellarrate
   |--partfunc
|--astroout
```

stellarrate

Subroutine for the calculation of the reaction rate for a Maxwell-Boltzmann distribution.

partfunc

Partition function for astrophysical calculations.

astroout

Subroutine for the output of astrophysical reaction rates.

8.4.28 endf

Subroutine for the output of cross sections and information for the production of an ENDF-6 file. The following subroutines are called:

```
endf
|--endfinfo
|--endfenergies
|--endfecis
   |--optical    >
   |--ecisinput  >
|--endfread
   |--tripathi   >
```

endfinfo

Subroutine for writing the general information (i.e. the main reaction parameters) needed to create an ENDF-6 file.

endfenergies

Subroutine to create the energy grid for cross sections for an ENDF-6 file. This grid ensures that the total, elastic and reaction cross section are calculated on a sufficiently precise energy grid. Thresholds for all partial cross sections are also added to this grid.

endfecis

In this subroutine the loop over the energy grid created in *endfenergies* is done to perform basic ECIS calculations. The optical model parameters are determined by calling *optical*. The subroutine *ecisinput* is called for the creation of the ECIS input files. At the end of this subroutine, *ecis06t* is called to perform the actual ECIS calculation.

endfread

In this subroutine the results from ECIS are read. For every incident energy we read the reaction (and for neutrons the total and elastic) cross sections. These are then written to a separate file for ENDF-6 formatting.

8.5 Programming techniques

In general, we aim to apply a fixed set of programming rules consistently throughout the whole code. Here are some of the rules we apply to enforce readability and robustness:

- We use suggestive variable names as much as possible.

- Every variable in a subroutine, apart from dummy variables appearing in e.g. a do loop, is explained once in the comment section. In addition, we aim to give as much explanation as possible for the used algorithms.
- We use **implicit none** as the first line of *talys.cmb* and all stand-alone subroutines and functions. This means that every variable must be declared, which is a powerful recipe against typing errors.
- We program directly "from the physics", as much as possible, i.e. we use array indices which correspond one-to-one to the indices of the physical formulae from articles and books.
- Cosmetical features:
  - Different tasks within a subroutine are clearly separated. A block, which contains one subtask, is separated by asterisks, e.g.
    c
    c *************************** Constants ******************************
    c
    The last asterisk is always in column 72. In the first block, the labels are numbered 10, 20, 30, etc. In the second block, the labels are numbered 110, 120, 130, etc.
  - We indent two blanks in do loops and if statements.
- In the file *talys.cmb*, we systematically store variables of type logical, character, integer, real and double precision in separate common blocks. The order of appearance of variables in *talys.cmb* follows that of the subroutines.
- Every subroutine has the same heading structure: We give the author, date and task of the subroutine. Next, the file *talys.cmb* is included, followed by the inclusion of declarations for possible local variables.
- We use nuclear model parameterisations that are as general as possible within the programmed nuclear reaction mechanisms, to enable easy implementation of future refinements. For example, level densities will never be hardwired "on the spot", but will be called by a function *density*. An improvement, or alternative choice, of a level density model will then have a consistent impact throughout the whole code.
- If there are exceptions to the procedures outlined above, it is probably since a few subroutines have been adopted from other sources, such as the collection of old style subroutines for the fission yields model.

As a general rule, although we aim to program as clever as possible, we always prefer readability over speed and memory economy. Some nuclear physicists are more expensive than computers, or at least should be.

8.6 Changing the array dimensions

As explained in the previous sections, almost all arrays are defined in the common block file *talys.cmb*. At the top of *talys.cmb*, the parameters are set for the dimensions of the various arrays. Their names all start with **num**. Most of these parameters should be left untouched, because they determine basic quantities of a nuclear model calculation. Some of them can however be changed. They can be reduced, for the case that the working memory of your computer is too small, or be increased, in cases where you want to perform more extensive or precise calculations than we thought were necessary. However, in normal cases you only need to change the keyword values in the input file and not the parameters in *talys.cmb*. In the standard version of TALYS, the latter already have reasonable values. Nevertheless, the following parameters can be changed and will have a significant effect:

- **memorypar**: general multiplication factor for dimensions of several arrays. Use a small value for a small computer. Normally, changing this parameter does not require any further changes of the parameters that follow below.

- **numbins**: the maximum number of continuum excitation energy bins in the decay chains. Obviously, this could be increased to allow for more precision.

- **numZchan**, **numNchan** and **numchantot**: the depth to which exclusive reaction channels are followed can be set by these parameters. However, as mentioned in Section 3.2.2, exclusive channels that go beyond 4 outgoing particles are rarely of interest (only for certain activation codes that work at high energies). Also, since the exclusive reaction calculation involves some large arrays, one may easily run into memory problems by choosing too large values. If one works on e.g. a 64 Mb machine it may be helpful, or even necessary, to choose smaller values if one is not interested in exclusive calculations at all. Table 8.1 displays the values that are theoretically possible. In this table, we use
$$\mathbf{numchantot} = \sum_{m=0}^{\mathbf{numchannel}} \binom{m+5}{m} \tag{8.1}$$
which is the total number of channels for 6 different outgoing particles (neutrons up to alpha particles) if we go **numchannels** particles deep. In practice, less are needed since many channels never open up and this is what we have assumed by setting the value for **numchantot** in *talys.cmb*.

- **numZ** and **numN**: The maximum number of proton and neutron units, respectively, away from the initial compound nucleus that can be reached after multiple emission. If you want to try your luck with TALYS at very high incident energies, these parameters may need to be increased.

- **numlev**: The maximum number of included discrete levels.

- **numang**: The maximum number of outgoing angles for discrete states.

- **numangcont**: The maximum number of outgoing angles for the continuum.

Obviously, after increasing these values you still need to set the associated keywords in the input file to use the increased limits, although some of them, e.g. **maxZ**, are always by default set to their maximum value. You could increase a parameter and simultaneously reduce another one that is of no relevance to the particular problem under study, to remain within the available memory of your computer. Of course, you should always completely re-compile TALYS after changing anything in *talys.cmb*.

Table 8.1: Theoretical number of exclusive channels for outgoing particles of 6 different types

numchannnel	number of channels	numchantot
0	1	1
1	6	7
2	21	28
3	56	84
4	126	210
5	252	462
6	462	924
7	792	1716
8	1287	3003
9	2002	5005
10	3003	8008

Chapter 9

Outlook and conclusions

This manual describes TALYS-1.0, a nuclear reaction code developed at NRG Petten and CEA Bruyères-le-Châtel. After several years of development, and application in various areas, by many users [1]-[50], we decided that after the previous (TALYS-0.64, TALYS-0.72) beta releases, the first official Version 1.0 of the code was ready to be released.

We note that various extensions are possible for the physics included in TALYS, and some will be mentioned below. Obviously, we can not guarantee that these will be included in a future release (if any). This depends on the required effort, future careers of the authors, your willingness to share your extensions with us, our willingness to implement them, and in the case of significant extensions, financial input from research programs that require nuclear data.

In general, the nuclear structure database can still be extended with more tables produced with microscopic methods, for e.g. particle-hole state densities. Through a trivial change in the TALYS code, the impact of these ingredients on reaction calculations can immediately be tested.

The default local and global spherical and deformed optical models that are used in TALYS are quite powerful. However, it would be good to extend the optical model database with more cases. A connection with the RIPL OMP database is then the most obvious. Another extension is needed for light nuclides $(A < 24)$. Also, TALYS is already being used with microscopic OMPs, but only with the spherical JLM method. An extension to deformed JLM is feasible. A few direct reaction items, such as the prediction of the Isobaric Analogue State, are also yet to be completed.

In the unresolved resonance range, we could implement an approach based on average resonance parameters, by allowing more flexibility per (l-dependent) transmission coefficient. This would improve especially the calculated capture and total cross sections in the tens to hundreds of keV range.

One type of observable still missing is the fission neutron spectrum. For this, both phenomenological and more physical approaches (in the latter, one would perform a loop over all excited fission fragments) are possible. Simultaneously, models for simulating the number of prompt and delayed neutrons could be included. In general, the fission parameter database for TALYS still needs to be settled. A general analysis of all actinides simultaneously should result in a stable, ready-to-use fission database. It is clear that the theoretical fission models themselves are also not yet mature, even though microscopic fission paths are now included.

Concerning continuum reactions, there exists a microscopic multi-step direct code, MINGUS, for quantum-mechanical pre-equilibrium calculations(MSD/MSC) [116], which still needs to be merged with TALYS.

Coupling with high-energy intranuclear cascade (INC) codes is possible, now that TALYS is able to take a pre-defined population distribution as the starting point. The INC code would take care of energies above e.g. 200 MeV, while TALYS takes over below that cut-off energy. The well-validated pre-equilibrium and Hauser-Feshbach approach at lower energies may then lead to more precise simulated data (including isomer production), even for reactions in the GeV range.

As for computational possibilities, the current day computer power enables to use nuclear model codes in ways that were previously thought impossible. Activities that have already proven to be possible are the generation of nuclear-model based covariances with Monte Carlo methods, automatic multi-parameter fitting of all partial cross sections to the existing experimental data, and dripline-to-dripline generation of all cross sections over the entire energy and projectile range. The applications range from basic science (e.g. astrophysics) to the production of nuclear data libraries for existing and future nuclear technologies.

We are considering a complete upgrade of TALYS to Fortran90/95. For the moment, however, we have restricted ourselves to adding as much modules to TALYS as possible, using Fortran77, without letting that project interfere with the use of other programming languages. Once we feel TALYS has reached a certain level, in terms of included physics and options, that calls for a global upgrade to a more modern language, we will certainly do so and we will apply such an update to the whole code *at once*. At the moment, all authors of TALYS master at least Fortran77, which is a strong argument in favor of the present approach. However, TALYS-1.0 is probably the last version for which we insist on full Fortran77 compatibility. A huge extra effort would be needed to make our methods fully quality assured, even though we know that already we are deviating from those currently practised in computational nuclear science.

There are two important satellite codes for TALYS, written at NRG, that have appeared in the literature: TASMAN [19], for determining nuclear model based covariances and automatic optimization to experimental data, and TEFAL [7], for translating the results of TALYS into ENDF-6 data libraries. However, this is proprietary software, and it is not yet foreseen that this software becomes generally available.

The development of TALYS has always followed the “first completeness, then quality” principle. This merely means that, in our quest for completeness, we tried to divide our effort equally among all nuclear reaction types. We think that, with the exception of a few issues the code is indeed *complete* in terms of predicted quantities. We now hope that TALYS also qualifies for “completeness and quality”. Nevertheless, it is certain that future theoretical enhancements as suggested above are needed to bring our computed results even closer to measurements.

Bibliography

[1] A.J. Koning, S. Hilaire and M.C. Duijvestijn, "TALYS: Comprehensive nuclear reaction modeling", *Proceedings of the International Conference on Nuclear Data for Science and Technology - ND2004*, AIP vol. 769, eds. R.C. Haight, M.B. Chadwick, T. Kawano, and P. Talou, Sep. 26 - Oct. 1, 2004, Santa Fe, USA, p. 1154 (2005).

[2] A.J. Koning, S. Hilaire and M.C. Duijvestijn, "TALYS-1.0", *Proceedings of the International Conference on Nuclear Data for Science and Technology - ND2007*, May 22 - 27, 2007, Nice, France.

[3] A.J. Koning and M.C. Duijvestijn, "New nuclear data evaluations for Ge isotopes" Nucl. Instr. Meth. B248, 197 (2006).

[4] A.J. Koning, M.C. Duijvestijn, S.C. van der Marck, R. Klein Meulekamp, and A. Hogenbirk, "New nuclear data libraries for Pb and Bi and their impact on ADS design", Nucl. Sci. Eng. 156, p. 357-390 (2007).

[5] M.C. Duijvestijn and A.J. Koning, "New intermediate-energy nuclear data libraries for Fe", Ann. Nuc. En. 33, 1196 (2006).

[6] A.J. Koning and M.C. Duijvestijn, "New nuclear data evaluations for Ca and Sc isotopes" Journ. Nucl. Sci. Techn. 44, no.6, p. 823-837 (2007).

[7] A.J. Koning, M.C. Duijvestijn, S.C. van der Marck, R. Klein Meulekamp, and A. Hogenbirk, "New nuclear data evaluations for Ca, Sc, Fe, Ge, Pb, and Bi isotopes" *Proceedings of the International Conference on Nuclear Data for Science and Technology - ND2004*, AIP vol. 769, eds. R.C. Haight, M.B. Chadwick, T. Kawano, and P. Talou, Sep. 26 - Oct. 1, 2004, Santa Fe, USA, p. 422 (2005).

[8] A.J. Koning and M.C. Duijvestijn, "Nuclear theory for high-energy nuclear reactions of biomedical relevance", Radiation Protection Dosimetry 2007; doi: 10.1093/rpd/ncm008 (Proceedings of the Tenth Symposium on Neutron Dosimetry, Uppsala, June 12-16 2006.)

[9] P. Romain, B. Morillon, and A.J. Koning, "Neutron actinides evaluations with the TALYS code", *Proceedings of the Workshop on Neutron Measurements, Evaluations and Applications - 2*, October 25-28, 2006 Borovets, Bulgaria (2006), EUR 22794 EN, p. 113-116 (2007).

[10] A.J. Koning and M.C. Duijvestijn, Nucl. Phys. **A744** (2004) 15.

[11] P. Demetriou, Ch. Dufauquez, E. El Masri, and A.J. koning, “Light charged-particle production from proton and alpha-induced reactions on ^{nat}Si at energies from 20 to 65 MeV: A theoretical analysis”, Phys Rev C72, 034607 (2005).

[12] S. Goko, H. Utsonomiya, S. Goriely, A. Makinaga, T. Kaihori, S. Hohara, H. Akimune, T. Yamagata, Y.-W. Lui, H. Toyokawa, A.J. Koning, and S. Hilaire, “Partial photoneutron cross sections for the isomeric state Ta-180m”, Phys. Rev. Lett. 96, 192501 (2006).

[13] V. Tatischeff, B. Kozlovsky, J. Kiener, R. J. Murphy, “Delayed X and GammaRay Line Emission from Solar Flare Radioactivity”, Astro. Journ. Supp. Series, 165:606-617 (2006).

[14] V. Semkova, R.J. Tornin, A.J. Koning, A. Moens, A. Plompen, “New cross section measurements for neutron-induced reactions on Cr, Ni, Cu, Ta and W isotopes obtained with the activation technique”, *Proceedings of the International Conference on Nuclear Data for Science and Technology - ND2007*, May 22 - 27, 2007, Nice, France.

[15] L.C. Mihailescu, P. Baumann, C. Borcea, P. Dessagne, E. Jericha, M. Kerveno, S. Lukic, A.J. Koning, A. Pavlik, A.J.M. Plompen, G. Rudolf, “High resolution neutron (n,xn) cross section measurements for 206,207,208Pb and 209Bi from threshold up to 20 MeV”, *Proceedings of the International Conference on Nuclear Data for Science and Technology - ND2007*, May 22 - 27, 2007, Nice, France.

[16] S. Goriely, S. Hilaire and A.J. Koning, “Improved predictions of nuclear reaction rates for astrophysics applications with the TALYS reaction code”, *Proceedings of the International Conference on Nuclear Data for Science and Technology - ND2007*, May 22 - 27, 2007, Nice, France.

[17] A.J. Koning, S. Hilaire and M.C. Duijvestijn, “Predicting nuclear reactions with TALYS”, *Proceedings of the Workshop on Neutron Measurements, Evaluations and Applications - 2*, October 20-23, 2004 Bucharest, Romania (2006), ed. A. Plompen,
htpp://www.irmm.jrc.be/html/publications/technical_reports/index.htm

[18] A.J. Koning, “Current status and future of nuclear model-based data evaluation”, in *Perspectives on Nuclear Data for the Next Decade*, CEA-DIF Bruyères-le-Châtel, France, September 26-28 2005.

[19] A.J. Koning,“Generating covariance data with nuclear models”, Proceedings of the International Workshop on “Nuclear data Needs for Generation IV Nuclear energy systems, Antwerpen, April 5-7, 2005, ed. P. Rullhusen, World Scientific (2006), p. 153.

[20] U. Tippawan, S. Pomp, A. Atac, B. Bergenwall, J. Blomgren, S. Dangtip, A. Hildebrand, C. Johansson, J. Klug, P. Mermod, L. Nilsson, M. Osterlund, N. Olsson, A.V. Prokofiev, P. Nadel-Turonski, V. Corcalciuc, and A.J. Koning, “Light-ion production in the interaction of 96 MeV neutrons with oxygen”, Phys. Rev. C73, 034611 (2006).

[21] E. Khan, S. Goriely, D. Allard, E. Parizot, T. Suomijarvi, A.J. Koning, S. Hilaire, and M.C. Duijvestijn,“Impact of the giant dipole resonance on the photodisintegration of ultrahigh energy cosmic rays”, Astroparticle physics Volume 23, Issue 2, 191 (2005).

[22] V. Avrigeanu, S.V. Chuvaev, R. Eichin, A.A. Filatenkov, R.A. Forrest, H. Freiesleben, M. Herman, A.J. Koning and K. Seidel, "Pre-equilibrium reactions on the stable tungsten isotopes at low energy", Nucl. Phys. A765, p. 1 (2006).

[23] M.C. Duijvestijn and A.J. Koning, "Exciton model calculations up to 200 MeV: the optical model points the way", *Proceedings of the International Conference on Nuclear Data for Science and Technology - ND2004*, AIP vol. 769, eds. R.C. Haight, M.B. Chadwick, T. Kawano, and P. Talou, Sep. 26 - Oct. 1, 2004, Santa Fe, USA, p. 1150 (2005).

[24] M.C. Duijvestijn and A.J. Koning, "Fission yield predictions with TALYS", *Proceedings of the International Conference on Nuclear Data for Science and Technology - ND2004*, AIP vol. 769, eds. R.C. Haight, M.B. Chadwick, T. Kawano, and P. Talou, Sep. 26 - Oct. 1, 2004, Santa Fe, USA, p. 1225 (2005).

[25] S. Hilaire, Ch. Lagrange, and A.J. Koning, "Comparisons between various width fluctuation correction factors for compound nucleus reactions", Ann. Phys. **306**, 209 (2003).

[26] E. Dupont, E. Bauge, S. Hilaire, A. Koning, and J.-C. Sublet, "Neutron Data Evaluation and Validation of Rhodium-103", *Proceedings of the International Conference on Nuclear Data for Science and Technology - ND2004*, AIP vol. 769, eds. R.C. Haight, M.B. Chadwick, T. Kawano, and P. Talou, Sep. 26 - Oct. 1, 2004, Santa Fe, USA, p. 95 (2005).

[27] Udomrat Tippawan, Stephan Pomp, Ayse Atac, Bel Bergenwall, Jan Blomgren, Somsak Dangtip, Angelica Hildebrand, Cecilia Johansson, Joakim Klug, Philippe Mermod, Leif Nilsson, Michael Osterlund, Klas Elmgren, Nils Olsson, Olle Jonsson, Alexander Prokofiev, P.-U. Renberg, Pawel Nadel-Turonski, Valentin Corcalciuc, Yukinobu Watanabe, Arjan Koning, "Light-ion production in the interaction of 96 MeV neutrons with silicon" *Proceedings of the International Conference on Nuclear Data for Science and Technology - ND2004*, AIP vol. 769, eds. R.C. Haight, M.B. Chadwick, T. Kawano, and P. Talou, Sep. 26 - Oct. 1, 2004, Santa Fe, USA, p. 1592 (2005).

[28] R. Michel, M. Gloris, J. Protoschill, M.A.M. Uosif, M. Weug, U. Herpers, J. Kuhnhenn, P.-W. Kubik, D. Schumann, H.-A. Synal, R. Weinreich, I. Leya, J.C. David, S. Leray, M. Duijvestijn, A. Koning, A. Kelic, K.H. Schmidt, and J. Cugnon, "From The HINDAS Project: Excitation Functions For Residual Nuclide Production By Proton-Induced Reactions", *Proceedings of the International Conference on Nuclear Data for Science and Technology - ND2004*, AIP vol. 769, eds. R.C. Haight, M.B. Chadwick, T. Kawano, and P. Talou, Sep. 26 - Oct. 1, 2004, Santa Fe, USA, p. 1551 (2005).

[29] R. Michel, W. Glasser, U. Herpers, H. Schuhmacher, H.J. Brede, V. Dangendorf, R. Nolte, P. Malmborg, A.V. Prokofiev, A.N. Smirnov, I. Rishkov, D. Kollar, J.P. Meulders, M. Duijvestijn, and A. Koning, "Residual Nuclide Production From Iron, Lead, And Uranium By Neutron-Induced Reactions Up To 180 MeV", *Proceedings of the International Conference on Nuclear Data for Science and Technology - ND2004*, AIP vol. 769, eds. R.C. Haight, M.B. Chadwick, T. Kawano, and P. Talou, Sep. 26 - Oct. 1, 2004, Santa Fe, USA, p. 861 (2005).

[30] M.A.M. Uosif, R. Michel, U. Herpers, P.-W. Kubik, M. Duijvestijn, and A. Koning, "Residual Nuclide Production By Proton-Induced Reactions On Uranium For Energies Between 20 MeV

And 70 MeV", *Proceedings of the International Conference on Nuclear Data for Science and Technology - ND2004*, AIP vol. 769, eds. R.C. Haight, M.B. Chadwick, T. Kawano, and P. Talou, Sep. 26 - Oct. 1, 2004, Santa Fe, USA, p. 1547 (2005).

[31] Vilen P. Eismont, Nikolay P. Filatov, Andrey N. Smirnov, Gennady A. Tutin, Jan Blomgren, Henri Conde, Nils Olsson, Marieke C. Duijvestijn, and Arjan J. Koning, "On Nuclear Structure Effects in the Nucleon-Induced Fission Cross Sections of Nuclei Near 208Pb at Intermediate Energies", *Proceedings of the International Conference on Nuclear Data for Science and Technology - ND2004*, AIP vol. 769, eds. R.C. Haight, M.B. Chadwick, T. Kawano, and P. Talou, Sep. 26 - Oct. 1, 2004, Santa Fe, USA, p. 629 (2005).

[32] Vilen P. Eismont, Nikolay P. Filatov, Sergey N. Kirillov, Andrey N. Smirnov, Jan Blomgren, Henri Conde, Nils Olsson, Marieke C. Duijvestijn, and Arjan J. Koning, "Angular Anisotropy of Intermediate Energy Nucleon-Induced Fission of Pb Isotopes and Bi", *Proceedings of the International Conference on Nuclear Data for Science and Technology - ND2004*, AIP vol. 769, eds. R.C. Haight, M.B. Chadwick, T. Kawano, and P. Talou, Sep. 26 - Oct. 1, 2004, Santa Fe, USA, p. 633 (2005).

[33] Andrey N. Smirnov, Vilen P. Eismont, Nikolay P. Filatov, Sergey N. Kirillov, Jan Blomgren, Henri Conde, Nils Olsson, Marieke C. Duijvestijn, and Arjan J. Koning, "Correlation of Intermediate Energy Proton- and Neutron-Induced Fission Cross Section in the Lead-Bismuth Region", *Proceedings of the International Conference on Nuclear Data for Science and Technology - ND2004*, AIP vol. 769, eds. R.C. Haight, M.B. Chadwick, T. Kawano, and P. Talou, Sep. 26 - Oct. 1, 2004, Santa Fe, USA, p. 637 (2005).

[34] Oleg I. Batenkov, Vilen P. Eismont, Mikhail I. Majorov, Andrey N. Smirnov, Kjell Aleklett, Walter Loveland, Jan Blomgren, Henri Conde, Marieke C. Duijvestijn, and Arjan J. Koning, "Comparison of Experimental and Calculated Mass Distributions of Fission Fragments in Proton-Induced Fission of 232Th, 235U, 238U and 237Np in the Intermediate Energy Region", *Proceedings of the International Conference on Nuclear Data for Science and Technology - ND2004*, AIP vol. 769, eds. R.C. Haight, M.B. Chadwick, T. Kawano, and P. Talou, Sep. 26 - Oct. 1, 2004, Santa Fe, USA, p. 625 (2005).

[35] C. Dufauquez, Y. El Masri, V. Roberfroid, J. Cabrera, Th. Keutgen, J. van Mol, V. Demetriou, and A.J. Koning, "Light charged and neutral particles emission in proton and alpha induced reactions on ^{nat}Si between 20 and 65 MeV, *Proceedings of the International Conference on Nuclear Data for Science and Technology - ND2004*, AIP vol. 769, eds. R.C. Haight, M.B. Chadwick, T. Kawano, and P. Talou, Sep. 26 - Oct. 1, 2004, Santa Fe, USA, p. 941 (2005).

[36] V. Avrigeanu, R. Eichin, R.A. Forrest, H. Freiesleben, M. Herman, A.J. Koning, and K. Seidel, "Sensitivity Of Activation Cross Sections Of Tungsten To Nuclear Reaction Mechanisms", *Proceedings of the International Conference on Nuclear Data for Science and Technology - ND2004*, AIP vol. 769, eds. R.C. Haight, M.B. Chadwick, T. Kawano, and P. Talou, Sep. 26 - Oct. 1, 2004, Santa Fe, USA, p. 1501 (2005).

[37] U. Tippawan, S. Pomp, A. Atac, B. Bergenwall, J. Blomgren, S. Dangtip, A. Hildebrand, C. Johansson, J. Klug, P. Mermod, L. Nilsson, M. Osterlund, N. Olsson, K. Elmgren, O. Jonsson, A.V.

Prokofiev, P.-U. Renberg, P. Nadel-Turonski, V. Corcalciuc, Y. Watanabe, and A.J. Koning, "Light-ion production in the interaction of 96 MeV neutrons with silicon", Phys. Rev. C **69**, 064609 (2004).

[38] A.J. Koning,"HINDAS: Experiments, models and data libraries below 200 MeV", Proceedings of the International Workshop on Nuclear Data for the Transmutation of Nuclear Waste, eds. A. Kelic and K.-H. Schmidt, GSI Darmstadt, Sep 1-5 2003. http://www-wnt.gsi.de/tramu/.

[39] P. Reimer, V. Avrigeanu, S.V. Chuvaev, A.A. Filatenkov, T. Glodariu, A.J. Koning, A.J.M. Plompen, S.M. Qaim, D.L. Smith, and H. Weigmann, "Reaction mechanisms of fast neutrons on stable Mo isotopes below 21 MeV", submitted for publication in Phys. Rev. C (2003).

[40] J.P. Meulders, E. Raeymackers, I. Slypen, S. Benck, N. Nica, V. Corcalciuc and A.J. Koning, "Neutron-induced Light-charged particle production (E_n=25-65 MeV) on elements of ADS-interest, AccApp'03, Accelerator Applications in a Nuclear Renaissance, San Diego, USA, June 1-5 2003.

[41] V. Semkova, V. Avrigeanu, A.J. Koning, A.J.M. Plompen, D.L. Smith, and S. Sudar,"A systematic investigation of reaction cross sections and isomer ratios up to 20 MeV on Ni-isotopes and ^{59}Co by measurements with the activation technique and new model studies of the underlying reaction mechanisms", Nucl. Phys. **A730**, 255 (2004).

[42] I. Slypen, N. Nica, A.J. Koning, E. Raeymackers, S. Benck, J.P. Meulders, and V. Corcalciuc, "Light charged particle emission induced by fast neutrons with energies between 25 and 65 MeV on Iron", Journ. Phys. **G30**, 45 (2004).

[43] E. Raeymackers, S. Benck, N. Nica, I. Slypen, J.P. Meulders, V. Corcalciuc and A.J. Koning, "Light charged particle emission in fast neutron (25-65 MeV) induced reactions on ^{209}Bi nuclei", Nucl. Phys. **A726**, 175 (2003).

[44] E. Raeymackers, S. Benck, I. Slypen, J.P. Meulders, N. Nica, V. Corcalciuc and A. Koning, "Light charged particle production in the interaction of fast neutrons (25-65 MeV) with Uranium nuclei", Phys. Rev. C **68**, 24604 (2003)

[45] M. Kerveno, F. Haddad, Ph. Eudes, T. Kirchner, C. Lebrun, I. Slypen, J.P. Meulders, C. Le Brun, F.R. Lecolley, J.F. Lecolley, F. Lefèbvres, S. Hilaire and A.J. Koning, "Hydrogen isotope double-differential production cross sections induced by 62.7 MeV neutrons on a lead target", Phys. Rev. C **66**, 014601 (2002).

[46] M. Pandurovic, S. Lukic, P. Baumann, S. Hilaire, J. Jeknic, E. Jericha, S. Jokic, M. Kerveno, C. Mihailescu, A. Pavlik, A. Plompen, and G. Rudolf, Nucl. Techn. Rad. Prot. **18**, no. 1 (2003) 22.

[47] V. Semkova, V. Avrigeanu, A.J.M. Plompen, P. Reimer, D.L. Smith, S. Sudar, A. Koning, R. Forrest,"Neutron activation cross sections for safety of nuclear reactors", European Commission JRC report, EUR Report 20820 EN, 2003, ISBN 92-894-6095-4.

[48] L.C. Mihailescu, C. Borcea, A.J.M. Plompen, and A.J. Koning, "High resolution measurement of neutron inelastic scattering and (n,2n) cross-sections for 52Cr" Nucl. Phys A786, p. 1-23 (2007).

[49] M. Segawa, T. Masaki, Y.Nagai, Y.Temma, T.Shima, K. Mishima, M.Igashira, S. Goriely, A. Koning, and S. Hilaire, "Neutron capture cross sections of ^{186}Os, ^{187}Os, and ^{189}Os for the Re-Os chronology", Phys. Rev. C 76, 022802 (2007)

[50] M. Kerveno, P. Baumann, A. Nachab, G. Rudolf, A. Pavlik, E. Jericha, S. Jokic, S. Lukic, L. Mihailescu, A. Plompen, R. Nolte, M. Reginatto, J.P. Meulders, J. Jeknic, S. Hilaire, A.J. Koning, and the n-TOF collaboration, "Measurements of (n,xn) cross sections for hybrid systems", Proceedings of the 8th Information Exchange Meeting on Actinide and Fission Product Partitioning and Transmutation, Las Vegas, USA Nov 9-11 2004.

[51] P.G. Young, E.D. Arthur, and M.B. Chadwick, in *Workshop on Computation and Analysis of Nuclear Data Relevant to Nuclear Energy and Safety*, edited by M.K. Mehta and J.J. Schmidt, Feb. 10 - March 13 1992, Trieste, Italy, (1993), p. 622.

[52] M. Blann, in *Workshop on Computation and Analysis of Nuclear Data Relevant to Nuclear Energy and Safety*, edited by M.K. Mehta and J.J. Schmidt, Feb. 10 - March 13 1992, Trieste, Italy, (1993), p. 622.

[53] M. Uhl and B. Strohmaier, *Computer code for particle induced activation cross sections and related quantities*, IRK report No. 76/01, Vienna (1976).

[54] M. Herman, in *Workshop on Nuclear Reaction Data and Nuclear Reactors: Physics, Design and Safety*, edited by N. Paver, M. Herman and A. Gandini, March 13 - April 14 2000, Trieste Italy, (2001), p. 137.

[55] J. Raynal, *Notes on ECIS94*, CEA Saclay Report No. CEA-N-2772, (1994).

[56] *Handbook for calculations of nuclear reaction data: Reference Input Parameter Library*, http://www-nds.iaea.or.at/RIPL-2/.

[57] A.M. Baldin, *Kinematics of Nuclear Reactions*, Oxford University Press, (1961).

[58] M.B. Chadwick, P.G. Young, S. Chiba, S.C. Frankle, G.M. Hale, G. Hughes, A.J. Koning, R.C. Little, R.E. Macfarlane, R.E. Prael, and L.S. Waters, Nucl. Sci. Eng. **131** (1999), 293.

[59] M.B. Chadwick, P.G. Young, R.E. Macfarlane, and A.J. Koning, "High Energy Nuclear Data Libraries for Accelerator-Driven Technologies: Calculational Method for Heavy Recoils", *Second International Conference on Accelerator-Driven Transmutation Technologies and Applications*, Kalmar, Sweden, June 3-7 1996, 483.

[60] A.J. Koning and J.P. Delaroche, Nucl. Phys. **A713**, 231 (2003).

[61] S. Watanabe, Nucl. Phys. **8**, 484 (1958).

[62] D.G. Madland, in *Proceedings of a Specialists' Meeting on preequilibrium nuclear reactions*, Semmering, Austria, February 10-12 (1988), p. 103.

[63] E.Bauge, J.P. Delaroche, M. Girod, Phys. Rev. C **63**, 024607 (2001).

[64] F. Maréchal, T. Suomijärvi, Y.Blumenfeld, A. Azhari, E. Bauge, D. Bazin, J.A. Brown, P.D. Cottle, J.P. Delaroche, M. Fauerbach, M. Girod, T. Glassmacher, S.E. Hirzebruch, J.K. Jewel, J.H. Kelley, K.W. Kemper, P.F. Mantica, D.J. Morissey, L.A. Riley, J.A. Scarpaci, H. Sheit, M. Steiner, Phys. Rev C **60**, 034615 (1999).

[65] H. Sheit, F. Maréchal, T. Glassmacher, E. Bauge, Y.Blumenfeld, J.P. Delaroche, M. Girod, R.W. Ibbotson, K.W. Kemper, J. Libert, B. Pritychenko, T. Suomijärvi, Phys. Rev. C **63** 014604 (2000).

[66] E. Khan, T. Suomijärvi, Y.Blumenfeld, Nguyen Van Giai, N. Alamanos, F. Auger, E. Bauge, D. Beaumel, J.P. Delaroche, P. Delbourgo-Salvador, A. Drouart, S. Fortier, N. Frascaria, A. Gilibert, M. Girod, C. Jouanne, K.W. Kemper, A. Lagoyannis, V. Lapoux, A. Lépine-Szily, I. Lhenry, J. Libert, F. Maréchal, J.M. Maison, A. Mussumara, S. Ottini-Hustache, P. Piattelli, S. Pita, E.C. Pollaco, P. Roussel-Chomaz, D. Santonocito, J.E. Sauvestre, J.A. Scarpacci, T. Zerguerras, Nucl. Phys **A 694**, 103 (2001).

[67] E. Bauge, J.P. Delaroche, M. Girod, G. Haouat, J. Lachkar, Y. Patin, J. Sigaud, J. Chardine, Phys. Rev. C **61**, 034306 (2000).

[68] J.P. Jeukenne, A. Lejeune, and C. Mahaux, Phys. Rep. **25C**, 83 (1976).

[69] J.P. Jeukenne, A. Lejeune, and C. Mahaux, Phys. Rev. C **14**, 1391 (1974).

[70] J.P. Jeukenne, A. Lejeune, and C. Mahaux, Phys. Rev. C **15**, 10 (1977).

[71] J.P. Jeukenne, A. Lejeune, and C. Mahaux, Phys. Rev. C **16**, 80 (1977).

[72] E.Bauge, J.P. Delaroche, M. Girod, Phys. Rev. C **58** 1118 (1998).

[73] R.R. Scheerbaum, Nucl. Phys. **A257**, 77 (1976).

[74] R.K. Tripathi, F.A. Cucinotta and J.W. Wilson, NASA technical paper 3621, January 1997.

[75] T. Tamura, Rev. Mod. Phys. **37**, 679 (1965).

[76] J.P. Delaroche, in Proceedings of the International Symposium on *Nuclear Data Evaluation Methodology*, ed. C.L. Dunford, October 12-16 1992, Brookhaven, USA, p. 347.

[77] N. Olsson, E. Ramström, and B. Trostell, Nucl. Phys. **A513**, 205 (1990).

[78] B.V. Carlsson, in *Workshop on Nuclear Reaction Data and Nuclear Reactors: Physics, Design and Safety*, edited by N. Paver, M. Herman and A. Gandini, March 13 - April 14 2000, Trieste Italy, (2001), p. 61.

[79] E. Sh Soukhovitskii, S. Chiba, J.-Y. Lee, O. Iwamoto and T. Fukahori, J. Phys. G: Nucl. Part. Phys. 30, 905 (2004).

[80] P.P. Guss, R.C. Byrd, C.R. Howell, R.S. Pedroni, G. Tungate, R.L. Walter, and J.P. Delaroche, Phys. Rev. C **39**, 405 (1989).

[81] G.R. Satchler, *Direct Nuclear Reactions*, Oxford University Press, New York, 1983.

[82] P.E. Hodgson, *Nuclear Reactions and Nuclear Structure*, Clarendon Press, Oxford, 1971.

[83] A. van der Woude, in *Electric and Magnetic Giant Resonances in Nuclei*, edited by J. Speth (World Scientific, Singapore, 1991), p. 99-232.

[84] C. Kalbach, Phys. Rev. C **62**, 44608 (2000).

[85] D.M. Brink, Nucl. Phys. **4**, 215 (1957); P. Axel, Phys. Rev. **126**, 671 (1962).

[86] J. Kopecky and M. Uhl, Phys. Rev. C **42**, 1941 (1990).

[87] J. Kopecky, M. Uhl and R.E. Chrien,, Phys. Rev. C **47**, 312 (1993).

[88] D.G. Gardner, in *Neutron Radiative Capture*, OECD/NEA Series on Neutron Physics and Nuclear Data in Science and Technology, eds. A. Michaudon et al., p. 62 (1984).

[89] J. Kopecky, private communication.

[90] M.B. Chadwick, P. Oblozinsky, P.E. Hodgson, and G. Reffo, Phys. Rev. C **44**, 814 (1991); Handbook on *photonuclear data for applications: Cross sections and spectra*, IAEA-TECDOC-1178 (2000).

[91] H. Gruppelaar, P. Nagel, and P.E. Hodgson, Riv. Nuovo Cimento **9**, No. 7, 1 (1986).

[92] E. Gadioli and P.E. Hodgson, *Pre-equilibrium nuclear reactions*, Oxford Univ. Press (1992).

[93] C. Kalbach, Phys. Rev. C **33**, 818 (1986).

[94] C.K. Cline and M. Blann, Nucl. Phys. **A172**, 225 (1971).

[95] J. Dobeš and E. Běták, Zeit. Phys. **A310**, 329 (1983).

[96] E. Běták and J. Dobeš, Zeit. Phys. **A279**, 319 (1976).

[97] C.Y. Fu, Nucl. Sci. Eng. **86**, 344 (1984).

[98] C. Kalbach, Phys. Rev. C **32**, 1157 (1985).

[99] C. Kalbach-Cline, Nucl. Phys. **A210**, 590 (1973).

[100] F. C. Williams, Nucl. Phys. **A166**, 231 (1971).

[101] J.M. Akkermans and H. Gruppelaar, Phys. Lett. **157B**, 95 (1985).

[102] H. Gruppelaar, *IAEA Advisory Group Meeting on Basic and Applied Problems on Nuclear Level Densities* (Brookhaven National Laboratory report, 1983), p. 143.

[103] C. Kalbach, Phys. Rev. C **71**, 034606 (2005).

[104] C. Kalbach, private communication (2007).

[105] A.J. Koning and J.M. Akkermans, Ann. Phys. **208**, 216 (1991).

[106] C. Kalbach, Phys. Rev. C **37**, 2350 (1988).

[107] W.D. Myers and W.J. Swiatecki, Nucl. Phys. **81**, 1 (1966).

[108] H.M. Hofmann, J. Richert, J.W. Tepel and H.A. Weidenmüller, Ann. Phys. (N.Y.) **90**, 403 (1975).

[109] J.W. Tepel, H.M. Hofmann and H.A. Weidenmüller, Phys. Lett. **49B**, 1 (1974).

[110] H.M. Hofmann, T. Mertelmeier, M. Herman and J.W. Tepel, Zeit. Phys. **A297**, 153 (1980).

[111] P.A. Moldauer, Phys. Rev. C **14**, 764 (1976).

[112] P.A. Moldauer, Nucl. Phys. **A344**, 185 (1980).

[113] J.J.M. Verbaarschot, H.A. Weidenmüller and M.R. Zirnbauer, Phys. Rep. **129**, 367 (1985).

[114] H. Gruppelaar and G. Reffo, Nucl. Sci. Eng. **62**, 756 (1977).

[115] M.B. Chadwick, P.G. Young, D.C. George and Y. Watanabe, Phys. Rev. C **50**, 996 (1994).

[116] A.J. Koning and M.B. Chadwick, Phys. Rev. C **56**, 970 (1997).

[117] A.J. Koning and S. Hilaire, to be published.

[118] T. Ericson, Adv. Phys. **9**, 425 (1960).

[119] A. Gilbert and A.G.W. Cameron, Can. J. Phys. **43**, 1446 (1965).

[120] W. Dilg, W. Schantl, H. Vonach, and M. Uhl, Nucl. Phys. **A217**, 269 (1973).

[121] H. Baba, Nucl. Phys. **A159**, 625 (1970).

[122] A.V. Ignatyuk, G.N. Smirenkin and A.S. Tishin, Sov. J. Nucl. Phys. **21**, no. 3, 255 (1975).

[123] G. Audi and A.H. Wapstra, Nucl. Phys. **A729**, 129 (2003).

[124] A. Mengoni and Y. Nakajima, J. Nucl. Sci. Techn. **31**, 151 (1994).

[125] S. Goriely, Nucl. Phys. **A605**, 28 (1996).

[126] S. Hilaire, PhD thesis, unpublished (1997).

[127] S.F. Mughabghab and C. Dunford, Phys. Rev. Lett. **81**, 4083 (1998).

[128] A.S. Iljinov, M.V. Mebel, N. Bianchi, E. De Sanctis, C. Guaraldo, V. Lucherini, V. Muccifora, E. Polli, A.R. Reolon, and P. Rossi, Nucl. Phys. **A543**, 517 (1992).

[129] M.K. Grossjean and H. Feldmeier, Nucl. Phys. **A444**, 113 (1985).

[130] O.T. Grudzevich, A.V. Ignatyuk, V.I. Plyaskin, A.V. Zelenetsky, in Proc. Nuclear Data for Science and Technology (Mito, JAERI), p 187 (1988)

[131] A.R. Junghans, M. de Jong, H.-G. Clerc, A.V. Ignatyuk, G.A. Kudyaev, and K.-H. Schmidt, Nucl. Phys. **A629**, 635 (1998).

[132] G. Hansen and A.S. Jensen, Nucl. Phys. **A406**, 236 (1983).

[133] P. Demetriou and S. Goriely, Nucl. Phys. **A695**, 95 (2001).

[134] S. Goriely, F. Tondeur, J.M. Pearson, Atom. Data Nucl. Data Tables **77**, 311 (2001).

[135] S. Hilaire and S. Goriely, accepted for Nucl. Phys. A.

[136] E.V. Gaï, A.V. Ignatyuk, N.S. Rabotnov, G.N. Smirenkin, 1969. *Physics and Chemistry of Fission,* I.A.E.A., Vienna, p.337.

[137] A.V. Ignatyuk, K.K. Istekov, and G.N. Smirenkin, Sov. J. Nucl. Phys. **29**, no. 4, 450 (1979).

[138] A.V. Ignatyuk, J.L. Weil, S. Raman, and S. Kahane, Phys. Rev. **C47**, 1504 (1993).

[139] A. J. Sierk, Phys. Rev. C **33**, 2039 (1986).

[140] S. Cohen, F. Plasil, and W. J. Swiatecki, *Ann. of Phys.* **82**, 557 (1974).

[141] M. Sin, R. Capote and A. Ventura, Phys. Rev. C **74**, 014608 (2006).

[142] A. Mamdouh, J.M. Pearson, M. Rayet and F. Tondeur, Nucl. Phys. **A679**, 337 (2001).

[143] A. D'Arrigo *et al.*, Journ. Phys. G **20**, 305 (1994).

[144] U. Brosa, S. Großmann and Müller, Phys. Rep. **197**, 167 (1990).

[145] M.C. Duijvestijn, A.J. Koning, and F.-J. Hambsch, Phys. Rev. C **64**, 014607 (2001).

[146] W.D. Myers and W.S. Swiatecki, Ark. Fysik **36**, 593 (1967).

[147] B.D. Wilkins, E.P. Steinberg, and R. R. Chasman, Phys. Rev. C **14**, 1832 (1976).

[148] J. Kopecky, M.G. Delfini, H.A.J. van der Kamp and D. Nierop: Revisions and extensions of neutron capture cross-sections in the European Activation File EAF-3, ECN-C–92-051, July 1992.

[149] S. Lemaire, P. Talou, T. Kawano, M.B. Chadwick, and D.G. Madland, Phys. Rev.C **72**, 024601 (2005).

[150] J.A. Holmes, S.E. Woosley, W.A. Fowler, B.A. Zimmerman, At. Data Nucl. Data Tables **18**, 306 (1976).

[151] P. Möller, J.R. Nix, W.D. Myers and W.J. Swiatecki, Atomic Data Nucl. Data Tab. **59**, 185 (1995).

[152] S. Goriely, J.M. Pearson, and M. Samyn, Nucl. Phys. **A773**, 279 (2006).

[153] J. Duflo and A. Zuker, unpublished.

[154] F. Vivès, F. -J. Hambsch, H. Bax, and S. Oberstedt, *Nucl. Phys.* **A662**, 63 (2000).

[155] S. Nagg, K.F. Flynn, J.E. Gindler, J.W. Meadows, and L.E. Glendening, Phys. Rev. C **17**, 163 (1978).

[156] T.C. Chapman, G.A. Anzelon, G.C. Spitale, and D.R. Nethaway Phys. Rev. C **17**, 1089 (1978).

[157] T.C. Chapman, G.A. Anzelon, G.C. Spitale, and D.R. Nethaway Phys. Rev. C **17**, 1089 (1978).

[158] L. McFadden, G.R. Satchler, Nucl. Phys. 84 (1966) 177.

[159] A.A. Cowley, A. van Kent, J.J. Lawrie, S.V. Förtsch, D.M. Whittal, J.V. Pilcher, F.D. Smit, W.A. Richter, R. Lindsay, I.J. van Heerden, R. Bonetti, and P.E. Hodgson, Phys. Rev. C **43**, 678 (1991).

[160] W. Scobel, M. Trabandt, M. Blann, B. A. Pohl, B. A. Remington, R. C. Byrd, C. C. Foster, R. Bonetti, C. Chiesa, and S. M. Grimes, Phys. Rev. C **41**, 2010 (1990).

[161] R. Michel, R. Bodemann, H. Busemann, R. Daunke, M. Gloris, H.-J. Lange, B. Klug, A. Krins, I. Leya, M. Luepke, S. Neumann, H. Reinhardt, M. Schnatz-Buettgen, U. Herpers, TH. Schiekel, F. Sudbrock, B. Holmqvist, H. Conde, P. Malmborg, M. Suter, B. Dittrich-Hannen, P.-W. Kubik, H.-A. Sinal, D. Filges, Nucl. Inst. Meth. **B129**, 153 (1997).

[162] B.L. Berman,J.T. Caldwell,R.R. Harvey,M.A. Kelly, R.L. Bramblett,S.C. Fultz, Phys. Rev. **162**, 1098 (1967).

[163] A. Marcinkowski, J. Rapaport, R. Finlay, X. Aslanoglou, and D. Kielan, Nucl. Phys. **A530**, 75 (1991).

[164] H. Vonach, A. Pavlik, M.B. Chadwick, R.C. Haight, R.O. Nelson, S.A. Wender, and P.G. Young, Phys. Rev. C **50**, 1952 (1994).

Appendix A

TERMS AND CONDITIONS FOR COPYING, DISTRIBUTION AND MODIFICATION

1. This License applies to any program or other work which contains a notice placed by the copyright holder saying it may be distributed under the terms of this General Public License. The ”Program”, below, refers to any such program or work, and a ”work based on the Program” means either the Program or any derivative work under copyright law: that is to say, a work containing the Program or a portion of it, either verbatim or with modifications and/or translated into another language. (Hereinafter, translation is included without limitation in the term ”modification”.) Each licensee is addressed as ”you”.

   Activities other than copying, distribution and modification are not covered by this License; they are outside its scope. The act of running the Program is not restricted, and the output from the Program is covered only if its contents constitute a work based on the Program (independent of having been made by running the Program). Whether that is true depends on what the Program does.

2. You may copy and distribute verbatim copies of the Program’s source code as you receive it, in any medium, provided that you conspicuously and appropriately publish on each copy an appropriate copyright notice and disclaimer of warranty; keep intact all the notices that refer to this License and to the absence of any warranty; and give any other recipients of the Program a copy of this License along with the Program.

   You may charge a fee for the physical act of transferring a copy, and you may at your option offer warranty protection in exchange for a fee.

3. You may modify your copy or copies of the Program or any portion of it, thus forming a work based on the Program, and copy and distribute such modifications or work under the terms of Section 1 above, provided that you also meet all of these conditions:

   a) You must cause the modified files to carry prominent notices stating that you changed the files and the date of any change.

b) You must cause any work that you distribute or publish, that in whole or in part contains or is derived from the Program or any part thereof, to be licensed as a whole at no charge to all third parties under the terms of this License.

c) If the modified program normally reads commands interactively when run, you must cause it, when started running for such interactive use in the most ordinary way, to print or display an announcement including an appropriate copyright notice and a notice that there is no warranty (or else, saying that you provide a warranty) and that users may redistribute the program under these conditions, and telling the user how to view a copy of this License. (Exception: if the Program itself is interactive but does not normally print such an announcement, your work based on the Program is not required to print an announcement.)

These requirements apply to the modified work as a whole. If identifiable sections of that work are not derived from the Program, and can be reasonably considered independent and separate works in themselves, then this License, and its terms, do not apply to those sections when you distribute them as separate works. But when you distribute the same sections as part of a whole which is a work based on the Program, the distribution of the whole must be on the terms of this License, whose permissions for other licensees extend to the entire whole, and thus to each and every part regardless of who wrote it.

Thus, it is not the intent of this section to claim rights or contest your rights to work written entirely by you; rather, the intent is to exercise the right to control the distribution of derivative or collective works based on the Program.

In addition, mere aggregation of another work not based on the Program with the Program (or with a work based on the Program) on a volume of a storage or distribution medium does not bring the other work under the scope of this License.

4. You may copy and distribute the Program (or a work based on it, under Section 2) in object code or executable form under the terms of Sections 1 and 2 above provided that you also do one of the following:

   a) Accompany it with the complete corresponding machine-readable source code, which must be distributed under the terms of Sections 1 and 2 above on a medium customarily used for software interchange; or,

   b) Accompany it with a written offer, valid for at least three years, to give any third party, for a charge no more than your cost of physically performing source distribution, a complete machine-readable copy of the corresponding source code, to be distributed under the terms of Sections 1 and 2 above on a medium customarily used for software interchange; or,

   c) Accompany it with the information you received as to the offer to distribute corresponding source code. (This alternative is allowed only for noncommercial distribution and only if you received the program in object code or executable form with such an offer, in accord with Subsection b above.)

   The source code for a work means the preferred form of the work for making modifications to it. For an executable work, complete source code means all the source code for all modules it contains, plus any associated interface definition files, plus the scripts used to control compilation and installation of the executable. However, as a special exception, the source code distributed need not include anything that is normally distributed (in either source or binary form) with the major components (compiler, kernel, and so on) of the operating system on which the executable runs, unless that component itself accompanies the executable.

If distribution of executable or object code is made by offering access to copy from a designated place, then offering equivalent access to copy the source code from the same place counts as distribution of the source code, even though third parties are not compelled to copy the source along with the object code.

5. You may not copy, modify, sublicense, or distribute the Program except as expressly provided under this License. Any attempt otherwise to copy, modify, sublicense or distribute the Program is void, and will automatically terminate your rights under this License. However, parties who have received copies, or rights, from you under this License will not have their licenses terminated so long as such parties remain in full compliance.

6. You are not required to accept this License, since you have not signed it. However, nothing else grants you permission to modify or distribute the Program or its derivative works. These actions are prohibited by law if you do not accept this License. Therefore, by modifying or distributing the Program (or any work based on the Program), you indicate your acceptance of this License to do so, and all its terms and conditions for copying, distributing or modifying the Program or works based on it.

7. Each time you redistribute the Program (or any work based on the Program), the recipient automatically receives a license from the original licensor to copy, distribute or modify the Program subject to these terms and conditions. You may not impose any further restrictions on the recipients' exercise of the rights granted herein. You are not responsible for enforcing compliance by third parties to this License.

8. If, as a consequence of a court judgment or allegation of patent infringement or for any other reason (not limited to patent issues), conditions are imposed on you (whether by court order, agreement or otherwise) that contradict the conditions of this License, they do not excuse you from the conditions of this License. If you cannot distribute so as to satisfy simultaneously your obligations under this License and any other pertinent obligations, then as a consequence you may not distribute the Program at all. For example, if a patent license would not permit royalty-free redistribution of the Program by all those who receive copies directly or indirectly through you, then the only way you could satisfy both it and this License would be to refrain entirely from distribution of the Program.

   If any portion of this section is held invalid or unenforceable under any particular circumstance, the balance of the section is intended to apply and the section as a whole is intended to apply in other circumstances.

   It is not the purpose of this section to induce you to infringe any patents or other property right claims or to contest validity of any such claims; this section has the sole purpose of protecting the integrity of the free software distribution system, which is implemented by public license practices.

Many people have made generous contributions to the wide range of software distributed through that system in reliance on consistent application of that system; it is up to the author/donor to decide if he or she is willing to distribute software through any other system and a licensee cannot impose that choice.

This section is intended to make thoroughly clear what is believed to be a consequence of the rest of this License.

9. If the distribution and/or use of the Program is restricted in certain countries either by patents or by copyrighted interfaces, the original copyright holder who places the Program under this License may add an explicit geographical distribution limitation excluding those countries, so that distribution is permitted only in or among countries not thus excluded. In such case, this License incorporates the limitation as if written in the body of this License.

10. The Free Software Foundation may publish revised and/or new versions of the General Public License from time to time. Such new versions will be similar in spirit to the present version, but may differ in detail to address new problems or concerns.

    Each version is given a distinguishing version number. If the Program specifies a version number of this License which applies to it and ”any later version”, you have the option of following the terms and conditions either of that version or of any later version published by the Free Software Foundation. If the Program does not specify a version number of this License, you may choose any version ever published by the Free Software Foundation.

11. If you wish to incorporate parts of the Program into other free programs whose distribution conditions are different, write to the author to ask for permission. For software which is copyrighted by the Free Software Foundation, write to the Free Software Foundation; we sometimes make exceptions for this. Our decision will be guided by the two goals of preserving the free status of all derivatives of our free software and of promoting the sharing and reuse of software generally.

    NO WARRANTY

12. BECAUSE THE PROGRAM IS LICENSED FREE OF CHARGE, THERE IS NO WARRANTY FOR THE PROGRAM, TO THE EXTENT PERMITTED BY APPLICABLE LAW. EXCEPT WHEN OTHERWISE STATED IN WRITING THE COPYRIGHT HOLDERS AND/OR OTHER PARTIES PROVIDE THE PROGRAM ”AS IS” WITHOUT WARRANTY OF ANY KIND, EITHER EXPRESSED OR IMPLIED, INCLUDING, BUT NOT LIMITED TO, THE IMPLIED WARRANTIES OF MERCHANTABILITY AND FITNESS FOR A PARTICULAR PURPOSE. THE ENTIRE RISK AS TO THE QUALITY AND PERFORMANCE OF THE PROGRAM IS WITH YOU. SHOULD THE PROGRAM PROVE DEFECTIVE, YOU ASSUME THE COST OF ALL NECESSARY SERVICING, REPAIR OR CORRECTION.

13. IN NO EVENT UNLESS REQUIRED BY APPLICABLE LAW OR AGREED TO IN WRITING WILL ANY COPYRIGHT HOLDER, OR ANY OTHER PARTY WHO MAY MODIFY AND/OR REDISTRIBUTE THE PROGRAM AS PERMITTED ABOVE, BE LIABLE TO YOU FOR DAMAGES, INCLUDING ANY GENERAL, SPECIAL, INCIDENTAL OR CONSEQUENTIAL DAMAGES ARISING OUT OF THE USE OR INABILITY TO USE THE PROGRAM

(INCLUDING BUT NOT LIMITED TO LOSS OF DATA OR DATA BEING RENDERED INACCURATE OR LOSSES SUSTAINED BY YOU OR THIRD PARTIES OR A FAILURE OF THE PROGRAM TO OPERATE WITH ANY OTHER PROGRAMS), EVEN IF SUCH HOLDER OR OTHER PARTY HAS BEEN ADVISED OF THE POSSIBILITY OF SUCH DAMAGES.